ESA Climate Change Initiative

Ozone_cci+

Product Validation and Intercomparison Report (PVIR)

Date: 12.05.2025

Version: 5.2 (Final)

Phase I, Task 4

Deliverable D4.1

WP Manager: J.-C. Lambert
WP Manager Organization: BIRA-IASB
Other partners:
VALT: AUTH, BIRA-IASB
EOST: BIRA-IASB, DLR-IMF, KNMI, RAL, ULB, FMI, IUP-UB

DOCUMENT PROPERTIES

Title	Product Validation and Intercomparison Report (PVIR)
Reference	Ozone_cci+_PVIR_5.2
Internal references	Ozone_cci+_D4.1
Issue / Revision	5.2 / 0
Status	Final
Date of issue	12.05.2025
Document type	QA/Validation Report

FUNCTION		NAME	DATE
LEAD AUTHOR	VALT Leader	Arno Keppens, BIRA-IASB	20.01.2025
CONTRIBUTING AUTHORS	VALT	Dimitris Balis, AUTH Katerina Garane, AUTH José Granville, BIRA-IASB Daan Hubert, BIRA-IASB Mariliza Koukouli, AUTH Jean-Christopher Lambert, BIRA-IASB Tijl Verhoelst, BIRA-IASB	20.01.2025
	EOST	Diego Loyola, DLR-IMF Alexei Rozanov, IUP-UB Richard Siddans, RAL Viktoria Sofieva, FMI Ronald van der A, KNMI Catherine Wespes, ULB	20.01.2025
REVIEWED BY	Science Leader	Daan Hubert, BIRA-IASB	12.05.2025
ISSUED BY	VALT Leader	Arno Keppens, BIRA-IASB	12.05.2025
ACCEPTED BY	ESA CCI Officer	Michael Eisinger, ESA/ECSAT	12.05.2025

Table of Contents

EXECUTIVE SUMMARY

The Ozone_cci+ project is the successor of Ozone_cci as part of ESA's Climate Change Initiative (CCI). The Validation Team (VALT) has developed a Product Validation Plan (PVP) translating user requirements into validation requirements, in order to ensure independent and traceable validation of the Ozone_cci+ data products and verification of compliance with the user requirements. This Product Validation and Intercomparison Report (PVIR) version 5.2 reports on the quality of the Climate Research Data Package (CRDP). For each of the Essential Climate Variable (ECV) data records provided by the project, the PVIR provides users with detailed validation results, with a list of quality indicators enabling the verification of fitness-for-purpose of the data for their own application, and with an assessment of the compliance of the CRDP with user requirements established by the Climate Research Group (CRG) based on their own research needs and on more generic needs formulated by international climate research and monitoring bodies like GCOS.

1 Introduction

1.1 *Purpose and scope*

The current Ozone_cci+ Climate Research Data Package (CRDP) includes records of total ozone columns, nadir-based ozone profiles, and limb-based ozone profiles. Requirements for the necessary quality assessment of the CRDP datasets are detailed in the Ozone_cci+ Product Validation Plan (PVP, [RD3]) established by a validation team working independently of the algorithm development teams. Based on the PVP, the present Product Validation and Intercomparison Report (PVIR) provides users and product developers of the CRDP with geophysical validation results and with a list of quality indicators enabling the verification of the fitness-for-purpose of the data. In particular, the PVIR discusses the compliance of the individual CRDP datasets with user requirements formulated by GCOS and the project's Climate Research Group (CRG) in a dedicated User Requirements Document (URD, [RD10]). This PVIR will be updated in a future phase of this project as improved and new data products and possibly validation approaches are developed.

1.2 *Document overview*

The Ozone_cci+ Product Validation and Intercomparison Report is organised as follows:

- Section 2 introduces the CRDP datasets addressed in this report.
- Section 3 describes the ECV validation methodology: Generic principles of the validation process, study of compliance with user requirements, information content and sensitivity studies, and confrontation to independent and traceable reference measurements.
- Section 4 describes validation results and compliance assessment for the nadir-based ozone profile ECV.
- Section 5 describes validation results and compliance assessment for the limb-based ozone profile ECV.
- Section 6 describes validation results and compliance assessment for the tropospheric ozone ECV.
- Section 7 lists applicable and reference documents.
- Section 8 defines the applicable terminology.

For each ECV data product, the results are reported as follows:

- A description of the reference measurements used for independent ECV validation.
- A description of the preparation of satellite and reference measurements, including quality control procedures applied for the selection of the most appropriate data, information on the uncertainties associated to them, co-location criteria applied, data manipulations applied to convert data units and representation systems...
- A description of the match-up analyses performed on the derived ECV products against the selected reference observations.
- A detailed analysis of the uncertainty of the ECV products with reference to the independent validation data.
- Statement of compliance with user requirements formulated in the project's User Requirement Document [RD10].

2 Climate Research Data Package (CRDP)

The Climate Research Data Package (CRDP) generated in the framework of the Ozone_cci+ project contains a list of ozone column and ozone profile data sets. The database can be accessed through the freely accessible ftp site ftp://cci_web@ftp-ae.oma.be/esacci/ozone, and Level-3 products through the CCI Open Data Portal (http://cci.esa.int/data) or at the Copernicus Climate Data Store (https://cds.climate.copernicus.eu). The data package is organised in four families of ozone data products: Total ozone data products (TC=Total Column), Nadir ozone profile data products (NP=Nadir Profile), Limb ozone profile data products (LP=Limb Profile) and Tropospheric ozone data products (TRC). All data sets are delivered in NetCDF-CF format and are compliant with CCI data format guidelines, as described in the Product User Guide (PUG) [RD5]. The Ozone_cci+ data products validated in this document are listed in the tables below. A full description of the retrieval algorithms and retrieval settings is given in the associated Algorithm Theoretical Basis Document (ATBD) [RD4]. A description of ex-ante uncertainty characterisation can be found in the End-to-End ECV Uncertainty Budget (E3UB) [RD6].

2.1 *Nadir ozone profile data sets*

Table 2.1 - Ozone_cci+ CRDP nadir ozone profile data products considered in this PVIR.

Product level	Product ID	Sensor	Product description	Provider	Time coverage	Validation report
Level-2	NP_L2_IASIA	Metop-A IASI	FORLI 20151001 CDR algorithm on fixed altitude levels	ULB-LATMOS	2008-2019	Section 4
	NP_L2_IASIB	Metop-B IASI	FORLI 20151001 CDR algorithm on fixed altitude levels	ULB-LATMOS	2019-2023	Section 4
	NP_L2_IASIC	Metop-C IASI	FORLI 20151001 CDR algorithm on fixed altitude levels	ULB-LATMOS	2019-2023	Section 4
Level-3	NP IASI-ABC	Merged	FORLI 20191122 algorithm on fixed altitude levels	ULB-LATMOS	2008-2023	Section 4
	NP_GOP-ECV	Merged	v3 from RAL L2 v2 and v3	DLR	1995-2022	Section 4

2.2 *Limb ozone profile data sets*

Table 2.2 - Ozone_cci+ CRDP limb ozone profile data products considered in this PVIR.

Product level	Product ID	Sensor	Product description	Provider	Time coverage	Validation report
HARMonized dataset of OZone profiles (HARMOZ) Level 2	LP_L2_GOMOS	Envisat GOMOS	Individual profiles of ozone mole concentrations on a common pressure or geometric altitude grid, and auxiliary information to convert to volume mixing ratio and/or geometric altitude/pressure	FMI	Entire mission, data screened for outliers (filtered data)	Section 5.4.2
	LP_L2_GBL	Envisat GOMOS		FMI		Section 5.4.3
	LP_L2_MIPAS	Envisat MIPAS		IMK/IAA		Section 5.4.4
	LP_L2_SCIA	Envisat SCIAMACHY		U Bremen		Section 5.4.5
	LP_L2_OSIRIS	Odin OSIRIS		U Saskatchewan		Section 5.4.6
	LP_L2_ACE	SciSat ACE FTS		U Toronto		Section 5.4.7
	LP_L2_OMPS_SNPP_USASK	Suomi-NPP		U Saskatchewan		Section 5.4.8
	LP_L2_OMPS_SNPP_UBR	Suomi-NPP		U Bremen		Section 5.4.9
	LP_L2_OMPS_N21_UBR	NOAA-21		U Bremen		Section 5.4.10
	LP_L2_SAGE-II	ERBS SAGE II		NASA-LaRC, U Bremen		Section 5.4.11
	LP_L2_HALOE	UARS HALOE		NASA-LaRC, U Bremen		Section 5.4.12
	LP_L2_SABER	TIMED SABER		NASA-LaRC, U Bremen		Section 5.4.13
	LP_L2_MLS	Aura MLS		NASA-JPL, U Bremen		Section 5.4.14
	LP_L2_POAM-III	SPOT-4 POAM III		NASA, U Bremen		Section 5.4.15
	LP_L2_SAGE-III/M3M	Meteor-3M SAGE III		NASA-LaRC, U Bremen		Section 5.4.16
	LP_L2_SAGE-III/ISS	ISS SAGE III		NASA-LaRC, U Bremen		Section 5.4.17
Level 3	LP_LIMB_HIRES	Aura MLS, GOMOS, MIPAS, SCIAMACHY, OSIRIS, OMPS-LP/SNPP, SAGE III/ISS, ACE-FTS	Daily 1° x 1° mean profile of ozone mole concentrations on a pressure grid	FMI	2004-2022	Section 5.5.2

2.3 *Tropospheric ozone data sets*

Table 2.3 - Ozone_cci+ CRDP tropospheric ozone data products considered in this PVIR.

Product level	Product ID	Sensor	Product description	Provider	Time coverage	Validation report
Level 3	TRC_L3_GTTO	GOME, SCIAMACHY, OMI, GOME-2A, GOME-2B, GOME-2C, TROPOMI	CCD algorithm, surface to 270 hPa	DLR	1995-2023	Section 6.2
	TRC_L3_OMI-LIMB	OMI, LIMB-HIRES	Limb-Nadir matching algorithm, surface to thermal tropopause	FMI	2004-2023	Section 6.3
	TRC_L3_GTO-LIMB	GTO-ECV, LIMB-HIRES	Limb-Nadir matching algorithm, surface to thermal tropopause	FMI	2004-2023	Section 6.3

3 ECV Validation Methodology

3.1 *General principles of the validation process*

The Ozone_cci+ Product Validation Plan [RD3] describes the validation protocol applied in this assessment. The prime objective of the Ozone_cci+ project is the production of ECV data products responding to the needs of the climate research community, represented by the Ozone_cci+ Climate research Group (CRG) and the CCI Climate Modelling User Group (CMUG). Every ECV data set produced by the project needs to be validated against the official user requirements formulated in the Ozone_cci+ User Requirement Document (URD, [RD10]). In the following section, we summarize the user requirements applicable to the present validation study. The translation of these user requirements into validation requirements is described in the Ozone_cci+ Product Validation Plan (PVP, [RD3]). The geophysical validation of ECV data products delivered in the CRDP relies primarily on comparisons with ground-based reference measurements. These comparisons are reported in the following sections. The reference measurements used in this study are summarised in Section 3.5. In preparation of the comparisons, the data sets must undergo a suite of data manipulations, including data filtering based on, e.g., quality flags, harmonisation of coordinate systems and of units, reduction of differences in vertical and horizontal smoothing, selection of co-locations meeting appropriate criteria… These operations depend on the ECV data product and associated retrieval algorithms; therefore, they are described in the respective sections reporting the comparisons. Prior to the data comparisons, the characterisation of the information content of the data products and their sensitivity to the real atmosphere may be required. This is definitely the case for a proper interpretation of nadir ozone profile data, for which the final data product is a mix of real contributions from the measurement and of a priori constraints. This aspect is addressed in Section 3.3.

3.2 *Compliance with user requirements*

The Ozone_cci+ User Requirement Document (URD) [RD10] defines climate user requirements based on the ozone requirements of the Global Climate Observing System (GCOS), the CCI Climate Modelling User Group (CMUG) [RD7], the Integrated Global Atmospheric Chemistry Observation theme (IGACO) of the Integrated Global Observing Strategy (IGOS) [RD9], and the WMO observational requirements [RD11]. They are summarised hereafter. These URD requirements were translated into validation requirements in the Product Validation Plan (PVP) [RD3] established by the Ozone_cci+ Validation Team (VALT).

The first category of user requirements addresses classical error bars. In the case of total ozone column TOC (expressed in DU) the error will be given as a delta total ozone value in DU (δTOC), usually equal to a few percent, such that TOC ± δTOC represents a symmetric 68 % confidence interval. This δTOC value contains a systematic term and a random term, corresponding to classical bias and precision (1σ standard deviation or equivalent) estimates. Validation is expected to verify the accuracy of ex-ante estimates of the systematic bias and precision provided by the ECV retrieval teams. This verification must further ensure that these quality indicators, which usually vary with several parameters of the measurement and the retrieval, remain within the acceptable ranges defined in URD.

In the case of ozone profiles two error bars are required, one representing an altitude range (requirement of ±500m for limb profile retrievals), the other representing a volume mixing ratio range (requirements between 8 % and 20 %), and both representing a symmetric 68 % confidence interval. Assessment of the error bar on altitude for nadir ozone profile data requires analysis of information content (e.g., calculation of centroids and Backus-Gilbert spread of the vertical averaging kernels, [RD27]). Details will be addressed in dedicated sections.

The second category of user requirements addresses (i) the temporal and spatial domains over which, and (ii) the associated temporal and spatial resolutions at which, data quality must meet the first category of user requirements:

- Temporal domain and sampling: continuous coverage with 3 days of observation frequency over the decadal range and beyond, with maximum uncertainty on interannual variability, annual cycle and shorter-term variability ranging from 2-3 % for total ozone data up to 20 % for tropospheric ozone data.
- Temporal stability: Long-term stability of 1 %-3 %/decade to allow trend detection.
- Geographical domain: global, regional, latitude-height monthly mean cross-sections.
- Horizontal resolution requirements: from 20 km to 300 km depending on the ECV.
- Vertical range and sensitivity: requirements reflect the vertical structure of ozone changes, namely total ozone column (TOC), and ozone in the lower troposphere (LT), upper troposphere (UT), lower stratosphere (LS), upper stratosphere and mesosphere (USM).
- Vertical resolution: depending on the ECV.

Other user requirements fall rather into categories of product specifications:

- Level of the ECV data set: off-line homogenized Level-2 time series for process evaluations on time scales spanning from hours/days to months/years, and homogenized multi-instrument long-term data sets for ozone-climate interactions (Level-3 and Level-4).
- Continuity of user requirements between data levels, e.g., aggregated multi-sensor Level-3 products should retain Level-2 requirements as much as possible. At least, Level-3 products should not be homogenized/degraded to the instrument with the lowest accuracy over the targeted time period.
- Requirements for ancillary data: cloud information per pixel (including cloud fraction, cloud height, cloud albedo) and surface information per pixel (surface albedo).
- Data format and metadata requirements.
- Visualisation requirements.

Compliance with requirements on observation frequency and geographical domain is straightforward to verify through visualisation of the data sets, a study hereafter referred to as dataset content study. Compliance with requirements on spatial resolution and spatial sampling need visualisation of the data and analysis of information content (e.g., calculation of centroids and Backus-Gilbert spread and use of cross-correlation techniques). Compliance with more specific requirements, especially requirements peculiar to Level-3/4 data products, e.g. in terms of actual geographical coverage and of point-to-zone representativeness, may need the use of statistical methods based on global model results. In addition to validation studies and quality checks performed by the validation teams (VALT) and by the ECV producers (EOSTs), user feedback provides valuable input for the assessment of effective usability of the data product. The latter quality checks are reported in another document, the Climate Assessment Report (CAR) [RD73].

Hereafter we reproduce the user requirements as described in Tables 5 to 10 of version 4.1 of the URD, against which Ozone_cci+ ECV data products must be verified and/or validated. For each ECV the tables in this document display specific requirements on the data, its characteristics and its errors (Table 3.1, Table 3.3 and Table 3.5), and requirements on the data format and associated metadata (Table 3.2, Table 3.4 and Table 3.6).

3.2.1 Total ozone data product requirements

Table 3.1 - Product requirements for total ozone column data. Achievable and future target requirements are given, separated by a '–' (adapted from URD v4.1).

Quantity	Driving Research topic	Geographical Zone		
		Tropics	Mid-latitudes	Polar region
Global horizontal resolution	Evolution of the ozone layer (radiative forcing); Seasonal cycle and interannual variability; Short-term variability*	20 – 100 km	20 – 50/100 km	20 – 50/100 km
Observation frequency	Evolution of the ozone layer (radiative forcing); Seasonal cycle and interannual variability; short-term variability*	Daily – weekly	Daily – weekly	Daily – weekly
Time period	Evolution of the ozone layer (radiative forcing)	(1980-2010) 1995-2011	(1980-2010) 1995-2011	(1980-2010) 1995-2011
Uncertainty	Evolution of the ozone layer (radiative forcing)	2 % (7 DU)	2 % (7 DU)	2 % (7 DU)
Uncertainty	Seasonal cycle and interannual variability; Short-term variability*	3 % (10 DU)	3 % (10 DU)	3 % (10 DU)
Stability (after corrections)	Evolution of the ozone layer (1980-2010 trend detection; radiative forcing)	1 – 3 % / decade (1995-2011)	1 – 3 % / decade (1995-2011)	1 – 3 % / decade (1995-2011)

** Short-term variability includes: Exchange of air masses, streamers, regime studies.*

Table 3.2 - Data format and metadata requirements for total ozone (adapted from URD v4.1)

Data feature	Requirement
Data format	Net-CDF [RD22]
Data conventions	CF
Data units	Total column (in DU; number of molecules per area or equivalent)
Error	Total area
Error characteristics (optional)	Total uncertainty and its subdivision per pixel into: - contribution measurement noise; - contribution of a priori uncertainties; - contribution of estimated spectroscopic uncertainty
Averaging kernels	Yes, for Level-2
Full covariance matrix included?	No
A priori data	Yes, per pixel
Quality flag	1: high quality data 2: contaminated data 3: missing value
Visualisation	Basic browsable archive visualisation (daily global maps; local/latitudinal time series of monthly means)

3.2.2 Nadir ozone profile and tropospheric ozone data product requirements

Table 3.3 - Product requirements for nadir-based ozone profile and tropospheric ozone Climate Data Records (CDRs). The ozone profile requirements are for ozone products in terms of (partial column mean) mixing ratios. The tropospheric altitude domain extends from the surface to the tropopause defined by an ozone concentration of 150 ppbv; the UT/LS extends from about 5 to 30 km, and the middle atmosphere extends from about 30 to 60 km altitude. The required coverage is global. Achievable and future target requirements are given, separated by a '–'. The first number is the future target. Note: requirements have been updated in Ozone_cci+ (adapted from URD v4.1).

Quantity	Driving Research topic	Height range		
		Troposphere	UT/LS	Middle Atmosphere
Horizontal resolution	Regional differences in evolution of the ozone layer and tropospheric ozone burden (radiative forcing); Seasonal cycle and interannual variability; Short-term variability*	20 – 200 km	20 – 200 km	200 – 400 km
Vertical resolution	Height dependence of evolution of the ozone layer and the tropospheric ozone burden (radiative forcing); Seasonal cycle and interannual variability; Short-term variability*	6 km – tropospheric column	6 km – partial column	6 km – partial column
Observation frequency	Evolution of the ozone layer and the tropospheric ozone burden (radiative forcing); Seasonal cycle and interannual variability; Short-term variability*	Daily – weekly	Daily – weekly	Daily – weekly
Time period	Evolution of the ozone layer and tropospheric ozone burden (radiative forcing)	(1980-2010) – (1996-2010)	(1980-2010) – (1996-2010)	(1980-2010) – (1996-2010)
Accuracy	Evolution of the ozone layer and tropospheric ozone burden (radiative forcing)	8 %	8 %	8 %
Accuracy	Seasonal cycle and interannual variability; Short-term variability*	16 %	16 % (< 20 km) 8 % (> 20 km)	8 %
Stability	Evolution of the ozone layer and tropospheric ozone burden (radiative forcing); trends	1 – 3 % / decade	1 – 3 % / decade	1 – 3 % / decade

** Short-term variability includes: Exchange of air masses, streamers, regime studies.*

Table 3.4 - Data requirements for nadir-based ozone profile Climate Data Records (adapted from URD v4.1)

Data feature	**Requirement**
Data format	Net-CDF
Data conventions	CF
Data units	Ozone mixing ratio (optional: also in partial ozone column and/or with co-located temperature profile)
Error characteristics	Total accuracy and its subdivision per pixel and per layer into: - contribution measurement noise; - contribution smoothing error - contribution of A Priori uncertainties;
Number of layers	To be chosen for optimal accuracy (not too few for information content, not too many by degrading the accuracy per layer)
Averaging kernels included?	Yes, per pixel
Full covariance matrix included?	Yes, per pixel
A priori data included?	Yes, per pixel
Flags	Quality per pixel (good, bad, uncertain); Pixel type; Snow/ice; Sun glint; Solar Eclipse; South-Atlantic Anomaly
Visualisations	Basic browsable archive visualisation (profile cross section per orbit; monthly maps at standard pressure levels; local/latitudinal time series of monthly means at standard pressure levels)

3.2.3 Limb ozone profile data product requirements

Table 3.5 - Product requirements for limb-based ozone profile Climate Data Records (CDRs). The ozone profile requirements are for ozone products in terms of (partial column mean) mixing ratios. The lower stratosphere (LS) extends from the tropopause (defined as ozone > 150 ppbv) to about 30 km, and the middle atmosphere extends from about 30 to 60 km altitude. The required coverage is global. Achievable and future target requirements are given, separated by a '–'. The first number is the future target (adapted from URD v4.1).

Quantity	Driving Research topic	Height Range	
		Lower Stratosphere	Middle Atmosphere
Horizontal resolution	Regional differences in the evolution of the ozone layer (radiative forcing); Seasonal cycle and interannual variability; Short-term variability	100 – 200 km	200 – 400 km
Vertical resolution	Height dependence of evolution of the ozone layer (radiative forcing); Seasonal cycle and interannual variability; Short-term variability	1 – 2 km	2 – 4 km
Observation frequency	Seasonal cycle and interannual variability; short-term variability	Daily – weekly	Daily – weekly
Time period	Evolution of the ozone layer (radiative forcing)	(1980-2010) – (2003-2010)	(1980-2010) – (2003-2010)
Uncertainty in height attribution	Evolution of the ozone layer (radiative forcing), Seasonal cycle and interannual variability; Short-term variability	±500 m	±500 m
Uncertainty on mixing ratio	Evolution of the ozone layer (radiative forcing)	8 %	8 %
Uncertainty on mixing ratio	Seasonal cycle and interannual variability; Short-term variability	16 % (<20 km) 8 % (>20 km)	8 %
Stability	Evolution of the ozone layer (radiative forcing); trends	1 – 3 % / decade	1 – 3 % / decade

Table 3.6 - Data format and metadata requirements for limb-based ozone profile requirements (adapted from URD v4.1)

Data feature	Requirement
Data format	Net-CDF [RD22]
Data conventions	CF
Data units	Ozone mixing ratio (optional: also in partial ozone column and/or with co-located temperature profile)
Error characteristics	Total accuracy and its subdivision per profile per layer into: - contribution measurement noise; - contribution horizontal smoothing error - contribution pointing accuracy - contribution of A Priori uncertainties;
Averaging kernels included?	Yes, per profile
Full covariance matrix included?	Yes, per profile
A priori data included?	Yes, per profile
Flags	Quality per profile per layer (good, bad, uncertain); Cloud contamination; Solar Eclipse; South-Atlantic anomaly
Visualisation	Basic browsable archive visualisation (profile cross section per orbit; monthly maps at standard pressure levels; local/latitudinal time series of monthly means at standard pressure levels)

3.2.4 Tropospheric ozone column data product requirements

Table 3.7 - Product requirements for tropospheric ozone Climate Data Records (CDRs). The ozone profile requirements are for ozone products in terms of (partial column mean) mixing ratios. The tropospheric altitude domain extends from the surface to the tropopause defined by an ozone concentration of 150 ppbv. The required coverage is global though not for the CCD technique-based tropospheric ozone products. Achievable and future target requirements are given, separated by a '–'. The first number is the future target (adapted from URD v4.1).

Quantity	**Driving Research topic**	**Height Range**		
		Tropospheric column	**Upper troposphere**	**Lower troposphere**
Horizontal resolution	Regional differences in the tropospheric ozone burden (radiative forcing); Seasonal cycle and interannual variability; Short-term variability	20 – 200 km	20 – 200 km	< 20 km
Vertical resolution	Height dependence of evolution of tropospheric ozone burden (radiative forcing); Seasonal cycle and interannual variability; Short-term variability	n/a	< 6 km	< 6 km
Observation frequency	Evolution of tropospheric ozone burden (radiative forcing); Seasonal cycle and interannual variability; Short-term variability	Daily – weekly	Daily – weekly	Hourly – weekly
Time period	Evolution of tropospheric ozone burden (radiative forcing)	(1980 -)	(1980 -)	(1980 -)
Uncertainty	Evolution of tropospheric ozone burden (radiative forcing)	8 %	8 %	8 %
Uncertainty	Seasonal cycle and interannual variability; Short-term variability	16 %	16 %	8 %
Stability	Evolution of the ozone layer (radiative forcing); trends	1-3 % / decade	1-3 % / decade	1-3 % / decade

Table 3.8 - Data format and metadata requirements for tropospheric ozone profile requirements (adapted from URD v4.1)

Data feature	Requirement
Data format	Net-CDF [RD22]
Data conventions	CF
Data units	Ozone mixing ratio (optional: also in partial ozone column and/or with co-located temperature profile)
Error characteristics	Total accuracy and its subdivision per profile per layer into: - contribution measurement noise; - contribution smoothing error - contribution of A Priori uncertainties;
Number of layers	To be chosen for optimal accuracy (not too few for information content, not too many by degrading the accuracy per layer)
Averaging kernels included?	Yes, per pixel
Full covariance matrix included?	Yes, per pixel
A priori data included?	Yes, per pixel
Flags	Quality per pixel (good, bad, uncertain); Pixel type; Snow/ice; Sun glint; Solar Eclipse; South-Atlantic Anomaly
Visualisation	Basic browsable archive visualisation (profile cross section per orbit; monthly maps at standard pressure levels; local/latitudinal time series of monthly means at standard pressure levels)

3.3 *Information content and sensitivity*

A key aspect in the validation of usability (the verification of “fitness for purpose” of a data product) is the characterisation of the information content of the data product. The retrieval of geophysical quantities from remote sounding measurements usually uses a set of a priori constraints, e.g., in the form of an assumed range of atmospheric profile shape around a first guess. Such constraints mix somehow in the retrieved quantities with the information really contributed by the measurement [RD76]. When a climatology is used in the retrieval, e.g., at altitudes where the measurement is not or less sensitive due to optically thick clouds or due to too low signal-to-noise ratios, it is important to understand what, in the final product, comes from the climatology and what comes really from the measurement. This kind of validation of the information content can rely on a combination of (1) comparisons with independent reference data sets, especially during events not considered in the climatology, (2) the study of deviations of the retrieved product from the a priori constraints, and (3) sensitivity analysis of the retrieval, e.g. based on a study of the associated averaging kernels and their eigenvectors [RD76, RD62, RD49]. E.g., plotting as a function of altitude the sum of the rows of the averaging kernel matrix associated with a retrieval shows at which altitudes the measurement offers sensitivity to atmospheric concentrations. Similarly, the real information content of the reference measurement itself should be known prior to performing a comparison. Information content studies might be an important aspect of the validation of model runs that have been initialised by climatology or by the output of another model, or that are constrained by a priori boundary conditions. They can also be of relevance in the assessment of data assimilation results when observations outside of a predetermined range are rejected as outliers by the data ingestion scheme, producing in the system a zero-information zone like the dead band or neutral zone used in voltage regulators and controllers to avoid unwanted oscillations and disruptions. Information content studies of the Level-2 data are also essential in understanding higher level data products generated by data merging and ensemble approaches.

3.4 *Validation of individual components of ECV processing chain*

ECV line components are the individual processing blocks by which ECV data products are generated in their interim or final version. For complex processing chains international standards require to validate or at least verify the good performance of every component and the accuracy of its output. Limiting validation to the final data product only is not sufficient. The validation of intermediate data products is highly desirable to avoid, e.g., that the apparently good behaviour of the final data product at the end of the chain hides large compensating errors affecting separate components of the data retrieval. Testing is one of many verification activities intended to confirm that software development output meets its input requirements. Other verification activities include various static and dynamic analyses, code and document inspections, walkthroughs, and other techniques. Most of these verification activities have been performed by the EOSTs developing and producing the data products and are reported in the associated Algorithm Theoretical Basis Documents (ATBDs) [RD4].

3.5 *Confrontation with independent reference measurements*

The performance of calibration procedures, retrieval algorithms and data merging systems, and the quality of the resulting ECV products is primarily assessed by comparison with traceable reference measurements supposed to provide the “true” atmospheric state. A key aspect is the appropriate selection of the reference data sets. The quality, traceability and fitness-for-purpose of the latter are essential to allow proper, unbiased and independent validation. Reference measurements must be well documented, and procedures must exist to ensure their quality control on the long term, as it is the case, e.g., within international ground-based networks where data acquisition and QA/QC are regulated by protocols.

Ground-based reference measurements of the total column and vertical distribution of atmospheric ozone are performed by networks of instruments contributing to WMO’s Global Atmosphere Watch (GAW) [RD24]. In the Ozone_cci+ project, ground-based data sets suitable for the validation of ECV products are collected from complementary instruments archiving routinely their data to the World Ozone and Ultraviolet Radiation Data Centre (WOUDC) and the Data Host Facility (DHF) of the Network for the Detection of Atmospheric Composition Change (NDACC). Details including data acquisition protocols, data quality estimates and data access conditions, are available on the web portals of the data archives (http://woudc.org and http://ndacc.org, respectively) and summarised in the Data Access Requirement Document (DARD) [RD8]. Additionally, satellite data sets of documented quality are also used to extend ground-based validation results to a more global coverage and identify features that cannot be detected by a network like, e.g., geographical patterns.

3.5.1 Total ozone column validation data sources

As described in DARD [RD8], the following measurement data sets are used hereafter as reference for validation studies and/or for cross-comparison studies of the total ozone column data products:

- Ground-based total ozone column (TOC) measurements by Dobson and Brewer ultraviolet spectrophotometers.

3.5.1.1 Brewer and Dobson total ozone measurements

The ground-based measurements database used for this validation report consists of archived Brewer and Dobson total ozone data that are downloaded from the World Ozone and Ultraviolet Radiation Data Centre (http://www.woudc.org). WOUDC is one of the World Data Centres which are part of the Global Atmosphere Watch (GAW) program of the World Meteorological Organization (WMO). These data are quality controlled, first by each station before submission and secondly by WOUDC. Brewer and Dobson ultraviolet spectrophotometers rely on the method of differential absorption in the Huggins band where ozone exhibits

strong absorption features in the ultraviolet part of the solar spectrum. This technique has been described in detail by the main reference papers [RD52] and references therein.

The Dobson spectrophotometer is a manually controlled two-beam instrument that measures TOC values with a total uncertainty of 2 – 3 % for solar zenith angles smaller than 75°. For Sun elevations higher than 15°, a well maintained and calibrated Dobson spectrophotometer measures the ozone column with an estimated total uncertainty better than 1 % for cloudless direct Sun observations. Since the International Geophysical Year in 1957, Dobson instruments have been deployed in a worldwide network. Figure 3.1 displays the geographical distribution of Dobson stations used in this study. It is known that Dobson measurements suffer from a temperature dependence of the ozone absorption coefficients used in the retrievals which might account for a seasonal variation in the error of ±0.9 % in the middle latitudes and ±1.7 % in the Arctic, and for systematic errors of up to 4 % (Bernhard et al., 2005, [RD29]).

The Brewer grating spectrophotometer is in principle similar to the Dobson. However, it has an improved optical design and is fully automated. The ozone column abundance is determined from a combination of five wavelengths between 306 nm and 320 nm. Since the 1980s, Brewer instruments are part of the ground-based network as well. Figure 3.2 displays the geographical distribution of Brewer stations used in this study. Most Brewers are single monochromators, but a small number of systems are double monochromators with improved stray light performance. Most of the Brewer instruments providing data to the WOUDC repository are operated at Northern Hemisphere stations. There are a few instruments of this type in the Southern Hemisphere, but they are not considered in this study because of their limited spatial representativeness. The uncertainty on total ozone Direct Sun (DS) measurements by a well-maintained Brewer instrument is about 1 % (e.g., [RD52]). When Brewer spectrophotometers are regularly calibrated and maintained, the DS TOC records can potentially maintain a precision of 1 % over long-time intervals [RD98].

Despite similar performance, small differences within ±0.6 % on an average are introduced between the Brewer and Dobson data because of the use of different wavelengths and different temperature dependence for the ozone absorption coefficients [RD85]. The seasonal cycle in atmospheric temperature results in a seasonal variation of the Dobson ozone data, where the contribution of the systematic offset is less than 1 % [RD93]. Dobson and Brewer instruments might also suffer from long-term drift associated with calibration changes. Additional problems arise at solar elevations lower than 15°, for which diffuse and direct radiation contributions can be of the same order of magnitude. Therefore, we do not rely on validation results that utilize limit the use of measurements by Dobson and Brewer ultraviolet spectrophotometers measurements that are, to data acquired for SZAs > up to 80° SZA for Brewers MK-III and MK-IV (double monochromators), and above up to 70-75° of SZA for Dobsons and other Brewers (single monochromators).

The Brewer and Dobson fiducial measurements retrieved from the WOUDC database are daily means (and thus there is no temporal treatment of the satellite observations), cover all latitudes from Antarctica to the Arctic and have been used as ground-truth in many recent validation studies (e.g. for GOME, GOME-2, SBUV, OMI and TROPOMI/S5P and GEMS).

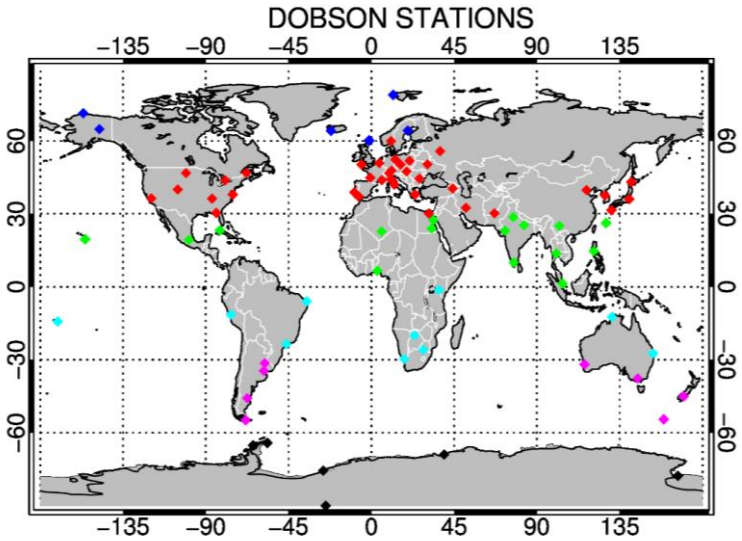

Figure 3.1 - Geographical distribution of Dobson network stations used in this study, colour-coded per latitude band; 90-60°S in black, 60-30°S in purple, 30°S – 0 in cyan, 0-30° N in green, 30-60° N in red and 60-90° N in blue.

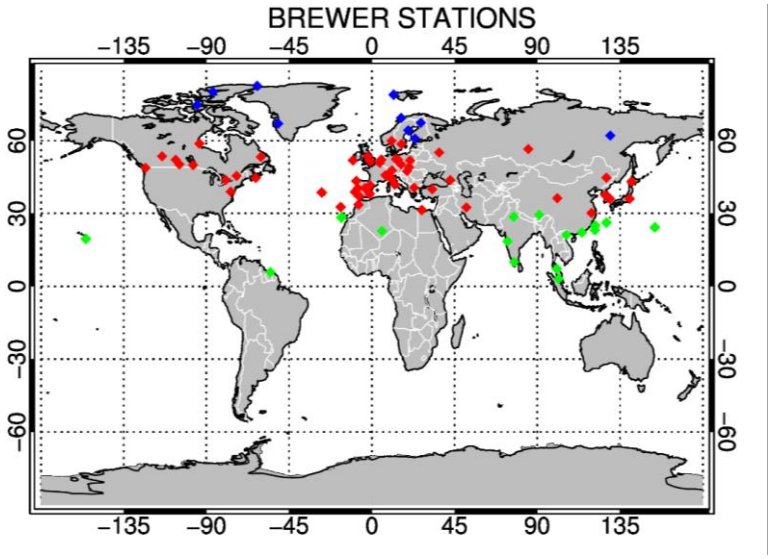

Figure 3.2 - Geographical distribution of Brewer network stations used in this study, colour-coded per latitude band; 0-30° in green, 30-60° in red and 60-90° in blue.

3.5.2 Nadir ozone profile validation data sources

As described in DARD [RD8], the following measurement data sets are used as reference for validation studies and/or for cross-comparison studies of the nadir ozone profile data products:

- Ground-based ozone profile measurements by balloon-borne electrochemical ozonesondes.
- Ground-based ozone profile measurements by stratospheric ozone lidars.

3.5.2.1 Ozonesonde measurements

In-situ measurements of ozone are carried out regularly by ozonesondes on-board small meteorological balloons launched at numerous sites around the world. They measure the vertical profile of ozone partial pressure with 100 to 150 meter vertical resolution from the ground to the burst point of the balloon, usually between 30 and 35 km. An interfaced radiosonde provides the pressure, temperature and GPS data

necessary to geolocate each measurement or to convert the ozone partial pressure to other units. Normalisation factors, if provided, are not applied. Different types of ozonesondes were developed over the years. Those still in use today are based on the electrochemical reaction of ozone with a potassium-iodide sensing solution. Laboratory tests and field campaigns indicate that between the tropopause and about 28 km altitude all sonde types produce consistent results when the standard operating procedures are followed [RD82]. The bias is smaller than ±5 % and the precision is about 3 %. Above 28 km the bias increases for all sonde types. Below the tropopause, due to lower ozone concentrations, the precision degrades slightly from 3 to 5 %, depending on the sonde type. The tropospheric bias also becomes larger, between ±5 to ±7 %. Other factors besides ozonesonde type influence the data quality as well. A detailed overview can be found in [RD82]. The present work relies on the ozonesonde data archived by the Network for the Detection of Atmospheric Composition Change (NDACC), Southern Hemisphere Additional Ozonesonde network (SHADOZ; [RD87], [RD88]) and WMO's Global Atmospheric Watch (GAW). Together these three data sources cover 82.5° N to 90.0° S and provide soundings at least once a week at many participating stations. Stations contributing to the present study are highlighted in Figure 3.3.

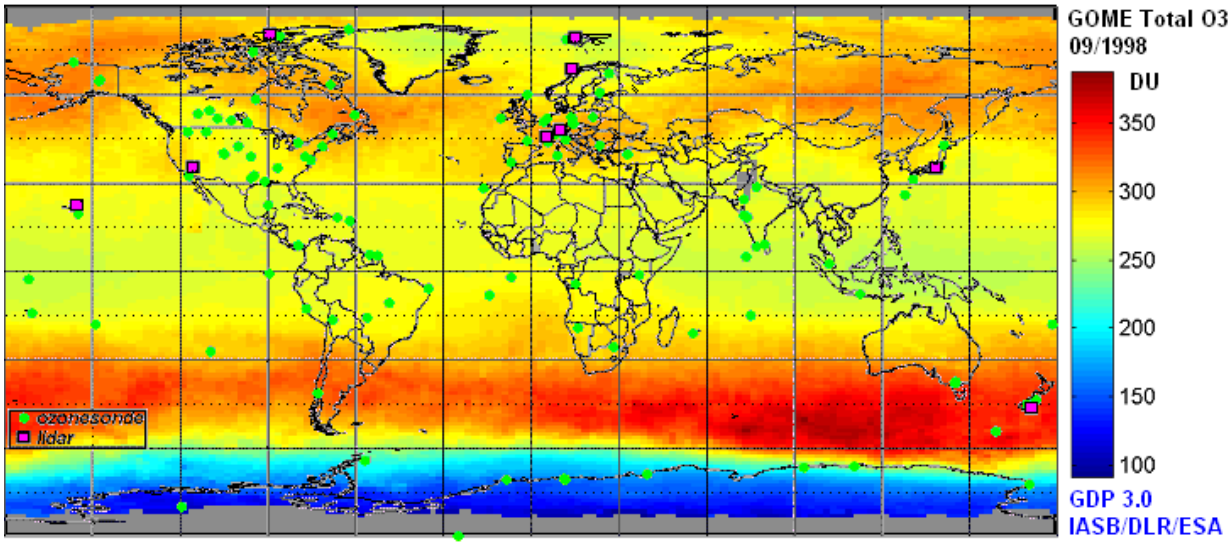

Figure 3.3 - Geographical distribution of ground-based NDACC lidar and GAW ozonesonde stations having archived regularly ozone profile data to the NDACC DHF, SHADOZ archive and/or the WOUDC during the Envisat era, displayed on top of a total ozone map typical of September.

3.5.2.2 Lidar measurements

A differential absorption lidar (DIAL) operates mostly during clear-sky nights, simultaneously emitting two pulsed laser beams at wavelengths with a different ozone absorption cross-section. The backscattered signal is integrated over a few hours to retrieve the vertical distribution of ozone [RD70]. A stratospheric ozone lidar system emits beams at 308 nm and 353 to 355 nm, which makes it sensitive from the tropopause up to about 45 to 50 km altitude with a vertical resolution that declines with altitude from 0.3 to 3 km. The profiles are reported as ozone number densities versus geometric altitude. The DIAL technique is in principle self-calibrating since the ozone profile is retrieved directly from the returned signals without introducing instrumental constants. However, interference by aerosols, signal induced noise and saturation of the data acquisition system can degrade the quality of the measurements. Unreliable measurements can be discarded based on the reported precision, which were shown to be realistic [RD42]. The bias and precision are about ±2 % between 20 to 35 km, increasing to ±5 to ±10 % outside this altitude range where the signal-to-noise ratio is smaller [RD48]. The consistency between six ozone lidars in the NDACC network was recently studied using various satellite data sets [RD72]. This study concluded that the different lidar records agree within ±5 % of the space-based observations over the range of 20 to 40 km. Data from all stratospheric ozone lidars

that have been operational in the NDACC network since the beginning of the 1990s and cover year 2008 are considered. The network covers 80.0° N to 67° S, but most sites are located in the northern hemisphere. Lidar stations contributing to the present study are highlighted in Figure 3.3.

3.5.3 Limb ozone profile validation data sources

The following measurement data sets are used as reference for validation studies and/or for cross-comparison studies of the limb ozone profile data products:

- Ground-based ozone profile measurements by balloon-borne electrochemical ozonesondes.
- Ground-based ozone profile measurements by stratospheric ozone lidars.
- Ground-based ozone profile measurements by ozone microwave radiometers.

3.5.3.1 Ozonesonde measurements

Details of the ozonesonde measurement technique, associated uncertainties and contributing stations are given in Section 3.5.2.1.

3.5.3.2 Lidar measurements

Details of the lidar measurement technique, associated uncertainties and contributing stations are given in Section 3.5.2.2.

3.5.3.3 Microwave radiometer measurements

Microwave radiometers (MWR) record the emission of a thermally excited rotational transition at 110 or 142 GHz. Observations are integrated over 1-4 hours, and they are carried out continuously during day and night, irrespective of cloud conditions or aerosol load. Vertical profiles of ozone VMR are retrieved on fixed pressure levels between 20-25 and 70 km from the pressure broadening of the integrated line spectra. Ozone VMR can be converted a posteriori into number density using meteorological (re)analyses of pressure and temperature. The total uncertainty of ozone retrievals is estimated at less than 10-15 % between 25-50 km and increases to 25 % at the profile top and bottom. When compared to ozonesonde and lidar the vertical resolution of MWR is much poorer, about 8-10km in the stratosphere up to 15 km in the mesosphere. On the other hand, the number of measurements is superior, so the co-location criteria can be stricter to reduce uncertainties in the comparison results due to spatiotemporal mismatch. We consider the MWR ozone profile data uploaded to NDACC data host facility by several stations: in Bern (47.0°N, 7.4°E), Payerne (46.8°N, 7.0°E), Mauna Loa (19.5°N, 155.6°W) and Lauder (45.0°S, 169.7°W).

3.5.4 Tropospheric ozone validation data sources

The following measurement data sets are used as reference for validation studies and/or for cross-comparison studies of the limb ozone profile data products:

- Ground-based ozone profile measurements by balloon-borne electrochemical ozonesondes.

3.5.4.1 Ozonesonde measurements

Details of the ozonesonde measurement technique, associated uncertainties and contributing stations are given in Section 3.5.2.1.

3.5.5 Error budget of the comparison of atmospheric data

A major objective of quantitative comparisons with reference measurements and modelling results of documented quality is to estimate uncertainties of the validated data product and to check the accuracy of its theoretical uncertainty estimates. However, in fact the systematic and random discrepancies between the validated data set and the validation data set combine uncertainties associated with each individual system,

plus uncertainties associated with the selection of data and the methodology of comparison [RD62]. Discrepancies include the effect of the following comparison uncertainties:

(1) Comparison uncertainties associated with the difference in sampling of atmospheric variability and structures: e.g., geographical mismatch, diurnal cycle effects in the upper stratosphere and mesosphere (USM), assumptions related to the area of representativeness.
(2) Comparison uncertainties associated with the difference in smoothing of atmospheric variability and structures: e.g., balloon-based in situ measurement at about 150 m vertical resolution by an electrochemical cell, compared with GOME ground pixels of 40 x 320 km^2 and vertical resolution of 3-8 km.

As far as possible, most comparison uncertainties will be reduced by a cautious design of the selection of data sets to be compared, and by considering that a multivariate analysis of the comparison results taking into account the specifics of the data being compared (modelling data or remote sensing data, atmospheric variability and gradients etc.) might be required and preferred over entirely statistical approaches. For traceability purposes it is essential to document for each validation exercise the selection method applied to the data sets (temporal and spatial co-location criteria, how differences in vertical and horizontal smoothing are handled etc.).

Although essential if a rigorous metrological approach is to be adopted, the derivation of a complete error budget for each comparison is still a matter of research at the time being and it falls partly beyond the scope of the Ozone_cci+ project. In Appendix to this document, a proof-of-concept is elaborated in which the agreement between satellite (S5P) and ground-based reference measurements of the total column of ozone is quantified in terms of their combined ex-ante error budgets. While agreement within the ex-ante uncertainties is found for this case, this cannot be assumed to hold also for products where the comparison method is more complex and introduces significant additional error sources, e.g. in the case of vertical profiles derived from nadir measurements. Validation teams as well as EOSTs are aware that neglecting uncertainties linked to the comparison method can spoil the value of the comparison and yield erroneous conclusions on the quality of the compared data product. With this disclaimer an awareness is transmitted to the reader of Ozone_cci+ Validation Reports for proper use of the validation results and, if fine, of the CCI ozone CRDP.

4 Validation of Nadir Ozone Profile Data Products

4.1 *Nadir ozone profile CRDP*

The ESA Ozone_cci+ Climate Research Data Package (CRDP) contains ten nadir ozone profile (NP) products. Table 4.9 lists these products, together with their time range and current availability. All Level-2 (L2) UV-VIS instrument retrievals are performed by the Rutherford Appleton Laboratory (RAL) algorithm, while the thermal infrared measurements of the IASI instruments are processed by a collaboration between the Belgian ULB (Université Libre de Bruxelles) and the French LATMOS, using their FORLI (Fast Optimal Retrievals on Layers for IASI) algorithm. A merged Level-3 (L3) product has been created from the three IASI instruments as well. Finally, DLR (Deutsche Luft- und Raumfahrt) has developed a L3 spatiotemporally gridded product from RAL's UV-VIS instrument retrievals combined (GOP-ECV).

This Ozone_cci+ PVIR focuses on the validation of the derived L3 GOP-ECV product, and on the updated (v20151001 CDR, called v2024, and v20191122 for the merged L3 product) FORLI products. The validation targets for this PVIR are therefore [RD2]:

- Validation of the L2 and L3 vertically integrated nadir ozone profiles (IASI and GOP-ECV only).
- Validation of the L2 and L3 nadir ozone profiles updated and new retrieval products.
- Comparison of RAL retrievals from GOME-2C for the L2 versions 3.00 and 4.01.
- Comparison of FORLI-O3 CDR retrievals to confirm consistency between the three IASI/Metop instruments.
- Drift assessments and consistency checks for all products.

4.2 *Validation of integrated nadir ozone data products*

The Ozone_cci+ phase 2 datasets include Level-2 and Level-3 integrated ozone profiles acquired by the IASI-Metop-A, -Metop-B and Metop-C sensors, as well as the integrated GOP-ECV ozone profiles. This section starts with the detailed validation results of the Level-2 IASI datasets (Section 4.2.1), and continues with the validation of the Level-3 merged IASI dataset (Section 4.2.2). Finally, in Section 4.2.3. the GOP-ECV integrated ozone profiles are validated.

While the objectives of the Level-2 validation are classical (determination of the systematic bias, dependences on SZA, etc.), the purpose of the Level-3 validation studies is to demonstrate that compared to reference ground-based measurements, no spurious features appear, as well as that they are temporally stable, suitable for long-term studies of the ozone layer evolution.

4.2.1 IASI-A, IASI-B and IASI-C CDR Level-2 integrated total ozone

In this section, integrated total ozone observations performed by the IASI instruments on board the Metop-A, Metop-B and Metop-C satellites (hereafter IASI-A, IASI-B and IASI-C), are validated against ground-based measurements. The current IASI ozone retrieval algorithm is the FORLI-O3 (Fast Optimal/Operational Retrieval on Layers for IASI) v20151001, which was validated by Boynard et al. (2018) [RD32].

The new, homogeneous IASI data use the Level1C dataset produced by EUMETSAT and utilize the EUMETSAT-CDR temperature and humidity profiles. The retrievals are available for 3.5 in 10 pixels and for all days per month. For reasons of consistency with previous validation works of the IASI datasets, a maximum co-location search radius up to 50 km was set. Note that only pixels with a cloud fraction equal to or lower than 13 % are processed by the algorithm. **Table 4.1** shows the time span of the available Level-2 datasets, as well as their source of their provision for the purposes of this validation work.

To ensure the good quality for the observations, the provided data were filtered by the following criteria:

- "retrieval_quality_flag" ≥ 1, as pixels with the value of 0 are recommended to not be used
- "O3_total_degrees_of_freedom" ≥ 2, as it was suggested by the algorithm team.

To limit the noise in the validation results and for reasons of consistency with previous validation studies of the IASI total ozone processed with FORLI v20151001 performed in the previous phase of the project, the O_3 error was restricted to values equal or lower to 0.02. As a result, less than 2 % of the co-locations to ground-based total ozone measurements were excluded, mainly attributed to measurements with high solar zenith angles. It should be noted that the application of this restriction for the ozone error leads to the elimination of all co-locations below 80°S for IASI-B and IASI-C, which are characterized by extremely high mean biases spanning 30-40 % with respect to ground-based measurements. IASI-A is also limited in co-locations close to South Pole, and its mean relative bias decreases (~24 %), but its dataset is not completely discarded (see **Figure 4.4**). Therefore, it was decided to use the latitudinal threshold of 80°S as a filter to avoid increasing the noise of our comparisons.

To prepare the ground-based data set, we have investigated the quality of the total ozone values of each station and instrument that deposited data at WOUDC. The selection methodology and associated criteria have been discussed in detail in [RD60, RD28, RD61, RD43 and RD44]. We offer a summary for completeness. For each ground-based station a series of statistics and plots are investigated. For the Level 2 products, daily coincidences of the satellite pixel's central latitude and longitude falling within the 50 km radius of the ground station are identified and used for the creation of monthly, seasonal and yearly time series and scatter plots. The percentage of the relative differences between ground and satellite TOC is used as the comparative tool for the validation. The statistics are then typically performed on a zonal average, on a hemispheric average and on a global average, always keeping the two types of ground-based instruments separate and using only direct sun observations, as they are deemed to be the most reliable.

In the following sections, the relative percentage differences between the co-located satellite and ground-based total ozone observations will be investigated in terms of systematic bias and stability. The temporal and geographical variation of the bias will be studied, as well as its dependence on various influence quantities.

Table 4.1: The time span of the available Level-2 IASI datasets.

Sensor	Algorithm	Time span	Dataset Source
IASI-A	Forli v2015 EUMETSAT CDR	1/1/2008– 31/12/2019	From IASI-ULB, via personal communication
IASI-B		1/11/2019 – 31/12/2023	(1) up to 12/2022: From IASI-ULB, via personal communication (2) 2023: via the Aeris portal
IASI-C		4/12/2019 – 31/12/2023	Aeris portal

4.2.1.1 Systematic bias and its variations

In **Figure 4.1**, the histograms (left column of plots) and scatter plots (right column) of the comparisons between the IASI instruments and the co-located Brewer ground-based total ozone measurements, representing the Northern Hemisphere (NH) only, are shown. The respective Dobson comparisons are not shown herein for reasons of brevity. The statistics of the analysis with respect to both Brewer and Dobson ground-based instruments are summarized in **Table 4.2**.

The histograms of the three sensors show normal distributions of the relative percentage differences around the mean bias, which ranges between 0 and +1.3 % for the Brewer co-locations. The respective Dobson

comparisons, which cover both hemispheres, are very similar. The mean relative bias with respect to Dobsons is +1.6 % for IASI-A and ~+0.4 % for IASI-B and IASI-C. The main result thus far is that **IASI-A reports higher TOCs than the ground-based networks by ~+1.5 % for the period of the available dataset**. **IASI-B and IASI-C are in excellent agreement to the reference measurements during the almost four years of observations covered herein**. The higher standard deviation of the Dobson comparisons is due to the contribution of the Southern Hemisphere (SH) co-locations, which are fewer in number.

The scatter plots show that the Pearson correlation coefficient between satellite measurements and the ground-based observations is higher than 0.9, and the slope of the linear regression is very close or even equal to unity.

To examine the temporal stability of the three satellite sensors' validation results, the hemispherical monthly mean time series of their relative percentage differences, seen in **Figure 4.2**, are exploited. Panels a and c show the comparisons to Dobson measurements (panel a: NH; panel c: SH), while panel b shows the Brewer comparisons for the NH only. The three sensors have a very good consistency, and no obvious step-function appears due to the transition from the IASI-A record and the start of the IASI-B and IASI-C datasets, in 2019. From the beginning of the IASI-A record until mid-2018, the NH and SH co-locations of **Figure 4.2** for both types of ground-based instruments, are temporally quite stable and have a mean relative bias of +1.0 ± 0.9 %[1]. Since the summer of 2018, a decrease of ~1 % in its bias occurs for both hemispheres and with respect to both types of instruments. The lower mean relative bias of IASI-A, now in the level of -0.5 ± 0.7 %, continues similarly for the IASI-B and IASI-C time series. These statistics refer to Brewer co-locations (panel b), which have a negligible seasonal cycle as reference measurements. The respective Dobson biases are of the same magnitude but have a higher standard deviation due to the seasonal features of the reference measurements. A further decrease in the mean bias of IASI-B and IASI-C is seen in mid-2022 for the Brewer co-locations, but this cannot be verified by the Dobson comparisons, therefore it could be a feature of the ground-based measurements.

[1] The statistics printed on the plots of **Figure 4.2** refer to the full IASI-A time series.

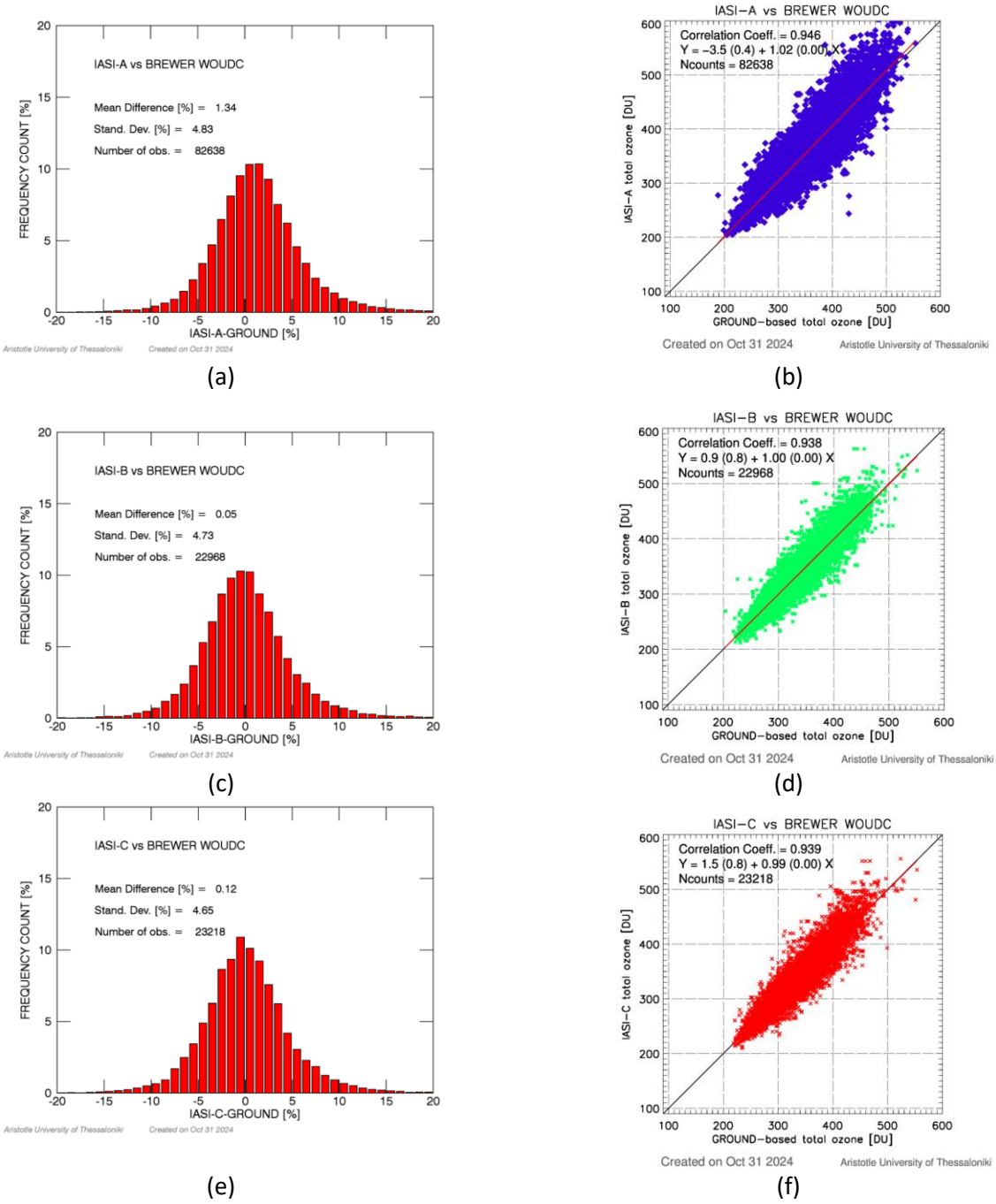

Figure 4.1 - The histograms (left) and scatter plots (right) of the comparisons between the three IASI instruments (IASI-A in panels a & b; IASI-B in panels c & d; IASI-C in panels e & f) and the co-located Brewer ground-based total ozone measurements, representing the NH only.

Table 4.2 - The overall statistics that result from the co-locations of the three satellite sensors to the Brewer (NH only) and Dobson ground-based observations.

		IASI-A	IASI-B	IASI-C
Mean rel. bias (%)	Dobson	+1.6	+0.3	+0.4
	Brewer	+1.3	+0.1	+0.1
St. Deviation (%)	Dobson	5.4	5.9	5.8
	Brewer	4.8	4.7	4.7
R^2	Dobson	0.932	0.905	0.905
	Brewer	0.946	0.938	0.939
Slope	Dobson	1.00	0.95	0.95
	Brewer	1.02	1.00	0.99
Annual cycle (% p-t-p)	Brewer	1.7	1.4	1.4

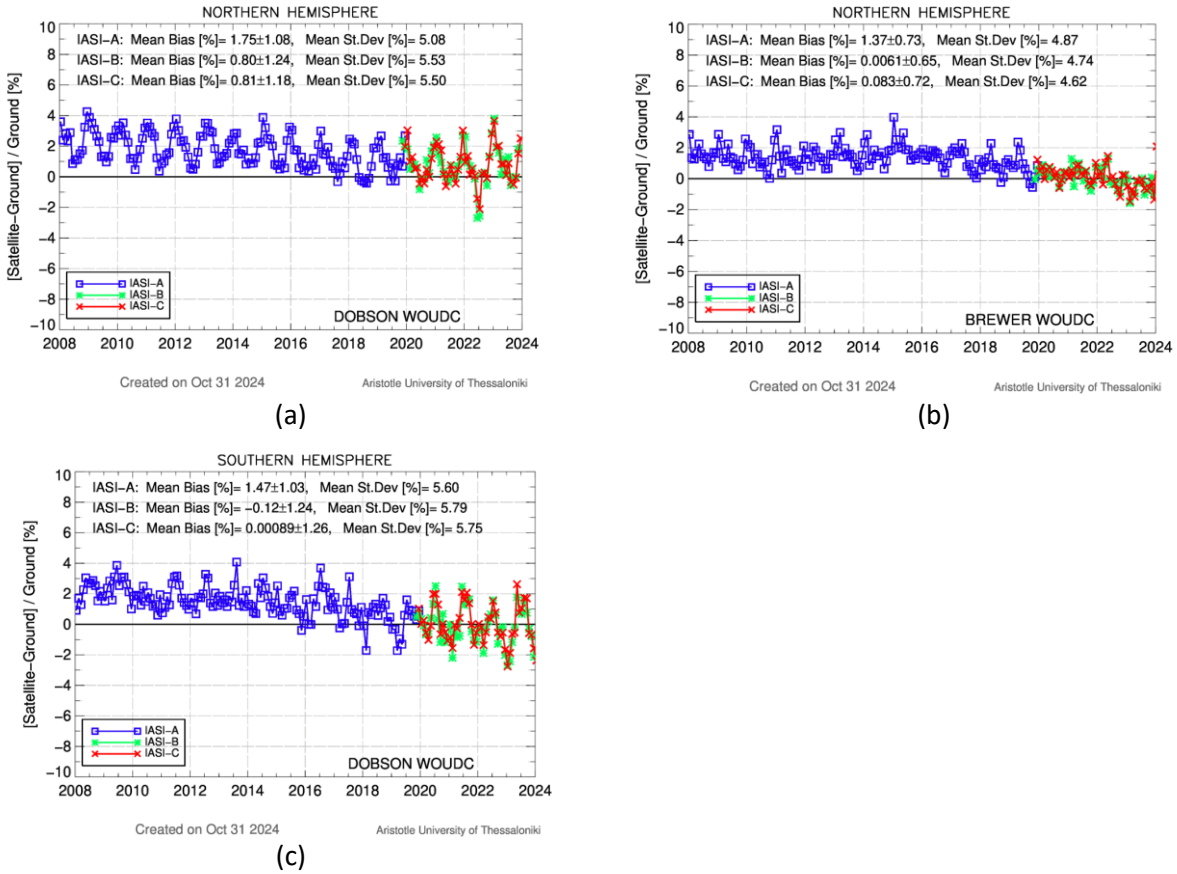

Figure 4.2 - The monthly mean time series of the relative percentage differences between IASI-A (blue), IASI-B (green) and IASI-C (red) and ground-based observations (panels a & c: Dobson, NH and SH, respectively; panel b: Brewer, NH).

The overall **drift of the IASI-A integrated ozone relative to the ground-based measurements is -0.8 %/decade**, resulting from the 12-years available dataset. The respective calculation of the IASI-B and IASI-C drifts is not meaningful due to the temporally short dataset of just 4 years.

In **Figure 4.3**, the mean annual cycle of the percentage differences between the three sensors and the Brewer total ozone measurements is shown. In terms of seasonality, only the Brewer comparisons are studied, due to the well-known dependency of the Dobson observations on effective temperature. The IASI-A comparisons have a higher bias from December until May with a maximum of ~ +2.2 ± 6.4 % in January, and a minimum of +0.5 ± 4.2 % in October with respect to ground-truth. The overall peak-to-peak annual cycle of the comparisons is ~ 1.7 %. IASI-B and -C appear to have a similar seasonal behaviour, with a maximum bias of +0.8 ± 4.8 % in May and a minimum of -0.6 ± 3.9 % in September or October, thus their annual cycle is also 1.4 %. The mean relative biases and the seasonal cycles of each satellite sensor are summarized in **Table 4.2**.

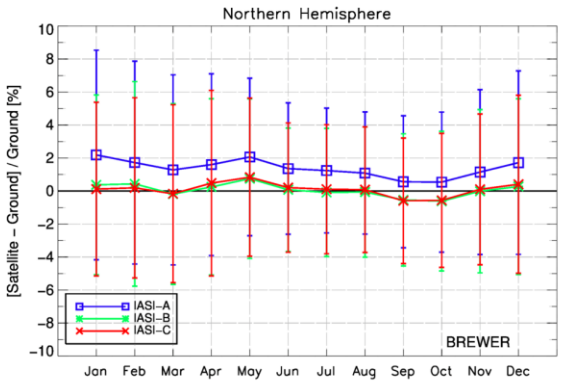

Figure 4.3: The seasonal dependence of the three IASI sensors with respect to co-located NH ground-based Brewer total ozone measurements.

In **Figure 4.4** and **Figure 4.5**, the percentage differences of the co-locations are averaged in 10° latitude bins using each ground-based station's latitude as reference and plotted as a pole-to-pole graph for the Dobson and the Brewer stations. The only difference between the two Dobson figures (**Figure 4.4** and **Figure 4.5**, left panel) is the y-axis scale, which in **Figure 4.4** is extended to +40 % so as to show the extremely high biases of the SH Dobson co-locations southwards 80° for IASI-A. As mentioned above, this was the reason for the use of the 80°S latitude threshold in this study.

A latitudinal dependency of the co-locations is seen for both ground-based networks (**Figure 4.5**). In the NH up to 60°N, the low biases show a very good agreement between the three sensors and the ground-reference, Brewer and Dobson. Northwards 60° the comparisons increase for the three satellite sensors, up to +2.5 % for IASI-B and -C and +5.3 % for IASI-A. The SH belts have similar features, with low biases up to 40° S which increase up to +5 % southwards. It should be noted that the temporal coverage of the IASI-A co-locations is different than the other two sensors, resulting in higher overall biases in all latitude belts. A very interesting feature shown in both panels is the increased bias for latitude belts that contain desert stations. For example, the comparisons within the latitude bin 20°-30° have a higher mean relative bias, +2.5 %, due to the contribution of the Tamanrasset station, in Algeria, located in the desert at an altitude of 1400 m. The mean relative bias of the IASI sensors with respect to the Brewer and the Dobson measurements of Tamanrasset is +9.6 ± 4.2 %. It is worth noting that the same station, when compared to other satellite sensors, e.g. OMI GODFIT v4 and GOME-2, has a lower mean bias of +1 to +2 %.

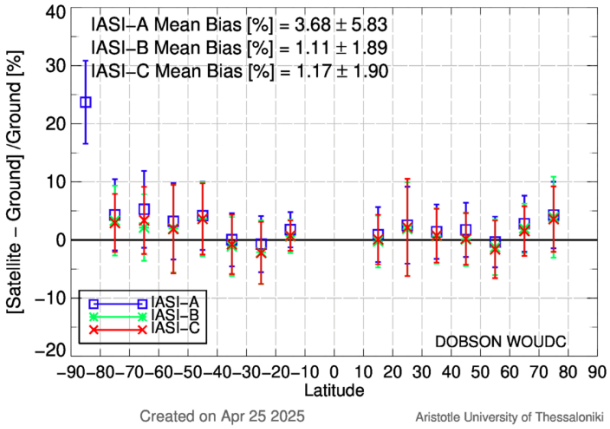

Figure 4.4 - The latitudinal dependence of the relative percentage differences between IASI-A, IASI-B and IASI-C and the Dobson ground-based observations, averaged in 10° latitude bins. No latitudinal filter has been applied for the Southern Hemisphere co-locations.

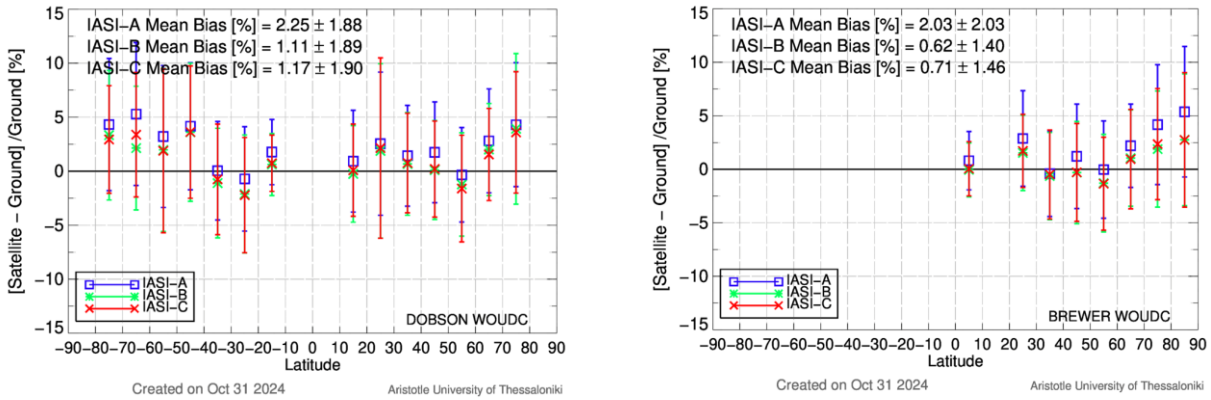

Figure 4.5: The latitudinal dependency of the percentage differences between the three IASI sensors and ground-based observations (left panel: Dobson; right panel: Brewer), averaged in 10° latitude bins. The left panel is identical to **Figure 4.4**, but the threshold of 80°S is now applied to the co-locations.

4.2.1.2 Dependency on various parameters of the retrieval algorithm

The influence of various parameters that affect the satellite integrated ozone profiles retrievals is also investigated, by plotting the percentage differences of the co-locations with respect to the parameter in question (**Figure 4.6**). Only comparisons to Brewer total ozone observations are shown herein, because their number of co-locations to the IASI sensors is higher than those against the Dobson network. Nevertheless, the Dobson results do not differ significantly from those shown here.

- **Solar Zenith Angle (SZA)**
  The dependency of the percentage differences of the three IASI sensors and Brewer total ozone measurements on SZA is shown in panel a:
  - IASI-A has a minor dependency on SZA, with a maximum of +2.5 % for 20°≤ SZAs ≤ 30° and SZAs>70°. For moderate SZAs, between 40° and 60°, the bias is slightly lower, +1.5 %.
  - IASI-B and IASI-C, studied for a different temporal range, have a higher dependency on SZA, with negligible biases for SZAs between 40° and 60° and equally high biases up to +3 % (as for IASI-A) for low SZAs below 30°.
- **Pixel of the scan**

Panel b shows that there is no dependence of the satellite and ground-based measurements comparisons on the satellite pixel.

- **Ozone profiles Degrees of Freedom (DOF)**

  Panel c shows the dependence of the percentage differences on the Degrees of Freedom of the signal, which is a quality flag for the data under investigation. As mentioned above, only data with DOF ≥2 are processed to avoid bad quality observations. The dependence of the co-locations on the DOF shows that for values below 2.8 the corresponding data points, which result from a very low number of co-locations, introduce high differences, up to +12 %. We suggest that these data could be excluded to limit the noise in the observations.

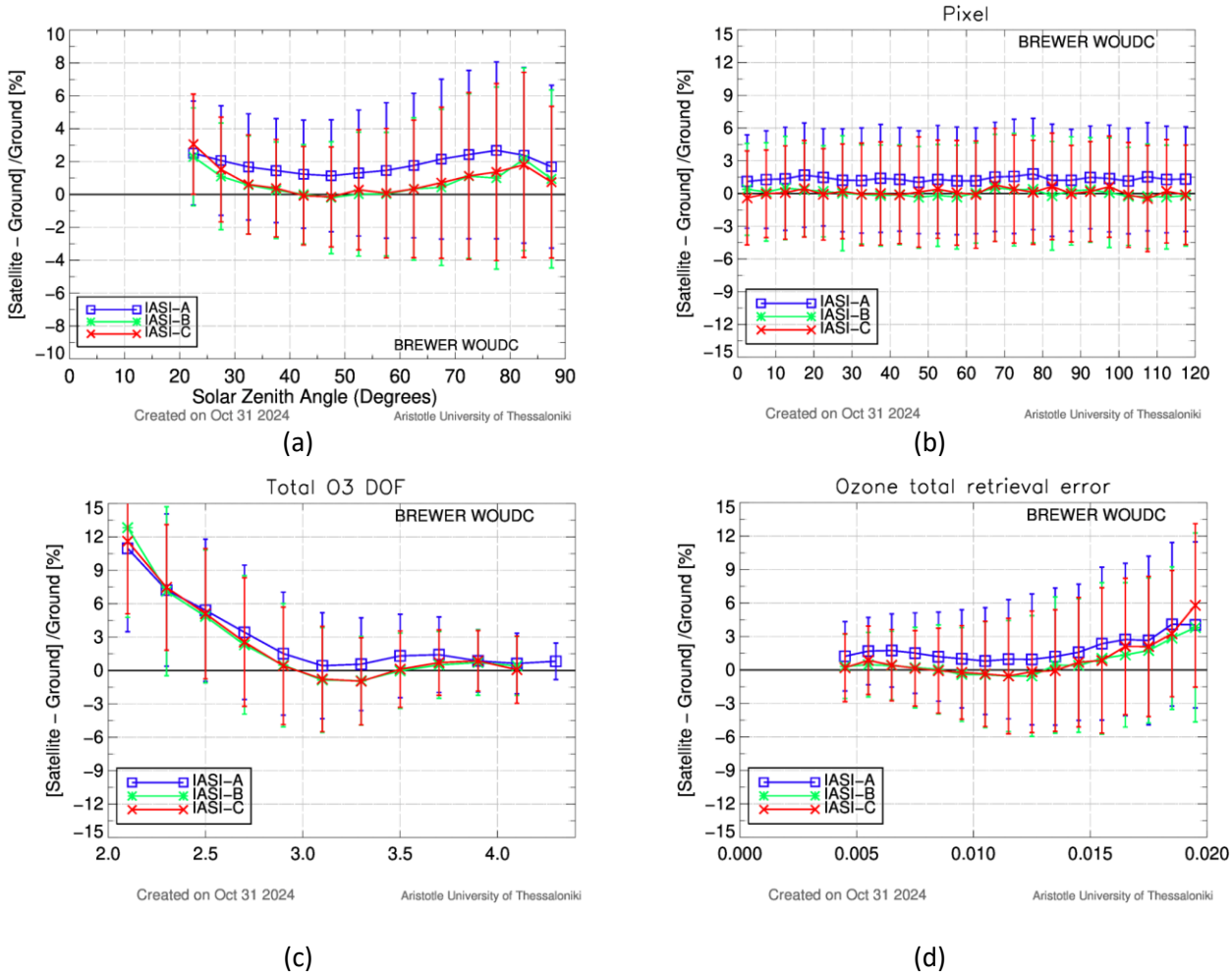

Figure 4.6 – The dependence of the relative percentage differences between the three IASI sensors and Brewer ground-based total ozone observations, on various influence parameters, such as solar zenith angle (a), pixel number of the sensor (b), the number of degrees of freedom (c) and the ozone retrieval error (d).

- **Ozone retrieval error**

  Panel d shows that the integrated ozone profiles comparisons from the three sensors have a very similar dependency on the errors of the retrievals: for errors up to 0.015 there is no dependency, but when the error increases up to 0.02 the biases increase up to +4 % for IASI-A and -B and +6 % for IASI-C. From a sensitivity test that was performed, it was seen that the dependency on the ozone error diminishes when data with DOFs < 3 are dismissed.

4.2.1.3 Summary and compliance with user requirements

The CDR integrated ozone profiles retrieved from IASI-A, IASI-B and IASI-C with the FORLI-O3 v20151001 algorithm based on the EUMETSAT Level1C dataset and the EUMETSAT-CDR temperature and humidity profiles, were validated against Brewer and Dobson ground-based measurements. The time span of the IASI observations is 12 years for IASI-A and 4 years for IASI-B and IASI-C. The validation results that are displayed in **Table 4.2** can be summarized as the follows:

- the **mean relative bias** between satellite and Brewer and Dobson reported TOCs is ~ +1.5 % for IASI-A and ~ +0.2 % for IASI-B and IASI-C, showing that IASI-A reports higher TOCs than the ground-based measurements of both networks,
- the **Pearson correlation coefficient** is above 0.9 for all sets of comparisons, therefore the agreement between the satellite and the ground-based data is very good,
- the peak-to-peak **annual cycle** of the relative differences with respect to Brewer observations are within 1.4 - 1.7 %, and
- the **temporal change** of IASI-A, which is the only dataset with a record long enough to be evaluated in this view, is -0.8 %/decade.

According to **Table 3.1**, the requirements that have to be met by the retrieved integrated ozone profiles from the three IASI sensors correspond to the stability of the TOC measurements, which must be in the range of 1 to 3 % per decade, the radiative forcing introduced by the evolution of the ozone layer that has to be less than 2 % and the short-term variability that must be less than 3 %. The level of compliance of the IASI datasets with these user requirements is shown in **Table 4.3** - **Table 4.5** and is highlighted with the following colour code:

- green indicates ascertained compliance with all users' requirements;
- yellow indicates compliance with some users' requirements but not all; and
- red indicates compliance with none of the user requirements.

Overall, the validation analysis of the IASI-A, IASI-B and IASI-C integrated ozone showed that the IASI CDR Level-2 records are compliant with the requirements in terms of stability and uncertainty. Therefore, we conclude that the studied datasets are of very good quality and temporal stability, suitable and useful for long term analysis of the ozone layer, such as decadal trend studies, the evaluation of model simulations, and data assimilation applications.

Table 4.3 - Compliance of IASI Metop-A integrated ozone profiles with user requirements (URD v3.1)

Topic	Requirement	Compliance / evaluation
Horizontal resolution	< 20-100 km	50 km along track
		50 km across track
Observation frequency	Daily – weekly	Twice a day
Time period	1980-	01/2008 – 12/2019
Total uncertainty	2 % (radiative forcing studies)	Bias: +1.5 %, Spread: ~5 % (includes the uncertainty of the reference dataset and some co-location mismatch), Seasonality: 1.7 % peak-to-peak
	3 % (Seasonal cycle & Short term variability)	
Stability	1 – 3 %/decade	-0.8 %/decade

Table 4.4 - Compliance of IASI Metop-B integrated ozone profiles with user requirements (URD v3.1)

Topic	Requirement	Compliance / evaluation
Horizontal resolution	< 20-100 km	50 km along track
		50 km across track
Observation frequency	Daily – weekly	Twice a day
Time period	1980-	11/2019 – 12/2023
Total uncertainty	2 % (radiative forcing studies)	Bias: +0.2 %, Spread: ~5 % (includes the uncertainty of the reference dataset and some co-location mismatch), Seasonality: 1.4 %
	3 % (variability studies)	
Stability	1 – 3 %/decade	N/A

Table 4.5 - Compliance of IASI Metop-C integrated ozone profiles with user requirements (URD v3.1)

Topic	Requirement	Compliance / evaluation
Horizontal resolution	< 20-100 km	50 km along track
		50 km across track
Observation frequency	Daily – weekly	Twice a day
Time period	1980-	12/2019 – 12/2023
Total uncertainty	2 % (radiative forcing studies)	Bias: +0.2 %, Spread: ~5 % (includes the uncertainty of the reference dataset and some co-location mismatch), Seasonality: 1.4 %
	3 % (variability studies)	
Stability	1 – 3 %/decade	N/A

4.2.2 IASI merged Level 3 integrated total O3 columns

The IASI merged integrated total ozone product is retrieved utilizing the following datasets for the respective time periods:

- IASI-A: 01/01/2008 – 07/03/2013
- IASI-A & -B: 08/03/2013 – 19/09/2019 and
- IASI-B & -C: 20/09/2019 - now

The retrieval algorithm of the merged IASI product is FORLI-O3 v20191122 and according to the files' metadata, an "*a posteriori filtering based on a combination of quality flags (e.g. neg. altitude, large cloudf, residuals biased or sloped, large RMS, suspect AK, max # of iteration exceeded, low DOFS) is applied*". The 16-year-long dataset consists of files that contain daily means of the merged product in a 1° x 1° grid and were provided to the validation team via personal communication.

For the comparison of the dataset to the ground-based reference measurements from Brewer and Dobson stations, the reported ground-based TOCs were gridded into the same 1° x 1° grid daily, with most grid points being represented by only one reporting station. In detail, direct Sun measurements were considered for the gridding of the ground-based TOCs into Level-3 grid points, even though in some cases this choice severely decreases the number of measurements. To better illustrate the differences between the ground-based and satellite observations, the time series of the daily co-locations were secondly averaged in monthly means and are presented herein. As a compromise between obtaining the highest global coverage possible and the most representative monthly means, especially at high latitudes, a lower limit of 5 daily means per month and per grid box was enforced so that the temporal representativeness errors are minimized.

4.2.2.1 Systematic bias and its variations

Figure 4.7 shows the hemispherical time series of the monthly mean percentage differences between the merged IASI integrated ozone and the ground-based reference total ozone measurements. Panel (a) depicts the Brewer NH comparisons, while panels (b) and (c) show the Dobson NH and SH differences. The NH time-series are stable, with no abrupt changes in their record, except for the Dobson comparisons in July and August 2022 that appear to deviate from the overall stability due to ground-based representativeness issues that can result from changes in the number of stations contributing with available data. In the SH the variability is higher due to the lower number of available stations in the area. The NH and SH curves are always below zero, showing that the **IASI integrated ozone product reports lower values than the ground reference, by about -2 ± 1 % in both hemispheres**. In panel (d) the total ozone time-series of the two datasets are shown in the form of monthly means. Except for the negative relative bias, the ozone variability is very well captured by IASI. The mean variability of the comparisons is ~ 3.5 % for the NH and ~5.2 % for the SH, also including the ground-based datasets' uncertainties.

Figure 4.8 shows the annual cycle of the monthly mean percentage differences between the merged IASI and the Brewer ground-based total ozone, resulting from the 16-year-long record of comparisons. The agreement between IASI and the ground-based reference is better during spring months such as April and May (relative bias ~ -1.5 %), during but their difference increases in September to -2.5 %, therefore **the peak-to-peak seasonality of the comparisons is ~1 %**.

(a)

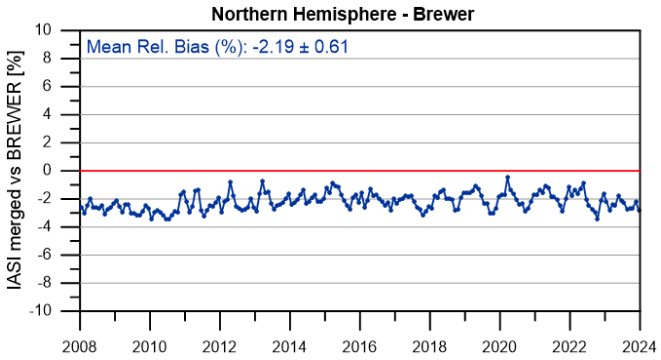

(b)

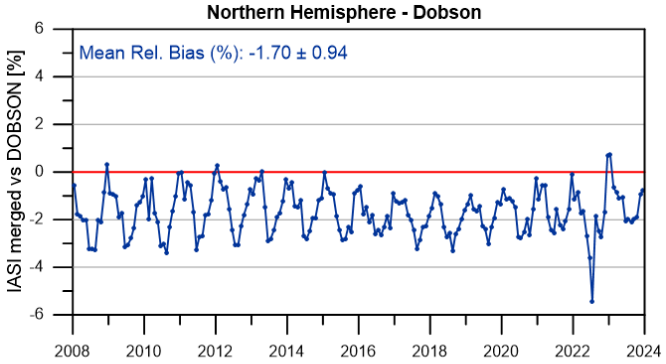

(c)

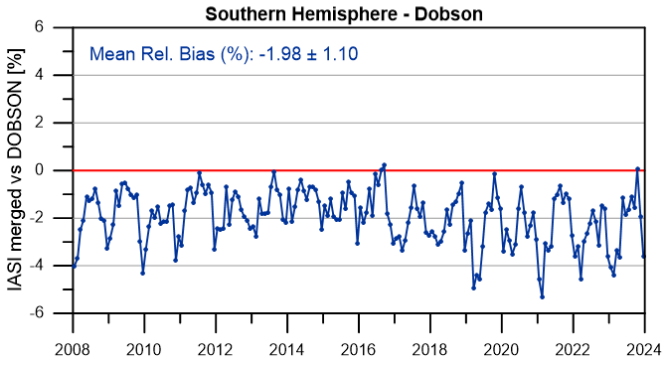

(d)

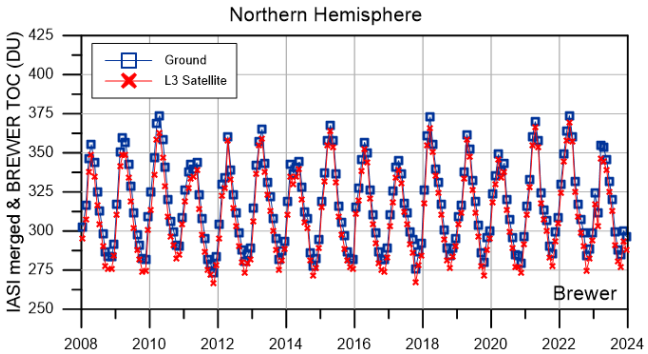

Figure 4.7: Monthly mean time series of the percentage differences between satellite observations and ground-based measurements for the Brewer network in the NH (panel a), the Dobson network in the NH (panel b) and in the SH (panel c). Panel (d) shows the respective NH timeseries of the Brewer total ozone from the Level-3 merged IASI integrated profiles and ground-based measurements TOC.

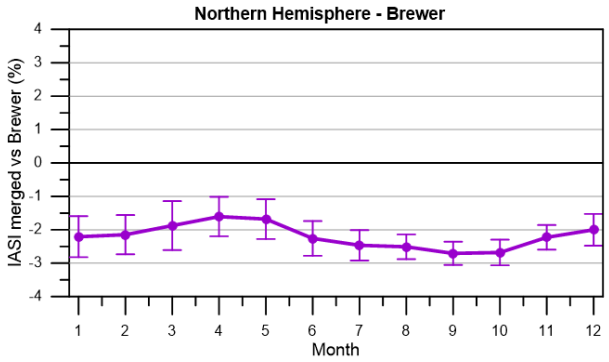

Figure 4.8: The annual cycle of the monthly mean percentage differences between the integrated Level-3 product and the NH Brewer ground-based observations.

(a)

(b)

(c)

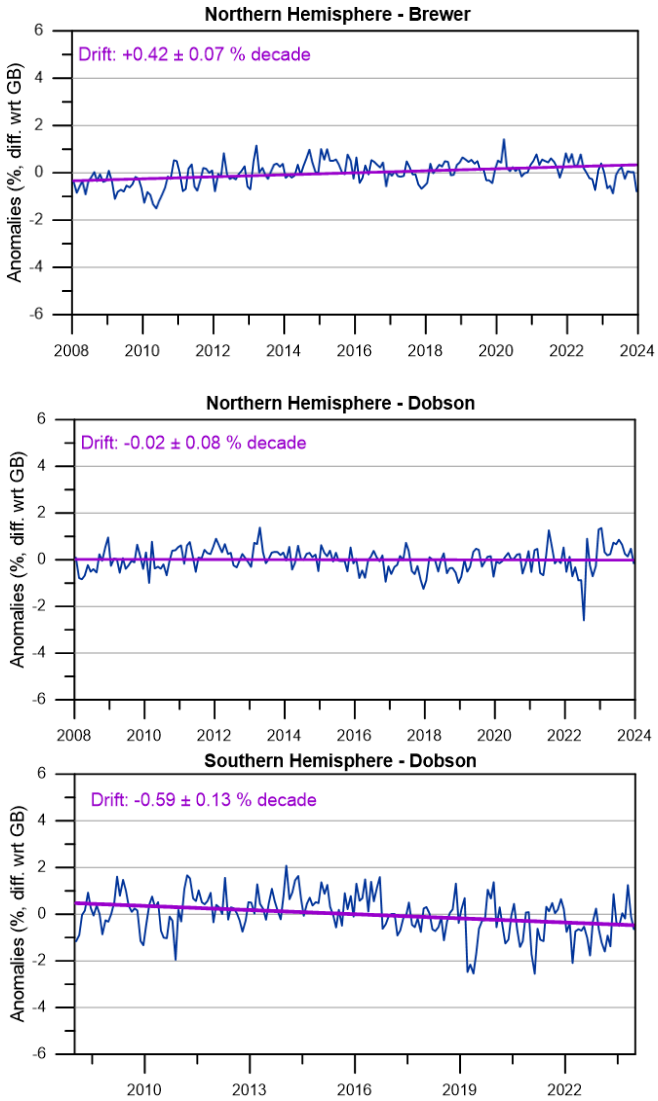

Figure 4.9: The de-seasonalized time series of the percentage differences between the Level-3 product and the ground-based measurements for the NH (panels a and b) and SH (panel c).

Moreover, the temporal stability of the satellite product is studied via the de-seasonalized time series shown in **Figure 4.9**. In the NH (panels a and b) the drift is +0.4 ± 0.1 %/decade for the Brewer and -0.0 ± 0.1 %/decade for the Dobson co-locations. The SH statistical analysis shows a slightly higher drift of -0.6 ± 0.1 %/decade. In all cases, these **very low drifts are well within the product requirements, showing that the merged IASI integrated total ozone is temporally very stable**.

Finally, the latitudinal dependency of the co-locations is shown in **Figure 4.10**, where the mean relative bias of each individual ground-based station is plotted against the station's latitude. The approach in this figure is different than before, since here the comparisons are performed in a one-pixel-per-station basis. Specifically, the pixel of the Level-3 grid containing each station is selected and then their daily total ozone (or integrated ozone, for the satellite product) are used to calculate the overall mean bias per station that is depicted in the figure. For stations in the latitudinal range from 70°N to 40°S, both Brewer and Dobson stations have negative overall negative mean biases, up to -4 %, with no particular patterns or dependencies. As an exception, the desert, high altitude station of Tamanrasset at 22.8°N appears to have a positive mean bias of +2 %, about 4 % higher than that of other stations' bias of similar latitude. Northwards 70° and southwards 40°S, the stations with available datasets have no or low positive biases, up to +1 % but they are highly variable due to the fewer number of co-locations. Overall, a U-pattern is seen in the figure.

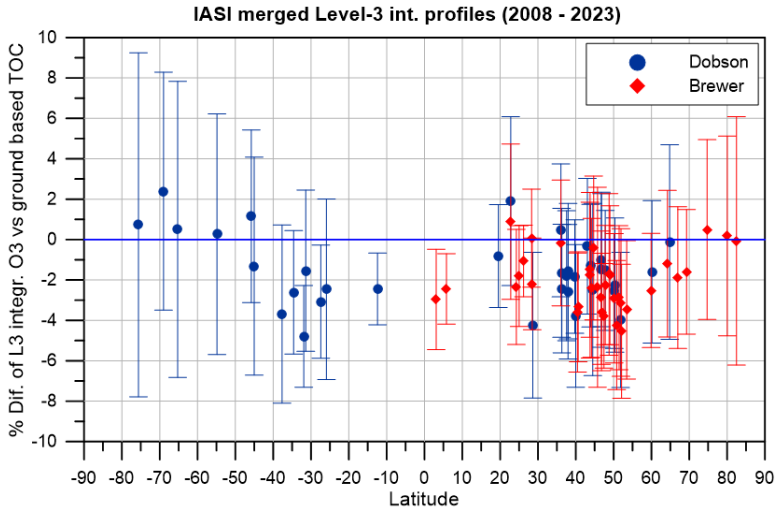

Figure 4.10: The latitudinal variability of the Level-3 mean relative biases with respect to the individual Brewer and Dobson ground-based stations' records. The 1-σ standard deviation of the average is also displayed as an error bar per station.

4.2.2.2 Summary and compliance with user requirements

The merged IASI Level-3 integrated ozone profiles were validated against Brewer and Dobson ground-based measurements. The time span of the IASI observations is 16 years, and the validation results can be summarized in the following points:

- the **mean relative bias** between the satellite product and ground based total ozone measurements is ~ -2 ± 1 %, showing that IASI reports higher TOCs than the ground-reference,
- the peak-to-peak **annual cycle** of the relative differences with respect to Brewer observations is 1 %, and
- the **temporal change** of merged IASI Level-3 product ranges between -0.6 and +0.4 %/decade, depending on the type of the ground based reference and the hemisphere of the co-locations.

According to **Table 3.1**, the requirements that have to be met by the retrieved merged IASI integrated ozone profiles correspond to the stability of the TOC measurements, which must be in the range of 1 to 3 % per

decade, the radiative forcing introduced by the evolution of the ozone layer that has to be less than 2 % and the short-term variability that must be less than 3 %. The level of compliance of the IASI dataset with these user requirements is shown in **Table 4.6** and highlighted with the following code:

- green indicates ascertained compliance with users' requirements;
- yellow indicates compliance with some users' requirements but not all; and
- red indicates compliance with none of the user requirements.

The merged IASI Level-3 integrated ozone dataset that was validated against ground-based reference measurements, was found to be compliant with the requirements in terms of uncertainty and stability. We hence conclude that the merged IASI Level-3 integrated ozone is a product of very good quality and temporal stability, suitable and useful for long term analysis of the ozone layer, such as decadal trend studies, the evaluation of model simulations, and data assimilation applications.

Table 4.6: Compliance of the merged IASI integrated ozone profiles with user requirements

Topic	Requirement	Compliance / evaluation
Horizontal resolution	< 20-100 km	~100 km (1°) along track
		~100 km (1°) across track
Observation frequency	Daily – weekly	Daily
Time period	(1980-…)	01/2008 – 12/2023
Total uncertainty	2 % (radiative forcing studies)	Bias: -2 %, Spread: ~3-5 % (includes the uncertainty of the reference dataset and some co-location mismatch), Seasonality: 1 % peak-to-peak
	3 % (Seasonal cycle & Short term variability)	
Stability	1 – 3 %/decade	-0.6 to +0.4 %/decade

4.2.3 GOP-ECV Level-3 integrated ozone profiles

The GOME-type Profile ECV (GOP-ECV) integrated total ozone, provided in monthly files and in a 5° x 5° grid, were made available for the time period July 1995 – October 2021. In this section, we report the validation results of the integrated total ozone with respect to fiducial ground-based total ozone measurements performed by quality-controlled Brewer and Dobson UV spectrometers.

In order to create the respective Level-3 TOC field based on the WOUDC ground-based stations, the reported TOCs were gridded into the same 5°x5° grid as the GOP-ECV data, on a monthly basis, with most grid points being represented by only one reporting station. In detail, direct Sun measurements were considered for the gridding of the ground-based TOCs into Level-3 grid points, even though in some cases this choice severely decreases the number of measurements. As a compromise between obtaining the highest global coverage possible and the most representative monthly means, especially at high latitudes, a lower limit of 5 measurements per month and per grid box was enforced so that the temporal representativeness errors are minimized.

4.2.3.1 Systematic bias and its variations

Figure 4.11 shows the hemispherical (Northern Hemisphere-NH in panels a and b, Southern Hemisphere-SH in panel c) percentage differences between the satellite Level-3 GOP-ECV integrated profiles and the Dobson (left) and Brewer (right) TOC records, in the form of monthly mean time series. The Dobson comparisons for NH and SH show very good agreement between the Level-3 product and the ground reference, with obvious

seasonal dependency due to the characteristics of the ground-based measurements that was discussed above. The percentage differences span between 0 and +4 %, with a very small number of outliers, but always showing that **the Level-3 product reports higher total ozone than the ground-based measurements**. The relative mean biases resulting from the 26-year data record are +1.7 ± 1.3 % for the NH and +1.6 ± 0.8 % for the SH. The Brewer comparisons (panel b) have a lower seasonal dependency and a mean relative bias of ~ **+1.0 ± 0.5 %,** showing a very good agreement between the two datasets. Moreover, the overall variability of the monthly mean comparisons is 2.6 % - 3.6 % for the NH and 3 % for the SH co-locations, but this is not only attributed to the satellite product since the ground-based data also contribute with their uncertainty. Panel d of **Figure 4.11** shows that the Level-3 product successfully captures the total ozone variability as observed by the ground-based stations. The annual cycle of the NH Brewer comparisons is shown in **Figure 4.12**, with a minor peak-to-peak seasonal variability of 0.8 %. The statistics of this analysis are summarized in **Table 4.7**.

Table 4.7: The overall statistics that result from the co-locations of the Level-3 GOP-ECV satellite product to the Brewer (NH only) and Dobson ground-based observations

		Dobson	Brewer
Mean rel. bias (%)	NH	+1.7 ± 1.3	+1.0 ± 0.5
	SH	+1.6 ± 0.8	N/A
St. Deviation (%)	NH	3.6	2.6
	SH	2.9	N/A
Annual cycle (% p-t-p)	NH	N/A	0.8

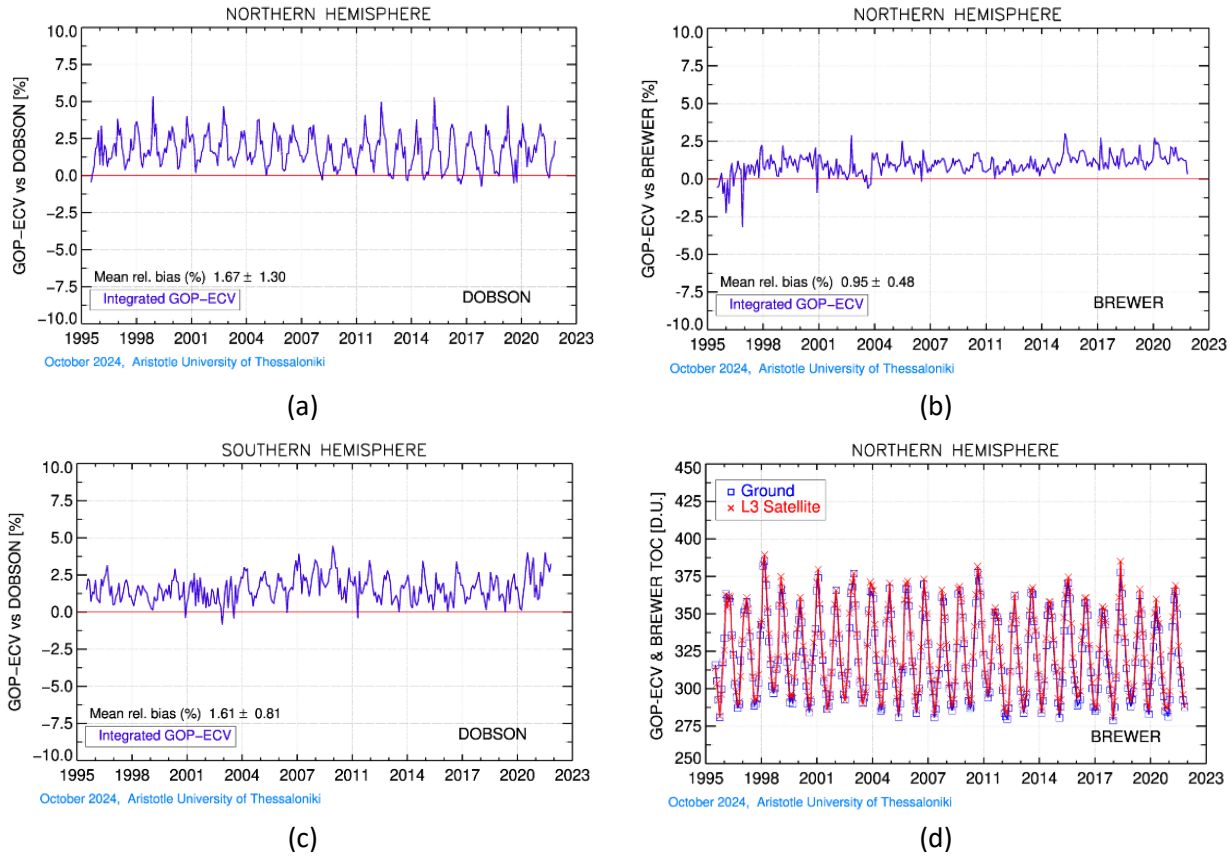

Figure 4.11: Monthly mean time series of the percentage differences between satellite observations and ground-based measurements for the Dobson network in the NH (panel a) and in the SH (panel c) and for the Brewer network, NH only (panel b). Panel (d) shows the respective NH timeseries of the Brewer total ozone from the integrated Level-3 GOP-ECV and ground-based measurements.

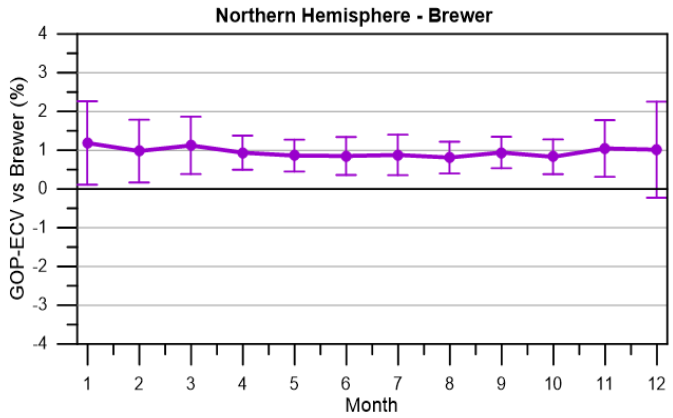

Figure 4.12: The annual cycle of the monthly mean percentage differences between the integrated Level-3 product and the NH Brewer ground-based observations.

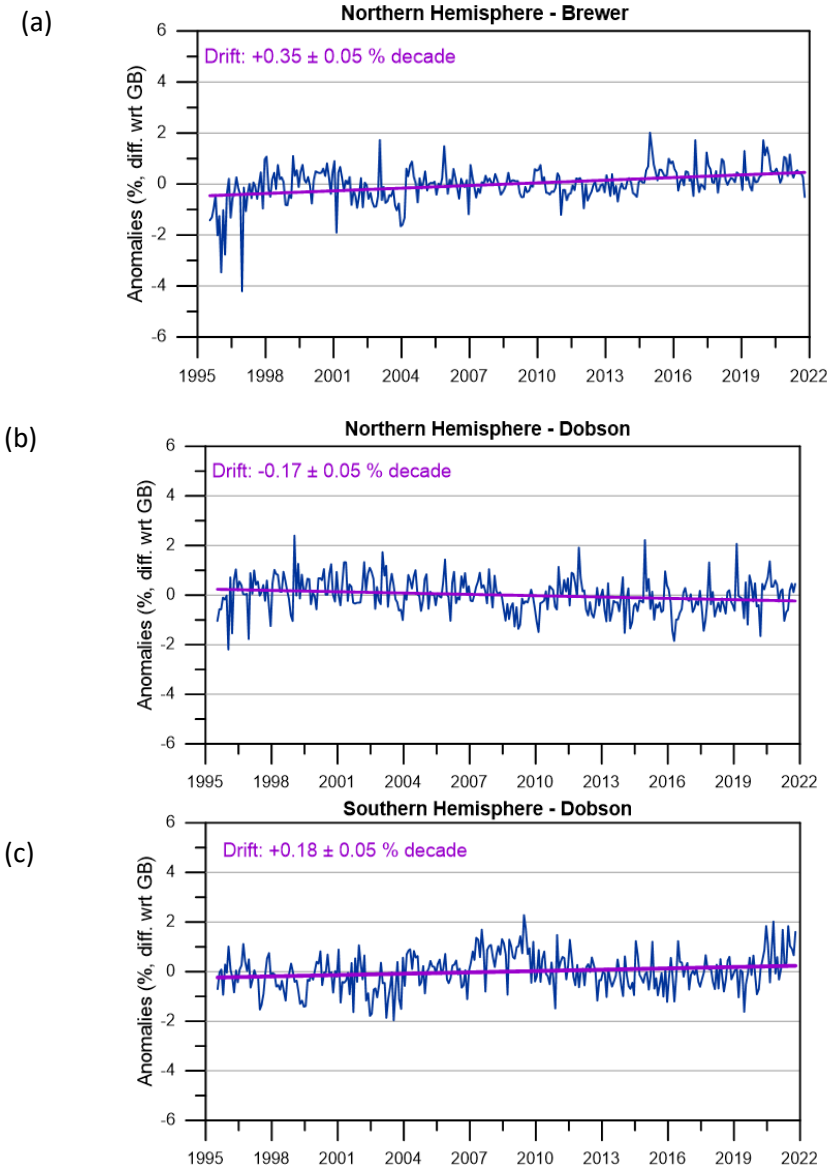

Figure 4.13: The de-seasonalized time series of the percentage differences between the Level-3 product and the ground-based measurements for the NH (panels a and b) and SH (panel c).

The respective de-seasonalized time series, depicted in **Figure 4.13** show even more clearly that the Level-3 comparisons are in general based on homogenous datasets (satellite and ground-based), with no particular abrupt changes in their records. In the NH, a minor drift per decade of the Level-3 product with respect to ground-based data is shown, +0.4 ± 0.1 % per decade for Brewer and -0.2 ± 0.1 % per decade for Dobson co-locations. The SH Dobson comparisons have a drift of the same order, +0.2 ± 0.1 % per decade. In any case, these drifts are well within the product requirements.

Finally, in **Figure 4.14** the mean relative bias of each individual ground-based station is plotted against the station's latitude, to investigate the spatial characteristics of the Level-3 integrated total ozone. The approach in this figure is different than before, since here the comparisons are performed in a one-pixel-per-station basis. Specifically, the pixel of the Level-3 grid containing each station is selected and then their monthly means are used to calculate the overall mean bias per station that is depicted in the figure. In the NH, where the density of the stations is high, the agreement between the two datasets, satellite and ground, is very

good and not particularly varying with latitude. Most stations have a relative bias within -1 and +3 %. The SH stations (Dobsons only) are clearly less in number. From the equator up to -40°, the biases are within 0 and +3 %, but southwards -40° and up to -70° the variability and the biases increase. Nevertheless, this should not be attributed to the satellite dataset, since similar features are seen in other Level-2 satellite products validation studies too (e.g. see Figure 5 of RD40).

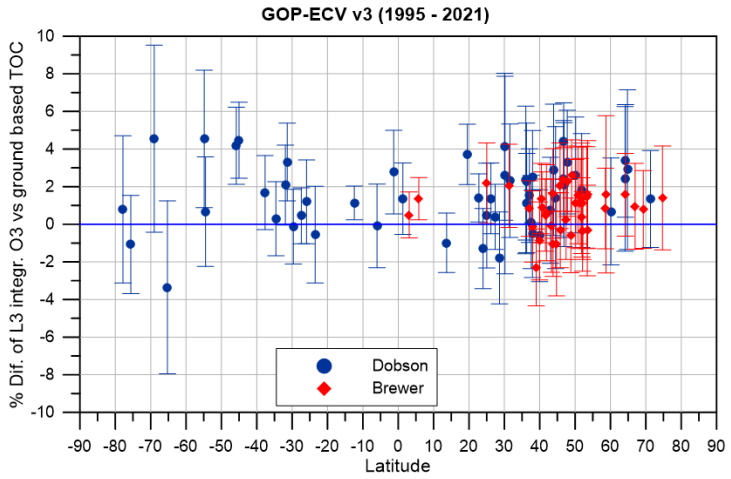

Figure 4.14: The latitudinal variability of the Level-3 mean relative biases with respect to the individual Brewer and Dobson ground-based stations' records. The 1-σ standard deviation of the average is also displayed as an error bar per station.

4.2.3.2 Summary and compliance with user requirements

The GOP-ECV integrated ozone profiles were validated against Brewer and Dobson ground-based measurements. The time span of the satellite observations is 26 years, and the validation results can be summarized in the following points:

- the **mean relative bias** between the satellite product and ground based total ozone measurements is ~ +1.5 ± 1 %, showing that the GOP-ECV integrated ozone is higher than the ground-reference total ozone columns,
- the peak-to-peak **annual cycle** of the relative differences with respect to Brewer observations is 0.8 %, and
- the **temporal change** of Level-3 satellite product ranges between -0.2 and +0.4 %/decade, depending on the type of the ground based reference and the hemisphere of the co-locations.

According to **Table 3.1**, the requirements that have to be met by the retrieved GOP-ECV integrated ozone profiles correspond to the stability of the TOC measurements, which must be in the range of 1 to 3 % per decade, the radiative forcing introduced by the evolution of the ozone layer that has to be less than 2 % and the short-term variability that must be less than 3 %. The level of compliance of the dataset under study with these user requirements is shown in **Table 4.8** and highlighted with the following code:

- green indicates ascertained compliance with users' requirements;
- yellow indicates compliance with some users' requirements but not all; and
- red indicates compliance with none of the user requirements.

Table 4.8: Compliance of the GOP-ECV integrated ozone profiles with user requirements

Topic	Requirement	Compliance / evaluation
Horizontal resolution	< 20-100 km	~500 km (5°) along track
		~500 km (5°) across track
Observation frequency	Daily – weekly	Monthly
Time period	(1980-…)	07/1995 – 10/2021
Total uncertainty	2 % (radiative forcing studies)	Bias: +1 to +1.7 %, Spread: ~3 % (includes the uncertainty of the reference dataset and some co-location mismatch), Seasonality: 0.8 % peak-to-peak
	3 % (Seasonal cycle & Short term variability)	
Stability	1 – 3 %/decade	-0.2 to +0.4 %/decade

We hence conclude that the GOP-ECV integrated ozone profiles, that showed an excellent agreement to the ground-based reference measurements as well as a negligible drift in their co-locations, is a product compliant with the requirements in terms of uncertainty and stability. Therefore, the GOP-ECV Level-3 integrated ozone profiles are of exceptional quality and temporal stability, suitable and useful for long term analysis of the ozone layer, such as decadal trend studies, the evaluation of model simulations, and data assimilation applications.

4.3 *Validation of full-profile nadir data*

Next to the post-retrieval screening by the data provider, additional filtering criteria have been applied (see Table 4.11). From all approved L2 nadir ozone profile data, only those that are located within 300 km of an NDACC, SHADOZ, or WOUDC ozonesonde or stratospheric lidar station location are retained for further analysis (see Section 5.2). This 300 km radius however is narrowed down for each instrument individually, depending on the instrument's pixel size (see Table 4.10).

Table 4.9 - Overview of Ozone_cci+ nadir ozone profile data products and their current availability.

L2 Data Product	Processing entity	Time period																									
		96	97	98	99	00	01	02	03	04	05	06	07	08	09	10	11	12	13	14	15	16	17	18	19	20	21	22	23
NP_GOME2B	RAL																												
NP_GOME2C	RAL																												
NP_OMI	RAL																												
NP_TROPOMI	RAL																												
NP_IASIA	ULB/LATMOS																												
NP_IASIB	ULB/LATMOS																												
NP_IASIC	ULB/LATMOS																												
NP_IASIABC	ULB/LATMOS																												
NP_GOP-ECV	DLR																												

Table 4.10 - Overview of Ozone_cci+ L2 nadir ozone profile data product specifications, including local solar time (LST) of the satellite overpass, pixel size, and co-location distance selection based on pixel size.

L2 data product	LST	pixel size (km²)	Co-location
NP_GOME2B/C	09:30AM	160 x 160 km²	100 km
NP_OMI	01:30PM	52 x 48 km²	50 km
NP_TROPOMI	01:30PM	28 x 28 km²	50 km
NP_IASIA/B/C	09:30AM(+PM)	12 km (diam.)	50 km

Table 4.11 - L2 nadir ozone profile filtering criteria considered in this work (first column) and their settings for the RAL UV-VIS retrieval algorithm (second column) and the FORLI TIR retrieval algorithm (third column). Values that do not comply with the settings are rejected as suggested by the respective data providers.

Filtering criterion	UV-VIS RAL algorithms	TIR FORLI algorithms
Averaging kernel matrix	/	- DFS > 1 - All elements < 2 - First derivative < 0.5 - Second derivative < 1
Chi-square test	1	1
Convergence	1	1
Cost function (normalised)	< 120 (< 2)	/
Effective cloud fraction	< 0.20	< 0.13
Negative ozone values	Rejected	Rejected
Product quality flag	- QA value > 0.5	- Retrieval quality flag = 1 - Ozone rejected if incomplete H2O retrieval
Solar zenith angle	< 80°	< 83° (daytime) or > 91° (nighttime)
Surface pressure	Rejected if unrealistic	Rejected if unrealistic

4.3.1 Validation approach

The ten-step nadir ozone profile QA/validation chain as applied in this work has already been extensively described within CCI context in [RD49] and [RD50]. Next to data and information content studies, ground-based data records are used as a transfer standard against which the nadir ozone profile retrievals are compared.

4.3.1.1 Information content studies

Each quantity that is retrieved using the optimal estimation technique contains information both from the satellite measurement and from the a-priori profile and covariance matrix. The contribution of prior information can be significant where the measurement is weakly or even not sensitive to the atmospheric ozone profile, e.g. in case of fine-scale structures of the profile, below optically thick tropospheric clouds, and at the lower altitudes. The information distribution is captured by the retrieval's ex-ante vertical averaging kernel matrix A (sometimes also AKM hereafter), which represents the sensitivity of the retrieved state $\hat{x}$ to changes in the true profile x_t at a given altitude: $A(m,n) = \partial\hat{x}(m)/\partial x_t(n)$. A study of the algebraic properties of this averaging kernel matrix, denoted information content study, can help understanding how the system captures actual atmospheric signals. Through straightforward analysis however, it can be easily demonstrated that typical information content measures as discussed in this section usually depend on the units of the averaging kernel matrices they are calculated from [RD49]. As these measures however should be unit-independent, fractional AKMs A_F must be considered.

Starting from the averaging kernels provided as part of the Ozone_cci+ CRDP L2 nadir ozone profile products, the degree of freedom in the signal (DFS) and the vertical sensitivity are studied. These quantities are given by the AKM trace and row sum profile, respectively. The DFS of a retrieved atmospheric profile is a non-linear measure for the number of independent quantities that can be determined and as such loosely related to the Shannon information content [RD76]. The vertical sensitivity to the measurement is a unit-normalised measure for how sensitive the retrieved ozone value at a certain height is to ozone values at all heights.

Besides the more common DFS and sensitivity information content quantities, in this work the vertical averaging kernels' offset and width are considered as well. The offset is an estimate of the uncertainty on the retrieval height registration, given here by the direct vertical distance (in km) between an averaging kernel's peak sensitivity altitude z_{peak} and its nominal retrieval altitude z_{nom} as $d(m) = z_{peak}(m) - z_{nom}(m)$. Ideally, within each kernel, this distance equals zero. Ozone_cci+ user requirements also specify an upper limit for the vertical resolution of the nadir ozone profile retrievals. Several methods have been proposed to estimate the vertical resolution from the width of the vertical averaging kernels (see overview in [RD49]), but usually it is determined either as a full width at half-maximum (FWHM) value around the kernel's peak altitude or as the Backus-Gilbert spread (BG) or resolving length around its centroid.

4.3.1.2 FRM comparisons

The ground-based FRM data considered for the nadir ozone profile validation in this report has been collected from ESA's Atmospheric Validation Data Centre (EVDC). The EVDC Cal/Val data portal contains ozonesonde data from the NDACC, SHADOZ, and WOUDC network archives. Stratospheric lidar data originate from the NDACC data archive and its rapid delivery section. The EVDC data portal redistributes the ground-based data in a harmonized HDF5 GEOMS format.

Like for the satellite data, prior to searching for co-locations with satellite ECV data, data screening has been applied to ground-based correlative measurements by ozonesondes and lidars, both on entire profiles and on individual altitude levels. The recommendations of the ground-based data providers to discard unreliable measurements are followed. Measurements with unrealistic pressure, temperature, or ozone readings are rejected automatically. Ozonesonde measurements at pressures below 5 hPa (beyond 30-33 km) and lidar measurements outside of the 15-47 km vertical range are rejected automatically as well. Prior to these data manipulations, the ground-based ozone profile data were converted to partial ozone column units (DU) by vertical integration. While ozonesondes report measurements in partial pressure, easily converted into VMR units (ppmv) and in ND using the on-board PTU measurements, the lidar data are given in number density.

Only co-locations with a maximal spatial distance of 100 km or smaller (see Table 4.10) and a maximal time difference of one day were allowed. When multiple satellite pixel co-locations with one unique ground measurement occur, only the closest satellite measurement is kept. Calculating difference profiles requires harmonisation of the satellite retrieval and ground-based reference ozone profiles in terms of at least their representation and vertical sampling. To down-sample a ground-based ozone profile measurement to the satellite retrieval grid, a mass-conserving regridding in subcolumn units on layers is preferably used [RD63]. Additionally, the satellite and ground-based profiles' vertical smoothing difference error is minimized by averaging kernel multiplication [RD51, RD76].

The baseline output of the L2 validation exercises consists of median absolute and relative nadir ozone profile differences at individual stations or within latitude bands for the entire time series. This median difference is a robust (against outliers) estimator of the vertically dependent systematic error, i.e. the bias, of the satellite data product. The bias profiles for the entire list of stations are then combined and visualized as a function of several influence quantities to reveal any dependences of the systematic error. Besides the median difference, also the Q84-Q16 interpercentile (IP68) of the differences is calculated as a robust spread

estimator of the random errors in the satellite data product, i.e. the precision profile. However, this spread on the differences will also include contributions from ground-based random uncertainties (limited to a few percent) and representativeness (sampling and smoothing) differences between the satellite and reference measurements, and therefore in fact provides and upper limit on the actual random satellite uncertainty. In case of a normal distribution of the ozone differences, median and IP68 are equivalent to mean and standard deviation, but they offer the advantage to be much less sensitive to occasional outliers.

The satellite-based L3 monthly gridded data is compared with monthly averages of the reference data (or, equivalently, a ground-based level-3-type dataset). This approach unavoidably introduces spatiotemporal representativeness errors into the difference statistics. However, these errors are reduced to a minimum in two ways. First, for monthly Level-3 data, as is the case here for GOP-ECV, the comparisons are limited to those months with a sufficient number of valid reference measurements. This number has been set to four in the ground-based validation presented here. As such, an implicit averaging of at least four ozonesonde or lidar measurements per month is introduced in the comparison statistics. This approach is not required for the IASI-ABC daily merged data, where daily comparisons can be considered. Second, the 1x1 degree box that overlaps with the ground measurement is taken for co-location, but the profiles from the four corners of this box are averaged, with the distances to the exact reference measurement location as weighting factors.

4.3.2 Validation results

4.3.2.1 L3 UV-VIS GOP-ECV

DLR's GOME-type Ozone Profile Essential Climate Variable (GOP-ECV) combines L2 retrievals by RAL from five nadir-viewing satellite sensors (GOME/ERS-2, SCIAMACHY/ENVISAT, GOME-2/Metop-A, GOME-2/Metop-B, and OMI/AURA) into a single L3 monthly gridded product, covering 1996-2022. Before merging the individual time series into one long-term data record, they are adjusted to match the total ozone column amounts from the GOME-type Total Ozone Essential Climate Variable (GTO-ECV). This procedure should lead to reduced inter-sensor biases and drifts. It should be taken into account, however, that the current GOP-ECV v3 is based on the fully available RAL v3.X L2 products, and not the v4.01 products discussed above.

The relative bias and dispersion plots as a function of latitude, season, and year (two-yearly) in **Figure 4.15**, for both ozonesonde and stratospheric lidar reference measurements, point at relative differences of the order of 10 % in the stratosphere and 20 % in the troposphere overall. The dispersion equals again 10 % on average in the stratosphere, but increases up to 60 % in the troposphere, pointing at larger difficulties to capture the tropospheric low-ozone dynamics. The GOP-ECV performance is more spatially dependent than temporally (given the little dependence on season and year, but also see drift assessment at the end of this section). Clearly, ozone values show negative biases of 20-50 % towards the poles throughout the entire vertical profile. The positive bias peak up to 50 % in the tropical UTLS seems to be real as well, as it is both captured by the ozonesonde and lidar comparisons. On the other hand, the increased dispersion that is only seen for the northern mid-latitude lidar comparisons for autumn 2011-2012 rather seems to be a reference measurement hiccup.

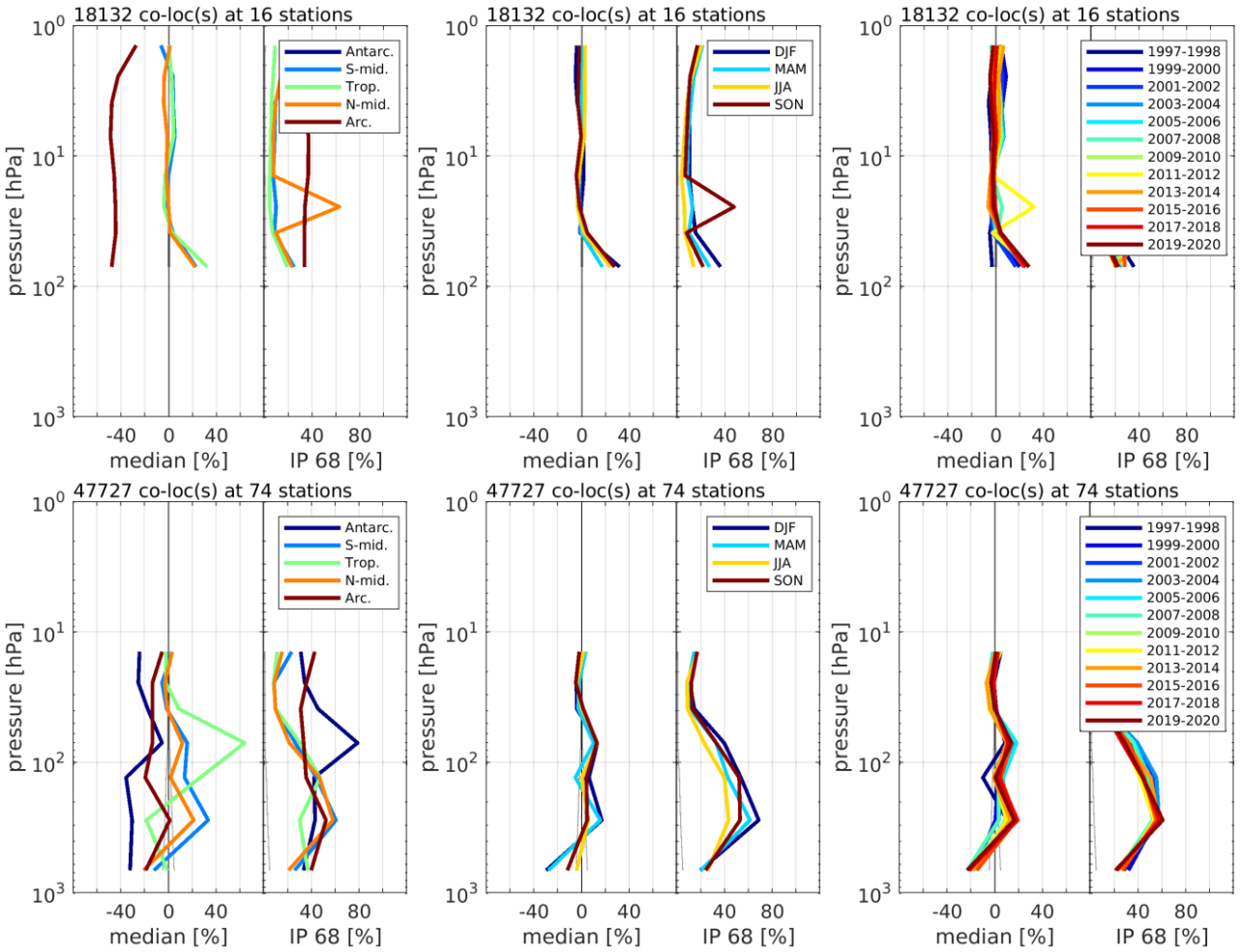

Figure 4.15 - Median relative differences and 68 % interpercentile spreads for comparison of GOP-ECV v3 with ozonesonde (bottom) and stratospheric lidar (top) reference measurements (at least four per month). Comparison statistics are plotted as a function of latitude (left), season (middle) and time (right), using the colour coding indicated by the plot legends.

4.3.2.2 IASI-A/B/C L2 CDR instrument retrievals and consistency

Figure 4.16 and **Figure 4.17** contain the median (relative) differences, 68 % interpercentile spreads, vertical sensitivities, offsets, and effective vertical resolutions (FWHMs) for the comparison of FORLI v20151001 CDR (also called v2024) retrieved IASI profiles with ozonesonde and lidar measurements, respectively, for SZA and DFS as influence quantities (others are not shown in this report). These results demonstrate that the retrieval results for all three IASI instruments are very similar, showing no significant differences between their respective statistics, and this despite the different time windows under consideration. The IASI instruments show a less than 10 % and insignificant stratospheric bias, a 10 to 30 % insignificant positive bias in the UTLS, and an order of 10-20 % negative bias at the edge of significance in the troposphere. The latter agrees with a tropospheric ozone (from IASI-A and IASI-B retrieved with FORLI v20151001) validation exercise performed by Boynard et al. [RD31]. Possible reasons for the positive UTLS bias are discussed in [RD37]. The comparison results show hardly any scan angle (VZA) dependence or seasonality, except for some larger systematic differences around the Antarctic ozone hole that can be partially attributed to co-location errors at the edge of the polar vortex (not shown here). The remaining meridian dependences are typically limited to stronger UTLS bias fluctuations in the tropics.

The vertical sensitivity profiles are close to unity around the ozone peak and above (25 to 35 km) for all three instruments. Typically, the sensitivity decreases above and below due to the smaller ozone concentrations. The FORLI retrievals show sensitivity fluctuations around the UTLS and down the troposphere, ranging between 0 and 2. Although the overall IASI sensitivity variability is strongest around the equator, these outliers typically occur in the Polar Regions and go together with excessively high retrieved ozone peaks. The strong sensitivity variability in general hampers the averaging kernel smoothing of the reference profiles before comparison, as this procedure then introduces a bias instead of reducing the vertical smoothing difference error. Usually however, except for decreased surface-level sensitivity (0.5) and a median 1.5 peak around the UTLS with slight compensation above and below, the FORLI sensitivity is vertically consistent.

The retrieval offset (vertical registration uncertainty) amounts to about 5-10 km on average but shows some discreteness due to the FORLI retrievals being performed on a fixed 1 km vertical grid. Moreover, the offset shows specific features for all three IASI instruments, like the peaks at 5 and 15 km, and a jump near 25 km altitude. The tropospheric offset sometimes even explodes to unrealistic values, when the corresponding averaging kernels have no clear maximum. The behaviour of an averaging kernel's sensitivity and offset is typically also reflected in its width, which is here measured by the kernel's FWHM. This FWHM ranges between 10 and 15 km on average for the IASI instrument retrievals, with oscillations occurring in the UTLS.

Looking at the FORLI v20151001 CDR comparison results into detail, it becomes clear that the highly positive difference outliers in the ULTS seem to go together with high SZA and low DFS values. In other words, poor quality retrievals with minimal retrieval sensitivities and DFS values appear to occur for the highest solar zenith angle observations. One could therefore consider screening the observations for high SZA (e.g. above 70°) or low DFS (e.g. below 2.5) to overall maintain the lowest-bias and dispersion observations.

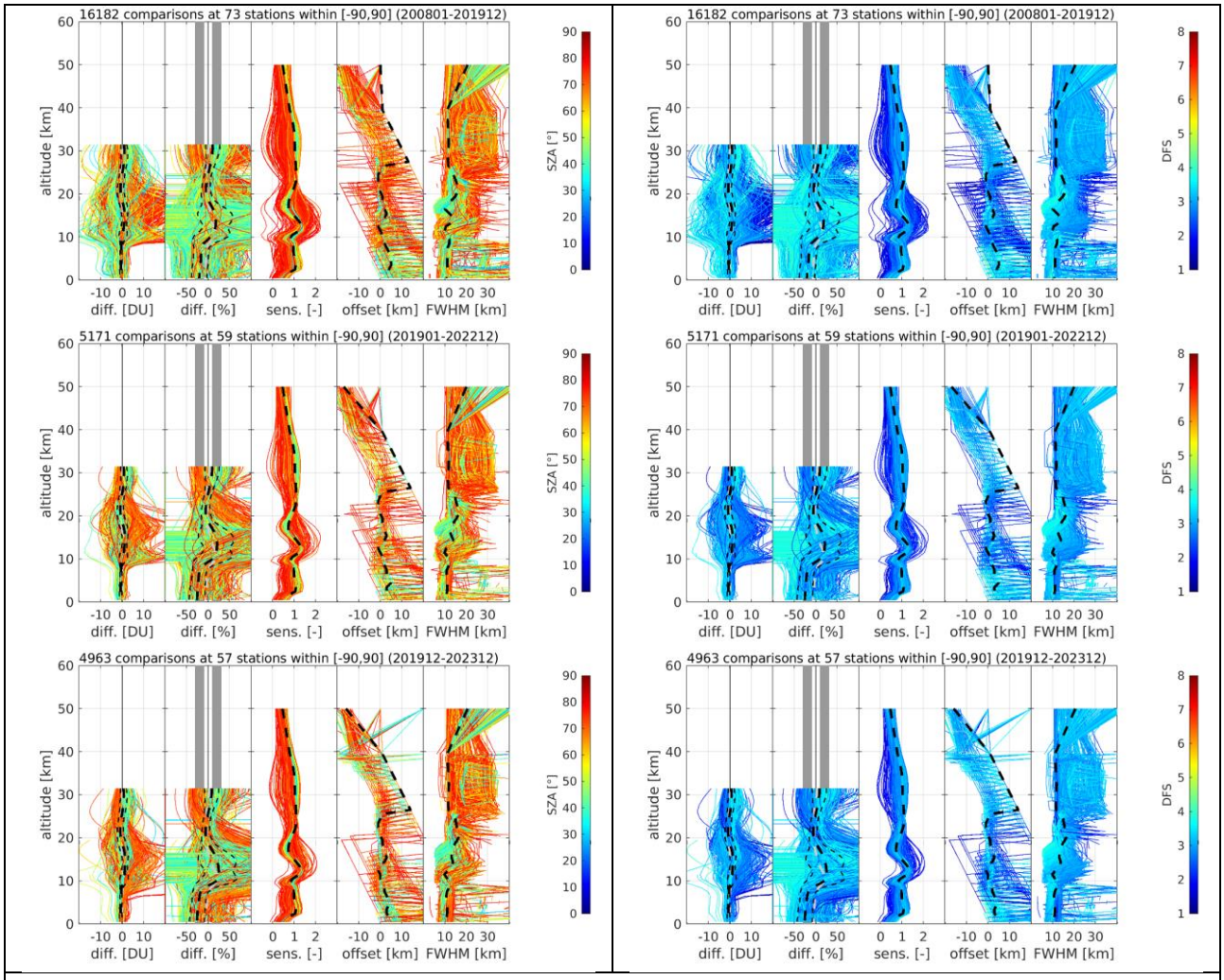

Figure 4.16 - Median absolute and relative differences (thick dashed lines), 68 % interpercentile spreads (thin dashed lines), and median vertical sensitivities, offsets and FWHMs (dashed lines) for comparison of FORLI L2 v20151001 CDR (v2024) IASI-A/B/C (top to bottom, respectively) retrieved profiles with ozonesonde reference measurements. Individual profile statistics are plotted as function of solar zenith angle (left) and DFS (right) using the colour coding indicated by the colour bar on each plot.

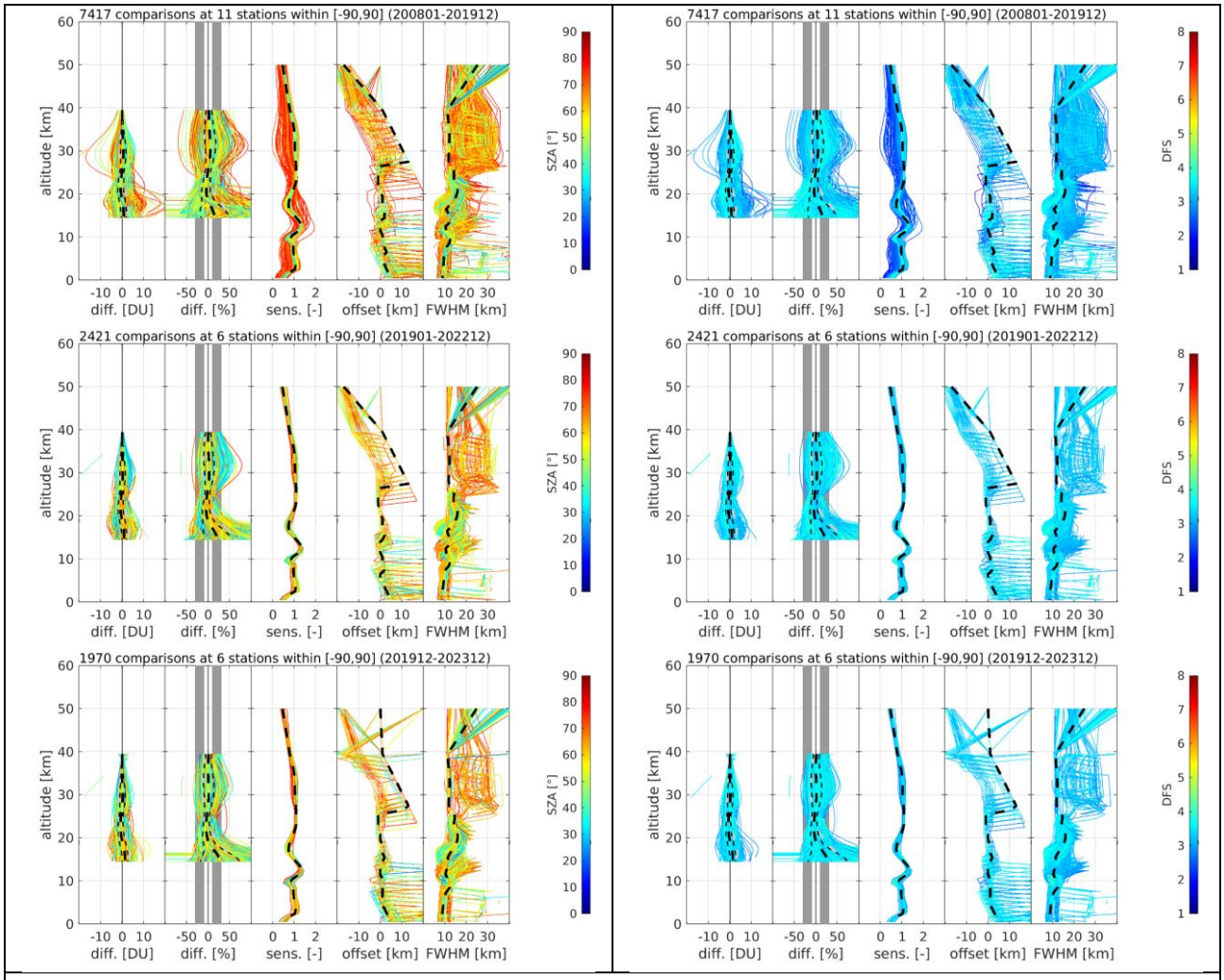

Figure 4.17 - Median absolute and relative differences (thick dashed lines), 68 % interpercentile spreads (thin dashed lines), and median vertical sensitivities, offsets and FWHMs (dashed lines) for comparison of FORLI L2 v20151001 CDR (v2024) IASI-A/B/C (top to bottom, respectively) retrieved profiles with stratospheric lidar reference measurements. Individual profile statistics are plotted as function of solar zenith angle (left) and DFS (right) using the colour coding indicated by the colour bar on each plot.

4.3.2.3 IASI-ABC L3 v2019

The individual FORLI L2 v20191122 retrievals – note the difference with the L2 v2015 CDR data in the previous section – for IASI-A, B, and C have been merged into a single Level-3 data record covering 2008-2023. This dataset consists of daily gridded (one-by-one degree) profile data on a 1 km vertical grid from the surface up to 40 km. Much in agreement with the L2 v2015 CDR data, the relative bias and dispersion plots as a function of latitude, season, and year (two-yearly) in **Figure 4.18**, for both ozonesonde and stratospheric lidar reference measurements, point at relative differences of less than 10 % and insignificant stratospheric bias, a 10 to 30 % insignificant positive bias in the UTLS, and an order of 20 % negative bias at the edge of significance in the troposphere. The dispersion equals again 10 % on average in the stratosphere, but increases up to 60 % in the UTLS, and to 20-30 % in the lower troposphere, pointing at larger difficulties to capture the tropospheric low-ozone dynamics.

As for the GOP-ECV L3 dataset, the IASI-ABC L3 performance is more spatially dependent than temporally (again also see the drift assessment at the end of this section), but the spatial dependence is now limited to the UTLS and troposphere. The high positive bias peak in the tropical UTLS again is real, as it is both captured by the ozonesonde and lidar comparisons. Moreover, in contrast with the other latitude bands, the Antarctic data show a 20 % positive tropospheric bias, while their UTLS bias is reduced to about 10 % on average (as for the Arctic). This bias shift is probably due to changes in the thermal contrast for high-latitude retrievals, but would require further investigation.

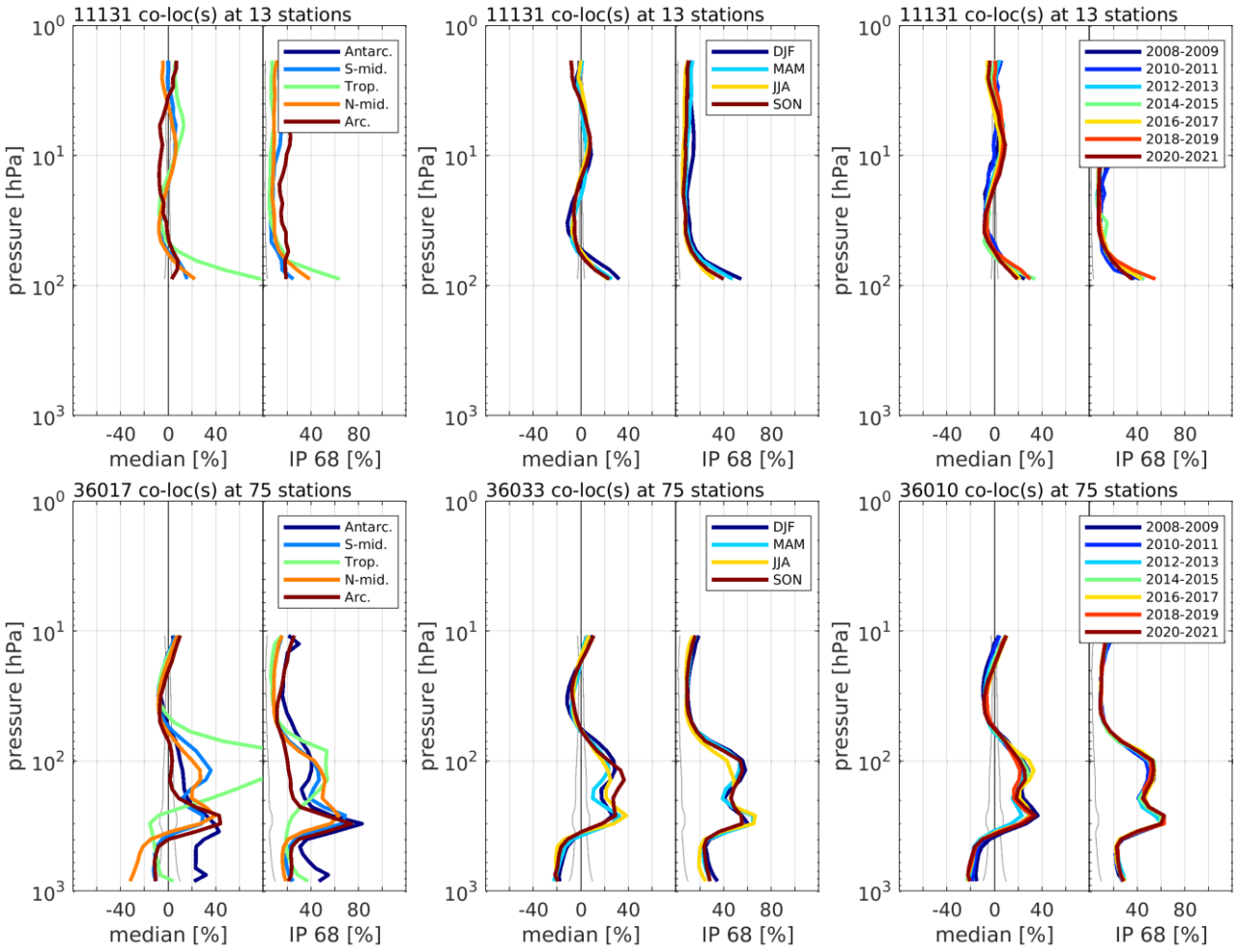

Figure 4.18 - Median relative differences and 68 % interpercentile spreads for comparison of IASI-ABC merged L3 data with ozonesonde (bottom) and stratospheric lidar (top) reference measurements (at least four per month). Comparison statistics are plotted as a function of latitude (left), season (middle) and time (right), using the colour coding indicated by the plot legends.

4.3.2.4 L2/L3 nadir profile drift assessment

Long-term stability of the systematic errors in the ozone data products is a key requirement for ESA's Climate Change Initiatives. The robust linear regression applied here includes an uncertainty estimate by means of the 95 % confidence interval. It is based on a bootstrapping approach with 1000 samples and performed on the satellite-ground difference profiles on the global scale. The results for GOP-ECV are shown in **Figure 4.19**. Results for the individual L2 IASI retrievals (FORLI v2015 CDR) and the L3 merged IASI-ABC product (from FORLI v2019) are collected in **Figure 4.20**. Note that results for ozonesonde and stratospheric lidar reference measurements are combined into single drift assessments and plots for the L2 data, while a composite graph is created for the L3 data (separated at 20 hPa, with ozonesonde results below and lidar results above), because of differences in the L3-like co-locations.

It is clear from **Figure 4.19** (left column) that the Level-3 GOP-ECV dataset shows a drift that is very comparable to the RAL L2 v3.X products where it is derived from (not included here), indicating that the L2/3 drift originates from L1(B) data degradation rather than from the retrieval process, including changes in prior information. The scaling of the integrated GOP-ECV profile by the GTO-ECV does not seem to play a significant role here. GOP-ECV shows a 5-10 %/decade positive drift in the troposphere and UTLS, while having a negative drift of the same order above (pressures below 20 hPa). Except for the UTLS, the drift results seem significant from the bootstrapping perspective, but they are still below the satellite products' random uncertainties as measured from the interpercentile spread (blue line in each plot).

Figure 4.20 demonstrates that the three individual IASI-A/B/C L2 retrievals (v2015 CDR) show very similar vertical drift profiles, despite covering only four years for IASI-B and IASI-C, while the IASI-A time series is three times longer. The latter is mostly reflected in the significance of the drift according to the bootstrapping technique (orange horizontal lines). All three instruments have a 5-10 %/decade negative lower tropospheric drift, and an order of 10 %/decade positive drift just above (10-17 km), although these values are also still within the satellite products' random uncertainties. No effective drift is observed for even higher altitudes. For the merged L3 IASI-ABC dataset, only a lower tropospheric (surface to 10 km) drift of -5 %/decade remains. This looks in agreement with previous results, reporting that the FORLI v2019 retrieval reduces the IASI ozone profiles' UTLS bias and (temporal) dependence.

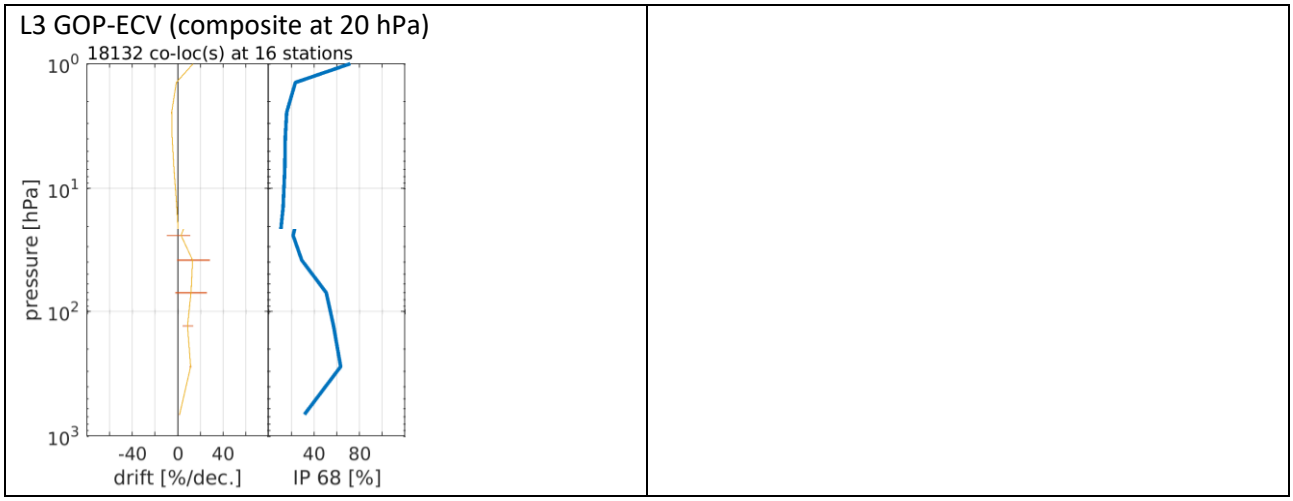

Figure 4.19 – Decadal drifts and 68 % interpercentile spreads for comparison of UV-VIS L3 data with ozonesonde and stratospheric lidar reference measurements combined (at least four per month and hence vertically distinguished at 20 hPa for L3).

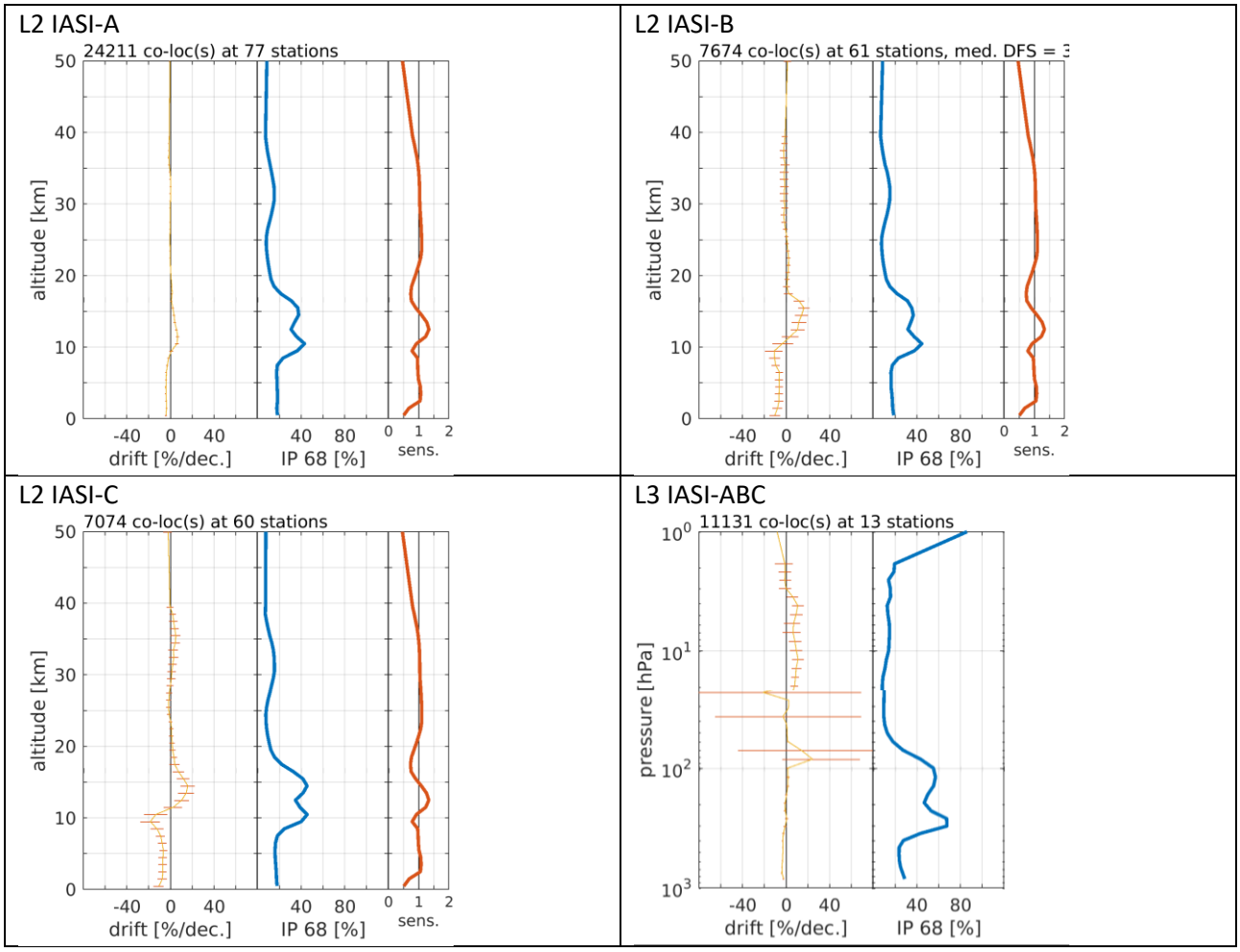

Figure 4.20 – Decadal drifts and 68 % interpercentile spreads for comparison of the IASI instruments' L2 and L3 data with ozonesonde and stratospheric lidar reference measurements combined (vertically distinguished at 20 hPa for L3).

4.3.3 Profile results discussion and conclusions

Table 4.12 collects the major QA/validation quantities discussed throughout this section, their corresponding typical values as discussed in the previous sections, and indications of their compliance with the GCOS user requirements. The nadir ozone profile products under study cover 1995 to 2023 globally, which is sufficiently long for (drift-corrected) ozone trend studies according to the GCOS user requirements (UR). They also fulfil the GCOS user requirements in terms of observation frequency and horizontal and vertical resolution. Only for the latter one must keep in mind that the L2 nadir products show UTLS sensitivity outliers and are strongly correlated vertically due to averaging kernel fluctuations that extend beyond the kernel's 10-15 km FWHM.

The Ozone_cci+ nadir ozone profile products under study typically do not comply with the GCOS user requirements in terms of total uncertainty. The total uncertainty is thereby determined as the quadratic sum of the products' systematic and random uncertainties, which on their turn are estimated from the comparison (with ground-based reference measurement) bias and dispersion, respectively. Total uncertainties range from about 10 % at minimum in the stratosphere to at least 20 % in the troposphere, and even higher values in the UTLS for IASI and for the UV-VIS instruments. The nadir ozone profile retrieval performance in terms systematic and random uncertainties mostly depends on the optical path (and thermal contrast for the IR retrievals, not included here).

Applying bias corrections to the nadir ozone profile CRDP presented in this work might not yield optimal results, however. Next to the L2 data screening recommended by the data providers (summarised in Table 4.11) the validation results presented in the previous sections point at additional data screening options. The highly positive ULTS biases for the FORLI v20151001 CDR products go together with high SZA and low DFS values. In other words, poor quality retrievals with minimal retrieval sensitivities and DFS values appear to occur for the highest solar zenith angle observations. One could therefore consider screening the observations for high SZA (e.g. above 70°) or low DFS (e.g. below 2.5) to overall maintain the lowest-bias and dispersion observations.

Table 4.12 - Major QA/validation quantities, their corresponding typical values, and indication user requirement (UR) compliance for the Ozone_cci+ L2 nadir ozone profile products.

QA quantity (GCOS UR)	**TIR: IASI-A/B/C v2015 CDR**
Time period (1996-2010)	2008-2023
L2 observation frequency (daily to weekly)	Both daytime and nighttime daily
Horizontal resolution (20-200 km)	12 km
Vertical resolution (6 km to troposphere)	Fixed 1 km grid but 10-15 km kernel width and UTLS oscillations
DFS	2-4 with meridian and seasonal dep.
Vertical sensitivity	Outliers around UTLS and below
Height registration uncertainty / retrieval offset	5-10 km on average, but strong features
Systematic uncertainty estimated from comp. bias	< 10 % (stratosphere) to 10-30 % (UTLS) pos. 10-20 % neg. (troposphere)
Random uncertainty estimated from comp. spread	10-50 %
Total uncertainty (16 % below 20 km, 8 % above 20 km)	~10 % in stratosphere, 20-30 % in troposphere, higher in UTLS
Dependence on influence quantities	SZA dependence, also reflected in sensitivity dependence
Stability (1-3 %/dec.)	5-10 %/decade pos. and neg.

5 Validation of Limb Ozone Profile Data Products

5.1 *Introduction*

This section reports on the assessment of the Level-2 and Level-3 limb ozone profile datasets of the Ozone_cci+ Climate Research Data Package (CRDP), accessible from https://climate.esa.int/en/projects/ozone/data.

The Level-2 CRDP consists of a HARMonized dataset of OZone profiles (also named HARMOZ) from the following list of limb/occultation sensors: GOMOS, MIPAS and SCIAMACHY on Envisat, OSIRIS on Odin, ACE-FTS on SciSat-1, OMPS-LP on Suomi-NPP and NOAA-21, SAGE II on ERBS, HALOE on UARS, SABER on TIMED, MLS on EOS-Aura, POAM III on SPOT-4, SAGE III on Meteor-3M and ISS. Each HARMOZ data set is screened for outliers by the instrument experts, presented on an identical vertical grid (altitude or pressure) and archived in the same NetCDF data format. The Level-3 CRDP consists of a gap-free 3D-gridded profile data record at high spatial (1° x 1°) and temporal (daily) resolution, combining data from eight sensors (Aura MLS, OSIRIS, GOMOS, MIPAS, SCIAMACHY, OMPS-LP/SNPP, ACE-FTS, SAGE III/ISS).

A description of data format, sensors, retrieval algorithms and ex-ante uncertainty characterisation can be found in the Product User Guide [RD5], the Algorithm Theoretical Baseline Document [RD4] and the End-to-End ECV Uncertainty Budget [RD6].

5.2 *Harmonized validation methodology*

The validation of the HARMOZ ozone profile datasets is based on comparisons with respect to correlative ground-based measurements. The validation methodology for Level-2 data products (Sect. 5.4) is described extensively by Hubert et al. [RD45], any deviations will be motivated below. Essentially the same method can be applied to the Level-3 LIMB-HIRES products (Sect. 5.5), given their high spatiotemporal resolution. Ground-based observations are acquired at a variety of ozonesonde, lidar and microwave radiometer (MWR) stations performing network operation within WMO's Global Atmosphere Watch (GAW), the Network for the Detection of Atmospheric Composition Change (NDACC) and the Southern Hemisphere Additional Ozonesonde program (SHADOZ).

Results for each of the Ozone_cci+ Level-2 and Level-3 limb profile CRDP are organized as follows

- Study of the co-location sample between HARMOZ and correlative datasets, and a brief discussion of the corresponding validation sample (Level-2 only);
- Presentation and analysis of the comparison results:
    - bias and dispersion as a function of altitude (or pressure), latitude and validation data source;
    - long-term stability over the entire time series as a function of altitude (or pressure);
    - dependence on other parameters, e.g. geophysical, instrument-related or auxiliary (Level-2 only);
    - compliance with user requirements [RD10].

5.3 *Conversion of profile representations*

The native representation of the ozone profile data reported for satellite, ozonesondes, lidars and MWRs differs from each other (see Table 5.1). In order to minimize the number of manipulations of the Ozone_cci+ satellite data records under investigation, the validation analyses are performed –whenever possible– in the reported representation of the satellite ozone data record under study: ozone mole concentration (equivalent to ozone number density) at either fixed altitude (e.g. HARMOZ ALT) or fixed pressure levels (e.g. HARMOZ PRS).

Conversions of ozone partial pressure measurements versus pressure or altitude by ozonesonde into other representations is done using pressure, temperature and (in recent years) GPS altitude measured by the coupled radiosonde. Conversions of lidar ozone number density measurements versus altitude into other representations was done using ancillary pressure and/or temperature information extracted from ERA5 meteorological reanalyses provided by ECMWF. Observations of atmospheric temperature by different ground-based and satellite instruments are quite consistent in the troposphere and lower stratosphere, but they tend to diverge above ~30 km [RD81]. Reanalysis temperature data in middle and upper stratosphere are hence more uncertain, which constitutes a potential non-negligible source of (time-dependent) uncertainty in representation-converted ozone profile data. MWR typically retrieve ozone profiles as volume mixing ratio versus pressure, but number density, altitude and temperature are reported in the data file as well. Several sources of ancillary meteorological data are used throughout the MWR network (NCEP, ECMWF operational, …) which may introduce uncertainty in the converted data sets. For this reason, all MWR validation analyses are performed in the pressure domain.

Table 5.1 summarizes the characteristics of each measurement source. Since the conversion of lidar data uses the same source of auxiliary data (ECMWF reanalysis) as that used for ESA and Third Party Mission data, the analyses remains insensitive to intrinsic deficiencies in the ERA5 data.

Table 5.1 - Characteristics of the satellite and ground-based measurements of the ozone profile. Bold indicates the native representation of the data files. In the case of HARMOZ data, this may differ from the native representation of the satellite ozone retrievals.

	Ozone unit	**Altitude**	**Air pressure**	**Air temperature**
HARMOZ PRS	**Mole concentration**	Retrieved / ERA-Interim / ERA5	**Retrieved / ERA-Interim / ERA5**	Retrieved / ERA-Interim / ERA5
HARMOZ ALT	**Mole concentration**	**Retrieved / ERA-Interim / ERA5**	Retrieved / ERA-Interim / ERA5	Retrieved / ERA-Interim / ERA5
Ozonesonde	**Partial pressure**	Provided	**Measured**	Measured
Stratospheric lidar	**Number density**	**Measured**	ERA5	ERA5
Microwave radiometer	**Volume mixing ratio**	Re/analysis	**Retrieved**	Re/analysis

5.4 *Level-2 limb profile products*

5.4.1 Validation method

The uncertainty of a single ozone profile by ground-based instruments is comparable to that obtained by satellite sensors. Nonetheless, a large sample of co-located satellite and ground-based profiles at numerous stations around the globe, allows us to derive meaningful estimates of systematic error, random uncertainty and long-term stability of the limb/occultation data records. The complementarity of the ozonesonde, lidar and MWR measurement techniques and network design allows further cross-checks which are crucial in achieving a robust assessment of satellite data quality.

As described in detail by Hubert et al. [RD45], the ground-based ozone profile observations are first screened according to the prescriptions by the data producers. Then, pairs of satellite and ground-based profiles that probe sufficiently overlapping air masses are searched for in a ±6 h (MIPAS, Aura-MLS and SABER) or ±12 h time window (all other instruments) and within 500 km radial distance (all instruments). Given the high sampling frequency of MWR instruments, the comparison to MWR profile data is done in a smaller window, less than 300 km and within 1 h or 6 h (depending on MWR station). When more than one satellite profile co-locates with a single ground-based profile, only the closest satellite profile is retained. Tightening the co-location window leaves the bias virtually unchanged and reduces the dispersion in the comparisons by a few percent. In a third step, the ozone unit is converted to mole concentration where necessary, see Section 5.3, after which sonde and lidar measurements are smoothed to the vertical resolution of the satellite data set. To this end, a triangular window function is applied to smoothen each ground-based ozone profile in the altitude domain. The base width of the triangle is equal to the (altitude-dependent) vertical resolution reported along with the co-locating satellite profile. The shape of the window function was found to have a negligible impact on the final conclusions. This smoothing step is omitted for the MWR profiles since their resolution is poorer than that of the satellite data. Finally, the vertically smoothed ground-based profiles are regridded to the fixed altitude or pressure grid of HARMOZ, using the pseudo-inverse interpolation method by Calisesi et al. [RD35]. These pre-processing steps lead to a screened and co-located set of satellite and ground-based profiles in the same ozone coordinate and the same vertical coordinate and grid.

Statistical indicators for the analysis are derived as described in Sections 4.1 and 5.1 of Hubert et al. [RD45]. The selection of sites used for the drift analysis are those mentioned in this paper. The MWR drift analysis only considers data from Mauna Loa and Lauder.

5.4.2 Envisat GOMOS ALGOM2s v1

The results in this section were obtained for Level-2 ALGOM2s version 1, file version 2, for the number density versus altitude profile representation (HARMOZ ALT).

5.4.2.1 Co-locations / Validation sample

Figure 5.1 shows the latitude–time distribution of the ozonesonde, lidar and microwave radiometer (MWR) measurements co-locating with GOMOS ALGOM2s v1 data. The sampling covers most latitude zones and is quite homogeneous in time, except for an interruption of GOMOS operations in the first half of 2005. Most GOMOS polar day profiles were screened out by the retrieval team at FMI, since twilight and bright limb viewing conditions degrade the quality of the retrieved profile.

5.4.2.2 Bias and dispersion

The median bias and half the 68 % interpercentile of the relative difference between GOMOS ALGOM2s v1 and GAW/NDACC/SHADOZ ozonesondes, NDACC lidars or NDACC MWRs are shown in the figures below. Figure 5.2 details the vertical and meridian dependence of the bias and dispersion at 5° latitude resolution, while Figure 5.3 shows the same information calculated in 30° latitude zones.

The median bias is less than 4 % between 20-45 km, except in the Arctic where it reaches -8 to -10 % around 25 km and 28 km. Above the stratopause, GOMOS occultation and MWR data are within 6 %. The meridian structure of the bias in the UTLS follows the meridian structure of the tropopause. Between the tropopause and 20 km the bias is positive in the Southern Hemisphere (5-10 %) and negative at other latitudes (5-15 %). At all latitudes a clear underestimation of ozone can be seen at the tropopause (-15 % or more).

The meridian structure of the dispersion $s_{\Delta x}$ follows that of the tropopause. Above 20-25 km the half IP-68 spread is about 5 % at the equator and increases gradually up to 10-15 % at the poles. Below ~20 km the dispersion increases rapidly, reaching 40 % around 18 km at the equator and around 11 km at the poles. The dispersion seen in the comparisons is a few percent larger than the ex-ante random uncertainty $s_{ex\text{-}ante}$ (not shown here) provided in the GOMOS data files. The latter is 1-4 % above ~20 km and increase rapidly up to 15-25 % at lower levels.

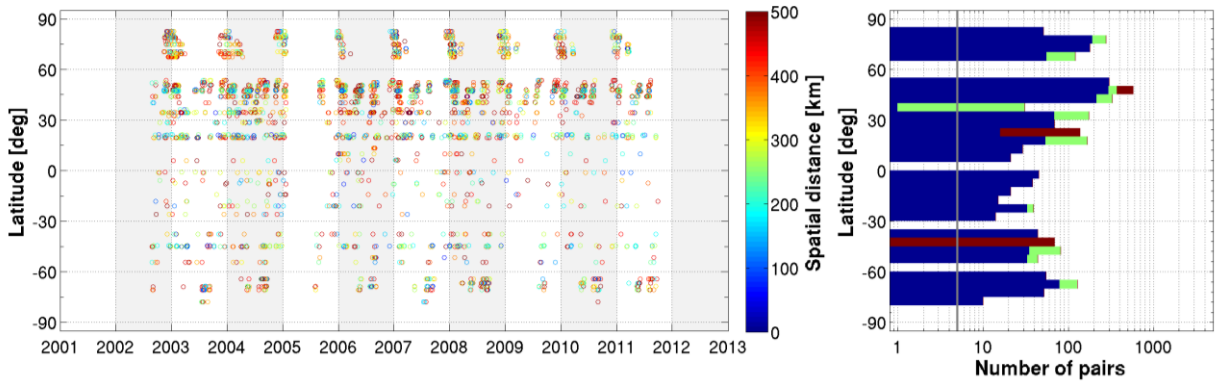

Figure 5.1 - (Left) Latitude–time distribution of co-locations between GOMOS ALGOM2s v1 ozone profiles and ground-based measurements (GAW/NDACC/SHADOZ ozonesonde, NDACC stratospheric ozone lidar and NDACC MWR). The colour code indicates the spatial distance between satellite/ground-based profile. (Right) Number of co-located pairs per 5° latitude band for ozonesonde (blue), lidar (green) and MWR (red).

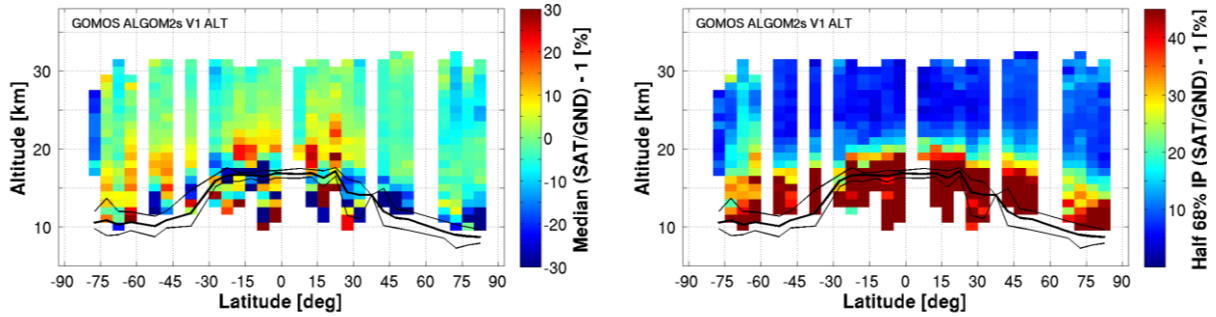

Figure 5.2 - Altitude–latitude cross-section of the median percent bias (left) and of the half IP-68 spread (right) between GOMOS ALGOM2s v1 ozone profile data and the global ozonesonde network, calculated over the entire GOMOS time period and in 5° bins. Black lines indicate the median (thick) and 1σ spread (thin) of the tropopause altitude.

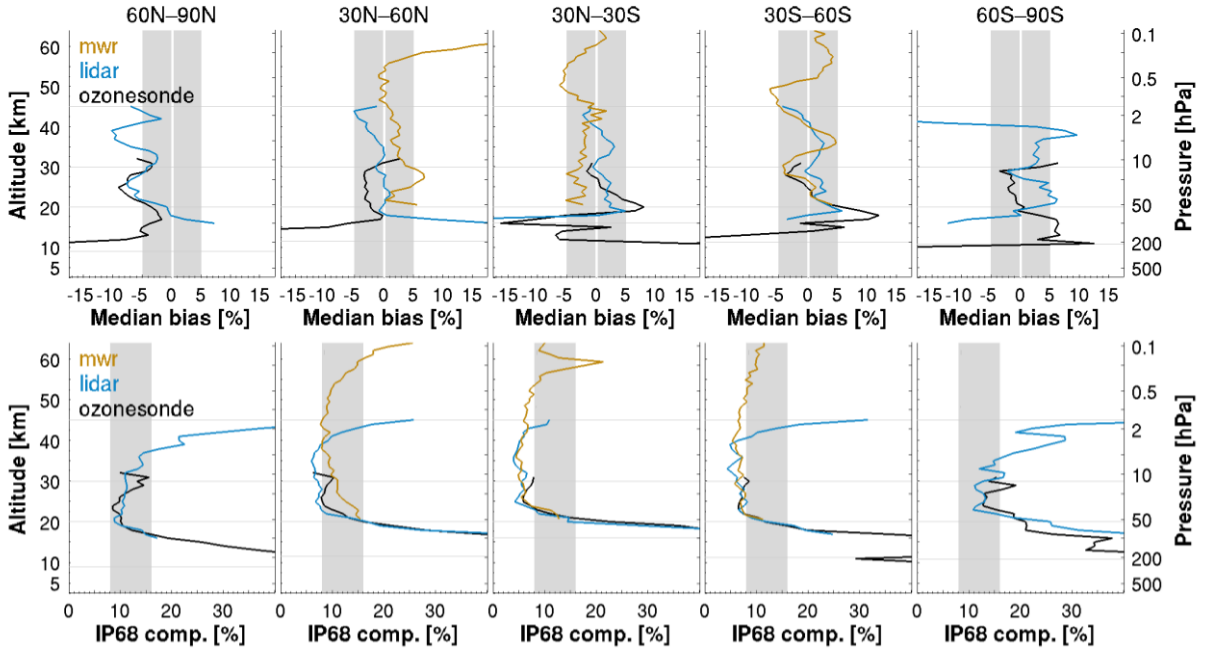

Figure 5.3 - (Top) Median bias between GOMOS ALGOM2s v1 ozone profile data and ozonesonde, lidar and MWR data, by 30° latitude. (Bottom) Same, but for the half IP-68 spread. The lowest horizontal line indicates the median tropopause altitude over the co-location sample.

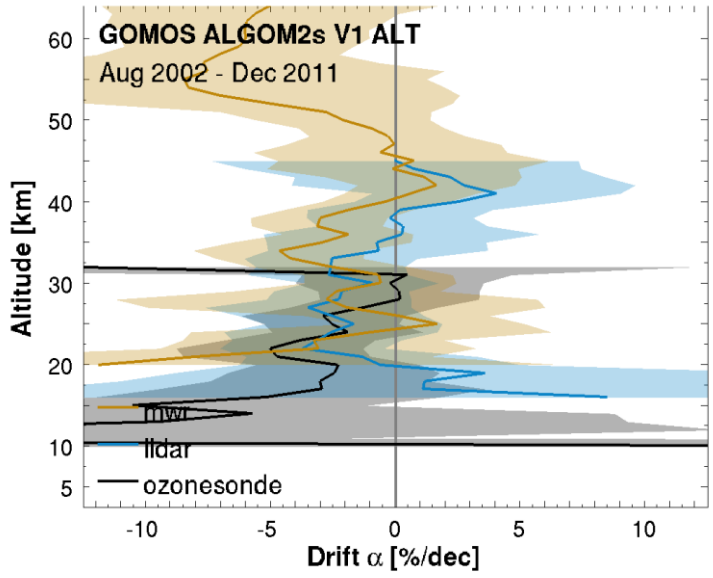

Figure 5.4 - Global network-averaged drift of GOMOS ALGOM2s v1 ozone profile data with respect to ozonesonde, lidar and MWR data, calculated over the 2002-2011 time period. The shaded region represents 2σ uncertainty on the average decadal drift.

5.4.2.3 Long-term stability

Figure 5.4 shows the drift of GOMOS ALGOM2s v1 ozone profile data with respect to co-located ozonesonde, lidar and MWR network data. Drift values are generally insignificant, negative and less than 3 % per decade between ~25-50 km. The -8 % per decade estimate around 55 km may be indicative of decreased stability in the mesosphere, though drift uncertainty is less reliable as only two MWR sites are used and uncertainties arise from the conversion of MWR VMR data to number density. Drift values in the lower stratosphere and UTLS region range from -5 % to -10 % per decade and reach the 2σ threshold for the sonde comparisons between 20-25 km. GOMOS drift relative to lower stratospheric lidar data, on the other hand, remains insignificant and flips sign at 20 km. Below ~20 km the uncertainty of the drift estimates increase rapidly due to increases in measurement noise and atmospheric variability; which explains the difference in sign between sonde and lidar results. This makes it difficult to obtain conclusive results in this part of the atmosphere.

5.4.2.4 Dependence of data quality on other parameters

The dependence of GOMOS ALGOM2s v1 data quality with respect to reference measurements has been studied also as a function of further parameters, including: star magnitude, star temperature, illumination condition, and occultation obliquity. There were no clear signs that the bias or dispersion correlate with any of these parameters. Any apparent dependence turned out to originate mainly from the correlation of the parameter with altitude and latitude.

In addition, the bias, the dispersion and the long-term stability of GOMOS ALGOM2s v1 ozone are in very good agreement in four different profile representations (combinations of altitude/pressure and number density/VMR). This indicates that the auxiliary pressure and temperature profiles included in the GOMOS HARMOZ data files and in the correlative data files are consistent.

5.4.2.5 Compliance with user requirements

From the results reported above it can be concluded that the GOMOS ALGOM2s v1 ozone profile data record is compliant with all but one sampling and resolution requirement. Data quality does not meet the requirements in the lowermost part of the ozone profile, but improves at higher altitudes. User requirements for random uncertainty are met for 60°N-60°S between 25-50 km and for decadal stability between 20-50 km. At lower and higher altitudes there are indications of a negative drift that is not compliant with requirements, though individual results are not significant. Assessing compliance of random uncertainty in polar regions proves challenging due to the unquantified but likely considerable contribution by natural variability to the observed dispersion. As a result, compliance is flagged as not fulfilled over the entire vertical range, even though this may not reflect the actual data quality.

Table 5.2 - Compliance of GOMOS ALGOM2s v1 with user requirements (URD v4.1): full compliance (green), partial compliance (orange) and no compliance (red).

	User requirement	Compliance / evaluation
Horizontal resolution	< 100–300 km	order of 100-250 km [RD91]
Vertical resolution	< 1–3 km	2–3 km
Observation frequency	< 3 days	3 days
Time period	(1980-2010) – (2003-2010)	08/2002 – 12/2011
Total uncertainty in height registration	< ± 500 m	60–150 m
Dependences	–	latitude, altitude

	Lower stratosphere				Middle atmosphere				
Layer [km]	10-15	15-20	20-25	25-30	30-35	35-40	40-45	45-50	50-60
	Uncertainty including only random component								
User requirement	< 8-16 %		< 8 %						
• Arctic			(large natural variability)						
• Mid NH									
• Tropics									
• Mid SH									
• Antarctic	(large natural variability)								
	Long-term stability								
User requirement	< 1-3 % per decade								
• Ground network									

5.4.3 Envisat GOMOS Bright Limb v1.2

The results in this section were obtained for Level-2 Bright Limb processor version 1.2, file version 1, for the number density versus altitude profile representation (HARMOZ ALT).

5.4.3.1 Co-locations / Validation sample

Figure 5.5 shows the latitude–time distribution of the ozonesonde, lidar and MWR measurements co-locating with GOMOS Bright Limb v1.2 data. The sampling covers most latitude zones and is quite homogeneous in time, except a short interruption of GOMOS operations in the first half of 2005. It is well distributed over the time series and over seasons, except at high latitudes during polar night.

5.4.3.2 Bias and dispersion

The median bias and half the 68 % interpercentile range of the relative difference between GOMOS BL v1.2 and GAW/NDACC/SHADOZ ozonesondes, NDACC lidars or NDACC MWRs are shown in the figures below. Figure 5.6 details the vertical and meridian dependence of the bias and dispersion at 5° latitude resolution, while Figure 5.7 show the same information calculated in 30° latitude zones.

GOMOS bright limb ozone data is biased low relative to ground-based data between 25-30 km and the stratopause. The underestimation varies slightly with latitude and becomes clearly larger with increasing altitude until ~40 km, where it reaches -10 % to -15 %. A rapid transition to positive bias values is seen towards the stratopause and extends well into the mesosphere. Below 25-30 km, there is an overestimation of up to 5 % in the Northern Hemisphere and the tropics, but not at more southern latitudes. Our analysis corroborates the findings by [RD89]. We refer to latter publication for a discussion of the origin of the bias structure.

The structure and magnitude of the dispersion is very similar to that of the ALGOM2s data. Below 25-30 km the bright limb data are slightly more noisy than GOMOS occultation data, the dispersion is ~1-2 % larger. The ex-ante uncertainty (not shown here) for both GOMOS data sets is generally very similar, except between 32-40 km and above the stratopause where the expected uncertainty is clearly larger (by ~5-10 %).

Figure 5.5 - (Left) Latitude–time distribution of co-locations between GOMOS Bright Limb v1.2 ozone profiles and ground-based measurements (GAW/NDACC/SHADOZ ozonesonde, NDACC stratospheric ozone lidar and NDACC MWR). The colour code indicates the spatial distance between each satellite/ground-based profile. (Right) Number of co-located pairs per 5° latitude band for ozonesonde (blue), lidar (green) and MWR (red).

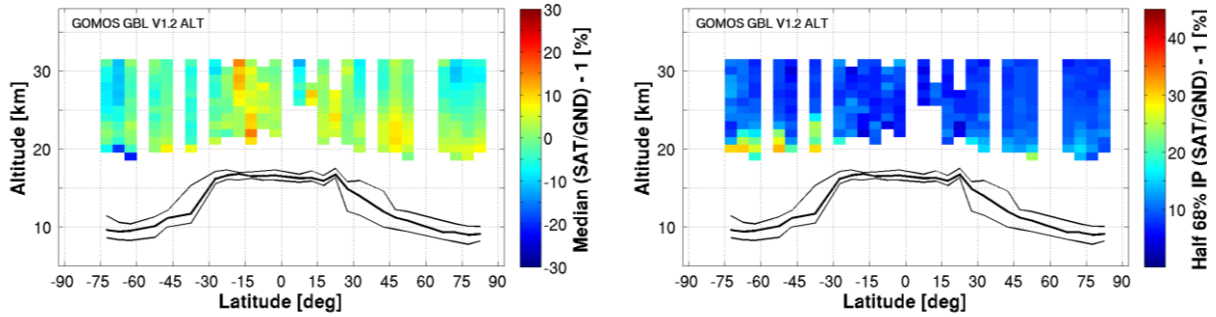

Figure 5.6 - Altitude–latitude cross-section of the median percent bias (left) and of the half IP-68 spread (right) between GOMOS Bright Limb v1.2 ozone profile data and the global ozonesonde network, calculated over the entire GOMOS time period and in 5° bins. Black lines indicate the median (thick) and 1σ spread (thin) of the tropopause altitude.

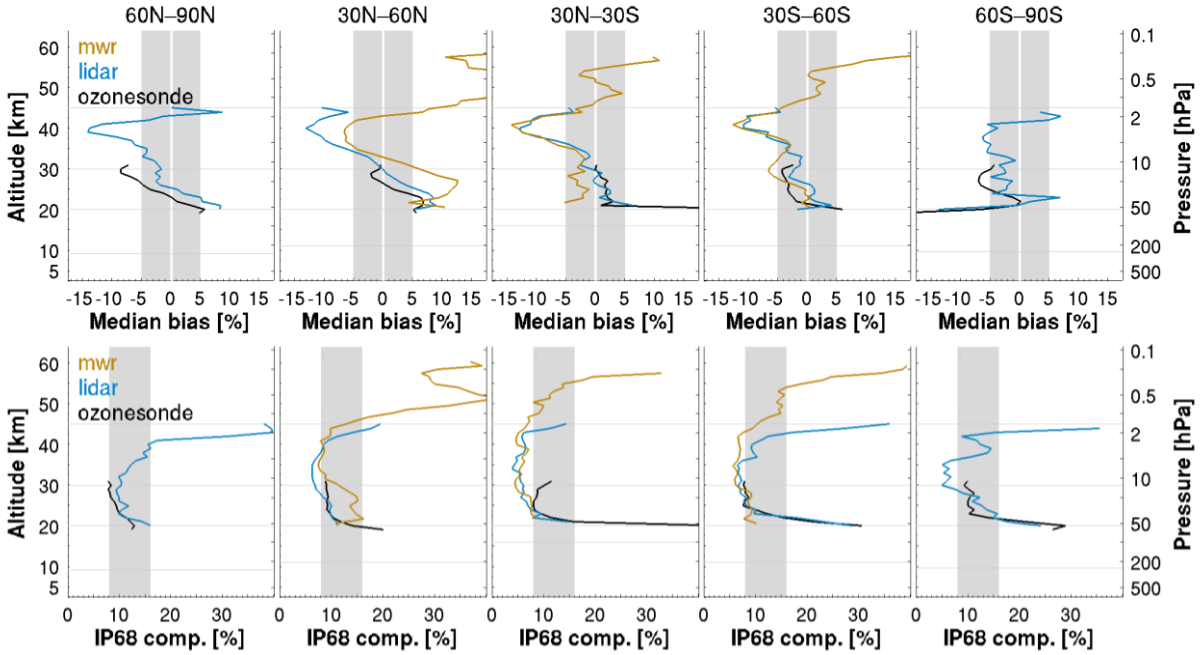

Figure 5.7 - (Top) Median bias between GOMOS Bright Limb v1.2 ozone profile data and ozonesonde, lidar and MWR data, by 30° latitude. (Bottom) Same, but for the half IP-68 spread. The lowest horizontal line indicates the median tropopause altitude over the co-location sample.

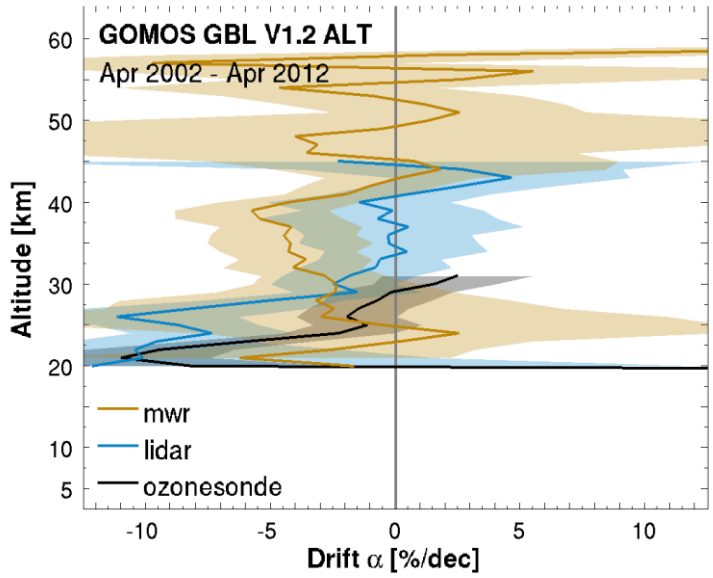

Figure 5.8 - Global network-averaged drift of GOMOS Bright Limb v1.2 ozone profile data with respect to ozonesonde, lidar and MWR data, calculated over the 2002-2012 time period. The shaded region represents 2σ uncertainty on the average decadal drift.

5.4.3.3 Long-term stability

Figure 5.8 shows the drift of GOMOS Bright Limb v1.2 ozone profile data with respect to the co-located ground-based data. The sign of the drift is generally negative between 20-40 km, but quantitative results and significance vary by reference instrument. The most compelling evidence of negative drift is found below ~25 km where both lidar and sonde results are significant. Drift is about -10 % per decade at 21 km and about -1 to -3 % per decade at 30 km. MWR comparisons over this vertical range are noisier but the derived drift is broadly consistent with the other results. The stability between 30-40 km is more difficult to assess given the tension between lidar and MWR results. The former is based on more than a handful of stations and does not show a significant drift. The latter, on the other hand, suggest a significant drift of -4 % per decade. But since that is based on just two sites we are inclined to put more confidence in the lidar results. In the mesosphere no drift is noted either.

5.4.3.4 Dependence of data quality on other parameters

The bias, the dispersion and the long-term stability of GOMOS BL v1.2 ozone are very similar in four different profile representations. This indicates that the auxiliary pressure and temperature profiles included in the GOMOS HARMOZ data files and in the correlative data files are consistent.

5.4.3.5 Compliance with user requirements

From the results reported above it can be concluded that the GOMOS Bright Limb v1.2 ozone profile data record is compliant with most of sampling and resolution requirements. No data are provided in the lower stratosphere, below 20 km. Requirements on random uncertainty are met between 25-40 km and partially slightly above and below. Requirements on decadal stability are met between 30-45 km, at lower altitudes a large negative drift is observed which becomes significant below 25 km. Assessing compliance of random uncertainty in polar regions proves challenging due to the unquantified but likely considerable contribution by natural variability to the observed dispersion. As a result, compliance is flagged as not fulfilled over the entire vertical range in the Arctic, even though this may not reflect the actual data quality.

Table 5.3 - Compliance of GOMOS Bright Limb v1.2 with user requirements (URD v4.1): full compliance (green), partial compliance (orange) and no compliance (red).

	Requirement	Compliance / evaluation
Horizontal resolution	< 100–300 km	300–400 km [RD90]
Vertical resolution	< 1–3 km	2–3 km [RD89]
Observation frequency	< 3 days	3 days
Time period	(1980-2010) – (2003-2010)	04/2002 – 04/2012
Total uncertainty in height registration	< ± 500 m	60–150 m
Dependences	–	latitude, altitude

	Lower stratosphere				Middle atmosphere				
Layer [km]	10-15	15-20	20-25	25-30	30-35	35-40	40-45	45-50	50-60
	Uncertainty including only random component								
User requirement	< 8-16 %		< 8 %						
• Arctic			(large natural variability)						
• Mid NH									
• Tropics									
• Mid SH									
• Antarctic									
	Long-term stability								
User requirement	< 1-3 % per decade								
• Ground network									

5.4.4 Envisat MIPAS IMK/IAA v8

The results in this section were obtained for Level-2 IMK/IAA version 8, file version 2, for the number density versus altitude profile representation (HARMOZ ALT). Validation results for an earlier processor version (v7) of the MIPAS IMK/IAA data set can be found in the Appendix of this document.

The Ozone_cci+ Level-2 CRDP includes MIPAS nominal mode observations acquired at full spectral resolution between July 2002 and March 2004 (L2 processor version V8H_O3_61) and at reduced spectral resolution between January 2005 and April 2012 (L2 processor version V8R_O3_261). There is an (altitude-dependent) bias between MIPAS O3 retrievals in both periods, which is why the validation analysis is differentiates each period.

5.4.4.1 Co-locations / Validation sample

Figure 5.9 shows the latitude–time distribution of the ozonesonde, lidar and MWR measurements co-locating with MIPAS nominal mode measurements for the full spectral resolution period (2002-2004) and the reduced spectral resolution period (2005-2012). The sampling covers most latitude bands and is homogeneous in time, except for an interruption of operations in 2004 and the reduced duty cycle during 2005-2006.

5.4.4.2 Bias and dispersion

The median bias and half the 68 % interpercentile range of the relative difference between MIPAS IMK-IAA v8 and GAW/NDACC/SHADOZ ozonesondes, NDACC lidars or NDACC MWRs are shown in the figures below. Figure 5.10 details the vertical and meridian dependence of the bias and dispersion at 5° latitude resolution, while Figure 5.11 and Figure 5.12 show the same information calculated in 30° latitude zones for both periods.

MIPAS bias differs considerably for both periods with a sign and magnitude that is altitude-dependent. Compared to the 2005-2012 data, ozone values during 2002-2004 are up to 5 % larger below 20-25 km and up to 5 % smaller at higher altitudes. A positive bias of 4-8 % relative to ground-based measurements is seen for both periods in the middle and upper stratosphere. It typically transitions to negative values in the lowermost stratosphere and around the stratopause. Below the tropopause vertical oscillations (10 % and more, peak to peak) are noted in the bias profile relative to ozonesonde.

The meridian structure of the dispersion $s_{\Delta x}$ is similar for both periods and follows at first order the meridian structure of the tropopause. In the middle and upper stratosphere the dispersion is about 4 % at the equator, and increases to 8-10 % at the poles. Dispersion increases rapidly below 20 km, reaching 40 % right above the tropopause. The dispersion seen in the comparisons is several percent larger than the ex-ante random uncertainty $s_{ex\text{-}ante}$ provided in the MIPAS data files (not shown here). The latter is 2-8 % in the mesosphere, 1-2 % in the stratosphere and rapidly increases below 20 km altitude to 20-30 % in the upper troposphere.

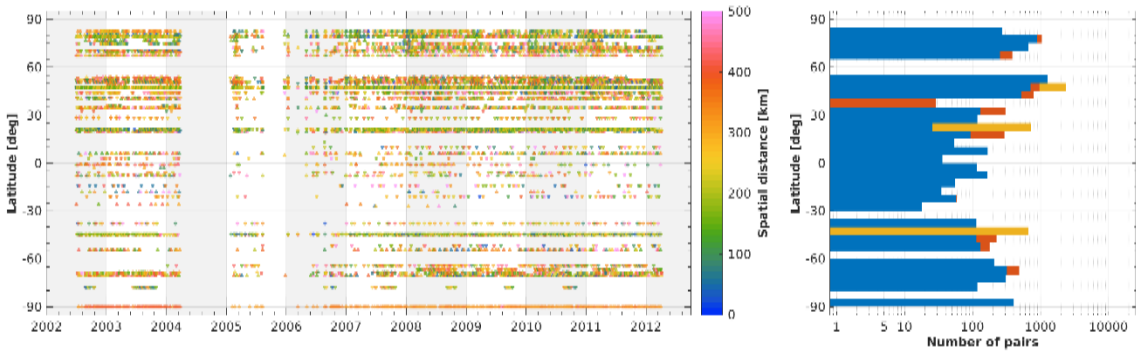

Figure 5.9 - (Left) Latitude–time distribution of co-locations between MIPAS IMK-IAA v8 ozone profiles and ground-based measurements (GAW/NDACC/SHADOZ ozonesonde, NDACC stratospheric ozone lidar and NDACC microwave radiometer). The colour code indicates the spatial distance of each satellite/ground-based pair. (Right) Number of co-located pairs per 5° latitude band for ozonesonde (blue), lidar (red) and MWR (orange).

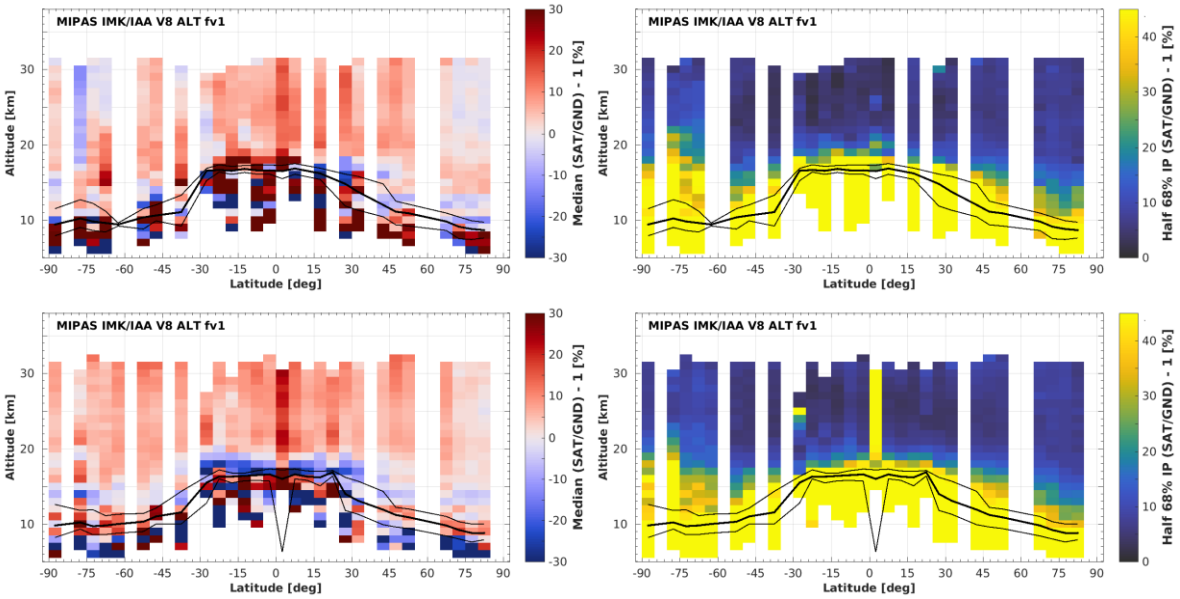

Figure 5.10 - Altitude–latitude cross-section of the median percent bias (left) and of the half IP-68 spread (right) between MIPAS IMK-IAA v8 ozone profile data and the global ozonesonde network, calculated over the 2002-2004 (top row) and 2005-2012 (bottom) time periods and in 5° bins. Black lines indicate the median (thick) and 1σ spread (thin) of the tropopause altitude.

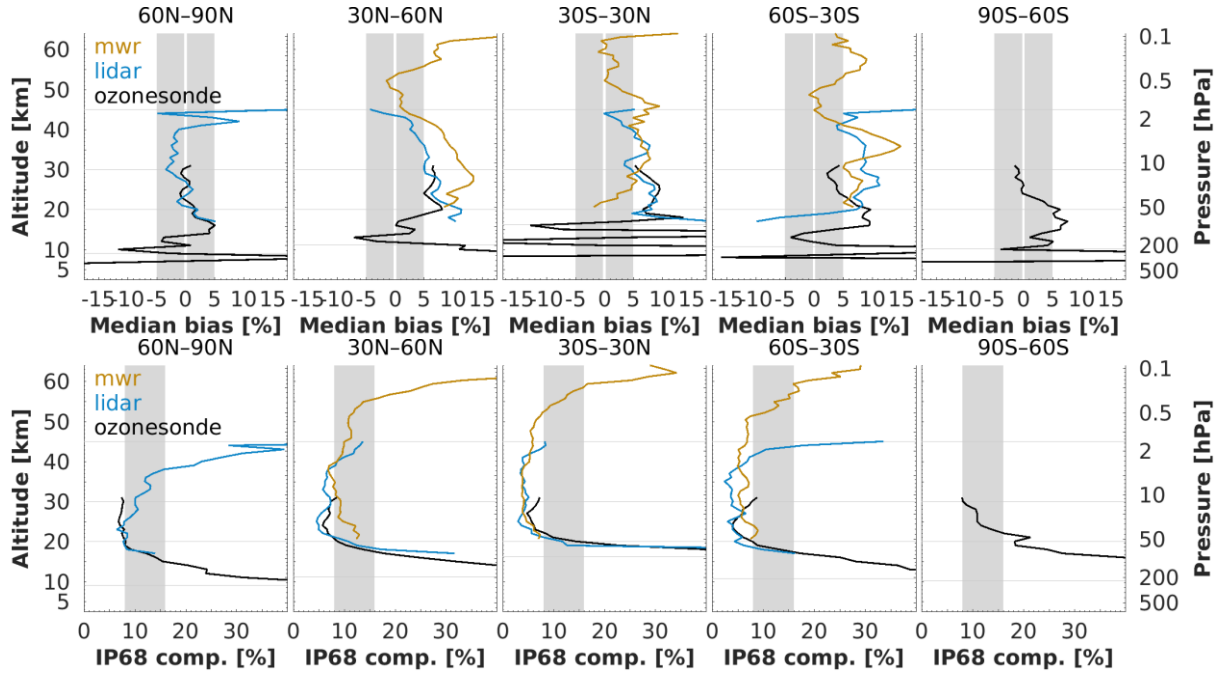

Figure 5.11 - (Top) Median bias between MIPAS IMK-IAA v8 (2002-2004) ozone profile data and ozonesonde, lidar and MWR data, by 30° latitude. (Bottom) Same, but for the half IP-68 spread. The lowest horizontal line indicates the median tropopause altitude over the co-location sample.

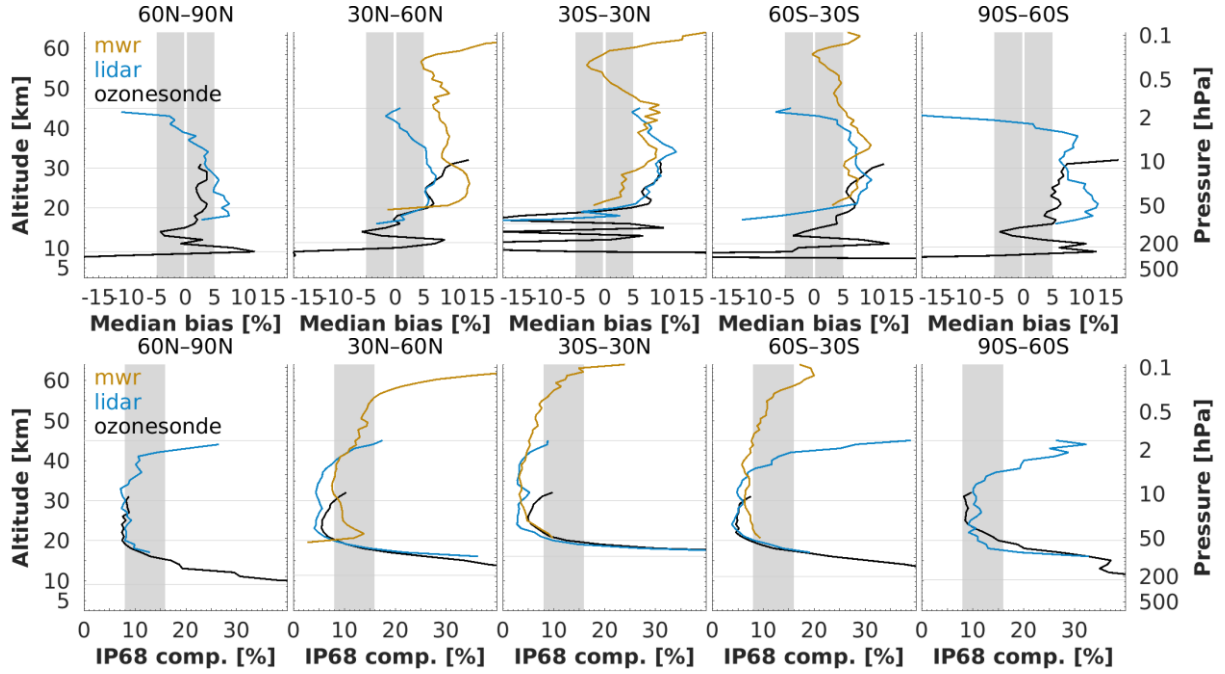

Figure 5.12 - As Figure 5.11, but for MIPAS data during the 2005-2012 period.

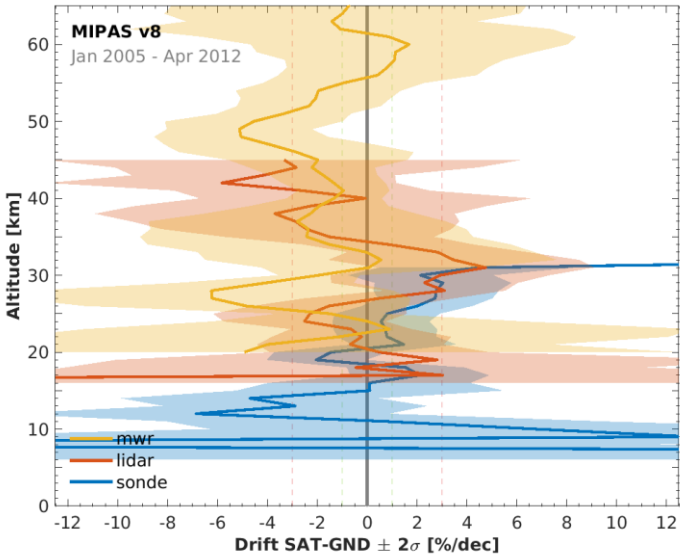

Figure 5.13 - Global network-averaged drift of MIPAS IMK-IAA v8 ozone profile data with respect to ozonesonde, lidar and MWR data, calculated for the 2005-2012 time period. The shaded region represents 2σ uncertainty on the average decadal drift.

5.4.4.3 Long-term stability

Figure 5.13 shows the drift estimates of MIPAS IMK-IAA v8 ozone profile data with respect to the co-located ozonesonde, lidar and MWR network data. The 2002-2004 period is not taken into account since it is too short for trend studies and, more importantly, the bias between the periods introduces artefacts when not accounted for in the regression [RD38]. Drift estimates between 15-40 km are insignificant and less than ±2 % per decade. Below 15 km, results from comparison to ozonesonde are statistically consistent with a no-drift hypothesis. Comparison to lidar and microwave radiometers, on the other hand, hint at a negative MIPAS drift of 3-4 % per decade in the uppermost stratosphere and lower mesosphere. However, above 40 km altitude, the drift estimates are, either, not well constrained due to considerable station-to-station variability (lidar), or, they are possibly overestimated as a result of too few stations (MWR). We advise caution to MIPAS users who require stable measurements above 40 km.

5.4.4.4 Dependence of data quality on other parameters

Further parameters which possibly impact the MIPAS data quality were studied, including the retrieval output parameters chi2 (normalized chi-square of retrievals), rms (root mean square of residual spectra) and DoF (degrees of freedom of target retrieval). There were no clear signs that the bias or dispersion correlates with any of these parameters. Any apparent dependence turned out to originate mainly from the correlation of the parameter with altitude and latitude.

The bias, the dispersion and the long-term stability of MIPAS ozone are very similar in four different profile representations (not shown here). This indicates that the auxiliary pressure and temperature profiles included in the MIPAS HARMOZ data files and in the correlative data files are consistent.

5.4.4.5 Compliance with user requirements (2005-2012 period)

From the results reported above it can be concluded that the MIPAS IMK-IAA v8 limb ozone profile data record is (nearly) compliant with most of sampling and resolution requirements. Data quality does not meet the requirements in the lowermost part of the ozone profile, below 15 km. The random uncertainty meets the 8 % or 8-16 % requirement between 20 and 40-50. The stability of the MIPAS data record over 2005-2012 complies with the requirement over most of the profile. Assessing compliance of random uncertainty in polar regions proves challenging due to the unquantified but likely considerable contribution by natural variability to the observed dispersion. As a result, compliance is flagged as not fulfilled over the part of the vertical range, even though this may not reflect the actual data quality.

Table 5.4 - Compliance of MIPAS IMK-IAA v8 (2005-2012 period) with user requirements (URD v4.1): full compliance (green), partial compliance (orange) and no compliance (red).

	Requirement	Compliance / evaluation
Horizontal resolution	< 100–300 km	200–400 km [RD94]
Vertical resolution	< 1–3 km	2.5–5 km [RD58]
Observation frequency	< 3 days	3 days
Time period	(1980-2010) – (2003-2010)	07/2002 – 04/2012
Total uncertainty in height attribution	< ± 500 m	[RD53]
Dependences	–	latitude, altitude

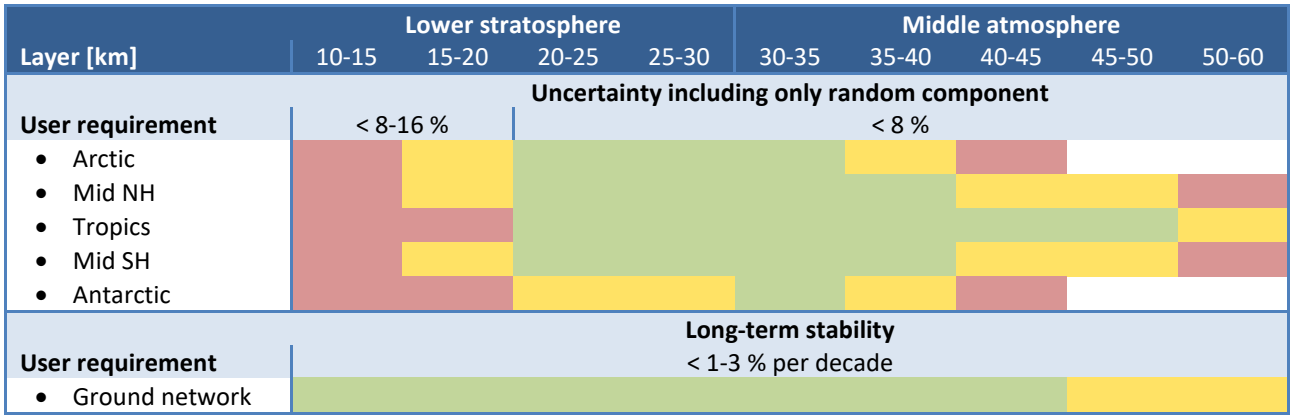

5.4.5 Envisat SCIAMACHY UBr v3.5

The results in this section were obtained for Level-2 UBr version 3.5, file version 5, for the number density versus altitude profile representation (HARMOZ ALT).

5.4.5.1 Co-locations / Validation sample

Figure 5.14 shows the latitude–time distribution of the ozonesonde, lidar and MWR measurements co-locating with the SCIAMACHY UBr v3.5 dataset. The sampling is very dense and covers all but the highest latitude zones. It is well distributed over the entire time series and over seasons, except poleward of 70° latitude where SCIAMACHY cannot observe the dark limb during polar night.

5.4.5.2 Bias and dispersion

The median bias and half the 68 % interpercentile of the relative difference between SCIAMACHY UBR v3.5 and GAW/NDACC/SHADOZ ozonesondes, NDACC lidars or NDACC MWRs are shown in the figures below. Figure 5.15 details the vertical and meridian dependence of the bias and dispersion at 5° latitude resolution, while Figure 5.16 show the same information calculated in 30° latitude zones.

Sonde and lidar comparisons show a very coherent picture of SCIAMACHY bias. It is generally less than 5 % between 20-30 km, positive southward of 30°S and positive elsewhere. Above 30 km, all lidar and MWR results indicate an increasing positive bias with altitude which peaks at 10-15 % around the stratopause. In the mesosphere, the slope of the bias profile changes sign at all four MWR sites considered. In the UTLS and below, a negative bias of ~10 % is found in the tropics and Arctic; at other latitudes a 10 % overestimation is noted.

The meridian structure of the dispersion $s_{\Delta x}$ in comparisons of SCIAMACHY to ground-based data is quite common. In the middle and upper stratosphere the dispersion is generally about 5 % at the equator, but increases gradually to 10 % at the poles. In the lower stratosphere the dispersion increases rapidly, reaching 40 % around 16 km at the equator and around 9 km at higher latitudes. The ex-ante random uncertainties $s_{ex\text{-}ante}$ provided in the SCIAMACHY record (not shown here) are 2-3 % above 20 km.

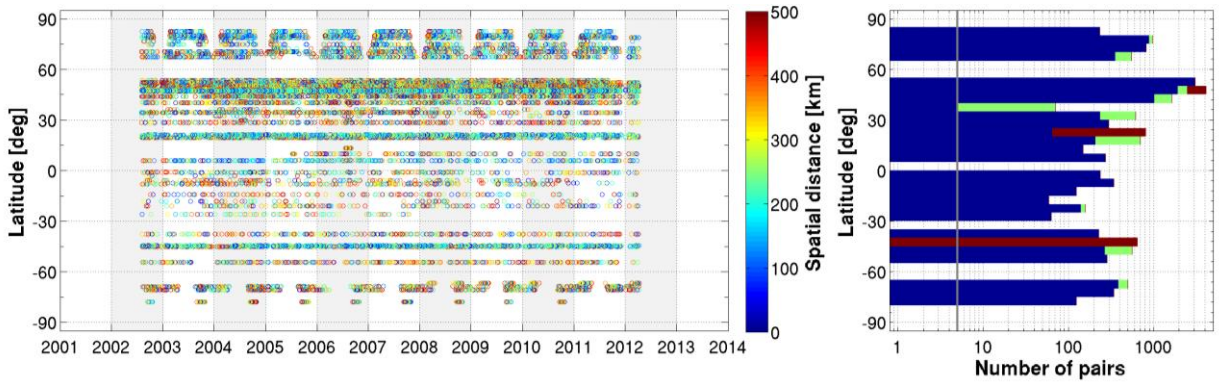

Figure 5.14 - (Left) Latitude–time distribution of co-locations between SCIAMACHY UBr v3.5 ozone profiles and ground-based measurements (GAW/NDACC/SHADOZ ozonesonde, NDACC stratospheric ozone lidar and NDACC MWR). The colour code indicates the spatial distance of each satellite/ground-based pair. (Right) Number of co-located pairs per 5° latitude band for ozonesonde (blue), lidar (green) and MWR (red).

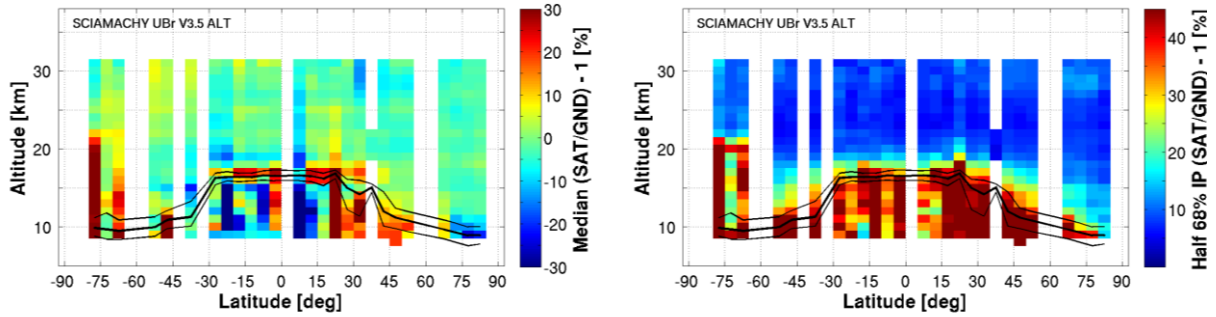

Figure 5.15 - Altitude–latitude cross-section of the median percent bias (left) and of the half IP-68 spread (right) between SCIAMACHY UBr v3.5 ozone profile data and the global ozonesonde network, calculated over the entire SCIAMACH time period and in 5° bins. Black lines indicate the median (thick) and 1σ spread (thin) of the tropopause altitude.

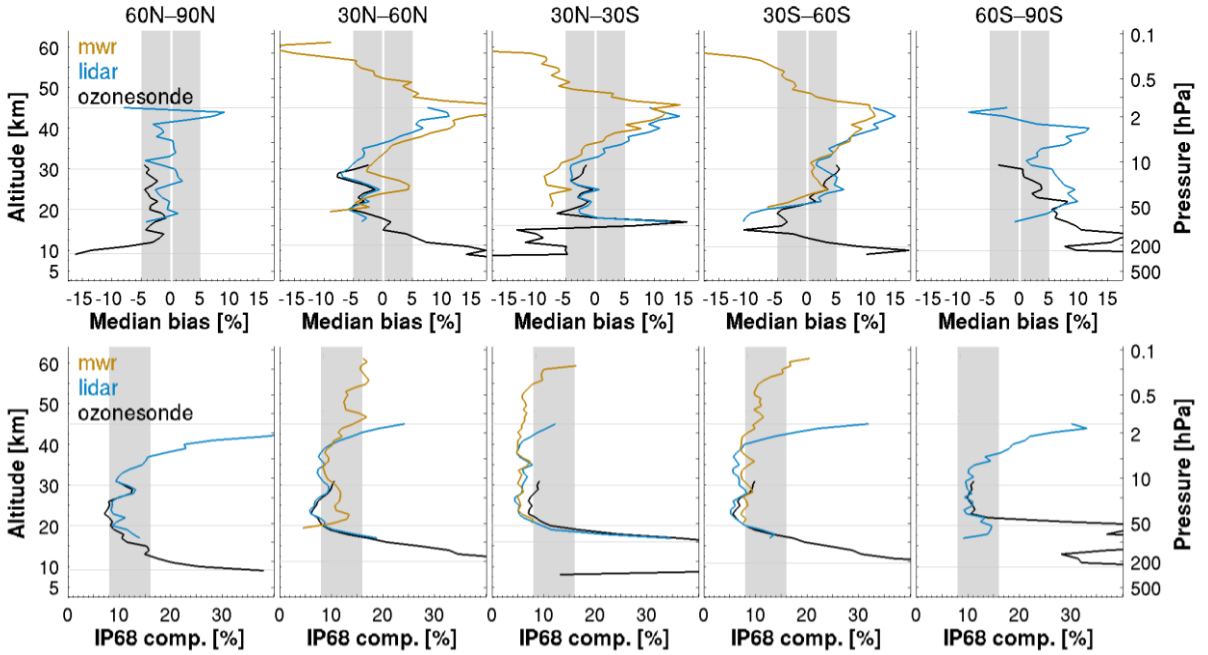

Figure 5.16 - (Top) Median bias between SCIAMACHY UBr v3.5 ozone profile data and ozonesonde, lidar and MWR data, by 30° latitude. (Bottom) Same, but for the half IP-68 spread. The lowest horizontal line indicates the median tropopause altitude over the co-location sample.

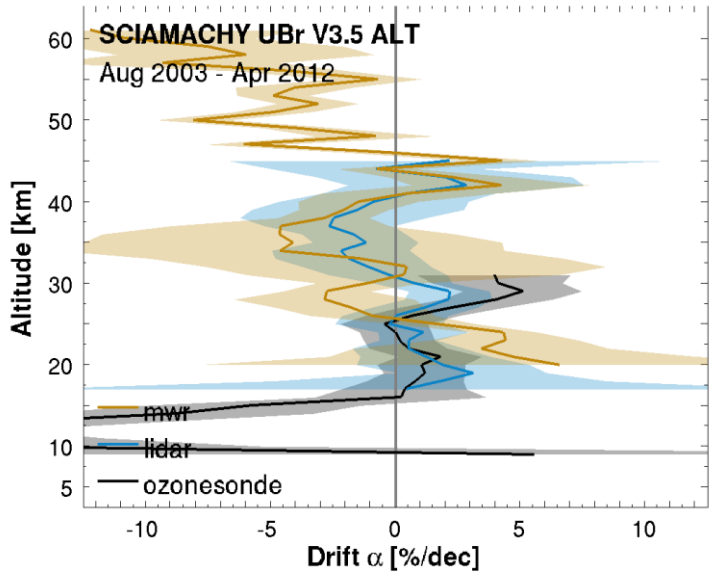

Figure 5.17 - Global network-averaged drift of SCIAMACHY UBr v3.5 ozone profile data with respect to ozonesonde, lidar and MWR network data, calculated over the 2003-2012 time period. The shaded region represents 2σ uncertainty on the average decadal drift.

5.4.5.3 Long-term stability

Pointing problems in the first year of SCIAMACHY operations may have led to reduced stability of the ozone profile data record. Here, we follow the suggestion by Sofieva et al. (2017, [RD84]) to exclude measurements before August 2003 from the analysis. Figure 5.17 shows that the stability of the screened SCIAMACHY UBr v3.5 ozone profile data record (Aug 2003 – Apr 2012) is better than 3 % per decade over a large part of the stratosphere. There are indications of negative drift of more than 5 % per decade below 15 km, above 45 km and perhaps around 35 km. However, significance may be either underestimated (mesosphere, only two MWR sites) or insufficient but with good agreement for both reference records (middle stratosphere). The most convincing sign of instability is in the UTLS, with a negative drift of more than 10 % per decade between 10-15 km.

5.4.5.4 Dependence of data quality on other parameters

Further parameters which possibly impact the SCIAMACHY data quality were studied, including solar zenith angle. There were no clear signs that the bias or dispersion correlate with this parameter. Any apparent dependence turned out to originate mainly from the correlation of the parameter with altitude and latitude.

The bias, the dispersion and the long-term stability of SCIAMACHY ozone are very similar in four different profile representations (not shown here). This indicates that the auxiliary pressure and temperature profiles included in the SCIAMACHY HARMOZ data files and in the correlative data files are consistent.

5.4.5.5 Compliance with user requirements

The SCIAMACHY record is nearly compliant with most sampling and resolution requirements. The data quality does not meet the requirements in the lowermost part of the ozone profiles, but improves at higher altitudes. The target on random uncertainty is reached around 15-20 km. Stability is compliant with requirements between 15-30 km and partially in parts of the upper stratosphere. Assessing compliance of random uncertainty in polar regions proves challenging due to the unquantified but likely considerable contribution by natural variability to the observed dispersion. As a result, compliance is flagged as not fulfilled over large part of the polar atmosphere, even though this may not reflect the actual data quality.

Table 5.5 - Compliance of SCIAMACHY UBr v3.5 with user requirements (URD v4.1): full compliance (green), partial compliance (orange) and no compliance (red).

	Requirement	Compliance / evaluation
Horizontal resolution	< 100–300 km	300–400 km [RD90]
Vertical resolution	< 1–3 km	4–5 km
Observation frequency	< 3 days	6 days
Time period	(1980-2010) – (2003-2010)	08/2002 – 04/2012
Total uncertainty in height attribution	< ± 500 m	± 200 m [RD95; RD33]
Dependences	–	latitude, altitude

	Lower stratosphere				Middle atmosphere				
Layer [km]	10-15	15-20	20-25	25-30	30-35	35-40	40-45	45-50	50-60
	Uncertainty including only random component								
User requirement	< 8-16 %		< 8 %						
• Arctic									
• Mid NH									
• Tropics									
• Mid SH									
• Antarctic	(large natural variability)								
	Long-term stability								
User requirement	< 1-3 % per decade								
• Ground network									

5.4.6 Odin OSIRIS v7.3

The results in this section were obtained for Level-2 SaskMART version 7.3, file version 1, for the number density versus altitude profile representation. Validation results for an earlier processor version (v5.10) of the OSIRIS data set can be found in the Appendix of this document (HARMOZ ALT).

5.4.6.1 Co-locations / Validation sample

Figure 5.18 shows the latitude–time distribution of the ozonesonde, lidar and MWR measurements co-locating with the OSIRIS v7.3 dataset. The co-locations cover most latitude zones and are reasonably well distributed over the time series, except the winter hemisphere where OSIRIS cannot observe the dark limb. Since about 2012 and, especially, 2019 OSIRIS operates in progressively reduced duty cycle in order to extend the lifetime of the mission. This yields much fewer comparisons in recent years.

5.4.6.2 Bias and dispersion

The median bias and half the 68 % interpercentile of the relative difference between OSIRIS v7.3 and GAW/NDACC/SHADOZ ozonesondes, NDACC lidars or NDACC MWRs are shown in the figures below. Figure 5.19 details the vertical and meridian dependence of the bias and dispersion at 5° latitude resolution, while Figure 5.20 shows the same information calculated in 30° latitude zones.

Negative biases are found in the lowermost stratosphere (5-12 %) and the tropical troposphere (more than 30 %). Around 20 km the bias changes to a positive sign and a local maximum appears around 22 km; it amounts to +3-5 % and up to +8 % at mid-latitudes in the SH. This bump, which is a few % more pronounced than that noted in earlier OSIRIS data versions, is supposedly related to a bias in the aerosol retrievals that serve as input to the ozone retrieval [RD25, RD26]. Between 30-45 km bias is generally positive (except in Arctic) and remains mostly less than 5 %. Above the stratopause, the sign of OSIRIS bias with respect to MWR is unclear. It is negative at two sites and positive at two other sites. The magnitude is less than 8 % up to 50 km.

The general structure of the dispersion $s_{\Delta x}$ follows that of the tropopause. Between 20-50 km, the dispersion is about 5-8 % at the equator, and increases gradually to ~10 % at the poles. Below 20 km, the dispersion increases rapidly, reaching 35 % around 16 km in the tropics and around 10-13 km at higher latitudes. The dispersion seen in the comparisons is a few percent larger than the ex-ante random uncertainty $s_{ex\text{-}ante}$ provided in the OSIRIS record (not shown here). The latter is about 2-3 % above 20 km and rapidly increases to ~15 % around the tropopause.

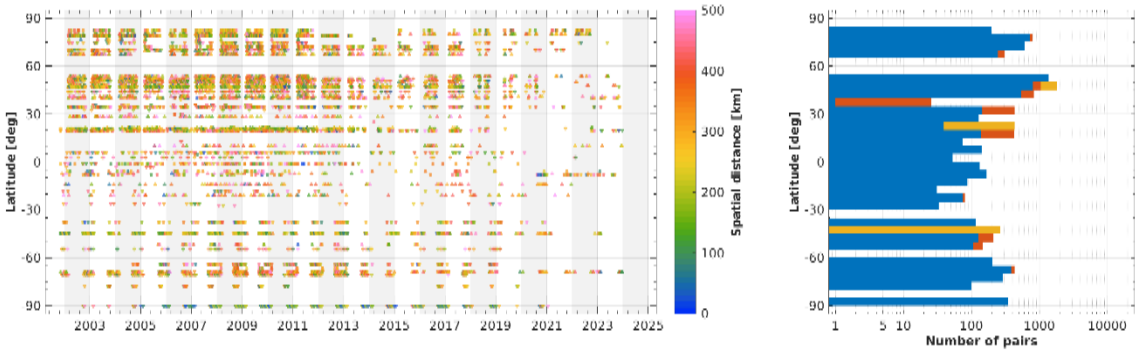

Figure 5.18 - (Left) Latitude–time distribution of co-locations between OSIRIS v7.3 ozone profiles and ground-based measurements (GAW/NDACC/SHADOZ ozonesonde, NDACC stratospheric ozone lidar and NDACC MWR). The colour code indicates the spatial distance of each satellite/ground-based pair. (Right) Number of co-located pairs per 5° latitude band for ozonesonde (blue), lidar (red) and MWR (orange).

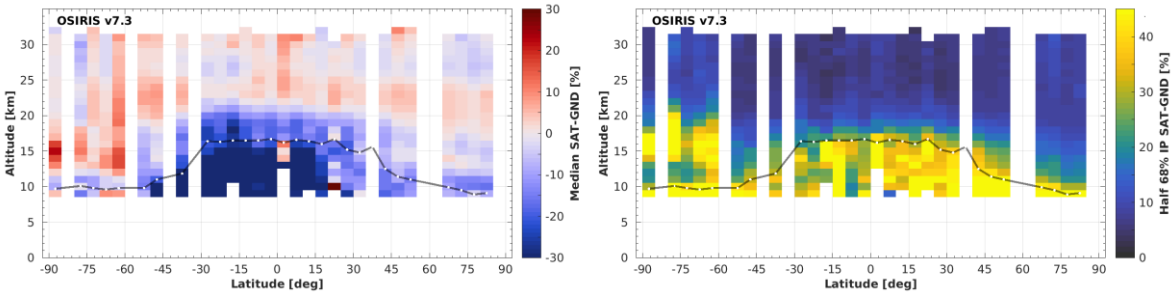

Figure 5.19 - Altitude–latitude cross-section of the median percent bias (left) and of the half IP-68 spread (right) between OSIRIS v7.3 ozone profile data and the global ozonesonde network, calculated over the entire OSIRIS time period and in 5° bins. The black line indicates the median tropopause altitude.

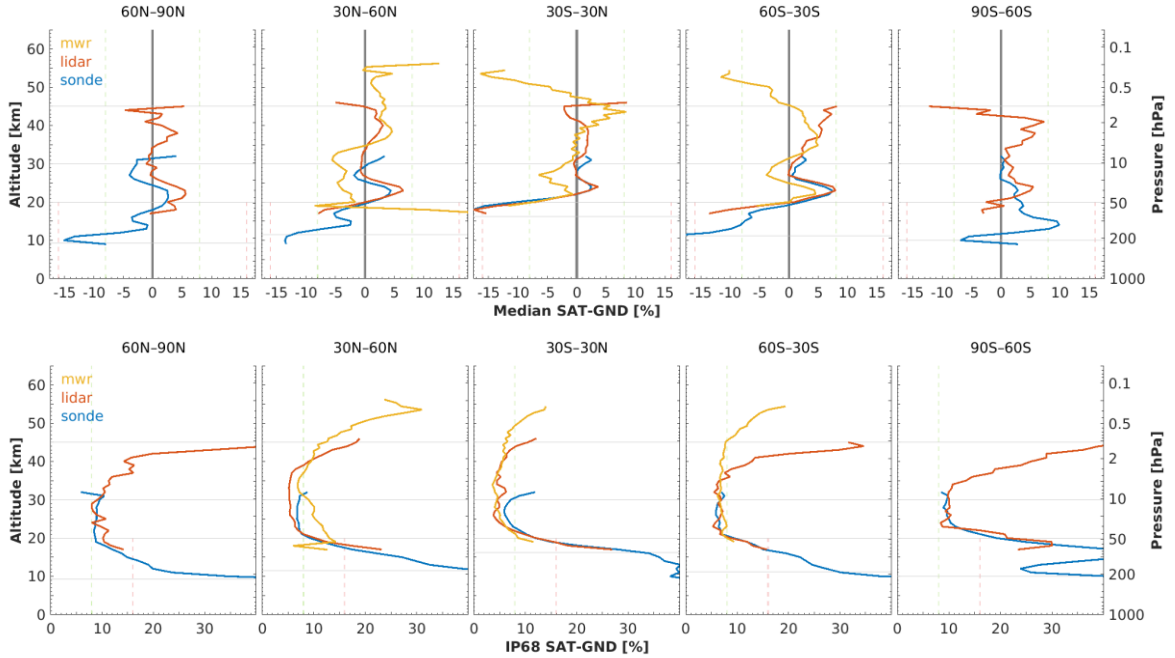

Figure 5.20 - (Top) Median bias between OSIRIS v7.3 ozone profile data and ozonesonde, lidar and MWR data, by 30° latitude. (Bottom) Same, but for the half IP-68 spread. The lowest horizontal line indicates the median tropopause altitude over the co-location sample.

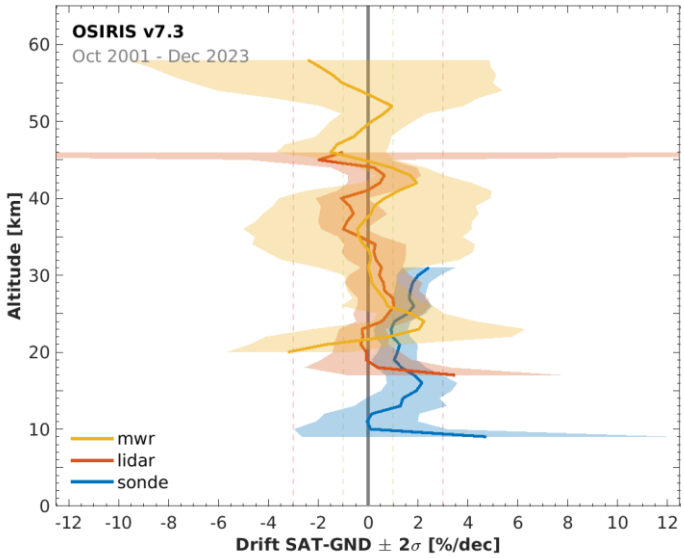

Figure 5.21 - Global network-averaged drift of OSIRIS v7.3 ozone profile data with respect to ozonesonde, lidar and MWR data, calculated over the 2001-2023 time period. The shaded region represents 2σ uncertainty on the average drift.

5.4.6.3 Long-term stability

Figure 5.21 shows the vertical structure of the decadal drift of OSIRIS v7.3 with respect to co-located ground-based data [RD30]. The two peaks in the drift profile (at 35 km and 43 km) noted for OSIRIS v5.10 have mostly disappeared in the v7.3 comparisons. The stability of the present version of OSIRIS is better than ±2 %/decade across the entire vertical domain. While the +1-2 %/decade drift estimated from the ozonesonde analysis is statistically significant, it remains close to the goal requirement and within the GCOS 2022 breakthrough requirements by GCOS (2022).

5.4.6.4 Dependence of data quality on other parameters

The bias, the dispersion and the long-term stability of OSIRIS ozone are very similar in four different profile representations. This indicates that the auxiliary pressure and temperature profiles included in the OSIRIS HARMOZ data files and in the correlative data files are consistent.

5.4.6.5 Compliance with user requirements

The OSIRIS v7.3 data record is nearly compliant with most of sampling and resolution requirements. The long-term stability of the OSIRIS record complies with user requirements over the entire profile. Random uncertainty generally meets the requirement between 20 km and the stratosphere, except in the polar regions. Assessing compliance of random uncertainty in polar regions proves challenging due to the unquantified but likely considerable contribution by natural variability to the observed dispersion. As a result, compliance is flagged as not fulfilled over the entire vertical range, even though this may not reflect the actual data quality.

Table 5.6 - Compliance of OSIRIS v7.3 with user requirements (URD v4.1): full compliance (green), partial compliance (orange) and no compliance (red).

	Requirement	Compliance / evaluation
Horizontal resolution	< 100–300 km	300–400 km [RD90]
Vertical resolution	< 1–3 km	2–4 km
Observation frequency	< 3 days	less frequent before June 2007 and since 2012/2019
Time period	(1980-2010) – (2003-2010)	11/2001 – 12/2023
Total uncertainty in height attribution	< ± 500 m	< ± 400 m [RD69]
Dependences	–	latitude, altitude

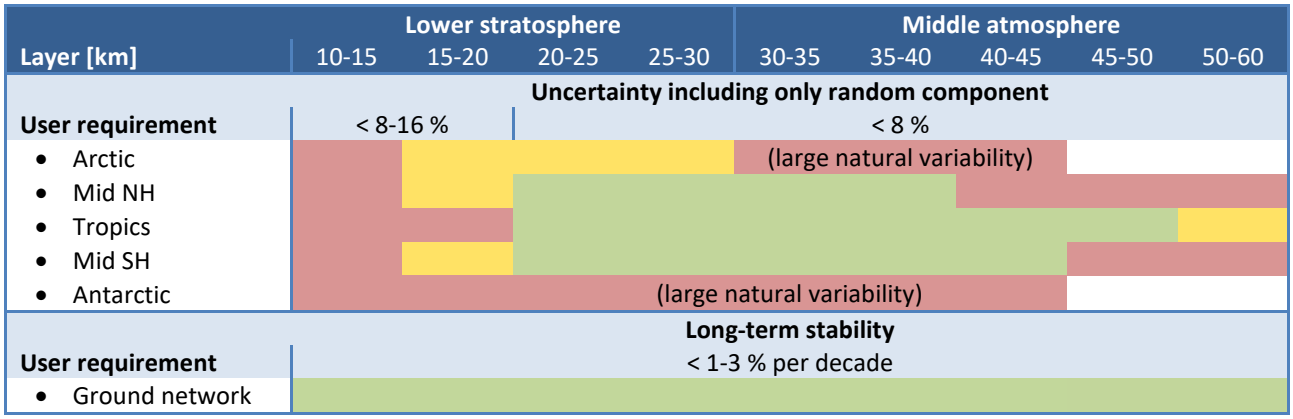

5.4.7 SCISAT-1 ACE-FTS v4.1/v4.2

The results in this section were obtained for Level-2 processor version 4.1/v4.2, file version 1, for the number density versus altitude profile representation (HARMOZ ALT). Validation results for an earlier processor version (v3.5/v3.6) of the ACE-FTS data set can be found in the Appendix of this document.

5.4.7.1 Co-locations / Validation sample

Figure 5.22 shows the latitude–time distribution of the ozonesonde, lidar and MWR measurements co-locating with the ACE-FTS v4.1/v4.2 dataset. The sampling is quite well distributed over the time series. Due to the 75° inclination orbit and the solar occultation mode mainly the polar regions and the middle latitudes are covered. Although the comparison statistics at tropical sites is limited it is possible to obtain some information by considering the entire tropical belt.

5.4.7.2 Bias and dispersion

The median bias and half the 68 % interpercentile of the relative difference between ACE-FTS v4.1/v4.2 and GAW/NDACC/SHADOZ ozonesondes, NDACC lidars or NDACC MWRs are shown in the figures below. Figure 5.23 details the vertical and meridian dependence of the bias and dispersion at 5° latitude resolution, while Figure 5.24 shows the same information calculated in 30° latitude zones.

ACE-FTS v4.1/v4.2 biases are generally positive and exhibit a pronounced vertical structure. Local minima are noted around 17-20 km (0 %) and around 35-42 km (+5-7 %). Local maxima are seen close to the tropopause (+7-10 %), around 30 km (+8-12 %) and around 50-55 km (+13-20 %). Biases may become negative in the polar upper stratosphere, although constraints are challenging in this region due to the limited number of lidar sites and their operation is limited to polar night.

The dispersion $s_{\Delta x}$ has similar behaviour as for most HARMOZ data sets. In the middle and upper stratosphere the dispersion is 3-5 % at mid latitudes and increases to 6-8 % towards the poles. In the Antarctic the variability is somewhat larger due to the occurrence of the ozone hole. Below 20 km, the dispersion increases rapidly, reaching 40 % at the tropopause. The dispersion seen in the comparisons is a few percent larger than the ex-ante random uncertainty $s_{ex\text{-}ante}$ provided in the ACE-FTS record (not shown here). The latter is of the order of 1-2 % above 20 km and increase up to 10-15 % in the UTLS and upper troposphere.

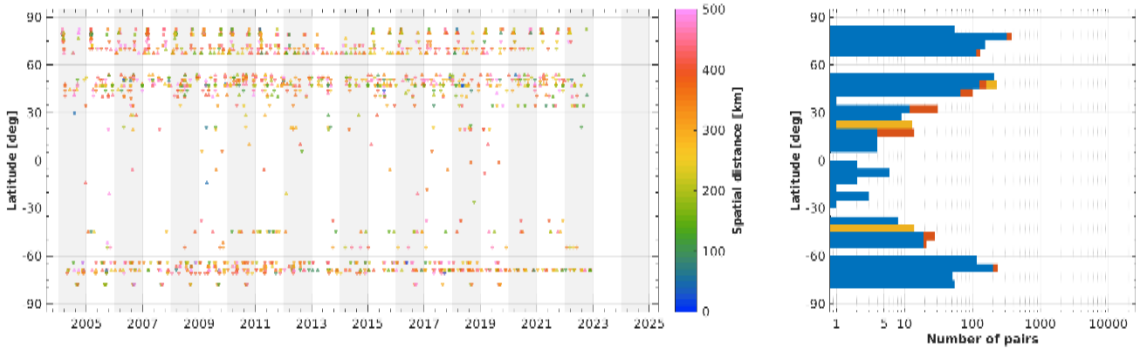

Figure 5.22 - (Left) Latitude–time distribution of co-locations between ACE-FTS v4.1/v4.2 ozone profiles and ground-based measurements (GAW/NDACC/SHADOZ ozonesonde, NDACC stratospheric ozone lidar and NDACC MWR). The colour code indicates the spatial distance of each satellite/ground-based pair. (Right) Number of co-located pairs per 5° latitude band for ozonesonde (blue), lidar (red) and MWR (orange).

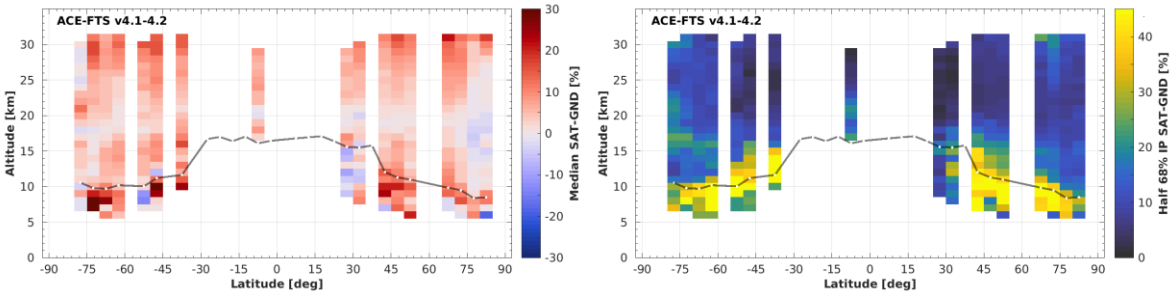

Figure 5.23 - Altitude–latitude cross-section of the median percent bias (left) and of the half IP-68 spread (right) between ACE-FTS v4.1/v4.2 ozone profile data and the global ozonesonde network, calculated over the entire ACE-FTS time period and in 5° bins. Black lines indicate the median (thick) and 1σ spread (thin) of the tropopause altitude.

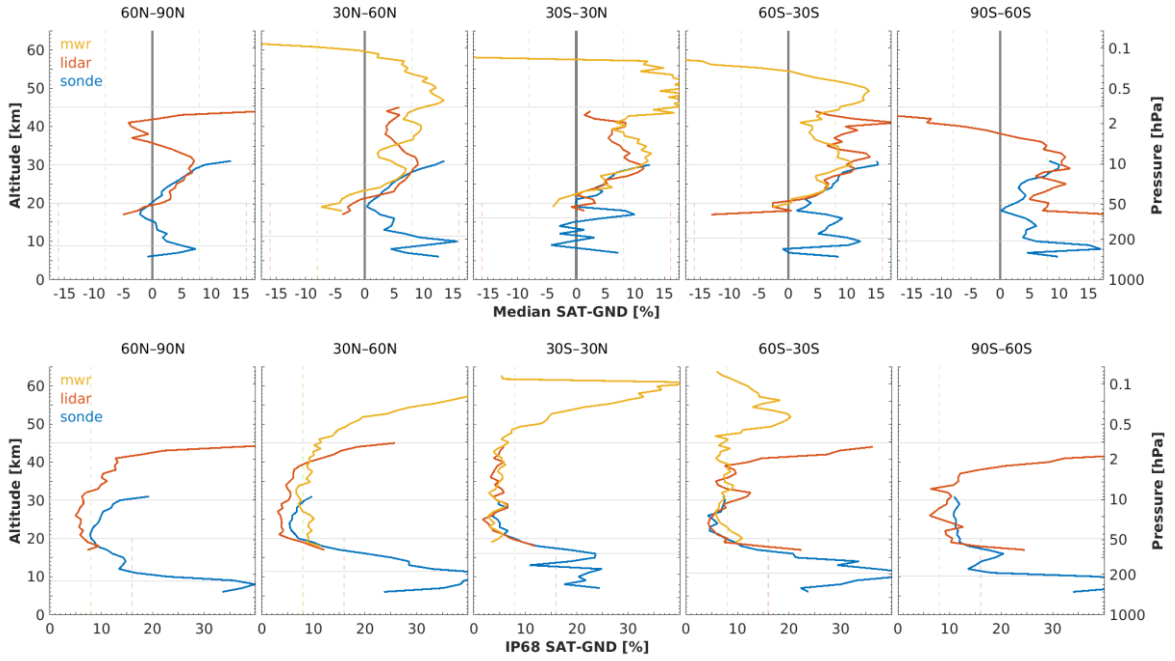

Figure 5.24 - (Top) Median bias between ACE-FTS v4.1/v4.2 ozone profile data and ozonesonde, lidar and MWR data, by 30° latitude. (Bottom) Same, but for the half IP-68 spread. The lowest horizontal line indicates the median tropopause altitude over the co-location sample.

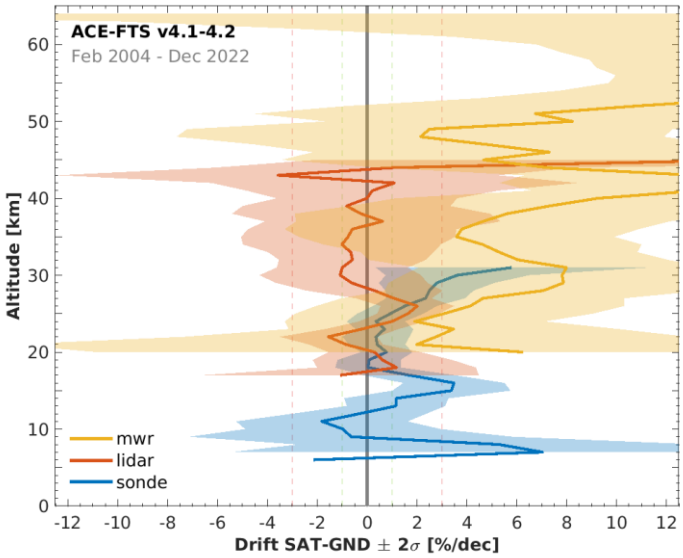

Figure 5.25 - Global network-averaged drift of ACE-FTS v4.1/v4.2 ozone profile data with respect to ozonesonde, lidar and MWR network data, calculated over the 2004-2022 time period. The shaded region represents 2σ uncertainty on the average decadal drift.

5.4.7.3 Long-term stability

Figure 5.25 shows the vertical structure of the decadal drift of ACE-FTS v4.1/v4.2 data relative to the ozonesonde, lidar and MWR networks. The number of co-locations with lidar measurements is limited, so the lidar constraints on stability are weaker than for other data sets discussed in this document. Nonetheless, the ozonesonde and lidar drift estimates are consistent and show no signs of drift between 17-27 km. In the UTLS and below, the data record is most likely stable as well. The bump in drift around 16 km is seen in the drift results for other limbs sensors as well, which indicates rather an issue with the ozonesonde data at this altitude. In the middle and upper stratosphere the ground-based networks provide different results. Given the good agreement of lidar and ozonesonde drift estimates for well-sampled satellite sensors (Aura MLS, SABER, OMPS-LP, …), we have reasonably high confidence in the ACE-FTS drift estimates up to 42 km. Hence, the ACE-FTS data record is very likely stable across the entire stratosphere, with drift less than ±1 %/decade. More data will be needed to further constrain drift in the mesosphere, currently large positive drifts are found but with (very) low confidence.

5.4.7.4 Dependence of data quality on other parameters

The bias, the dispersion and the long-term stability of ACE-FTS ozone are very similar in four different profile representations. This indicates that the auxiliary pressure and temperature profiles included in the ACE-FTS HARMOZ data files and in the correlative data files are consistent.

5.4.7.5 Compliance with user requirements

The ACE-FTS v4.1/v4.2 ozone profile data record is compliant with most sampling and resolution requirements. The data quality was assessed against ground-based measurements at high and middle latitudes. It generally meets the user requirements between 20 km and the stratopause. Stability is compliant with requirements across the entire stratosphere. Assessing compliance of random uncertainty in polar regions proves challenging due to the unquantified but likely considerable contribution by natural variability to the observed dispersion. As a result, compliance is flagged as not fulfilled in the Antarctic, even though this may not reflect the actual data quality.

Table 5.7 - Compliance of ACE-FTS v4.1/v4.2 with user requirements (URD v4.1): full compliance (green), partial compliance (orange) and no compliance (red).

	Requirement	Compliance / evaluation
Horizontal resolution	< 100–300 km	uncertain
Vertical resolution	< 1–3 km	3 km
Observation frequency	< 3 days	not compliant, ~30 solar occultation profiles per day
Time period	(1980-2010) – (2003-2010)	02/2004 – 12/2022
Total uncertainty in height attribution	< ± 500 m	likely compliant (solar occultation)
Dependences	–	latitude, altitude

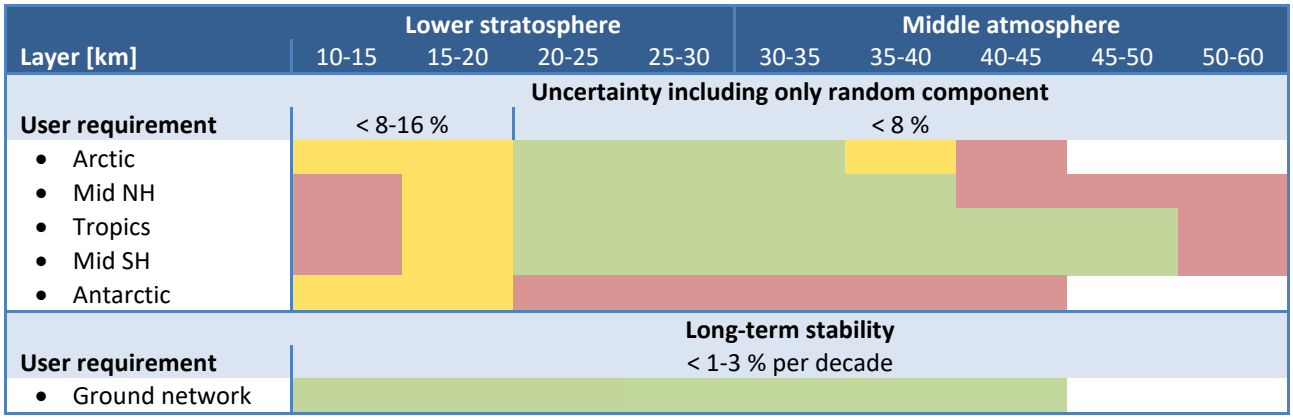

5.4.8 Suomi-NPP OMPS-LP USask-2D v1.3.0

The results in this section were obtained for Level-2 USask-2D version 1.3.0, file version 1, for the number density versus altitude profile representation (HARMOZ ALT). Validation results for earlier processor versions (v1.0.2, v1.1.0) of the OMPS-LP / SNPP USask-2D data set can be found in the Appendix of this document.

5.4.8.1 Co-locations / Validation sample

Figure 5.26 shows the latitude–time distribution of the ozonesonde, lidar and MWR measurements co-locating with OMPS-LP/SNPP USask-2D v1.3.0 data. The sampling covers nearly all latitude belts and is homogeneous in time except during polar night.

5.4.8.2 Bias and dispersion

The median bias and half the 68 % interpercentile of the relative difference between OMPS-LP/SNPP v1.3.0 and GAW/NDACC/SHADOZ ozonesondes, NDACC lidars or NDACC microwave radiometers are shown in the figures below. Figure 5.27 details the vertical and meridian dependence of the bias and dispersion at 5° latitude resolution, while Figure 5.28 shows the same information calculated in 30° latitude zones.

Ground-based comparisons show a coherent picture of the vertical structure of OMPS-LP/SNPP bias in the stratosphere. About 5 km above the tropopause a local maximum of +5-8 % is noted in the bias profile followed by a local minimum of -5 % around 25 km at most latitudes. In the middle and upper stratosphere, the OMPS-LP bias remains constant and positive by +3-5 % over the range 30-50 km. The positive bias becomes progressively smaller in the lowermost stratosphere and changes to a large negative bias of 5-15 % at the tropopause. Agreement and differences between OMPS-LP/SNPP USask-2D and UBr data are discussed in Sect. 5.4.9.2.

The meridian structure of the dispersion $s_{\Delta x}$ follows that of the tropopause. Above 20-25 km, the half IP-68 spread is about 5 % at the equator and increases gradually up to 6-10 % at the poles. Below ~20 km, the dispersion increases rapidly, reaching 25-30 % at the tropopause.

The ex-ante random uncertainties provided in the OMPS-LP/SNPP data files are too conservative, especially below 30 km. The reported mean ex-ante error is 11-14 % at 25 km and 6-7 % at 35 km, whereas the dispersion is 5-7 %.

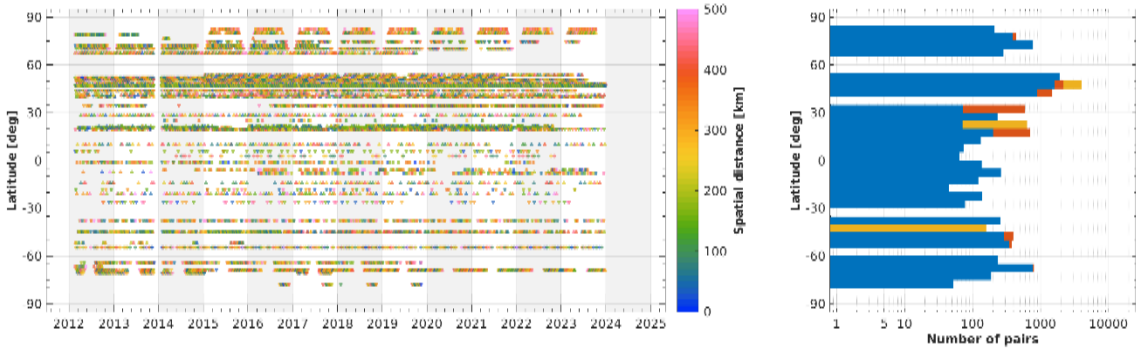

Figure 5.26 - (Left) Latitude–time distribution of co-locations between OMPS-LP/SNPP USask-2D v1.3.0 ozone profiles and ground-based measurements (GAW/NDACC/SHADOZ ozonesonde, NDACC stratospheric ozone lidar and NDACC MWR). The colour code indicates the spatial distance of each satellite/ground-based pair. (Right) Number of co-located pairs per 5° latitude band for ozonesonde (blue), lidar (red) and MWR (orange).

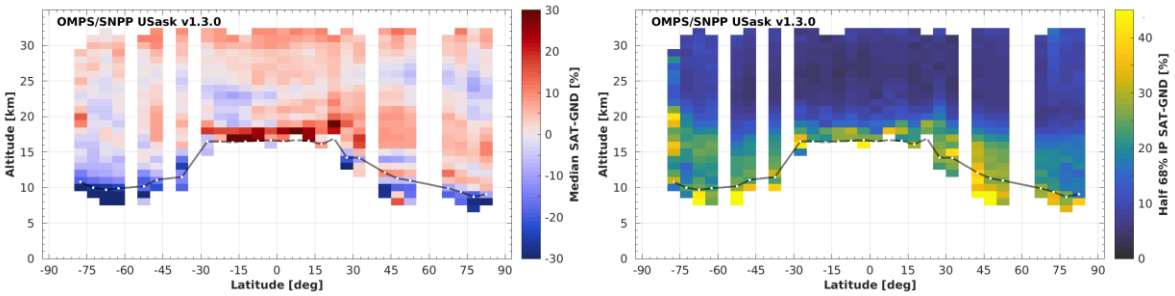

Figure 5.27 - Altitude–latitude cross-section of the median percent bias (left) and of the half IP-68 spread (right) between OMPS-LP/SNPP USask-2D v1.3.0 ozone profile data and the global ozonesonde network, calculated over the entire OMPS/SNPP time period and in 5° bins. Black lines indicate the median tropopause altitude.

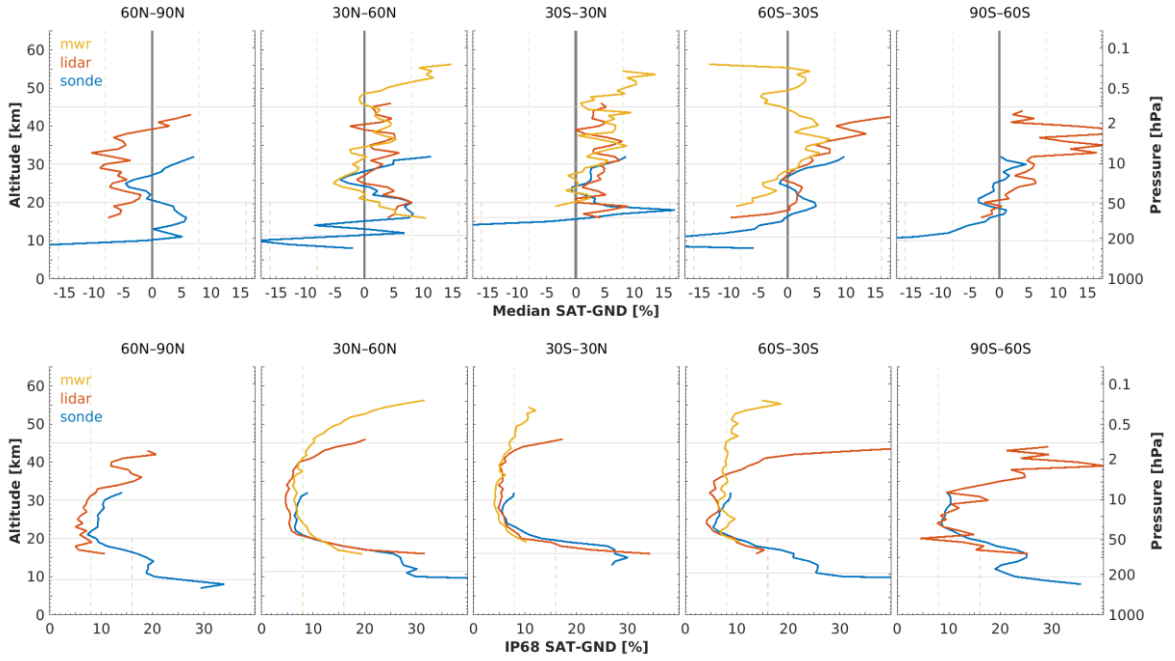

Figure 5.28 - (Top) Median bias between OMPS-LP/SNPP USask-2D v1.3.0 ozone profile data and ozonesonde, lidar and MWR data, by 30° latitude. (Bottom) Same, but for the half IP-68 spread. The lowest horizontal line indicates the median tropopause altitude over the co-location sample.

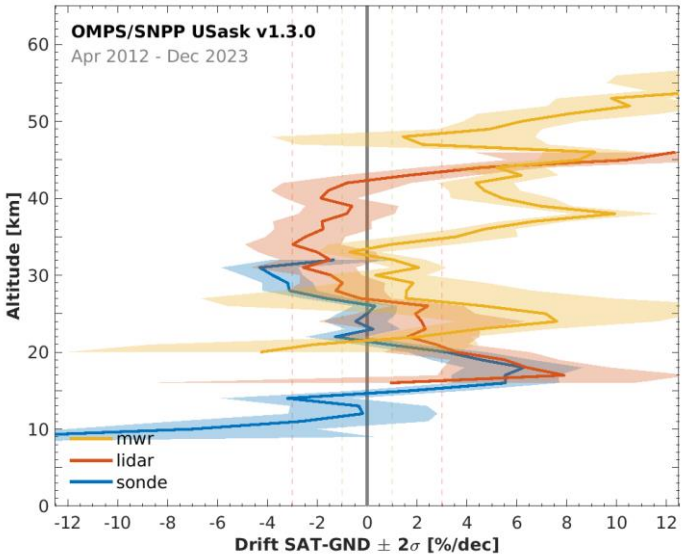

Figure 5.29 - Global network-averaged drift of OMPS-LP/SNPP USask-2D v1.3.0 ozone profile data with respect to ozonesonde, lidar and MWR network data, calculated over the 2012-2023 time period. The shaded region represents 2σ uncertainty on the average decadal drift.

5.4.8.3 Long-term stability

Figure 5.29 shows the drift of OMPS-LP/SNPP USask-2D v1.3.0 ozone profile data with respect to co-located ozonesonde, lidar and MWR network data. The ample co-location statistics allows to estimate drift with a precision of about 0.5-1 % per decade (1σ) over the 20-45 km range. While drift magnitude differs between ground-based techniques a consistent picture of the vertical structure of drift emerges. Between 15-19 km, there is high confidence in a positive drift of +4 % to +6 % per decade. Between 20-40 km the sign of drift depends on the reference data set used, though we find it more likely that OMPS drift is negative over the 25-40 km range. Across this range drift remains below ±3 % per decade. A large positive drift of 5 % per decade, and more, is found around the stratopause and above, but these results have fairly low confidence.

5.4.8.4 Dependence of data quality on other parameters

Bias, dispersion and long-term stability of OMPLS-LP/SNPP USask-2D v1.3.0 are very similar in four different profile representations. This indicates that the auxiliary pressure and temperature profiles included in the OMPS-LP HARMOZ data files and in the correlative data files are consistent.

5.4.8.5 Compliance with user requirements

From the results reported above we conclude that the OMPS-LP/SNPP USask-2D v1.3.0 ozone profile data record is nearly compliant with the sampling and resolution requirements. Random uncertainty meets the requirements almost everywhere between 20-40 km. However, the long-term drift exceeds the threshold in the lowermost stratosphere and possible the upper stratosphere as well. Also, assessing compliance of random uncertainty in polar regions proves challenging due to the unquantified but likely considerable contribution by natural variability to the observed dispersion. As a result, compliance is flagged as not fulfilled in the Antarctic, but it is understood that this may not reflect the actual data quality.

Table 5.8 - Compliance of OMPS-LP/SNPP USask v1.3.0 with user requirements (URD v4.1): full compliance (green), partial compliance (orange) and no compliance (red).

	Requirement	Compliance / evaluation
Horizontal resolution	< 100–300 km	250-400 km
Vertical resolution	< 1–3 km	1–2 km
Observation frequency	< 3 days	3-4 days [RD57]
Time period	(1980-2010) – (2003-2010)	01/2012 – 12/2023
Total uncertainty in height registration	< ± 500 m	~400 m [RD71]
Dependences	–	latitude, altitude

	Lower stratosphere				Middle atmosphere				
Layer [km]	10-15	15-20	20-25	25-30	30-35	35-40	40-45	45-50	50-60
	Uncertainty including only random component								
User requirement	< 8-16 %		< 8 %						
• Arctic									
• Mid NH									
• Tropics									
• Mid SH									
• Antarctic	(large natural variability)								
	Long-term stability								
User requirement	< 1-3 % per decade								
• Ground network									

5.4.9 Suomi-NPP OMPS-LP UBr v4.1

The results in this section were obtained for Level-2 UBr v4.1, file version 8, for the number density versus altitude profile representation (HARMOZ ALT).

5.4.9.1 Co-locations / Validation sample

Figure 5.30 shows the latitude–time distribution of the ozonesonde, lidar and MWR measurements co-locating with OMPS-LP/SNPP UBr v4.1 data. The sampling covers nearly all latitude belts and is homogeneous in time except for polar night.

5.4.9.2 Bias and dispersion

The median bias and half the 68 % interpercentile of the relative difference between OMPS-LP/SNPP UBr v4.1 and GAW/NDACC/SHADOZ ozonesondes, NDACC lidars or NDACC microwave radiometers are shown in the figures below. Figure 5.31 details the vertical and meridian dependence of the bias and dispersion at 5° latitude resolution, while Figure 5.32 shows the same information calculated in 30° latitude zones.

Ground-based comparisons show a reasonably coherent picture of 3 minima and 2 maxima in the vertical structure of OMPS-LP/SNPP bias in the stratosphere. Local minima are seen at ~12 km (-2 % to +1 %), 20-25 km (-5 % to +4 %) and at 45-50 km (-3 % to 0 %). Local maxima are located at 16-19 km (+4 % to +14 %) and around 30 km (+4 % to +8 %). The peaks at 18 km, 25 km and 30 km) coincide with those noted in the USask-2D data record. Interestingly, the UBr bias profile above 30 km depends on altitude, unlike that of USask-2D. The UBr bias profile is less noisy in the vertical domain. Finally, between 45-90° S, UBr bias is 5 % larger (more positive) than USask-2D which leads to a clear hemispheric asymmetry for the former data record at mid to high latitudes (Figure 5.31).

The meridian structure of the dispersion $s_{\Delta x}$ follows that of the tropopause. Above 20-25 km, the half IP-68 spread is about 5 % at the equator and increases gradually up to 6-10 % at the poles. Below ~20 km, the dispersion increases rapidly, reaching 25-30 % at the tropopause. Results are very similar to OMPS-LP/SNPP USask-2D.

The ex-ante random uncertainties provided in the OMPS-LP/SNPP data files range between 1-3 % above 20 km, rapidly increasing to 10 % (mid and high latitudes) or 30 % (tropics) at the tropopause. It is plausible that ex-ante uncertainty underestimates the actual random measurement uncertainty.

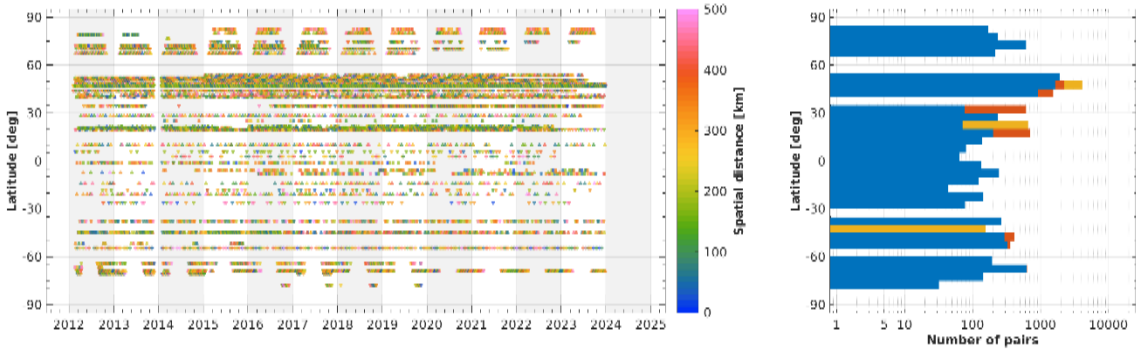

Figure 5.30 - (Left) Latitude–time distribution of co-locations between OMPS-LP/SNPP UBr v4.1 ozone profiles and ground-based measurements (GAW/NDACC/SHADOZ ozonesonde, NDACC stratospheric ozone lidar and NDACC MWR). The colour code indicates the spatial distance of each satellite/ground-based pair. (Right) Number of co-located pairs per 5° latitude band for ozonesonde (blue), lidar (red) and MWR (orange).

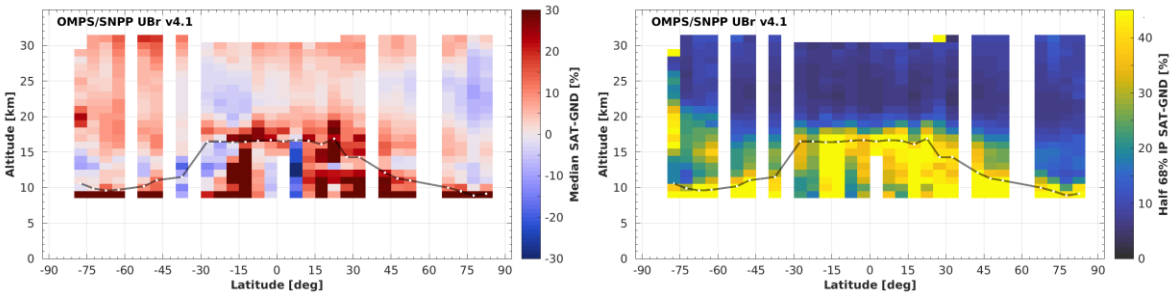

Figure 5.31 - Altitude–latitude cross-section of the median percent bias (left) and of the half IP-68 spread (right) between OMPS-LP/SNPP UBr v4.1 ozone profile data and the global ozonesonde network, calculated over the entire OMPS/SNPP time period and in 5° bins. Black lines indicate the median (thick) and 1σ spread (thin) of the tropopause altitude.

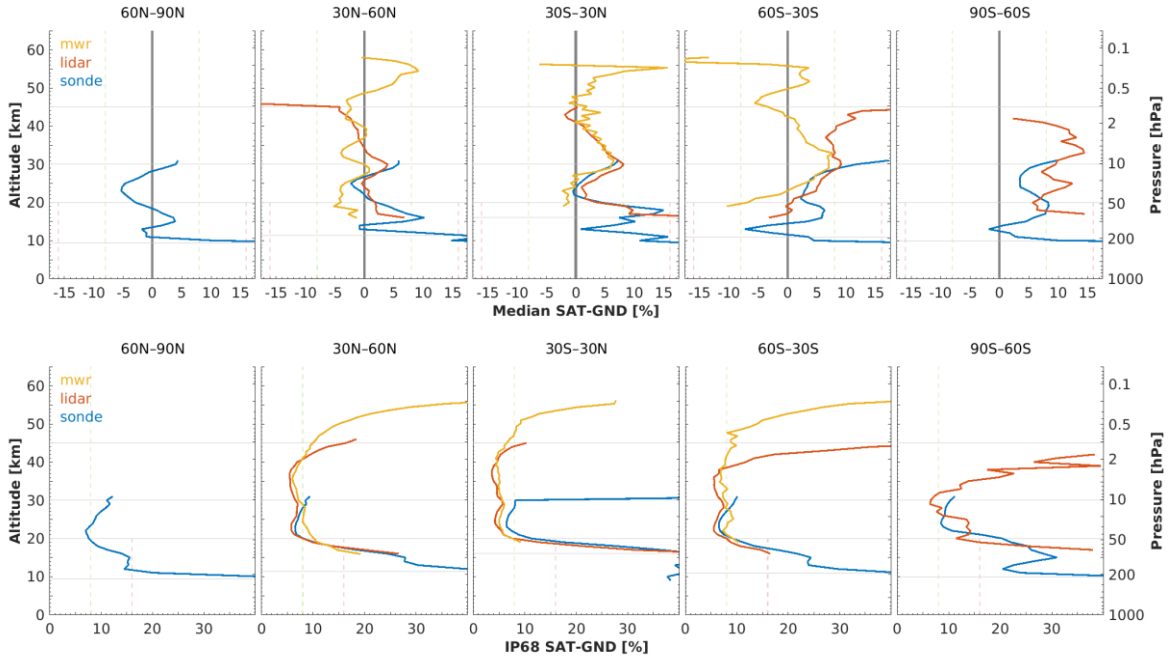

Figure 5.32 - (Top) Median bias between OMPS-LP/SNPP UBr v4.1 ozone profile data and ozonesonde, lidar and MWR data, by 30° latitude. (Bottom) Same, but for the half IP-68 spread. The lowest horizontal line indicates the median tropopause altitude over the co-location sample.

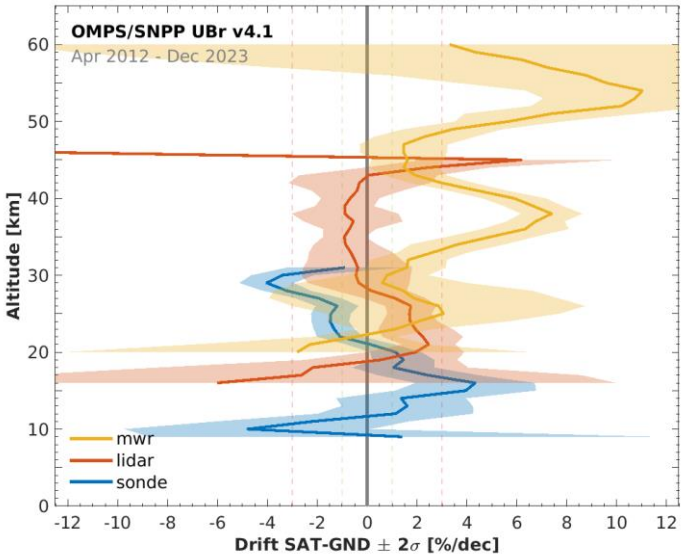

Figure 5.33 - Global network-averaged drift of OMPS-LP/SNPP UBr v4.1 ozone profile data with respect to ozonesonde, lidar and MWR data, calculated over the 2012-2023 time period. The shaded region represents 2σ uncertainty on the average decadal drift.

5.4.9.3 Long-term stability

Figure 5.29 shows the drift of OMPS-LP/SNPP UBR v4.1 ozone profile data with respect to co-located ozonesonde, lidar and MWR network data. The ample co-location statistics allows to estimate drift with a precision of about 0.5-1 % per decade (1σ) over the 20-45 km range. While drift magnitude differs between ground-based techniques a consistent picture of the vertical structure of drift emerges. Between 14-17 km, there is high confidence in a positive drift of +3 % to +4 % per decade. Between 20-40 km, the results are less coherent. The sign of drift depends on the reference data set used, and drift estimates differ by 3 % per decade between ground-based techniques. Overall, we drift remains below ±3 % per decade across 14-47 km range. A large positive drift of 5 % per decade, and more, is found around the stratopause and above, but these results have fairly low confidence.

5.4.9.4 Dependence of data quality on other parameters

Bias, dispersion and long-term stability of OMPLS-LP/SNPP UBr v4.1 are very similar in four different profile representations. This indicates that the auxiliary pressure and temperature profiles included in the OMPS-LP HARMOZ data files and in the correlative data files are consistent.

5.4.9.5 Compliance with user requirements

From the results reported above we conclude that the OMPS-LP/SNP UBr v4.1 ozone profile data record is nearly compliant with the sampling and resolution requirements. Random uncertainty meets the requirements almost everywhere between 20-40 km. Long-term drift exceeds the threshold only around 16 km. Also, assessing compliance of random uncertainty in polar regions proves challenging due to the unquantified but likely considerable contribution by natural variability to the observed dispersion. As a result, compliance is flagged as not fulfilled in the Antarctic, but it is understood that this may not reflect the actual data quality.

Table 5.9 - Compliance of OMPS-LP USask v1.1.0 with user requirements (URD v4.1): full compliance (green), partial compliance (orange) and no compliance (red).

	Requirement	Compliance / evaluation
Horizontal resolution	< 100–300 km	250-400 km
Vertical resolution	< 1–3 km	1–2 km
Observation frequency	< 3 days	3-4 days [RD57]
Time period	(1980-2010) – (2003-2010)	01/2012 – 01/2020
Total uncertainty in height registration	< ± 500 m	~400 m [RD71]
Dependences	–	latitude, altitude

	Lower stratosphere				Middle atmosphere				
Layer [km]	10-15	15-20	20-25	25-30	30-35	35-40	40-45	45-50	50-60
	Uncertainty including only random component								
User requirement	< 8-16 %		< 8 %						
• Arctic									
• Mid NH									
• Tropics									
• Mid SH									
• Antarctic									
	Long-term stability								
User requirement	< 1-3 % per decade								
• Ground network									

5.4.10 NOAA-21 OMPS-LP UBr v1.1

The results in this section were obtained for Level-2 UBr version 1.1, file version 1, for the number density versus altitude profile representation (HARMOZ ALT).

5.4.10.1 Co-locations / Validation sample

Figure 5.30 shows the latitude–time distribution of the ozonesonde, lidar and MWR measurements co-locating with OMPS-LP/N21 UBr v1.1 data. The sample is limited due to recent start of OMPS-LP/N21 operations and the latency in the upload of ground-based data to the public data archives. Nonetheless, at least 5 comparison pairs, the minimum requirement to obtain statistics, are found at eighteen 5° latitude belts. This enables us to explore the meridian structure of quality indicators with just one year of data.

5.4.10.2 Bias and dispersion

The median bias and half the 68 % interpercentile of the relative difference between OMPS-LP/N21 UBr v1.1 and GAW/NDACC/SHADOZ ozonesondes, NDACC lidars or NDACC microwave radiometers are shown in the figures below. Figure 5.35 details the vertical and meridian dependence of the bias and dispersion at 5° latitude resolution, while Figure 5.36 shows the same information calculated in 30° latitude zones.

Bias with respect to ozonesonde is mostly less than ±5 %, except in the lowermost stratosphere where a local maximum of +7 % to +15 % is noted between 15-20 km and a local minimum of -10 % to -20 % at 12 km. The spatial bias structure bears early signs of resemblance with that of OMPS-LP/SNPP UBr (Sect. 5.4.9.2). The meridian structure of the dispersion $s_{\Delta x}$ follows that of the tropopause. The half IP-68 spread is about 8 % at mid-latitudes and 8-10 % at the poles. Below 20-25 km, the dispersion increases rapidly, reaching 20-35 % at the tropopause. The ex-ante random uncertainties provided in the OMPS-LP/N21 data files range between 2-4 % above 20 km, rapidly increasing to 15-25 % at the tropopause. It is plausible that ex-ante uncertainty underestimates the actual random measurement uncertainty.

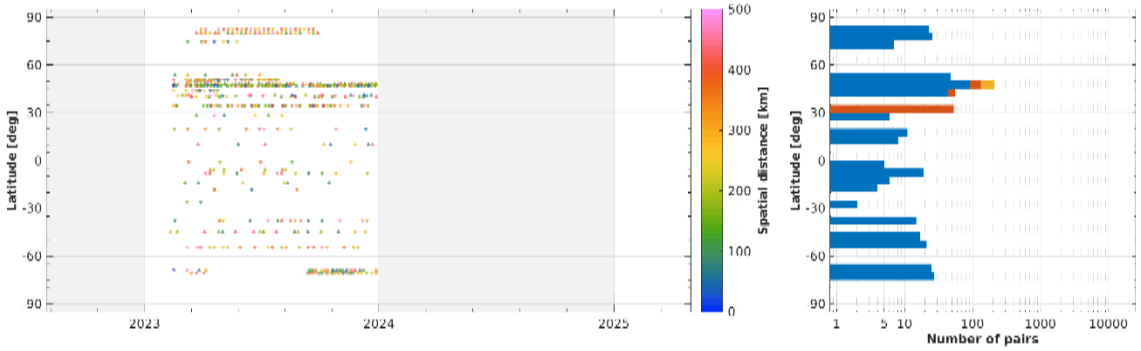

Figure 5.34 - (Left) Latitude–time distribution of co-locations between OMPS-LP/N21 UBr v1.1 ozone profiles and ground-based measurements (GAW/NDACC/SHADOZ ozonesonde, NDACC stratospheric ozone lidar and NDACC MWR). The colour code indicates the spatial distance of each satellite/ground-based pair. (Right) Number of co-located pairs per 5° latitude band for ozonesonde (blue), lidar (red) and MWR (orange).

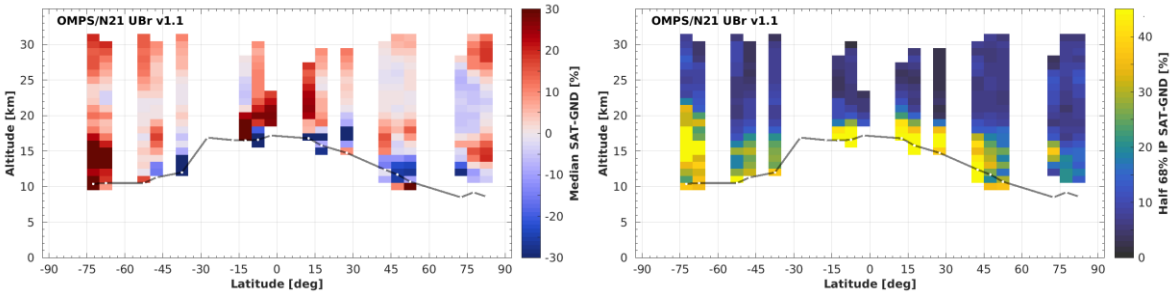

Figure 5.35 - Altitude–latitude cross-section of the median percent bias (left) and of the half IP-68 spread (right) between OMPS-LP/N21 UBr v1.1 ozone profile data and the global ozonesonde network, calculated over the entire OMPS/N21 time period and in 5° bins. Black lines indicate the median (thick) and 1σ spread (thin) of the tropopause altitude.

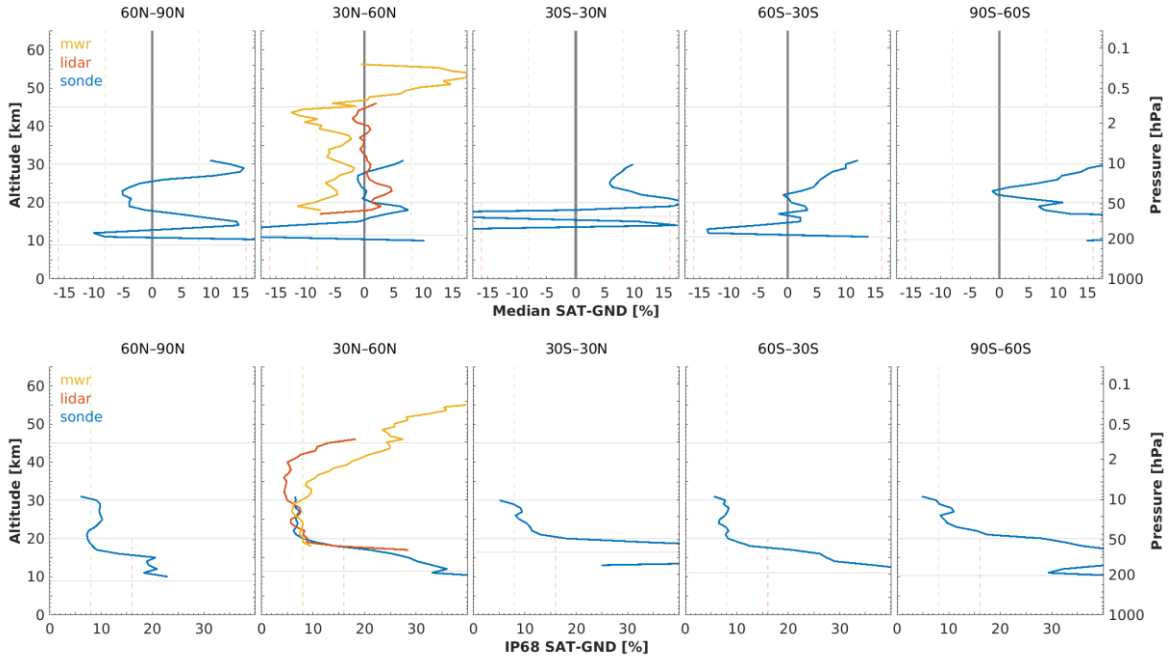

Figure 5.36 - (Top) Median bias between OMPS-LP/N21 UBr v1.1 ozone profile data and ozonesonde, lidar and MWR data, by 30° latitude. (Bottom) Same, but for the half IP-68 spread. The lowest horizontal line indicates the median tropopause altitude over the co-location sample.

5.4.10.3 Long-term stability

No meaningful drift can be estimated, at least 3 years of observations are needed.

5.4.10.4 Dependence of data quality on other parameters

Bias and dispersion of OMPS-LP/N21 UBr v1.1 are very similar in four different profile representations. This indicates that the auxiliary pressure and temperature profiles included in the OMPS-LP HARMOZ data files and in the correlative data files are consistent.

5.4.10.5 Compliance with user requirements

From the results reported above we conclude that it is too early to find compliance of OMPS-LP/N21 UBr v1.1 data with requirements. Additional will be needed to constrain the quality indicators to the point where they can be compared to requirements. Below, we give a first assessment given the limited data sets currently available.

Table 5.10 - Compliance of OMPS-LP/N21 UBr v1.1 with user requirements (URD v4.1): full compliance (green), partial compliance (orange) and no compliance (red).

	Requirement	Compliance / evaluation
Horizontal resolution	< 100–300 km	250-400 km
Vertical resolution	< 1–3 km	1–2 km
Observation frequency	< 3 days	3-4 days [RD57]
Time period	(1980-2010) – (2003-2010)	02/2023 – 12/2023
Total uncertainty in height registration	< ± 500 m	~400 m [RD71]
Dependences	–	latitude, altitude

	Lower stratosphere				Middle atmosphere				
Layer [km]	10-15	15-20	20-25	25-30	30-35	35-40	40-45	45-50	50-60
	Uncertainty including only random component								
User requirement	< 8-16 %				< 8 %				
• Arctic									
• Mid NH									
• Tropics									
• Mid SH									
• Antarctic									
	Long-term stability								
User requirement	< 1-3 % per decade								
• Ground network									

5.4.11 ERBS SAGE II v7.0

The results in this section were obtained for Level-2 processor version 7.0, file version 7, for the number density versus altitude profile representation (HARMOZ ALT).

5.4.11.1 Co-locations / Validation sample

Figure 5.37 shows the latitude–time distribution of the ozonesonde, lidar and MWR measurements co-locating with SAGE II v7.0 data. Very few comparisons are available in the tropics, the sample mainly covers middle and high latitudes. It is fairly homogeneous in time, but increases of ground network size are clear in the 1990s.

5.4.11.2 Bias and dispersion

The median bias and half the 68 % interpercentile of the relative difference between SAGE II v7.0 and GAW/NDACC/SHADOZ ozonesondes, NDACC lidars or NDACC MWRs are shown in the figures below. Figure 5.38 details the vertical and meridian dependence of the bias and dispersion at 5° latitude resolution, while Figure 5.39 shows the same information calculated in 30° latitude zones.

The SAGE II bias is negative at all latitudes below 20 km. At higher altitudes (20-45 km) the bias is mostly less than 3-4 % when compared to all three ground-based techniques. Although some tension arises between sonde and lidar comparison results in polar regions, this can be traced to either poor co-location statistics and hence larger uncertainties on the bias estimates (Arctic), or to a known negative bias in the lidar data between 1991 and 1998 at Dumont d'Urville (Antarctica, [RD43]). In the mesosphere SAGE II reports larger ozone values than MWR instruments, by 5-10 %.

The meridian structure of the dispersion $s_{\Delta x}$ follows that of the tropopause. Above 20 km the half IP-68 spread is 4-6 % at the equator and increases gradually up to ~10 % at the poles. The dispersion increases rapidly at lower altitudes and reaches 40 % around the tropopause. The dispersion seen in the comparisons is clearly larger than the ex-ante random uncertainty $s_{ex\text{-}ante}$ (not shown here) provided in the SAGE II data files. The latter is only 1-2 % above 20 km and increases to about 20 % at the tropopause.

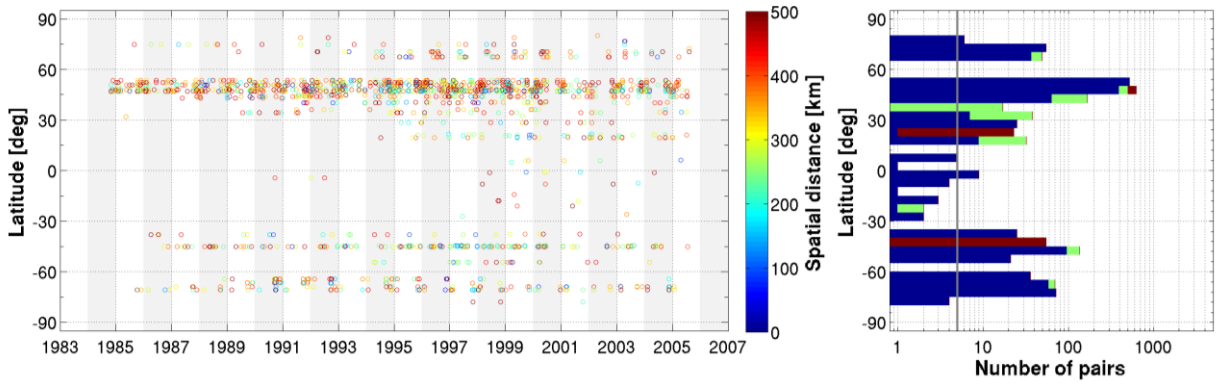

Figure 5.37 - (Left) Latitude–time distribution of co-locations between SAGE II v7 ozone profiles and ground-based measurements (GAW/NDACC/SHADOZ ozonesonde, NDACC stratospheric ozone lidar and NDACC MWR). The colour code indicates the spatial distance of each satellite/ground-based pair. (Right) Number of co-located pairs per 5° latitude band for ozonesonde (blue), lidar (green) and MWR (red).

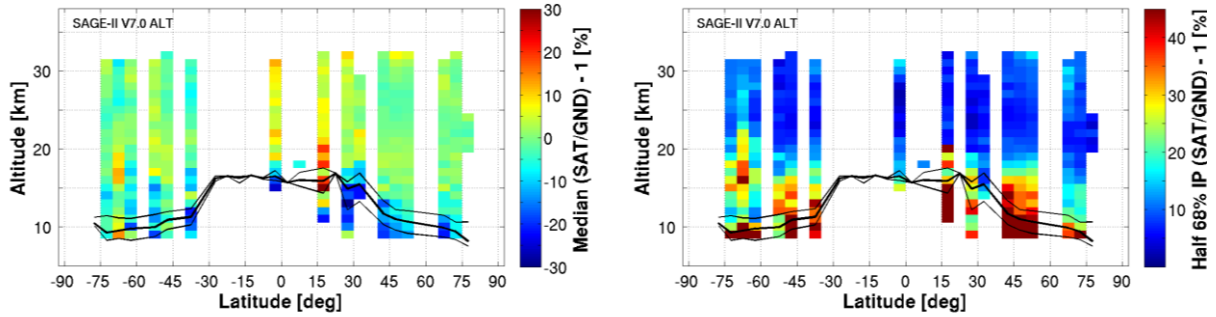

Figure 5.38 - Altitude–latitude cross-section of the median percent bias (left) and of the half IP-68 spread (right) between SAGE II v7 ozone profile data and the global ozonesonde network, calculated over the entire SAGE II time period and in 5° bins. Black lines indicate the median (thick) and 1σ spread (thin) of the tropopause altitude.

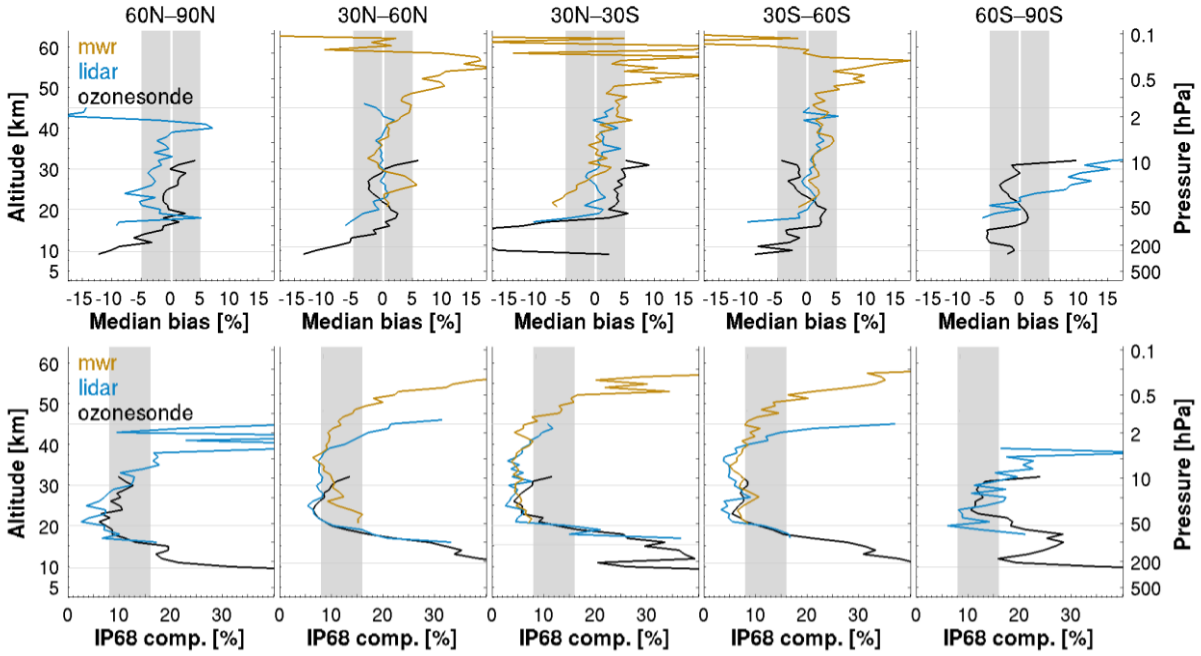

Figure 5.39 - (Top) Median bias between SAGE II v7 ozone profile data and ozonesonde, lidar and MWR data, by 30° latitude. (Bottom) Same, but for the half IP-68 spread. The lowest horizontal line indicates the median tropopause altitude over the co-location sample.

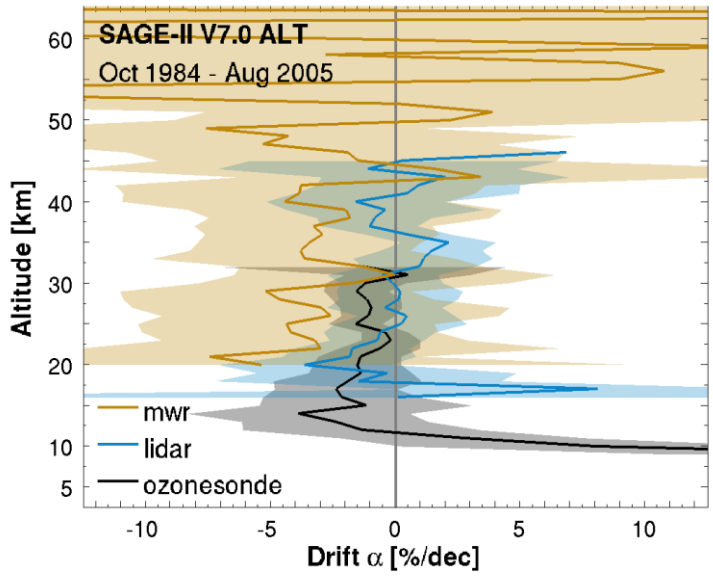

Figure 5.40 - Global network-averaged drift of SAGE II v7 ozone profile data with respect to ozonesonde, lidar and MWR network data, calculated over the 1984-2005 time period (sonde, lidar) or the 1995-2005 period (MWR). The shaded region represents 2σ uncertainty on the average decadal drift.

5.4.11.3 Long-term stability

Figure 5.40 shows the vertical structure of the decadal drift of SAGE II v7.0 data relative to the ozonesonde, lidar and MWR networks. Drift estimates are virtually independent of altitude and they remain between -2 % and 1 % per decade over the entire stratosphere. Estimates of drift relative to MWR are based on a different period in time than sonde and lidar since regular MWR observations started mostly after 1995. This may explain the quantitative differences in drift, yet the qualitative conclusion remains the same. SAGE II drift values are small and not significant, hereby showing the excellent stability of the SAGE II data record for studies of long-term changes in ozone.

5.4.11.4 Dependence of data quality on other parameters

Bias, dispersion and long-term stability of SAGE II ozone are in excellent agreement in four different profile representations. This indicates that the auxiliary pressure and temperature profiles included in the SAGE II HARMOZ data files and in the correlative data files are consistent.

5.4.11.5 Compliance with user requirements

From the results reported above it can be concluded that the SAGE II v7 ozone profile data record is compliant with most sampling and resolution requirements. Data quality meets the random uncertainty requirements between 20 km and the stratopause, except in polar regions where random mismatch uncertainty due to natural variability obfuscates the analysis results. Decadal stability is fully compliant between 15-45 km and partially at other levels.

Table 5.11 - Compliance of SAGE II v7.0 with user requirements (URD v4.1): full compliance (green), partial compliance (orange) and no compliance (red).

	Requirement	Compliance / evaluation
Horizontal resolution	< 100–300 km	uncertain [RD91]
Vertical resolution	< 1–3 km	1 km
Observation frequency	< 3 days	not compliant, ~30 solar occultation profiles per day
Time period	(1980-2010) – (2003-2010)	10/1984 – 08/2005
Total uncertainty in height registration	< ± 500 m	likely compliant (solar occultation)
Dependences	–	latitude, altitude, sunset/sunrise

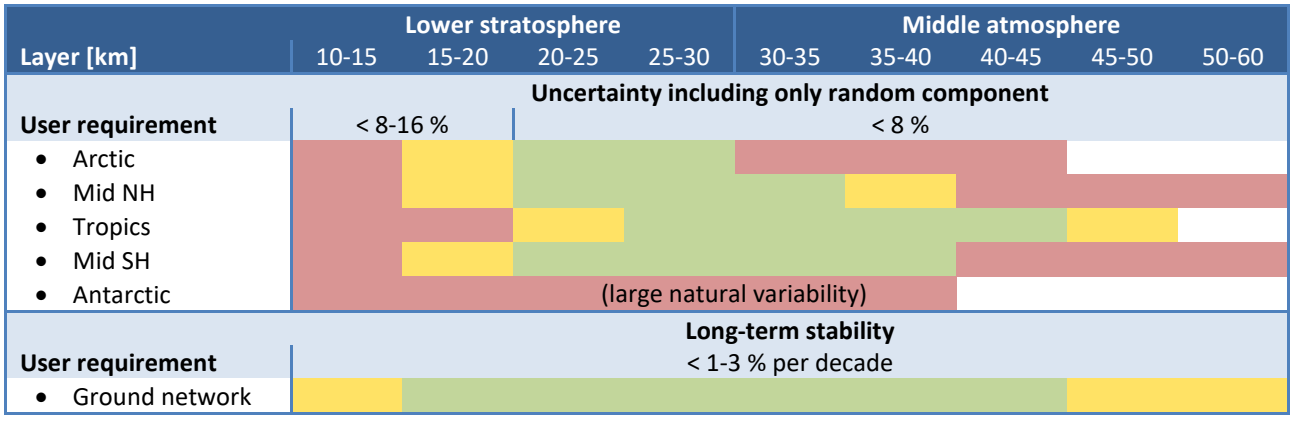

5.4.12 UARS HALOE v19

The results in this section were obtained for Level-2 processor version 19, file version 4, for the volume mixing ratio versus pressure profile representation (HARMOZ PRS).

5.4.12.1 Co-locations / Validation sample

Figure 5.41 shows the latitude–time distribution of the ozonesonde, lidar and MWR measurements co-locating with HALOE v19 data. The sampling covers most latitude zones and is reasonably homogeneous in time.

5.4.12.2 Bias and dispersion

The median bias and half the 68 % interpercentile of the relative difference between HALOE v19 and GAW/NDACC/SHADOZ ozonesondes, NDACC lidars or NDACC MWRs are shown in the figures below. Figure 5.42 details the vertical and meridian dependence of the bias and dispersion at 5° latitude resolution, while Figure 5.43 shows the same information calculated in 30° latitude.

HALOE underestimates ozone by 10-15 % and more below 20-50 hPa (~15-20 km). The bias remains negative but is much smaller, less than 3-4 %, in the middle stratosphere. In the upper stratosphere the sign remains less than ~4 % and its sign varies with latitude and altitude. Above the stratopause MWR comparisons indicate a negative bias of 5-10 % increasing towards the top of the profile. The apparent tension between the sonde and lidar comparison results in the polar regions can be traced to either poor co-location statistics and hence larger uncertainties on the bias estimates (Arctic), or to a known negative bias of the lidar data between 1991 and 1998 at Dumont d'Urville (Antarctica, [RD43]).

The meridian structure of the dispersion $s_{\Delta x}$ follows that of the tropopause. Above the 20 hPa level (~25 km) the half IP-68 spread is 4-5 % at the equator and increases gradually up to 8-10 % at the poles. The dispersion increases rapidly at lower altitudes, and reaches 40 % and more around tropopause. The dispersion seen in the comparisons is a clearly larger than the ex-ante random uncertainty $s_{ex\text{-}ante}$ (not shown here) provided in the HALOE data files. The latter is only 1-3 % at altitudes above the 50 hPa level (20 km) and increases to about 20-40 % at the tropopause.

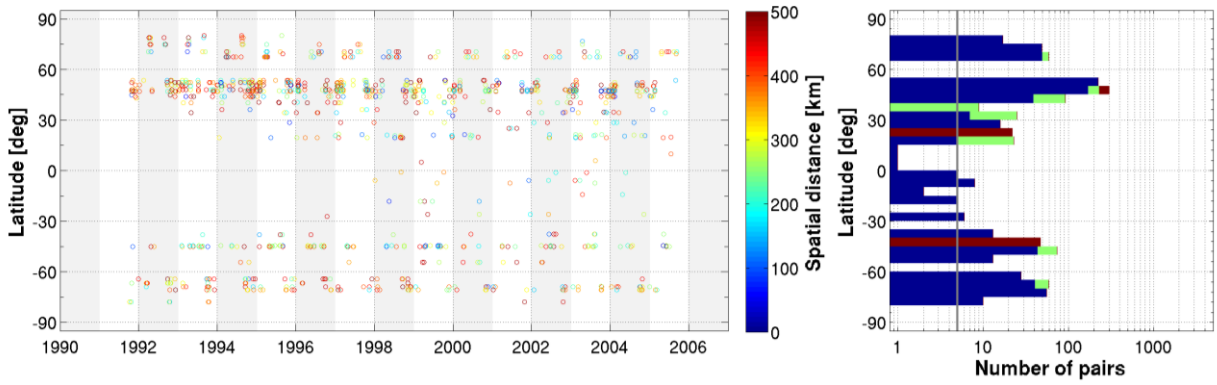

Figure 5.41 - (Left) Latitude–time distribution of co-locations between HALOE v19 ozone profiles and ground-based measurements (GAW/NDACC/SHADOZ ozonesonde, NDACC stratospheric ozone lidar and NDACC MWR). The colour code indicates the spatial distance of each satellite/ground-based pair. (Right) Number of co-located pairs per 5° latitude band for ozonesonde (blue), lidar (green) and MWR (red).

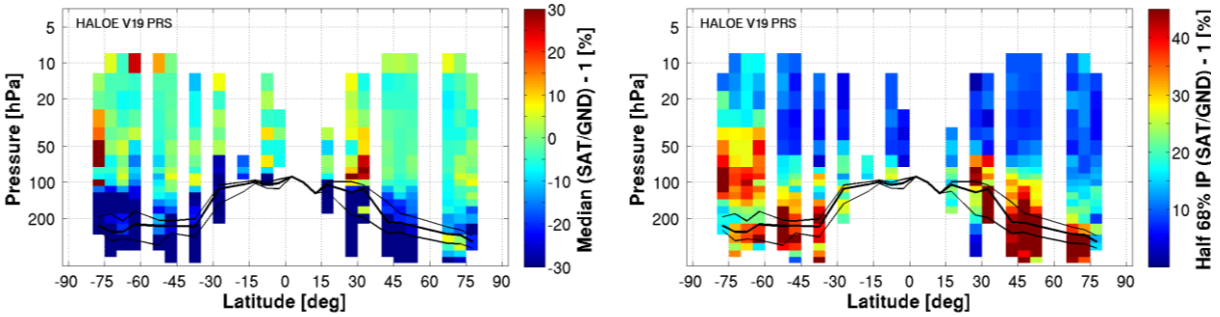

Figure 5.42 - Altitude–latitude cross-section of the median percent bias (left) and of the half IP-68 spread (right) between HALOE v19 ozone profile data and the global ozonesonde network, calculated over the entire HALOE time period and in 5° bins. Black lines indicate the median (thick) and 1σ spread (thin) of the tropopause altitude.

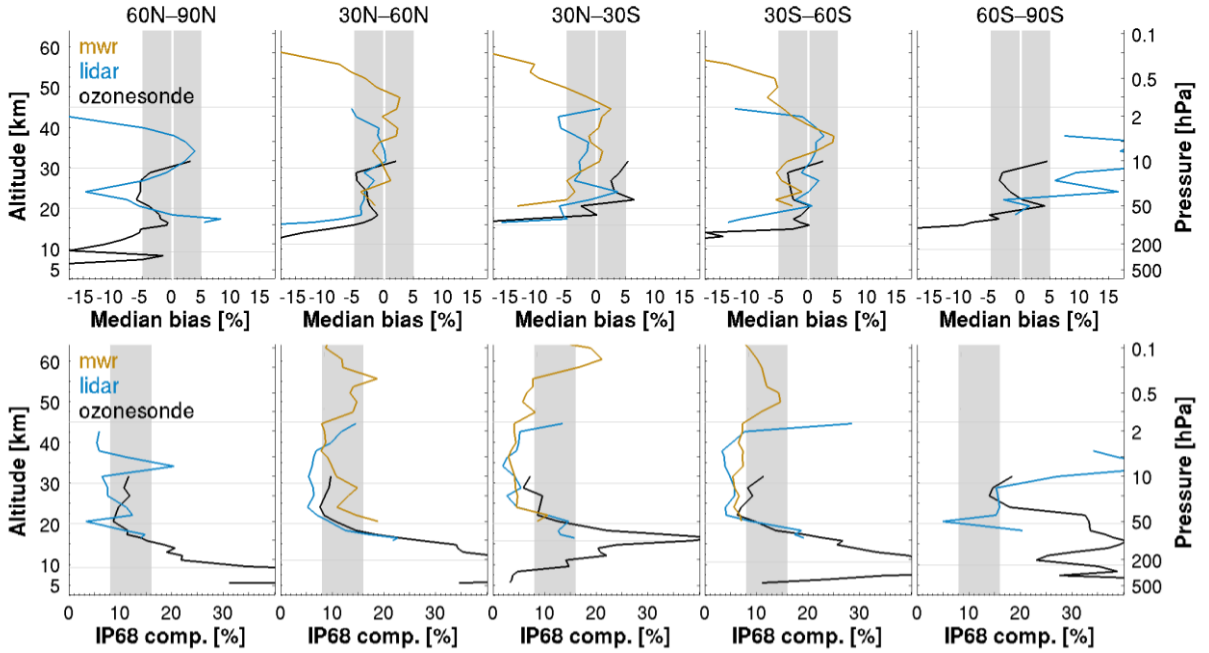

Figure 5.43 - (Top) Median bias between HALOE v19 ozone profile data and ozonesonde, lidar and MWR data, by 30° latitude. (Bottom) Same, but for the half IP-68 spread. The lowest horizontal line indicates the median tropopause altitude over the co-location sample.

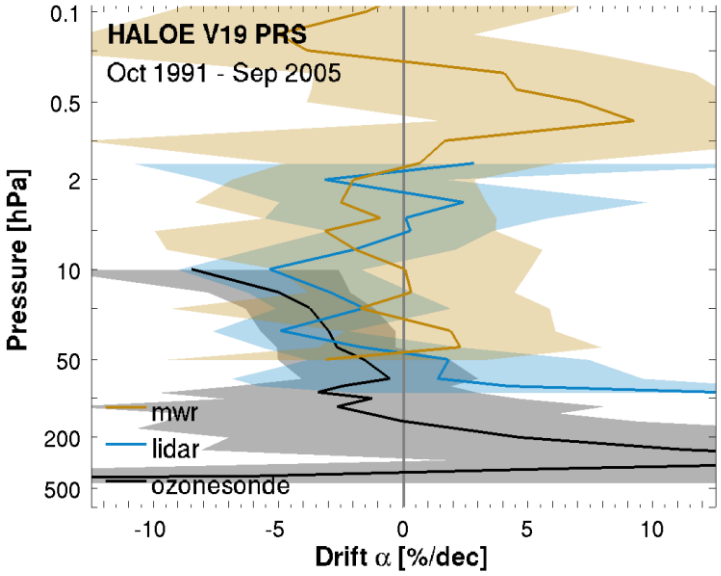

Figure 5.44 - Global network-averaged drift of HALOE v19 ozone profile data with respect to ozonesonde, lidar and MWR data, calculated over the 1991-2005 time period. The shaded region represents 2σ uncertainty on the average decadal drift.

5.4.12.3 Long-term stability

Figure 5.44 shows the vertical structure of the decadal drift of HALOE v19 data relative to the ozonesonde, lidar and MWR networks. Drift estimates are negative between 200-2 hPa and significant between 10-40 hPa (~23-30 km) for both the sonde and the lidar comparisons. In the lower mesosphere values are positive but insignificant. The negative drift in the middle stratosphere amounts to 3-4 % per decade. We therefore advice caution when using HALOE data for studies of long-term changes in ozone.

5.4.12.4 Dependence of data quality on other parameters

The bias, the dispersion and the long-term stability of HALOE ozone are very similar in four different profile representations. This indicates that the auxiliary pressure and temperature profiles included in the HALOE HARMOZ data files and in the correlative data files are consistent.

5.4.12.5 Compliance with user requirements

From the results reported above it can be concluded that the HALOE v19 ozone profile data record is compliant with most of sampling and resolution requirements. Data quality meets the requirements on random uncertainty at altitudes above the 50 hPa level (~20 km). A significant negative drift of 3-4 % per decade is seen between 10-40 hPa (~23-30 km) and has to be considered in long-term studies. Assessing compliance of random uncertainty in polar regions proves challenging due to the unquantified but likely considerable contribution by natural variability to the observed dispersion. As a result, compliance is flagged as not fulfilled in the Antarctic, but it is understood that this may not reflect the actual data quality.

Table 5.12 - Compliance of HALOE v19 with user requirements (URD v4.1): full compliance (green), partial compliance (orange) and no compliance (red).

	Requirement	Compliance / evaluation
Horizontal resolution	< 100–300 km	uncertain [RD91]
Vertical resolution	< 1–3 km	2.3 km
Observation frequency	< 3 days	not compliant, ~30 solar occultation profiles per day
Time period	(1980-2010) – (2003-2010)	10/1991 – 11/2005
Total uncertainty in height registration	< ± 500 m	likely compliant (solar occultation)
Dependences	–	latitude, altitude, sunset/sunrise

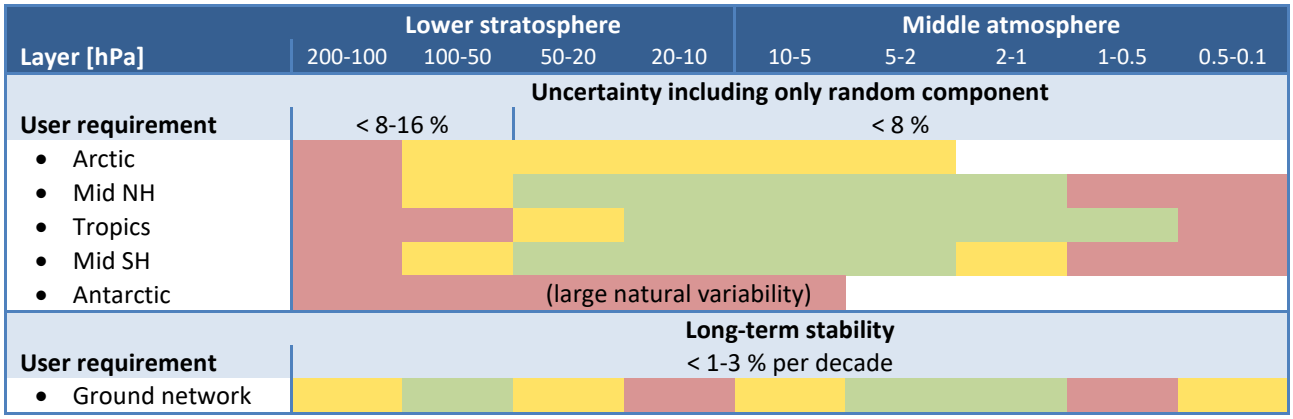

5.4.13 TIMED SABER 9.6 µm v2.0

The results in this section were obtained for Level-2 processor version 2.0, file version 5, for the volume mixing ratio versus pressure profile representation (HARMOZ PRS).

5.4.13.1 Co-locations / Validation sample

Figure 5.45 shows the latitude–time distribution of the ozonesonde, lidar and MWR measurements co-locating with SABER 9.6µm v2.0 data. The sampling is very dense as SABER measures ~1400 profiles per day [RD77]. All latitude zones are covered and temporal sampling is very homogeneous. Slightly fewer co-locations are also seen in the last few years of the mission, due to the unavailability of publicly released correlative data.

5.4.13.2 Bias and dispersion

The median bias and the half 68 % interpercentile of the relative difference between SABER 9.6µm v2.0 and GAW/NDACC/SHADOZ ozonesondes, NDACC lidars or NDACC MWRs are shown in the figures below. Figure 5.46 details the vertical and meridian dependence of the bias and dispersion at 5° latitude resolution, while Figure 5.47 shows the same information calculated in 30° latitude zones.

All ground-based comparisons show a similar pronounced vertical structure of SABER bias. Around 30-40 hPa (~21-24 km) SABER bias ranges from -5 % to 0 %. At higher altitudes, there is a clear overestimation which increases with altitude, reaching 5-10 % (NH) to 10-15 % (NH) at the stratopause. SABER overestimates ozone w.r.t. ozonesonde in the lowermost stratosphere by 5-15 % around 50 hPa. This vertical structure is similar to that reported for an earlier version of the SABER data [RD77]. Opposed to the previous SABER data release (fv0003), the current file version (fv0005) does include measurements below the 50 hPa level. We recommend caution in using SABER ozone profile data in the UTLS and below due to a positive bias of at least 30 %.

The meridian structure of the dispersion $s_{\Delta x}$ follows that of the tropopause. In the upper stratosphere, the half IP-68 spread is about 6-8 % at the equator and increases gradually towards the poles. Higher variability is seen in the mesosphere (~15 %) and middle stratosphere (~12 %). In the lower stratosphere and below, dispersion in the comparisons rapidly increases from 15 % to more than 40 %. Ex-ante uncertainties in the current SABER data release (fv0005) have decreased significantly with respect to the previous file version (fv0003). Median reported uncertainty drops from 16 % to 5 % between 10-50 hPa and from 9 % to 1 % at pressures below 2 hPa. These much smaller ex-ante uncertainties appear too optimistic, as the observed dispersion in the comparisons is much higher across the entire profile.

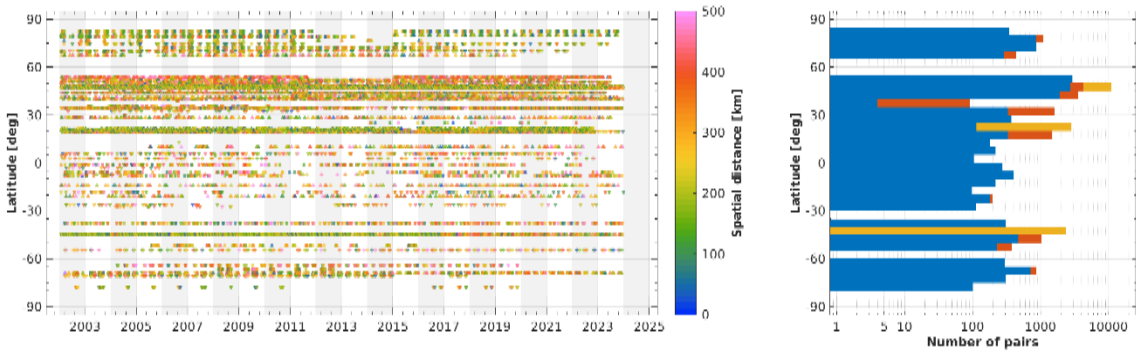

Figure 5.45 - (Left) Latitude–time distribution of co-locations between SABER 9.6µm v2.0 ozone profiles and ground-based measurements (GAW/NDACC/SHADOZ ozonesonde, NDACC stratospheric ozone lidar and NDACC MWR). The colour code indicates the spatial distance of each satellite/ground-based pair. (Right) Number of co-located pairs per 5° latitude band for ozonesonde (blue), lidar (red) and MWR (orange).

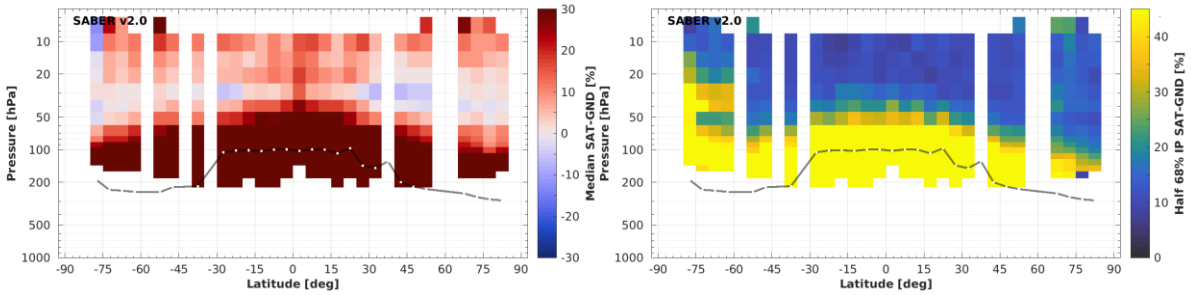

Figure 5.46 - Altitude–latitude cross-section of the median percent bias (left) and of the half IP-68 spread (right) between SABER 9.6µm v2.0 ozone profile data and the global ozonesonde network, calculated over the entire SABER time period and in 5° bins. Black lines indicate the median tropopause altitude.

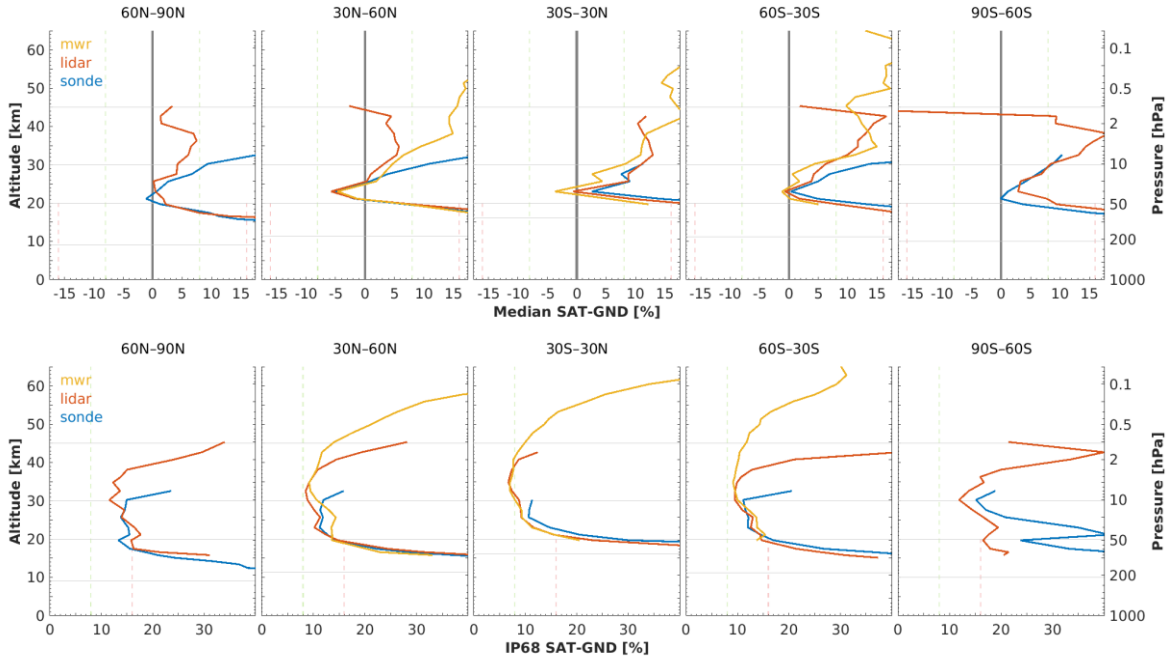

Figure 5.47 - (Top) Median bias between SABER 9.6µm v2.0 ozone profile data and ozonesonde, lidar and MWR data, by 30° latitude. (Bottom) Same, but for the half IP-68 spread. The lowest horizontal line indicates the median tropopause altitude over the co-location sample.

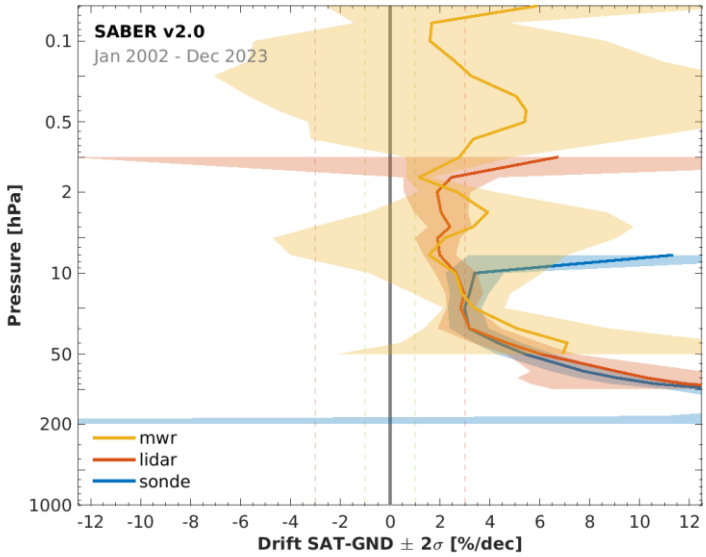

Figure 5.48 - Global network-averaged drift of SABER 9.6µm v2.0 ozone profile data with respect to ozonesonde, lidar and MWR network data, calculated over the 2002-2023 time period. The shaded region represents 2σ uncertainty on the average decadal drift.

5.4.13.3 Long-term stability

Figure 5.48 shows the drift of SABER 9.6µm v2.0 ozone profile data with respect to co-located ground-based network data. We find a consistent picture that SABER ozone drifts towards higher values relative to all independent ground-based data records, across the entire profile. The drift estimates are highly significant from the stratopause down to the lowest profile level. SABER drifts by more than +6 % per decade below the 50 hPa level and by about +2-3 % per decade at all higher altitudes. We therefore recommend great caution when using these data for studies of long-term changes in ozone.

5.4.13.4 Dependence of data quality on other parameters

Bias, dispersion and long-term stability of SABER 9.6µm v2.0 ozone are very similar in four different profile representations. This indicates that the auxiliary pressure and temperature profiles included in the SABER HARMOZ data files and in the correlative data files are consistent.

5.4.13.5 Compliance with user requirements

From the results reported above it can be concluded that the SABER 9.6 µm v2.0 ozone profile data record is compliant with most of sampling and resolution requirements. Data quality does not meet the requirements over most of the profile. Random uncertainty exceeds the 8 % threshold nearly everywhere and there is solid evidence of a +2-3 % per decade or more drift across the entire profile which will impact long-term studies.

Table 5.13 - Compliance of SABER 9.6µm v2.0 with user requirements (URD v4.1): full compliance (green), partial compliance (orange) and no compliance (red).

	Requirement	Compliance / evaluation
Horizontal resolution	< 100–300 km	500 km [RD77]
Vertical resolution	< 1–3 km	2 km [RD77]
Observation frequency	< 3 days	3 days
Time period	(1980-2010) – (2003-2010)	01/2002 – 12/2023
Total uncertainty in height registration	< ± 500 m	unknown
Dependences	–	latitude, altitude

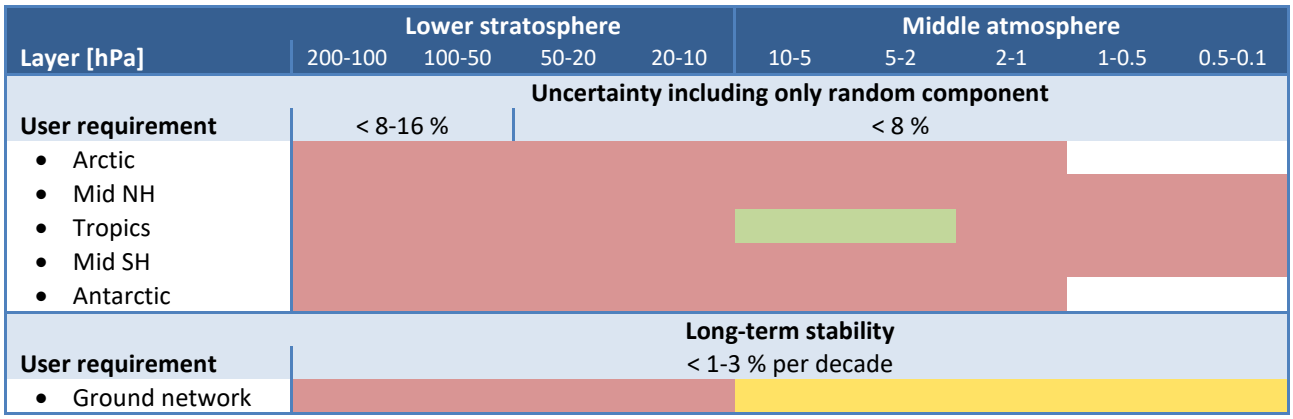

5.4.14 EOS-Aura MLS v5.0

The results in this section were obtained for Level-2 processor version 5.0, file version 8, for the volume mixing ratio versus pressure profile representation. Validation results for an earlier processor version (v4.2) of the Aura MLS data set can be found in the Appendix of this document (HARMOZ PRS).

5.4.14.1 Co-locations / Validation sample

Figure 5.49 shows the latitude–time distribution of the ozonesonde, lidar and MWR measurements co-locating with Aura MLS v5.0 data. The sampling covers most latitude zones and is very homogeneous in time. Slightly fewer co-locations are also seen in the last few years of the mission, due to the unavailability of publicly released correlative data.

5.4.14.2 Bias and dispersion

The median bias and half the 68 % interpercentile of the relative difference between Aura MLS v5.0 and GAW/NDACC/SHADOZ ozonesondes, NDACC lidars or NDACC MWRs are shown in the figures below. Figure 5.50 details the vertical and meridian dependence of the bias and dispersion at 5° latitude resolution, while Figure 5.51 shows the same information calculated in 30° latitude zones.

The vertical-meridian structure of the median bias follows that of the tropopause. Stratospheric and mesospheric bias is mostly less than 3-4 % and has almost no vertical structure. Imprints of vertical oscillations are clearly visible in the UTLS region, starting around 70 hPa (~17 km). This feature is known [RD66] but is diluted in the Ozone_cci+ product since the original Aura MLS profiles are interpolated to another vertical grid.

The meridian structure of the dispersion $s_{\Delta x}$ follows that of the tropopause. Above 30-40 hPa (~21-24 km) the half IP-68 spread is 3-4 % at the equator and increases gradually up to 6-8 % at the poles. At lower altitudes, the dispersion increases rapidly. Around the tropopause the dispersion is 25 % in the tropics and 35-40 % at higher latitudes. The dispersion seen in the comparisons is generally larger than the ex-ante random uncertainty $s_{ex\text{-}ante}$ (not shown here) provided in the Aura MLS data files (2-3 % above 50 hPa/20 km).

No notable changes were seen in these quality indicator with respect to those obtained for Aura MLS v4.2.

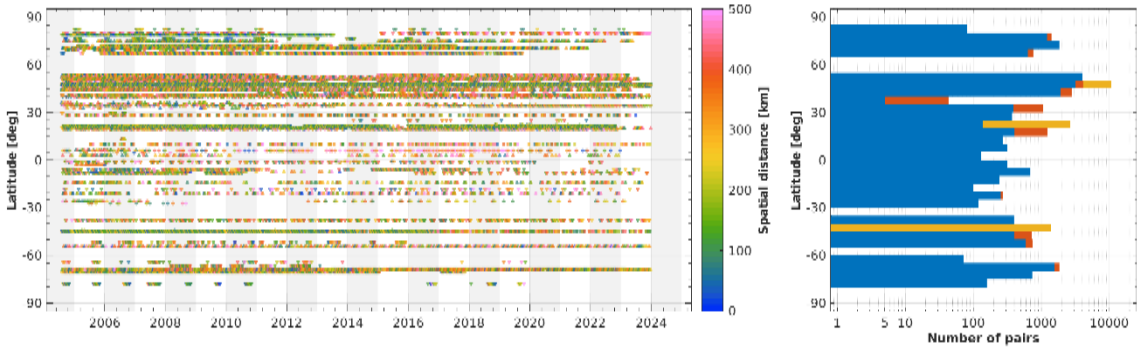

Figure 5.49 - (Left) Latitude–time distribution of co-locations between Aura MLS v5.0 ozone profiles and ground-based measurements (GAW/NDACC/SHADOZ ozonesonde, NDACC stratospheric ozone lidar and NDACC MWR). The colour code indicates the spatial distance of each satellite/ground-based pair. (Right) Number of co-located pairs per 5° latitude band for ozonesonde (blue), lidar (red) and MWR (orange).

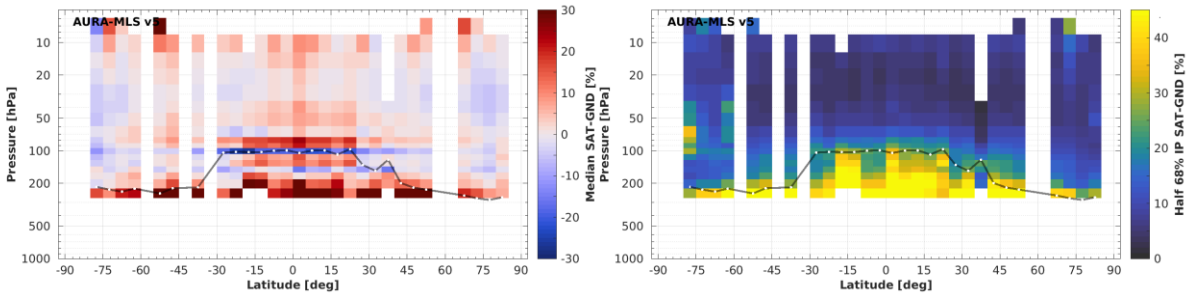

Figure 5.50 - Altitude–latitude cross-section of the median percent bias (left) and of the half IP-68 spread (right) between Aura MLS v5.0 ozone profile data and the global ozonesonde network, calculated over the entire Aura MLS time period and in 5° bins. Black lines indicate the median tropopause altitude.

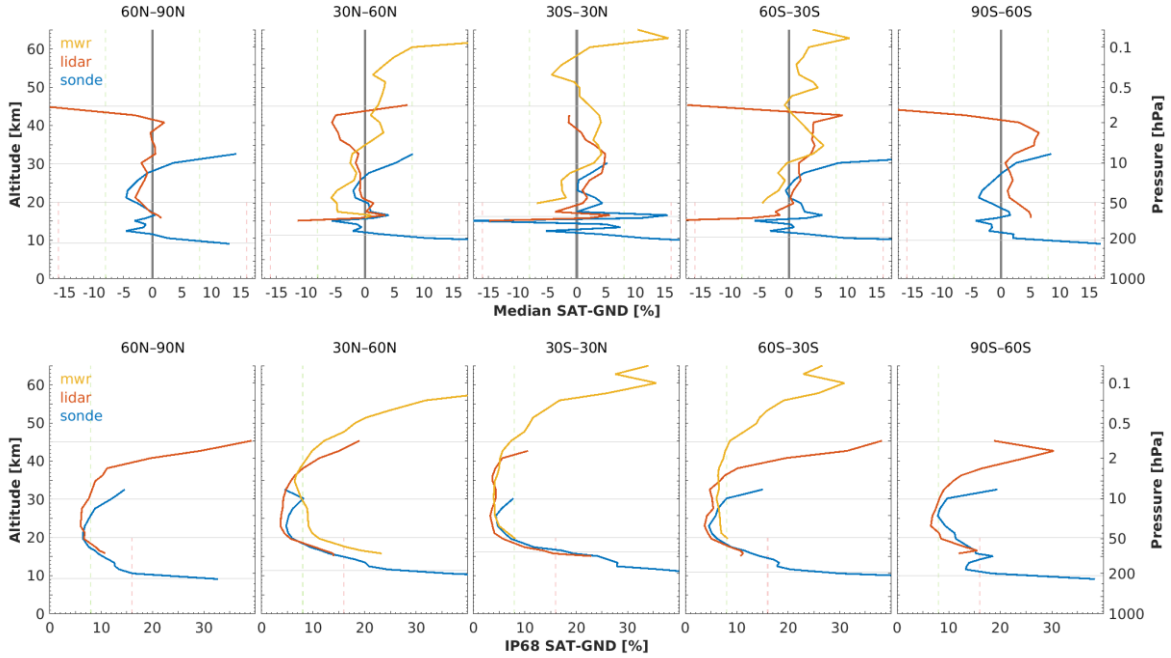

Figure 5.51 - (Top) Median bias between Aura MLS v5.0 ozone profile data and ozonesonde, lidar and MWR data, by 30° latitude. (Bottom) Same, but for the half IP-68 spread. The lowest horizontal line indicates the median tropopause altitude over the co-location sample.

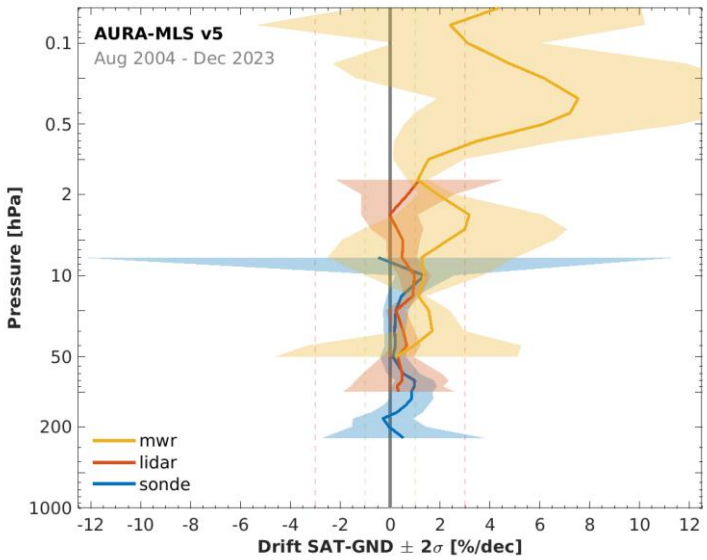

Figure 5.52 - Global network-averaged drift of Aura MLS v5.0 ozone profile data with respect to ozonesonde, lidar and MWR data, calculated over the 2004-2023 time period. The shaded region represents 2σ uncertainty on the average decadal drift.

5.4.14.3 Long-term stability

Figure 5.52 shows the drift of Aura MLS v5.0 ozone profile data with respect to the co-located ozonesonde, lidar and MWR network data. Drift estimates are positive but small: less than 1 % per decade between 200-2 hPa (~10-41 km) and less than 2 % per decade in the uppermost stratosphere, between 2-0.9 hPa (~41-46 km). In the mesosphere, the drift estimates are larger but also become too uncertain to conclude anything. Overall, results from all ground-based techniques are in good agreement in regions where they are most sensitive. There is therefore substantial support for an essentially drift-free Aura MLS data record (at the level of about 1 % per decade) across the entire stratosphere. No notable changes were seen in these drift estimates with respect to those obtained for Aura MLS v4.2.

5.4.14.4 Dependence of data quality on other parameters

Bias, dispersion and long-term stability of Aura MLS v5.0 ozone are very similar in four different profile representations. This indicates that the auxiliary pressure and temperature profiles included in the Aura MLS HARMOZ data files and in the correlative data files are consistent.

5.4.14.5 Compliance with user requirements

From the results reported above, we conclude that the Aura MLS v5.0 ozone profile data record is nearly compliant with all sampling and resolution requirements. Requirements on random uncertainty are met at altitudes above the 50 hPa level (~20 km). Also decadal stability is compliant over the entire stratosphere. Assessing compliance of random uncertainty in polar regions proves challenging due to the unquantified but likely considerable contribution by natural variability to the observed dispersion. As a result, random uncertainty compliance is flagged as not fulfilled in the polar upper stratosphere, but it is understood that this may not reflect the actual data quality.

Table 5.14 - Compliance of Aura MLS v5.0 with user requirements (URD v4.1): full compliance (green), partial compliance (orange) and no compliance (red).

	Requirement	Compliance / evaluation
Horizontal resolution	< 100–300 km	200–500 km [RD66]
Vertical resolution	< 1–3 km	2.5–5 km [RD66]
Observation frequency	< 3 days	Daily global coverage [RD97]
Time period	(1980-2010) – (2003-2010)	08/2004 – 12/2023
Total uncertainty in height registration	< ± 500 m	unknown
Dependences	–	latitude, altitude

	Lower stratosphere				Middle atmosphere				
Layer [hPa]	200-100	100-50	50-20	20-10	10-5	5-2	2-1	1-0.5	0.5-0.1
	Uncertainty including only random component								
User requirement	< 8-16 %		< 8 %						
• Arctic					(large natural variability)				
• Mid NH									
• Tropics									
• Mid SH									
• Antarctic					(large natural variability)				
	Long-term stability								
User requirement	< 1-3 % per decade								
• Ground network									

5.4.15 SPOT-4 POAM III v4

The results in this section were obtained for Level-2 processor version 4, file version 4, for the number density versus altitude profile representation (HARMOZ ALT).

5.4.15.1 Co-locations / Validation sample

Figure 5.22 shows the latitude–time distribution of the ozonesonde and lidar measurements co-locating with the POAM III v4 dataset. Due to the orbital inclination of the satellite and its solar occultation viewing geometry, comparisons are mostly found at high latitudes. Co-locations are noted at two sites at Northern mid-latitudes but we deem that results are likely not representative outside of the polar regions. No co-locations with MWR measurements were found. The temporal sampling is fairly continuous given annual interruptions during polar winter. In addition, the type of occultation differs between the Northern (sunrise) and Southern (sunset) Hemispheres, which should be considered in the (lidar) comparisons above ~35 km where the magnitude of the diurnal cycle in ozone becomes stronger.

5.4.15.2 Bias and dispersion

The median bias and half the 68 % interpercentile of the relative difference between POAM III v4 and GAW/NDACC/SHADOZ ozonesondes and NDACC lidars are shown in the figures below. Figure 5.53 details the vertical and meridian dependence of the bias and dispersion at 5° latitude resolution, while Figure 5.54 shows the same information calculated in 30° latitude zones.

POAM III underestimates ground-based data by up to 5 % between 15-30 km at high latitudes. At lower and higher altitudes, there is a positive bias with respect to sonde and/or lidar, which reaches 10-15 % close to the tropopause and 5-10 % in the Arctic upper stratosphere. The apparent tension between the sonde and lidar comparison results in the polar regions can be traced to a known negative bias of the lidar data between 1991 and 1998 at Dumont d'Urville (Antarctica, [RD43]).

The dispersion $s_{\Delta x}$ in the Arctic is 8-10 % between 20-30 km and increases to 30-40 % at the tropopause and at 40 km altitude. In the Antarctic the variability is somewhat larger due to the presence of the ozone hole. The dispersion seen in the comparisons is slightly larger than the ex-ante random uncertainty $s_{ex\text{-}ante}$ provided in the POAM III record (not shown here). The latter is of the order of 4-7 % between 20-30 km and increases up to 20-40 % in the UTLS and upper troposphere.

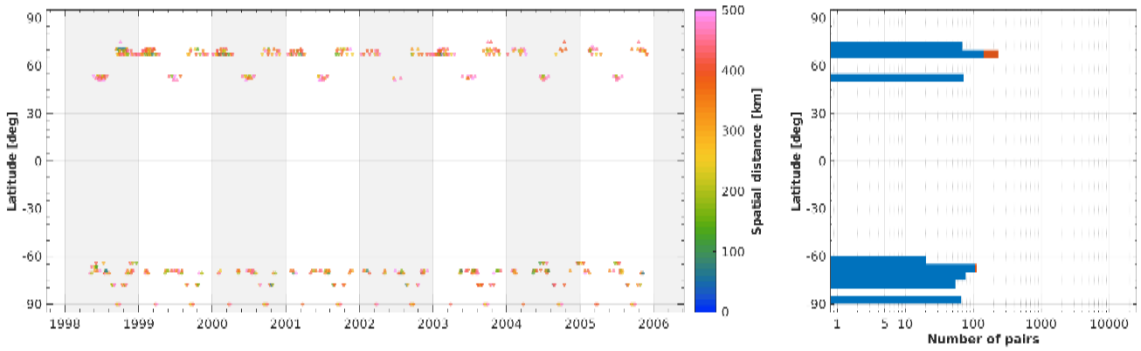

Figure 5.53 - (Left) Latitude–time distribution of co-locations between POAM III v4 ozone profiles and ground-based measurements (GAW/NDACC/SHADOZ ozonesonde and NDACC stratospheric ozone lidar). The colour code indicates the spatial distance of each satellite/ground-based pair. (Right) Number of co-located pairs per 5° latitude band for ozonesonde (blue) and lidar (red).

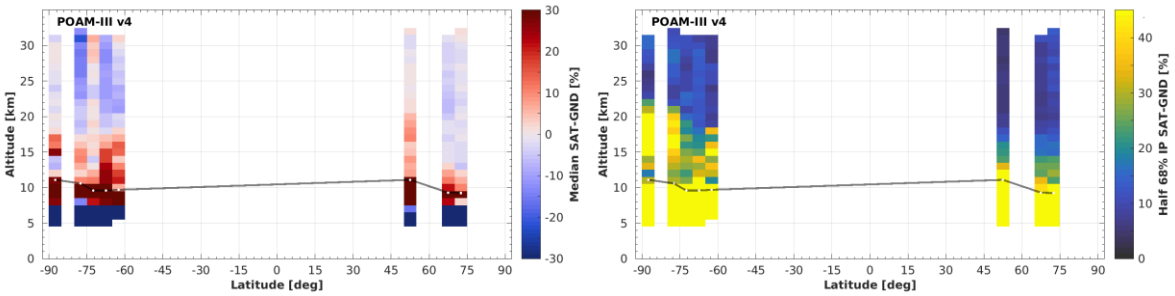

Figure 5.54 - Altitude–latitude cross-section of the median percent bias (left) and of the half IP-68 spread (right) between POAM III v4 ozone profile data and the global ozonesonde network, calculated over the entire POAM III time period and in 5° bins. Black lines indicate the median tropopause altitude. Results outside the polar regions are likely not representative.

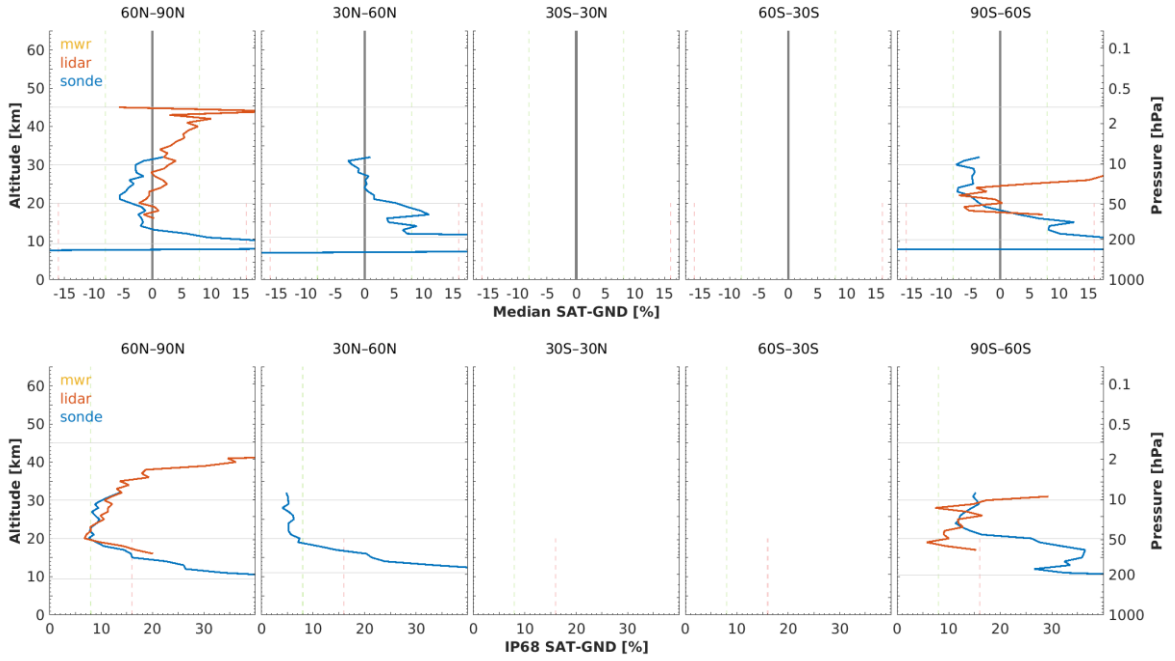

Figure 5.55 - (Top) Median bias between POAM III v4 ozone profile data and ozonesonde and lidar data, by 30° latitude. (Bottom) Same, but for the half IP-68 spread. The lowest horizontal line indicates the median tropopause altitude over the co-location sample. Results outside the polar regions are likely not representative.

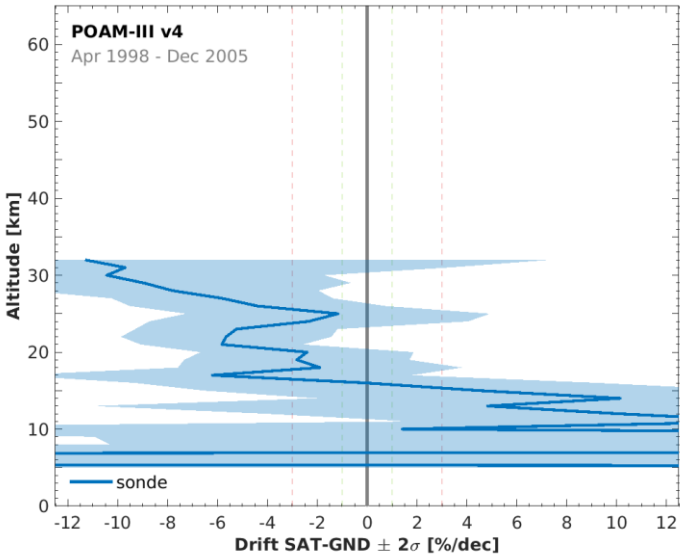

Figure 5.56 - Global network-averaged drift of POAM III v4 ozone profile data with respect to ozonesonde data, calculated over the 1998-2005 time period. The shaded region represents 2σ uncertainty on the average decadal drift.

5.4.15.3 Long-term stability

Figure 5.25 shows the vertical structure of the decadal drift of POAM III v4 data relative to the ozonesonde network. There are not enough co-locations to obtain meaningful estimates of drift relative to lidar measurements. Co-locations with ozonesonde are available at just a handful of sites due to POAM III's limited spatial coverage. Estimates of network-averaged drift will therefore be more prone to inhomogeneities (spatial and temporal) in the ozonesonde records than those for other satellite sensors. The drift uncertainty, estimated at 2-4 % per decade between 20-30 km (1σ), is likely smaller than in reality. For this reason, we have low confidence in the 5-10 % per decade negative drift between 20-30 km. Nonetheless, we recommend users of POAM III data to verify their stability as our analysis can not exclude the presence of drift.

5.4.15.4 Dependence of data quality on other parameters

Bias and dispersion of POAM III ozone are in excellent agreement in four different profile representations. This indicates that the auxiliary pressure and temperature profiles included in the POAM III HARMOZ data files and in the correlative data files are consistent.

5.4.15.5 Compliance with user requirements

Our ground-based assessment of the quality of the POAM III v4 ozone profile data record is restricted to high latitudes. The data record meets the user's uncertainty requirements only in the Arctic lowermost stratosphere. However, assessing random uncertainty in the polar regions proves challenging due to the unquantified but likely considerable contribution by natural variability to the observed dispersion in the comparisons. Furthermore, the ground-based analysis is unable to test compliance of POAM III stability at the 1-3 % per decade level, mainly due to the scarcity of comparison data.

Table 5.15 - Compliance of POAM III v4 with user requirements (URD v4.1): full compliance (green), partial compliance (orange) and no compliance (red).

	Requirement	Compliance / evaluation
Horizontal resolution	< 100–300 km	uncertain [RD91]
Vertical resolution	< 1–3 km	1-2 km
Observation frequency	< 3 days	not compliant
Time period	(1980-2010) – (2003-2010)	04/1998 – 12/2005
Total uncertainty in height attribution	< ± 500 m	likely compliant (solar occultation)
Dependences	–	latitude, altitude

	Lower stratosphere				Middle atmosphere				
Layer [km]	10-15	15-20	20-25	25-30	30-35	35-40	40-45	45-50	50-60
	Uncertainty including only random component								
User requirement	< 8-16 %				< 8 %				
• Arctic									
• Mid NH									
• Tropics									
• Mid SH									
• Antarctic									
	Long-term stability								
User requirement	< 1-3 % per decade								
• Ground network									

5.4.16 Meteor-3M SAGE III v4

The results in this section were obtained for Level-2 processor version 4, file version 2, for the number density versus altitude profile representation (HARMOZ ALT).

5.4.16.1 Co-locations / Validation sample

Figure 5.57 shows the latitude–time distribution of the ozonesonde, lidar and MWR measurements co-locating with SAGE III/M3M v4 data. The sampling pattern is quite peculiar due to the orbit of the satellite. There is no homogeneous sampling in the time domain and comparisons are only available at mid-latitudes and in the Arctic.

5.4.16.2 Bias and dispersion

The median bias and half the 68 % interpercentile of the relative difference between SAGE III/M3M v4 and GAW/NDACC/SHADOZ ozonesondes, NDACC lidars or NDACC MWRs are shown in the figures below. Figure 5.58 details the vertical and meridian dependence of the bias and dispersion at 5° latitude resolution, while Figure 5.59 shows the same information calculated in 30° latitude zones.

The SAGE III/M3M bias is less than ±5 % in the middle and lower stratosphere, underestimating ground-based data in the Arctic and overestimating at mid-latitudes. Larger positive biases of 5-15 % are noticed in the uppermost stratosphere and in the UT/LS region. Between 20-40 km, the half IP-68 spread lies between 3-8 % at mid-latitudes and between 8-16 % in the Arctic. The dispersion increases rapidly at lower altitudes and reaches 40 % around the tropopause. The dispersion seen in the comparisons is clearly larger than the ex-ante random uncertainty $s_{ex\text{-}ante}$ (not shown here) provided in the SAGE III/M3M data files. The latter is less than 1-2 % above 20 km and increases to about 25 % at the tropopause.

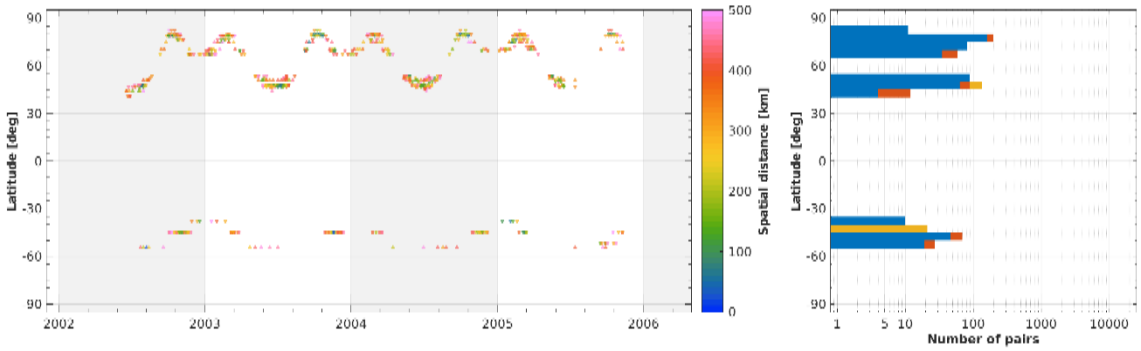

Figure 5.57 - (Left) Latitude–time distribution of co-locations between SAGE III/M3M v4 ozone profiles and ground-based measurements (GAW/NDACC/SHADOZ ozonesonde, NDACC stratospheric ozone lidar and NDACC MWR). The colour code indicates the spatial distance of each satellite/ground-based pair. (Right) Number of co-located pairs per 5° latitude band for ozonesonde (blue), lidar (red) and MWR (orange).

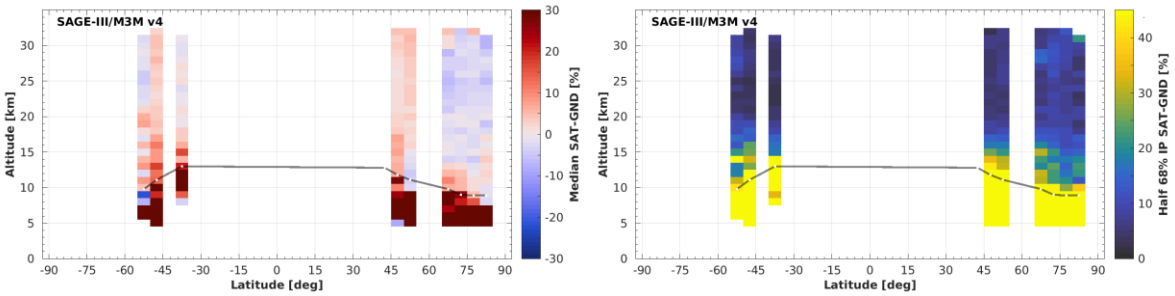

Figure 5.58 - Altitude–latitude cross-section of the median percent bias (left) and of the half IP-68 spread (right) between SAGE III/M3M v4 ozone profile data and the global ozonesonde network, calculated over the entire SAGE III/M3M time period and in 5° bins. Black lines indicate the median tropopause altitude.

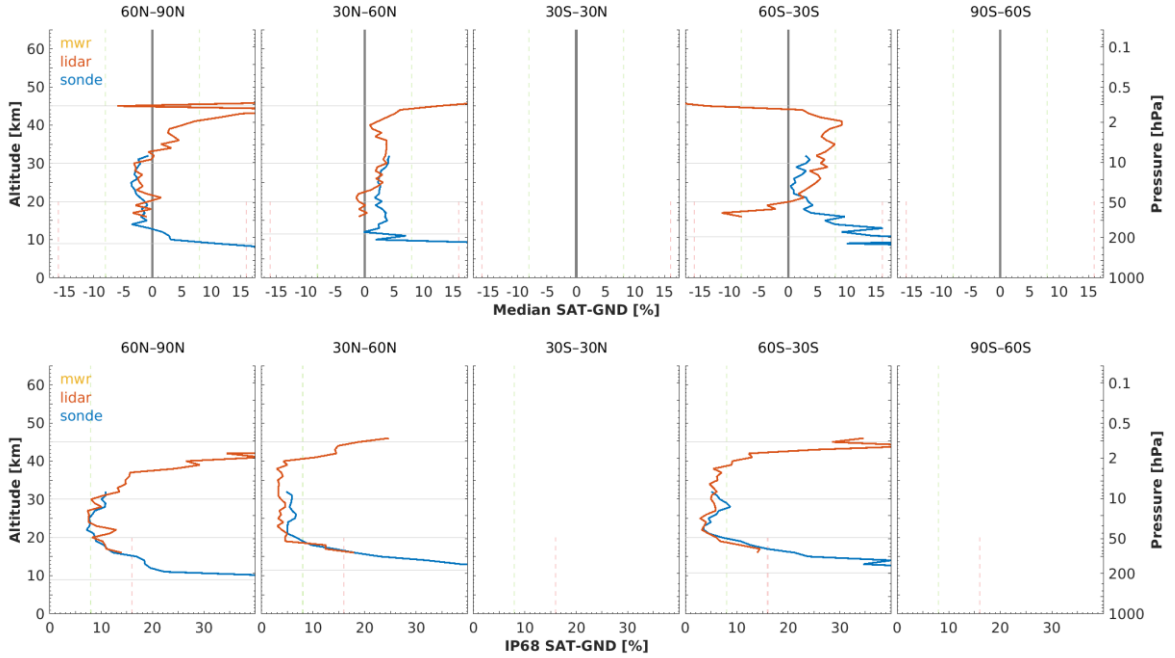

Figure 5.59 - (Top) Median bias between SAGE III/M3M v4 ozone profile data and ozonesonde, lidar and MWR data, by 30° latitude. (Bottom) Same, but for the half IP-68 spread. The lowest horizontal line indicates the median tropopause altitude over the co-location sample.

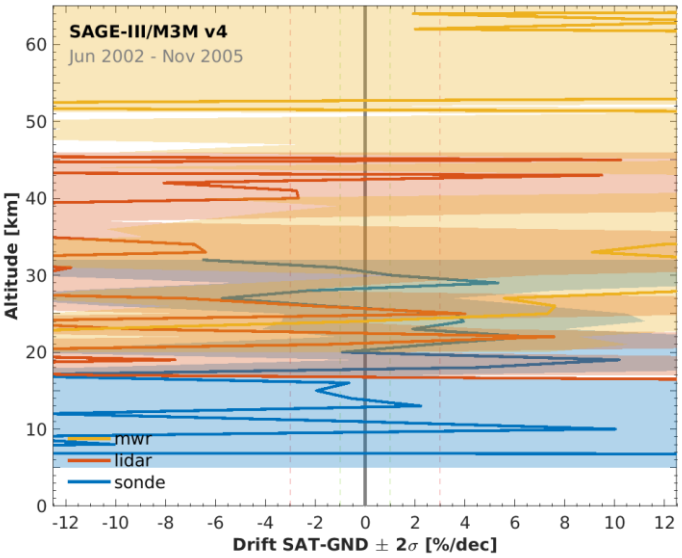

Figure 5.60 - Global network-averaged drift of SAGE III/M3M v4 ozone profile data with respect to ozonesonde, lidar and MWR data, calculated over the 2002-2005 time period. The shaded region represents 2σ uncertainty on the average decadal drift.

5.4.16.3 Long-term stability

Figure 5.60 shows the vertical structure of the decadal drift of SAGE III/M3M v4 data relative to the ozonesonde, lidar and MWR networks. Due to its short data record (3.5 years) SAGE III/M3M drift cannot be well constrained. The uncertainty (1σ) of the estimates is at best 5-10 % per decade across the stratosphere. Hence, we can only conclude that SAGE III/M3M drift, if any, is not worse than 10 % per decade.

5.4.16.4 Dependence of data quality on other parameters

Bias, dispersion and long-term stability of SAGE III/M3M ozone are in excellent agreement in four different profile representations. This indicates that the auxiliary pressure and temperature profiles included in the SAGE III/M3M HARMOZ data files and in the correlative data files are consistent.

5.4.16.5 Compliance with user requirements

Verifying the compliance of the short SAGE III/M3M data record with user requirements is very hard. What is already clear is that an UV-visible occultation mission, like SAGE, is unable to meet the temporal sampling requirements but that it does have the required vertical resolution and accuracy in altitude registration. Besides this, the random uncertainty requirements between 20-40 km are likely to be met at middle latitudes and in the lowermost stratosphere of the Arctic. Verification of compliance with user requirements for long-term stability is not possible.

Table 5.16 - Compliance of SAGE III/M3M v4 with user requirements (URD v4.1): full compliance (green), partial compliance (orange) and no compliance (red).

	Requirement	Compliance / evaluation
Horizontal resolution	< 100–300 km	uncertain [RD91]
Vertical resolution	< 1–3 km	0.5 km
Observation frequency	< 3 days	not compliant, ~30 solar occultation profiles per day
Time period	(1980-2010) – (2003-2010)	06/2002 – 11/2005
Total uncertainty in height registration	< ± 500 m	likely compliant (solar occultation)
Dependences	–	latitude, altitude, sunset/sunrise

	Lower stratosphere				Middle atmosphere				
Layer [km]	10-15	15-20	20-25	25-30	30-35	35-40	40-45	45-50	50-60
	Uncertainty including only random component								
User requirement	< 8-16 %		< 8 %						
• Arctic									
• Mid NH									
• Tropics									
• Mid SH									
• Antarctic									
	Long-term stability								
User requirement	< 1-3 % per decade								
• Ground network									

5.4.17 ISS SAGE III v5.3

The results in this section were obtained for Level-2 processor version 5.3, file version 4, for the number density versus altitude profile representation (HARMOZ ALT). Retrievals from lunar occultation data are released by NASA, but not used by the Ozone_cci project. Validation results for an earlier processor version (v5.1) of the SAGE III / ISS data set can be found in the Appendix of this document.

5.4.17.1 Co-locations / Validation sample

Figure 5.61 shows the latitude–time distribution of the ozonesonde, lidar and MWR measurements co-locating with SAGE III/ISS v5.3 data. The number of co-locations is fairly low due to the sparse sampling by SAGE III/ISS. It must therefore be kept in mind that sampling uncertainty and spatial inhomogeneities in ground-based network data may contribute considerably to the observed differences. The region with best robustness of the results is at Northern mid-latitudes, elsewhere additional data will be very helpful in future analyses.

5.4.17.2 Bias and dispersion

The median bias and half the 68 % interpercentile of the relative difference between SAGE III/ISS v5.3 and GAW/NDACC/SHADOZ ozonesondes, NDACC lidars or NDACC MWRs are shown in the figures below. Figure 5.62 details the vertical and meridian dependence of the bias and dispersion at 5° latitude resolution, while Figure 5.63 shows the same information calculated in 30° latitude zones.

SAGE III/ISS generally overestimates middle stratospheric ozone by 2-5 % (between 20-35 km altitude) with respect to observations by the different ground-based networks. Below 20 km, SAGE III/ISS is biased positive versus ozonesonde (up to 10-15 % at tropopause) and negative versus lidar. Results above 40 km have very low confidence at the moment; at two sites a negative bias is seen (~3-5 %), but and one sites indicates a positive bias (~10-12 %).

The dispersion $s_{\Delta x}$ between 20-40 km lies between 5-8 %. A slow increase (up to 16-20 % at the stratopause) is noted at higher altitudes and a rapid increase below 20 km (up to 40-50 % at the tropopause). Similar values are found for SAGE II (Figure 5.39) and SAGE III/M3M (Figure 5.59). The dispersion seen in the comparisons is clearly larger than the ex-ante random uncertainty $s_{ex\text{-}ante}$ (not shown here) provided in the SAGE III/ISS data files. The latter is only 0.5-1.5 % between 20-35 km and increases to about 25-30 % at the tropopause.

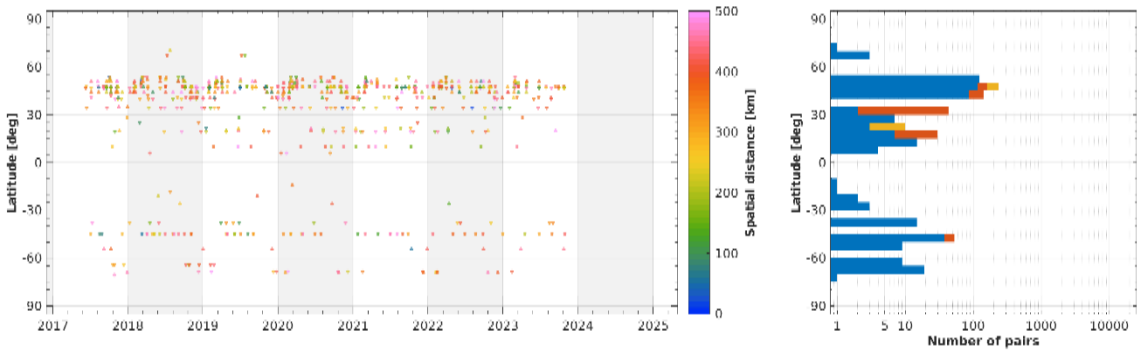

Figure 5.61 - (Left) Latitude–time distribution of co-locations between SAGE III/ISS v5.3 ozone profiles and ground-based measurements (GAW/NDACC/SHADOZ ozonesonde, NDACC stratospheric ozone lidar and NDACC MWR). The colour code indicates the spatial distance of each satellite/ground-based pair. (Right) Number of co-located pairs per 5° latitude band for ozonesonde (blue), lidar (red) and MWR (orange).

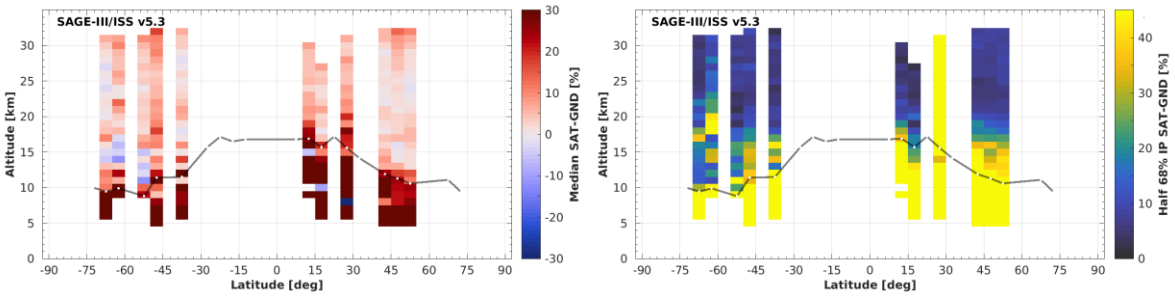

Figure 5.62 - Altitude–latitude cross-section of the median percent bias (left) and of the half IP-68 spread (right) between SAGE III/ISS v5.3 ozone profile data and the global ozonesonde network, calculated over the entire SAGE III/ISS time period and in 5° bins. Black lines indicate the median tropopause altitude.

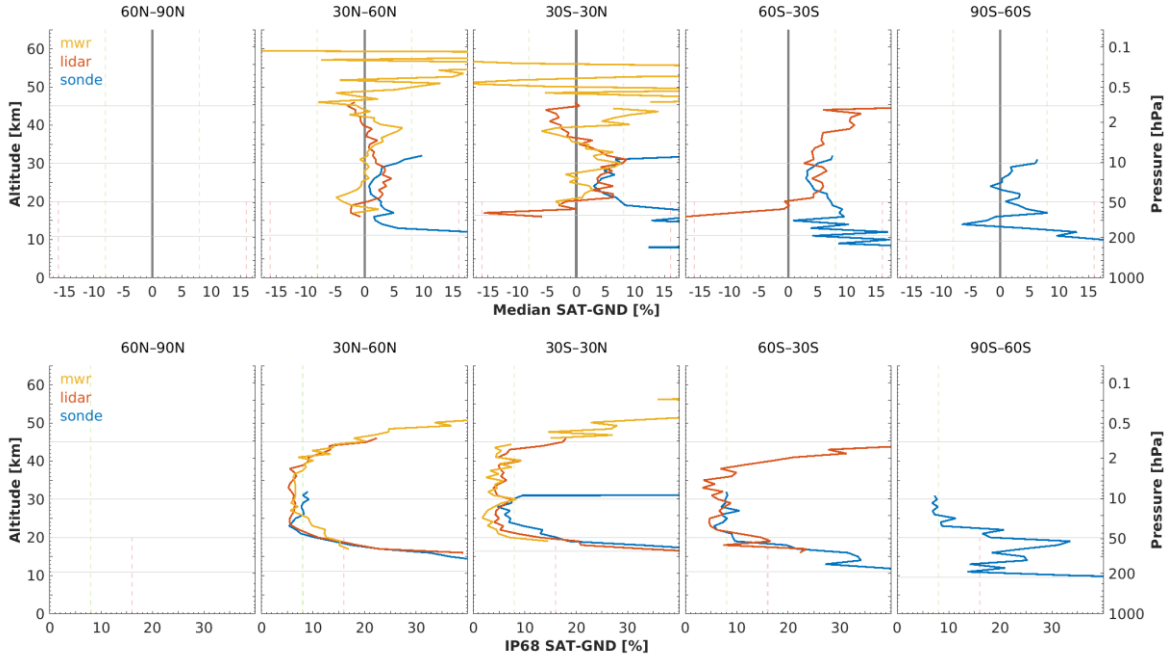

Figure 5.63 - (Top) Median bias between SAGE III/ISS v5.3 ozone profile data and ozonesonde, lidar and MWR data, by 30° latitude. (Bottom) Same, but for the half IP-68 spread. The lowest horizontal line indicates the median tropopause altitude over the co-location sample.

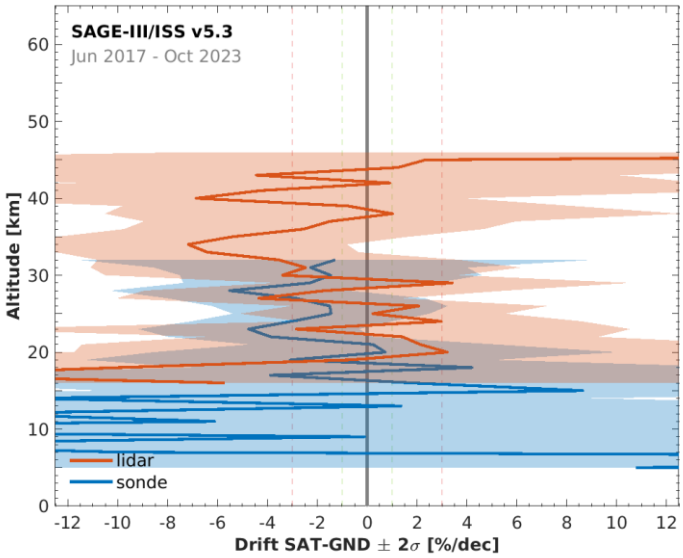

Figure 5.64 - Global network-averaged drift of SAGE III/ISS v5.3 ozone profile data with respect to ozonesonde and lidar data, calculated over the 2017-2023 time period. The shaded region represents 2σ uncertainty on the average decadal drift.

5.4.17.3 Long-term stability

Figure 5.64 shows the vertical structure of the drift of SAGE III/ISS v5.3 data relative to the ozonesonde and lidar networks. The confidence in SAGE III/ISS drift estimates is fairly low due to the sparse co-location sample. The uncertainty of the drift estimates (1σ) is at best 2-3 % per decade in the middle stratosphere (20-30 km) and 3.5-5 % per decade in the upper stratosphere (30-40 km). With this in mind, both ozonesonde and lidar comparisons hint at a small, negative drift in the SAGE III/ISS data record. Current drift estimates are about -(2-3) % per decade over the 20-40 km range. Longer time series are needed to verify the stability of the data record.

5.4.17.4 Dependence of data quality on other parameters

Bias, dispersion and long-term stability of SAGE III/ISS ozone are in excellent agreement in four different profile representations. This indicates that the auxiliary pressure and temperature profiles included in the SAGE III / ISS HARMOZ data files and in the correlative data files are consistent.

5.4.17.5 Compliance with user requirements

Verifying the compliance of the short SAGE III/ISS data record with user requirements is fairly challenging at this point, especially for stability. For now, we report provisional results which will need to be consolidated after analysis of longer time series. What is already clear is that an UV-visible occultation mission, like SAGE, is unable to meet the temporal sampling requirements but that it does have the required vertical resolution and accuracy in altitude registration. Besides this, the random uncertainty requirements between 20-40 km are likely to be met at middle and low latitudes. Verification of long-term stability will require several more years of data.

Table 5.17 - Compliance of SAGE III/ISS v5.3 with user requirements (URD v4.1): full compliance (green), partial compliance (orange) and no compliance (red).

	Requirement	Compliance / evaluation
Horizontal resolution	< 100–300 km	uncertain [RD91]
Vertical resolution	< 1–3 km	1 km
Observation frequency	< 3 days	not compliant, ~30 solar occultation profiles per day
Time period	(1980-2010) – (2003-2010)	06/2017 – 10/2023
Total uncertainty in height registration	< ± 500 m	likely compliant (solar occultation)
Dependences	–	latitude, altitude, sunset/sunrise

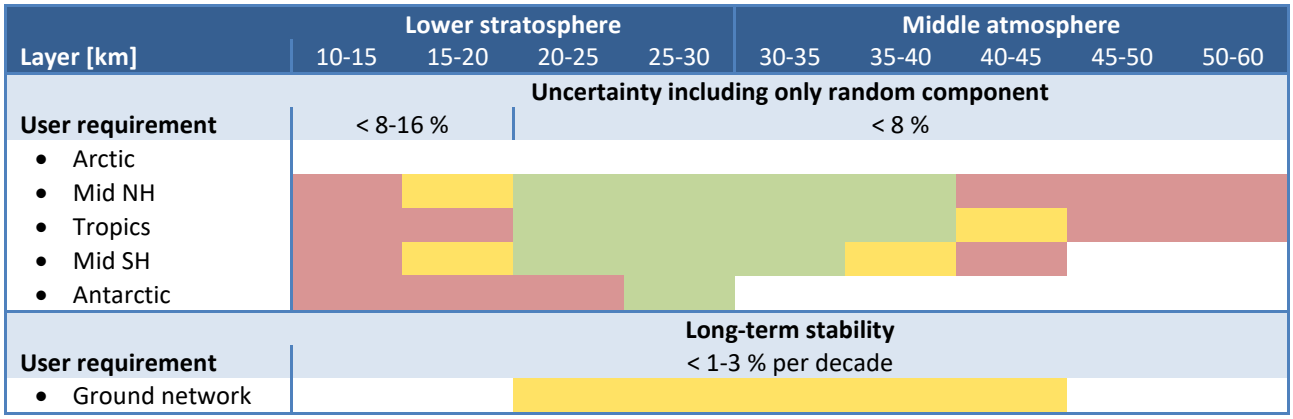

5.5 *Level-3 limb profile products*

Validation results (with respect to ozonesonde) for single-sensor or merged Level-3 data sets produced in earlier phases of Ozone_cci+ can be found in the Appendix of this document. The validated products include monthly zonal mean data from GOMOS (ALGOM2s v1), MIPAS (IMK/IAA v8), SCIAMACHY (UBr v3.5), OSIRIS (USask v5.10), ACE-FTS (v4), OMPS-LP/SNPP (USask-2D v1.1.0), SAGE II (v7.0), HALOE (v19), Aura MLS (v4.2), and SAGE-CCI-OMPS (v1). Also validation results for MEGRIDOP (v1), a monthly latitude-longitude gridded data product, can be found in Appendix. The Level-3 limb ozone profile data products listed above are part of the Copernicus Climate Change Service (C3S) and updated and/or extended on an annual basis. The validation results of these data sets are reported in the C3S Product Quality Assessment Report (https://cds.climate.copernicus.eu/datasets/satellite-ozone-v1?tab=documentation).

5.5.1 Validation method

The LIMB-HIRES data record is gap-free and has a high sampling resolution in the horizontal (1° latitude x 1° longitude) and the temporal (daily) domain, hence the same validation method is followed as for the Level-2 limb products (Sect. 5.4.1). The only difference lies in the colocation. We consider that LIMB-HIRES and ground-based ozone profiles co-locate when they are obtained on the same day and when the LIMB-HIRES grid cell contains the ground station. MWRs measure multiple ozone profiles per day; we only use the measurement closest to 13:45 local solar time. The latter is the effective local time of the LIMB-HIRES product since all limb sensors are debiased with respect to Aura MLS (in a 13:45 orbit).

5.5.2 LIMB-HIRES v1

The LIMB-HIRES v1 data files contain two ozone variables covering different vertical ranges: “ozone_satellite” (250-0.05 hPa) and “ozone_extended” (900-0.05 hPa). In this section, we distinguish both ozone products as “LIMB-HIRES” and “LIMB-HIRES extended”, respectively. The input data used by the merging algorithm may differ for the two products, depending on the vertical range (Table 5.18). Identical ozone values are produced for both products between 130-0.05 hPa but differences appear between 250-150 hPa. The merging algorithm debiases all contributing limb sensors with respect to Aura MLS. It is therefore expected that the data quality of LIMB-HIRES resembles that of Aura MLS v5 (Sect. 5.4.14).

Table 5.18 – Ozone information used to produce LIMB-HIRES and LIMB-HIRES extended.

Vertical range	LIMB-HIRES	LIMB-HIRES extended
900-300 hPa	*no data*	SILAM model (FMI)
250-150 hPa	limb observations	SILAM & limb observations
130-0.05 hPa	limb observations	limb observations

5.5.2.1 Co-locations / Validation sample

Figure 5.65 shows the latitude–time distribution of the ozonesonde, lidar and microwave radiometer (MWR) measurements co-locating with LIMB-HIRES v1 data. The co-location sample covers all latitude zones and is homogeneous in the time domain. This sample is the largest possible, since every (screened) ground-based profile can be utilised (LIMB-HIRES is a gap-free data product). Since the satellite product is gap-free, every ozonesonde and lidar measurement is used in the validation analysis, hereby reaching the largest possible co-location sample offered by these ground networks.

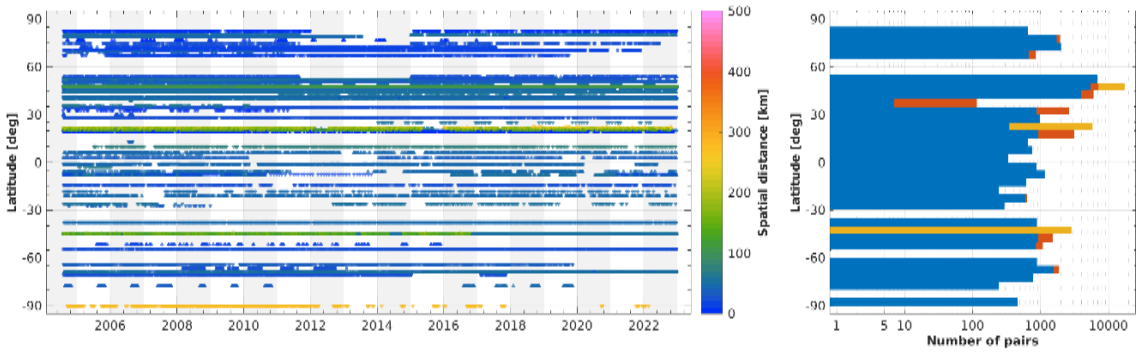

Figure 5.65 - (Left) Latitude–time distribution of co-locations between LIMB-HIRES v1 ozone profiles and ground-based measurements (GAW/NDACC/SHADOZ ozonesonde, NDACC stratospheric ozone lidar and NDACC MWR). The colour code indicates the spatial distance between satellite/ground-based profile. (Right) Number of co-located pairs per 5° latitude band for ozonesonde (blue), lidar (red) and MWR (orange).

5.5.2.2 Bias

The median bias between both LIMB-HIRES products and GAW/NDACC/SHADOZ ozonesondes, NDACC lidars or NDACC MWRs are shown in the figures below. Figure 5.66 details the vertical and meridian dependence of the bias relative to ozonesonde at 5° latitude resolution, while Figure 5.67 shows the same information calculated in 30° latitude zones with respect to ozonesonde, lidar and MWR.

In the stratosphere, LIMB-HIRES biases are generally less than 3-4 %. Larger biases are found in the mesosphere (above 0.5 hPa) and the troposphere (below 200 hPa). The sign of these biases is mostly positive: in the mesosphere, the lowermost stratosphere and upper troposphere. Negative biases are noted between 20-50 hPa. The difference between LIMB-HIRES and LIMB-HIRES extended is less than 1 % in the vertical range where the input data differs (250-150 hPa). In the middle and lower troposphere, negative biases are seen for LIMB-HIRES extended across the southern hemisphere and tropics, and positive biases at northern mid and high latitudes.

The vertical oscillations in the UTLS region (starting around 70 hPa , ~17 km) noted in the validation analysis of Aura MLS (Figure 5.50 left and Figure 5.51 top) are found for both LIMB-HIRES products as well. Overall, the spatial pattern of the bias is very similar to that of Aura MLS but LIMB-HIRES bias values are up to 1-2 % percent larger than for Aura MLS, depending on location.

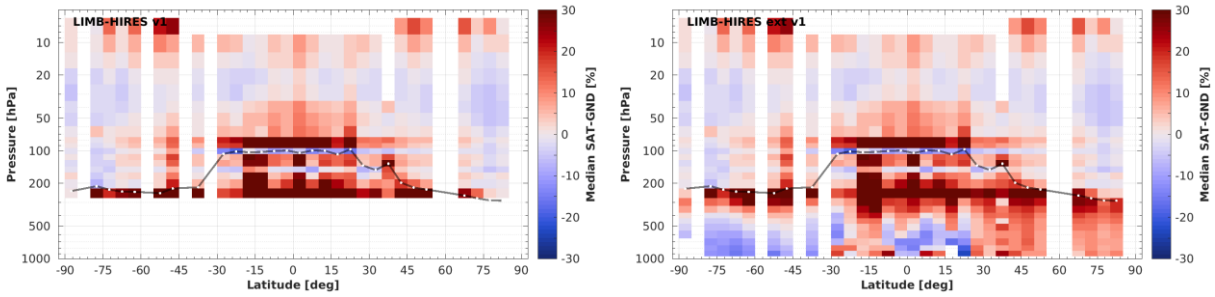

Figure 5.66 - Altitude–latitude cross-section of the median percent bias between LIMB-HIRES (left) and LIMB-HIRES extended (right) v1 ozone profile data and the global ozonesonde network, calculated over the entire LIMB-HIRES time period and in 5° bins. The black line indicates the median tropopause altitude.

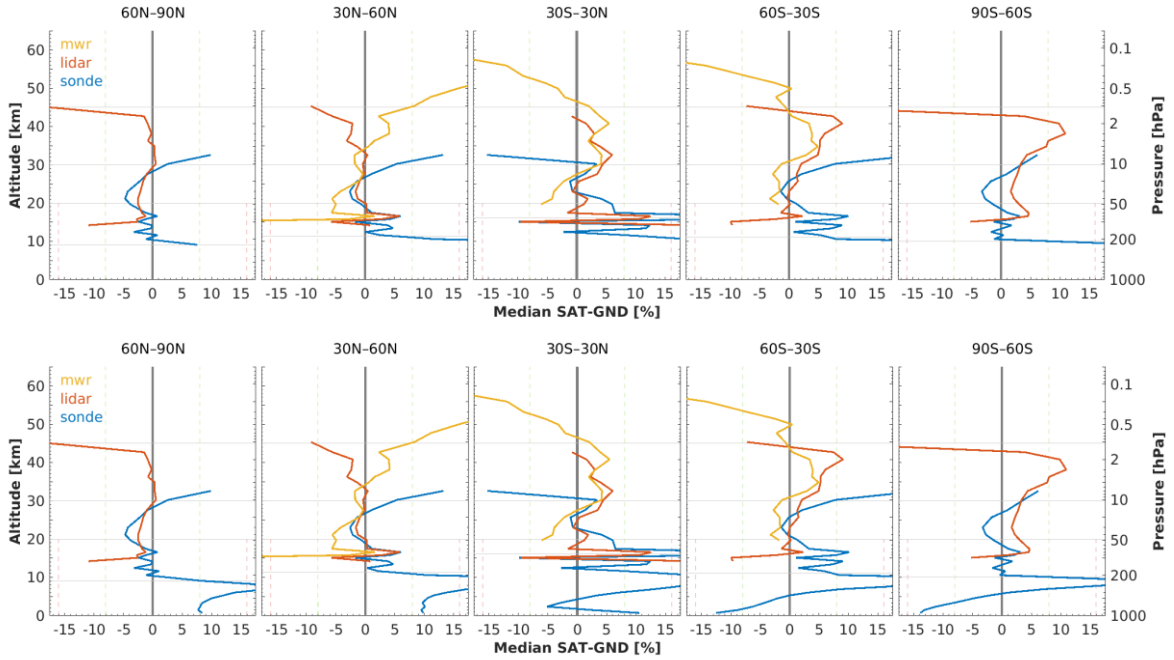

Figure 5.67 - Median bias between LIMB-HIRES (top) and LIMB-HIRES extended (bottom) v1 ozone profile data and ozonesonde, lidar and MWR data, by 30° latitude. The lowest horizontal line indicates the median tropopause altitude over the co-location sample.

5.5.2.3 Dispersion

The meridian structure of the dispersion follows that of the tropopause. Above 30-40 hPa (~21-24 km) the half IP-68 spread is ~4 % at the equator and increases gradually up to 7-8 % at the poles. At lower altitudes, the dispersion increases rapidly. Around the tropopause the dispersion is 30 % in the tropics and (at least) 40 % at in the polar regions. The difference in dispersion between LIMB-HIRES and LIMB-HIRES extended is negligible in the vertical range where the used input data differs (250-150 hPa).

When compared to Aura MLS dispersion estimates (Figure 5.50 right and Figure 5.51 bottom), the dispersion in the LIMB-HIRES comparisons is slightly larger (~1 %) in the stratosphere and (at least) 5 % larger below the 70 hPa level in the UTLS. In the mesosphere (above 0.5 hPa), however, smaller dispersions (up to ~5 %) are found than for Aura MLS.

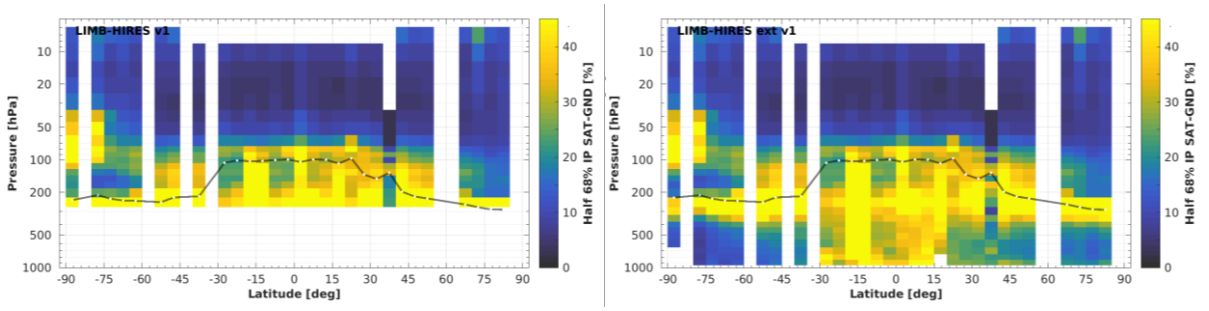

Figure 5.68 - Altitude–latitude cross-section of the dispersion between LIMB-HIRES (left) and LIMB-HIRES extended (right) v1 ozone profile data and the global ozonesonde network, calculated over the entire LIMB-HIRES time period and in 5° bins. The black line indicates the median tropopause altitude.

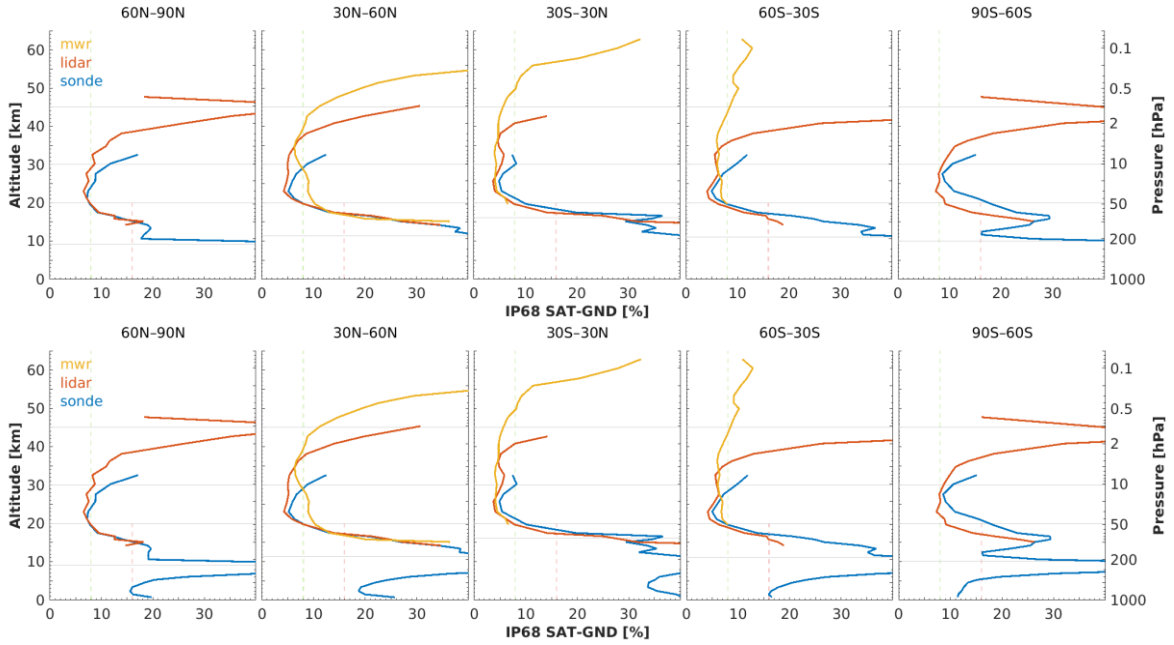

Figure 5.69 - Dispersion between LIMB-HIRES (top) and LIMB-HIRES extended (bottom) v1 ozone profile data and ozonesonde, lidar and MWR data, by 30° latitude. The lowest horizontal line indicates the median tropopause altitude over the co-location sample.

5.5.2.4 Long-term stability

Figure 5.70 shows the drift of LIMB-HIRES v1 ozone profile data with respect to co-located ozonesonde, lidar and MWR network data. Drift estimates are mostly positive but small: less than 1 % per decade between 200-2 hPa (~10-41 km) and less than 2 % per decade in the uppermost stratosphere, between 2-0.9 hPa (~41-46 km). In the mesosphere, the drift estimates are larger but also become too uncertain to conclude anything. The drift of the extended LIMB-HIRES product changes sign in the troposphere (below 200 hPa) but is also less than 1 % per decade and not significant. Overall, results from all ground-based techniques are in good agreement in regions where these sensors are most sensitive. There is therefore substantial support for an essentially drift-free LIMB-HIRES data record (at the level of about 1 % per decade) across the entire stratosphere and troposphere. These are essentially the same findings as for Aura MLS v5 (Sect. 5.4.14.3).

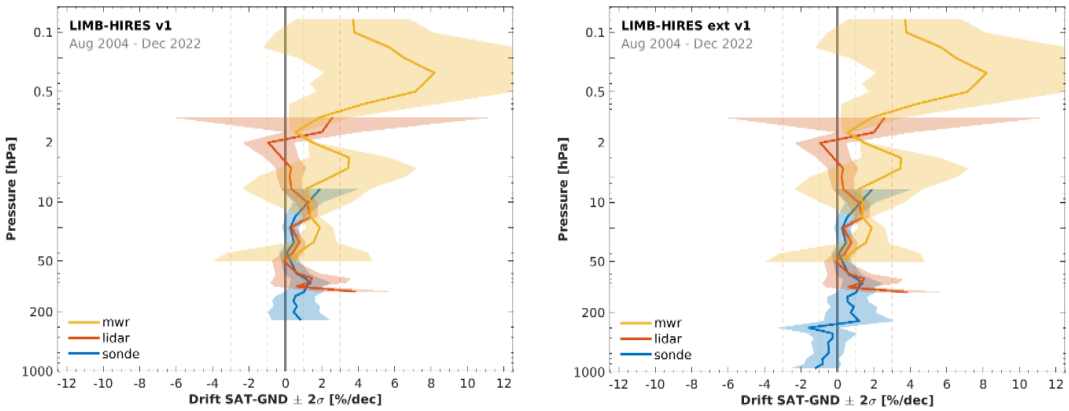

Figure 5.70 - Global network-averaged drift of LIMB-HIRES v1 (left) and LIMB-HIRES v1 extended (right) ozone profile data with respect to ozonesonde, lidar and MWR data, calculated over the 2004-2023 time period. The shaded region represents 2σ uncertainty on the average drift.

5.5.2.5 Compliance with user requirements

From the results reported above, we conclude that the LIMB-HIRES v1 ozone profile data record is fully compliant with nearly all sampling and resolution requirements. There is partial compliance for vertical resolution as in some parts of the atmosphere the effective resolution will be larger than 3 km. Requirements on random uncertainty are met at altitudes above the 50 hPa level (~20 km). Also decadal stability is compliant over the entire stratosphere and troposphere. Assessing compliance of random uncertainty in polar regions proves challenging due to the unquantified but likely considerable contribution by natural variability to the observed dispersion. As a result, random uncertainty compliance is flagged as not fulfilled in the polar upper stratosphere, but it is understood that this may not reflect the actual data quality.

Table 5.19 - Compliance of LIMB-HIRES v1 with user requirements (URD v4.1): full compliance (green), partial compliance (orange) and no compliance (red).

	Requirement	Compliance / evaluation
Horizontal resolution	< 100–300 km	100 km
Vertical resolution	< 1–3 km	2.5–5 km [RD66]
Observation frequency	< 3 days	Daily global coverage
Time period	(1980-2010) – (2003-2010)	08/2004 – 12/2022
Total uncertainty in height registration	< ± 500 m	unknown
Dependences	–	latitude, altitude

	Troposphere		Lower stratosphere				Middle stratosphere				
Layer [hPa]	900-500	500-200	200-100	100-50	50-20	20-10	10-5	5-2	2-1	1-0.5	0.5-0.1
	Uncertainty including only random component										
User requirement	< 8 – 16 %						< 8 %				
• Arctic											
• Mid NH											
• Tropics											
• Mid SH											
• Antarctic											
	Long-term stability										
User requirement	< 1-3 % per decade										
• Ground network											

6 Validation of Tropospheric Ozone Data products

The three tropospheric ozone data records (GTTO-ECV v6lc, OMI-LIMB v1 and GTO-LIMB v1) considered in this section combine measurements by multiple satellite sensors and consist of monthly mean 1° latitude by 1° longitude gridded partial columns of ozone with a vertical range depending on the product. The ground-based validation of tropospheric ozone data obtained through the retrieval of the vertical ozone profile by nadir sensors can be found in Sect. 4.

6.1 *Validation method*

The satellite data are validated using ozonesonde measurements as a reference. These balloon-borne sensors measure the vertical distribution of ozone with high accuracy and at high vertical resolution at many sites across the globe, from the surface up to about 5 hPa (Sect. 3.5.2.1). We take advantage of the homogenised ozonesonde data recently prepared by the HEGIFTOM working group of the second Tropospheric Ozone Assessment Report (Van Malderen et al., 2024 [RD92]). For each ozonesonde station, the sample of ozone profiles was quality screened, then aggregated into monthly means and, finally, integrated between surface and the top level of the considered Ozone_cci+ tropospheric ozone product. This results in a monthly mean tropospheric column time series by ozonesonde at each site in the ground network. None of the 1° x 1° satellite grid cells contain more than one ozonesonde site, so the combination of time series from different sites is not needed. Hence, the processed sonde data are directly comparable to the satellite products.

Statistical indicators for systematic error (*bias*), random uncertainty (*dispersion* or *comparison spread*) and stability (*drift*) are derived as described in Sections 4.1 and 5.1 of Hubert et al., 2016 [RD45].

6.2 *GTTO-ECV v6lc*

There are two GTTO-ECV v6 data products, differing only in their top level: v6lc contains tropospheric ozone columns between surface and 270 hPa (~10.5 km), v6hc columns between surface and 200 hPa (~12 km). The results in this section were obtained for GTTO-ECV version 6lc, file version 2.

6.2.1 Bias

Figure 6.1 (left) shows the median value (bias) of the GTTO-ECV v6lc minus ozonesonde comparisons, at 12 sites in the tropical[2] SHADOZ network. The tropospheric ozone column cover surface to 270 hPa. GTTO-ECV systematically overestimates ozonesonde measurements across the ground network. The network-averaged mean and its standard error (1σ) are +4.6 ± 0.5 DU (or +24 ± 3 %). At seven sites the positive bias ranges between +3 DU and +8 DU. Biases are smaller (+2 to +3 DU) at four sites in the 101° E – 172° W region (Sepang Airport, Watukosek, Suva, Samoa). Since this coincides with the region where the CCD algorithm estimates the stratospheric ozone column (70° E – 170° W) it is likely that the assumption, by the CCD algorithm, of zonal symmetry of the stratospheric column does not hold to the few DU level. An alternative but less likely cause could be residual measurement biases between sites that were not completely removed in the homogenisation process by the TOAR II HEGIFTOM working group (Van Malderen et al., 2024 [RD92]).

GTTO-ECV bias exhibits a seasonal cycle over several sites (Figure 6.2). The largest amplitude is found at Hilo, with a maximum of +15 DU in boreal winter and a minimum of +3 DU in August-October. At most sites around the Atlantic basin (Heredia, Paramaribo, San Cristobal, Natal, Nairobi, Natal) a temporary increase of GTTO-ECV bias varying between +3 DU to +6 DU is seen during July-October/November. This coincides with the season of active biomass burning in South America and South Africa. It is currently not clear whether the coincidence is causal.

[2] Due to the requirement of a sufficient number of convective clouds at high altitude, the GTTO-ECV data product only covers the 20° S-20° N tropical belt.

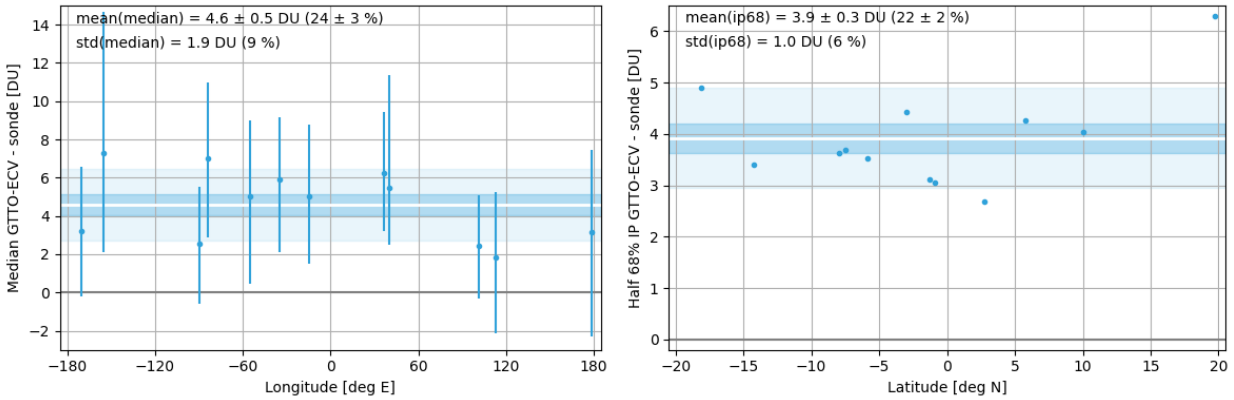

Figure 6.1 – Left: Bias (marker) and dispersion (error bar, 1σ) of GTTO-ECV v6lc versus ozonesonde data at each site in the network (longitudinally resolved). Positive values indicate that GTTO-ECV overestimates ozonesonde. Right: Dispersion (1σ) of GTTO-ECV versus ozonesonde at each site (latitudinally resolved). On both panels the network-averaged statistics are shown as white line and blue shaded areas.

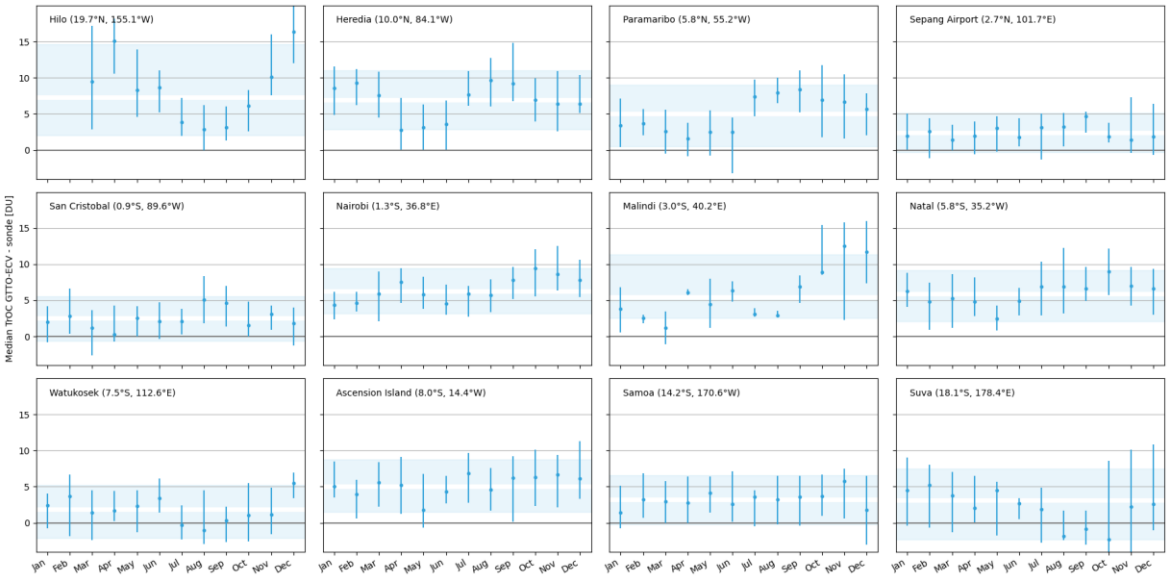

Figure 6.2 – Annual cycle of GTTO-ECV v6lc bias (marker) and dispersion (error bar, 1σ) versus ozonesonde data at each site in the tropical network (different panels). Also shown are the median (white line) and 68 % inter-percentile (blue area) of the comparisons. Positive values indicate that GTTO-ECV overestimates sonde data.

6.2.2 Dispersion

Figure 6.1 (right) shows the half-width of the 68 % interpercentile (dispersion) of the GTTO-ECV v6lc minus ozonesonde comparisons. Largest values (5-6 DU) are found over stations in the outer tropics (Suva 18.1° S, Hilo 19.7° N) which are often exposed to ozone rich air from the extratropics. At other sites, GTTO-ECV dispersion ranges between 3.0 DU and 4.5 DU. The network-averaged mean dispersion and its standard error (1σ) are 3.9 ± 0.3 DU (or 22 ± 2 %). Hubert et al. (2021) discuss that dispersion estimates derived from pairwise comparisons of S5P tropospheric ozone column data to ozonesonde are dominated by the random uncertainty due to differences in spatio-temporal smoothing and sampling (Sect. 4.5 in [RD46]). Hubert et al. (2021) analysed daily S5P data, so the smoothing/sampling mismatch uncertainty for monthly GTTO-ECV data will be even more important. In conclusion, it is expected that the random uncertainty of GTTO-ECV v6c is (much) smaller than the reported 3.9 DU (22 %).

6.2.3 Long-term stability

The GTTO-ECV v6c comparison time series at each ozonesonde station are shown in Figure 6.3 (thin lines), as well as their 5-year moving mean (grey) and a purely linear fit inferred with a robust regression method (blue line). Almost all sites offer measurements over 20 years or more, albeit sometimes with a gap of several years in the time series. The comparison data in the different periods are consistent at most sites, apart from the comparisons at San Cristobal since late 2021. The long-term behaviour of the difference time series is reasonably linear at all sites (within 1-2 DU). The only exception is Hilo, where a temporary excursion in bias is noted during the 2006-2014 period, peaking at +3 DU in 2010 with respect to the multi-decadal background. Figure 6.4 shows GTTO-ECV v6c drift relative to ozonesonde at each site, with its 95 % confidence interval. We conclude that GTTO-ECV is stable, the drift estimates average to +0.1 ± 0.3 DU per decade (2σ), or 0 ± 2 % per decade, over the network (when inverse-variance weighted).

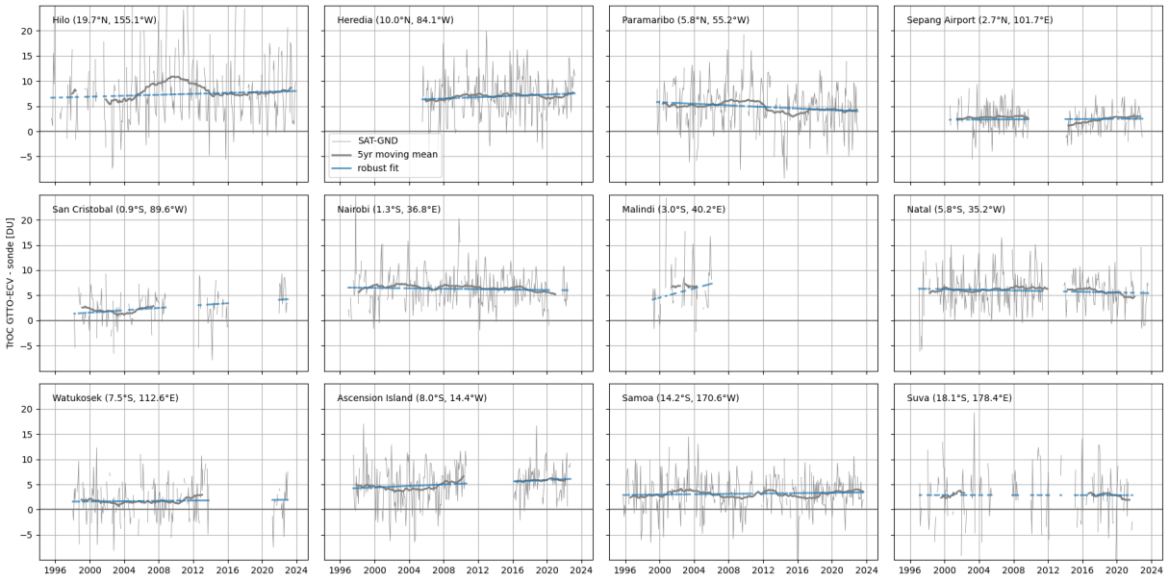

Figure 6.3 – Comparison time series of GTTO-ECV tropospheric ozone column data versus ozonesonde at each site in the tropical network (ordered North to South). Also shown are a robust linear fit (blue line) and a 5-year moving mean (grey line) of the comparisons. Positive values indicate that GTTO-ECV overestimates sonde data.

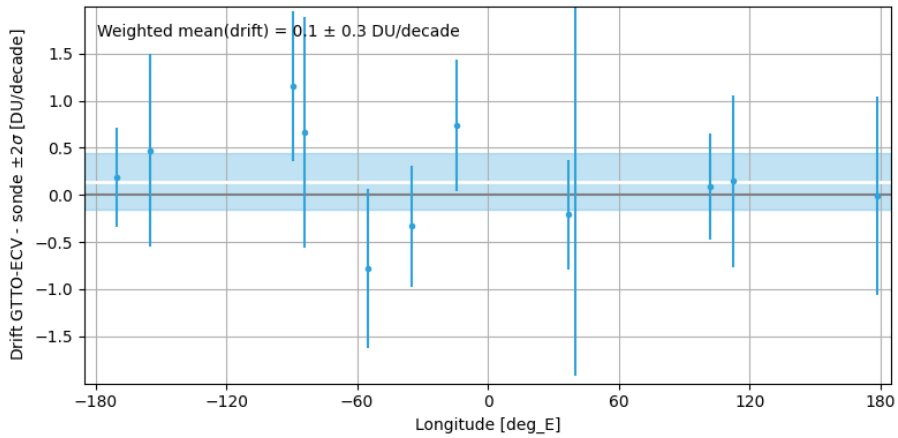

Figure 6.4 - Drift estimate and its 2σ uncertainty of GTTO-ECV v6lc tropospheric ozone column data (surface to 270 hPa) with respect to ozonesonde data at each site, calculated over the 1995-2023 time period. The white line and blue shaded region represents the network-averaged drift and its 95 % confidence interval.

6.3 *OMI-LIMB v1 and GTO-LIMB v1*

The tropospheric ozone column of these global satellite data products covers surface to thermal tropopause. Both data records are generated with the same algorithm and differ only in the source of total ozone column data used to compute the tropospheric column. OMI-LIMB relies on daily total column data by OMI, GTO-LIMB uses daily GTO-ECV data combines 7 nadir sensors (including OMI). OMI data are fully cloud screened, but GTO-ECV data are not. Please note that GTO-LIMB v1 data in the period January 2003 to August 2004 should be screened for science applications, further work is needed to brings the quality in line with the rest of the record. This period is therefore not considered when computing bias, dispersion or drift for GTO-LIMB.

6.3.1 Bias

Figure 6.5 (markers) shows the median value (bias) of the OMI-LIMB v1 (left) and GTO-LIMB v1 (right) differences to ozonesonde. Both data sets systematically underestimate ozonesonde measurements across the ground network, with a magnitude that depends on season at mid/high latitudes.

The network-averaged mean and its standard error (1σ) are -5.7 ± 0.6 DU (or -17 ± 2 %) for OMI-LIMB v1 and -6.9 ± 0.6 DU (or -21 ± 2 %) for GTO-LIMB v1. The difference in bias (1.2 DU) between both satellite data records is seen across most of the network but especially at low latitudes. Overall, there is very little spatial structure in the OMI-LIMB or GTO-LIMB bias, apart from a reduction towards high latitudes (see also discussion in next paragraph). Outside the polar regions, the bias estimates range between -(3-12) DU for OMI-LIMB and -(4-14) DU for GTO-LIMB, with a site-to-site spread of about 3.5 DU (10 %). Part of this dispersion could be due to residual measurement biases between sites that were not completely removed in the homogenisation process by the TOAR II HEGIFTOM working group (Van Malderen et al., 2024 [RD92]).

There are very clear signs of temporal structure of the bias at the seasonal scale. Figure 6.6 and Figure 6.7 show a pronounced seasonal cycle at all sites in the mid and high latitudes (40° or higher) with a minimum consistently appearing in local winter and a maximum during local summer. No seasonal structure is found across the tropical belt (20° S to 20° N). The amplitude of the seasonal cycle is largest at high latitudes (min/max difference of 10-20 DU) and still considerable at mid latitudes (about 5-7 DU). The cycle for OMI-LIMB and GTO-LIMB are very similar. Between May to August, these satellite data records overestimate Arctic ozonesonde data by about +5 DU. This period is followed by negative biases of -5 DU to -15 DU during winter. This leads to the smaller negative bias in the Arctic when compared to other latitudes. At mid-latitudes the summer maximum bias remains negative.

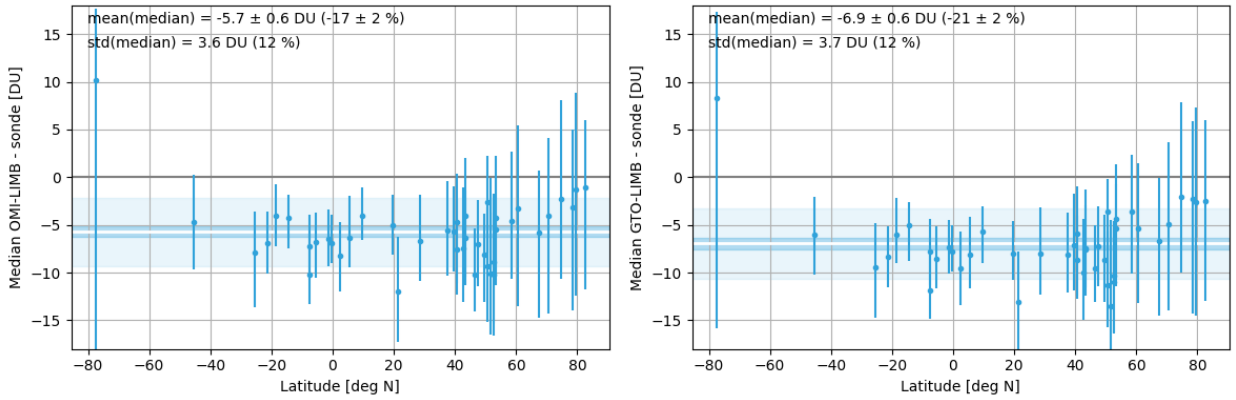

Figure 6.5 –Bias (marker) and dispersion (error bar, 1σ) of OMI-LIMB v1 (left) and GTO-LIMB v1 (right) versus ozonesonde data at each site in the network. Positive values indicate that the satellite data record overestimates ozonesonde. Network-averaged statistics are shown as white line and blue shaded areas.

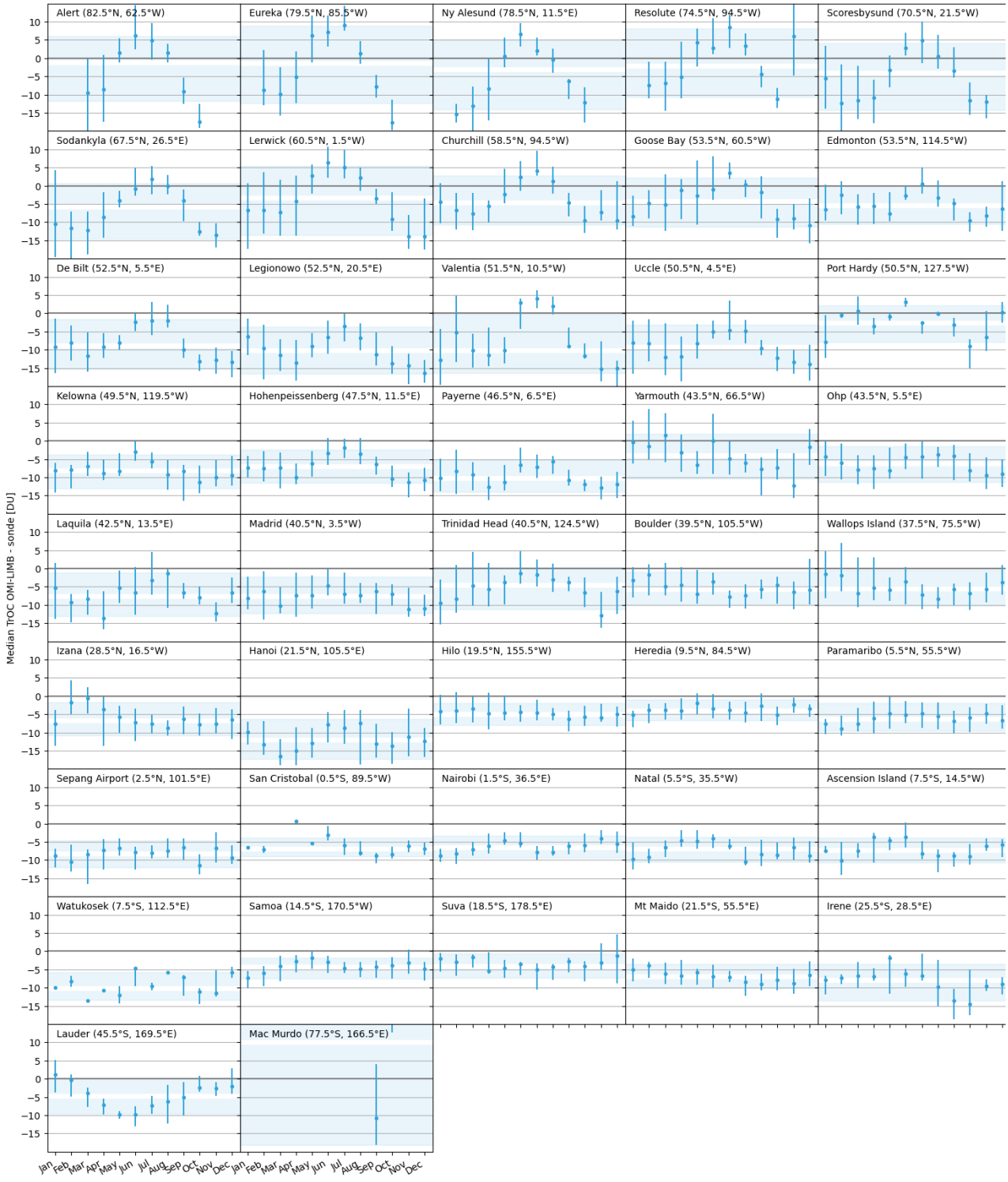

Figure 6.6 – Annual cycle of OMI-LIMB v1 bias (marker) and dispersion (error bar, 1σ) versus ozonesonde data at each site in the tropical network (different panels). Also shown are the median (white line) and 68 % inter-percentile (blue area) of the comparisons. Positive values indicate that OMI-LIMB overestimates ozonesonde data.

Figure 6.7 – As Figure 6.6, but for GTO-LIMB v1

6.3.2 Dispersion

Figure 6.8 shows the half-width of the 68 % interpercentile (dispersion) of the OMI-LIMB v1 (left) and GTO-LIMB v1 (right) comparisons. There is a clear latitudinal dependence, with the smallest dispersion (3-4 DU) found over the tropics, increasing to 5-7 DU at mid-latitudes and up to 8-10 DU in the polar regions. The network-averaged mean dispersion and its standard error (1σ) are 5.8 ± 0.4 DU (or 18 ± 2 %) for OMI-LIMB v1 and 5.5 ± 0.4 DU (or 17 ± 2 %) for GTO-LIMB v1. GTO-LIMB dispersion is slightly smaller than for OMI-LIMB, mostly due to reduced dispersion at mid-latitude ozonesonde sites.

The seasonal cycle of the bias, discussed previously (Sect. 6.3.1), is a large contributor to the dispersion at mid and high latitudes. Data users that take this seasonal bias into account, e.g., by analysing deseasonalised anomalies, will be able to reduce dispersion greatly. Dispersion around the monthly bias values, instead of around the bias for the full data record, is about 4-6 DU in summer and 8-10 DU in winter for Arctic sites. At mid-latitudes the dispersion during summer months is 2-3 DU and 4-5 DU in winter months. In the tropics, the seasonal cycle is absent so monthly dispersion values are in line with those calculated for the entire data record (about 2-3 DU).

Hubert et al. (2021) discuss that dispersion estimates derived from pairwise comparisons of S5P tropospheric ozone column data to ozonesonde are dominated by the random uncertainty due to differences in spatio-temporal smoothing and sampling (Sect. 4.5 in [RD46]). Hubert et al. (2021) analysed daily S5P data, so the smoothing/sampling mismatch uncertainty for monthly OMI-LIMB and GTO-LIMB data will be even more important. In conclusion, it is expected that the random uncertainty of the satellite products is (much) smaller than the reported 5.5-5.8 DU (17-18 %).

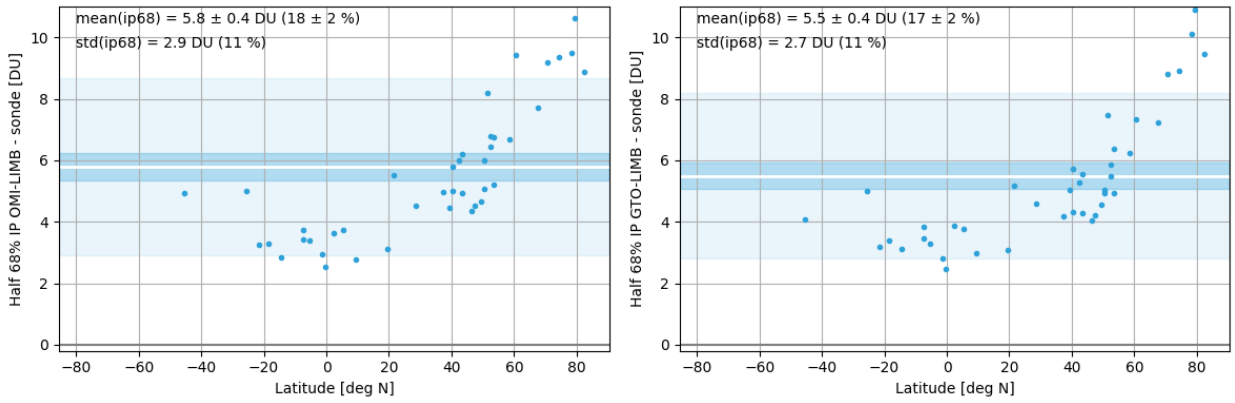

Figure 6.8 – Dispersion (1σ) of the comparisons of OMI-LIMB v1 (left) and GTO-LIMB v1 (right) versus ozonesonde data at each site in the network. Network-averaged statistics are shown as a white line and blue shaded areas.

6.3.3 Long-term stability

The OMI-LIMB and GTO-LIMB comparison time series at each ozonesonde station are shown, respectively, in Figure 6.10 and Figure 6.11 (thin lines), as well as their 5-year moving mean (grey) and a linear fit inferred with a robust regression method (blue line). About 80 % of the ozonesonde stations provide two decades of measurements, albeit sometimes with a gap of several years in the time series. In case of gaps, the difference time series during the disconnected periods are generally either similar and, if not, at least consistent with the temporal structure of the comparisons in other grid cells. We exclude three sites in the drift analysis, either because of a too pronounced discontinuity between two periods (Hanoi) or due to too few data in combination with a long gap (San Cristobal and Watukosek).

The comparison time series show non-linear structure at many ozonesonde sites for both satellite data records. Excursions of the 5-year moving mean from a robust linear regression remain mostly within 2-4 DU. The non-linearity is most prominent in the Arctic, with a zero or slightly negative drift prior to 2012 followed by a positive drift in the past decade. At most sites in the 0°N – 40°N range, a local maximum is noted around 2010, followed by a minimum around 2015, then returning to a maximum again around 2020-2022. Such change points are visible at most sites, often with a similar sign but with only a broadly consistent timing.

The long-term structure of the ground-based comparison time series are very similar for both satellite data records; any differences are largest in the Arctic. Hence, the different total ozone column data used to construct the satellite tropospheric ozone column data does not appear to impact the stability a lot[3]. Figure 6.9 shows OMI-LIMB (left) and GTO-LIMB (right) drift relative to ozonesonde at each site, with its 95 % confidence interval. The network-averaged drift estimates (inverse-variance weighted) are positive for both data records and right at the 2σ threshold: for OMI-LIMB we find +0.4 ± 0.4 DU per decade (or +1 ± 1 % per decade), for GTO-LIMB +0.3 ± 0.4 DU per decade (or +1 ± 1 % per decade). The quoted uncertainty represents 2 standard deviations or 95 % confidence. Irrespective of whether the observed drift is present or not, the magnitude is small and well within the user requirement of 1-3 % per decade.

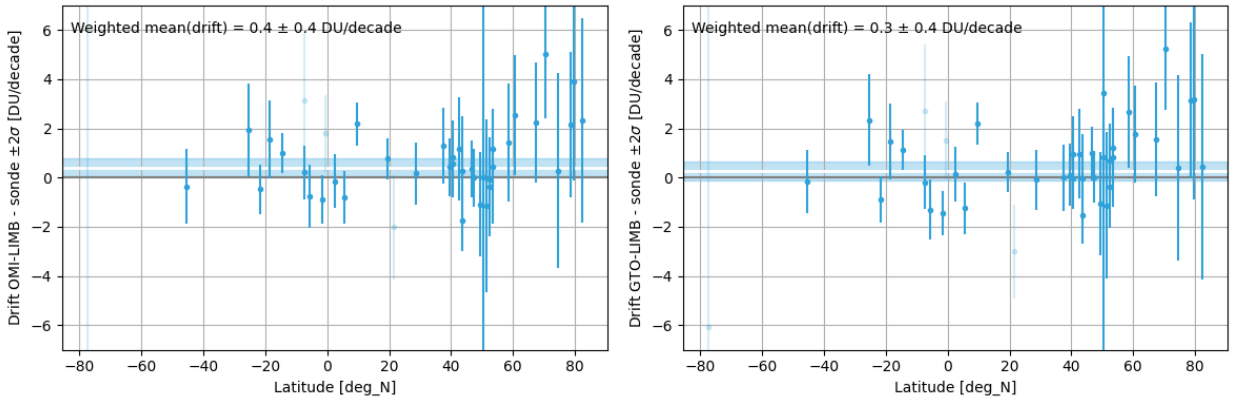

Figure 6.9 – Drift estimate and its 2σ uncertainty of OMI-LIMB v1 (left) and GTO-LIMB v1 (right) tropospheric ozone column data (surface to thermal tropopause) with respect to ozonesonde data at each site, calculated over the September 2004 – December 2023 time period. The white line and blue shaded region represents the network-averaged drift and its 95 % confidence interval.

[3] Possibly because OMI serves as a reference sensor in the construction of the GTO-ECV data record.

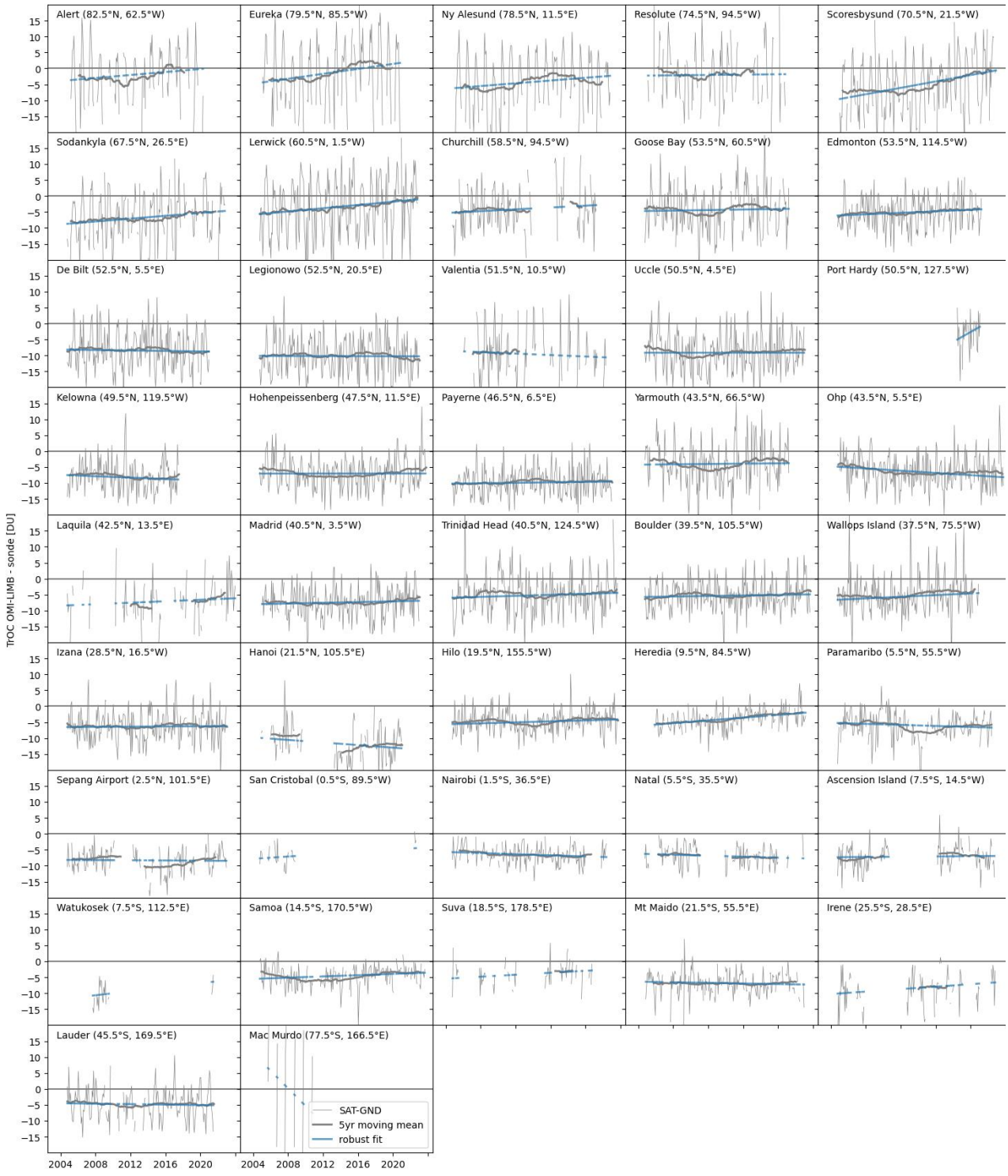

Figure 6.10 – Comparison time series of OMI-LIMB v1 tropospheric ozone column data (surface to thermal tropopause) versus ozonesonde data at each site in the tropical network (ordered North to South). Also shown are a robust linear fit (blue line) and a 5-year moving mean (grey line) of the comparisons. Positive values indicate that OMI-LIMB overestimates ozonesonde data.

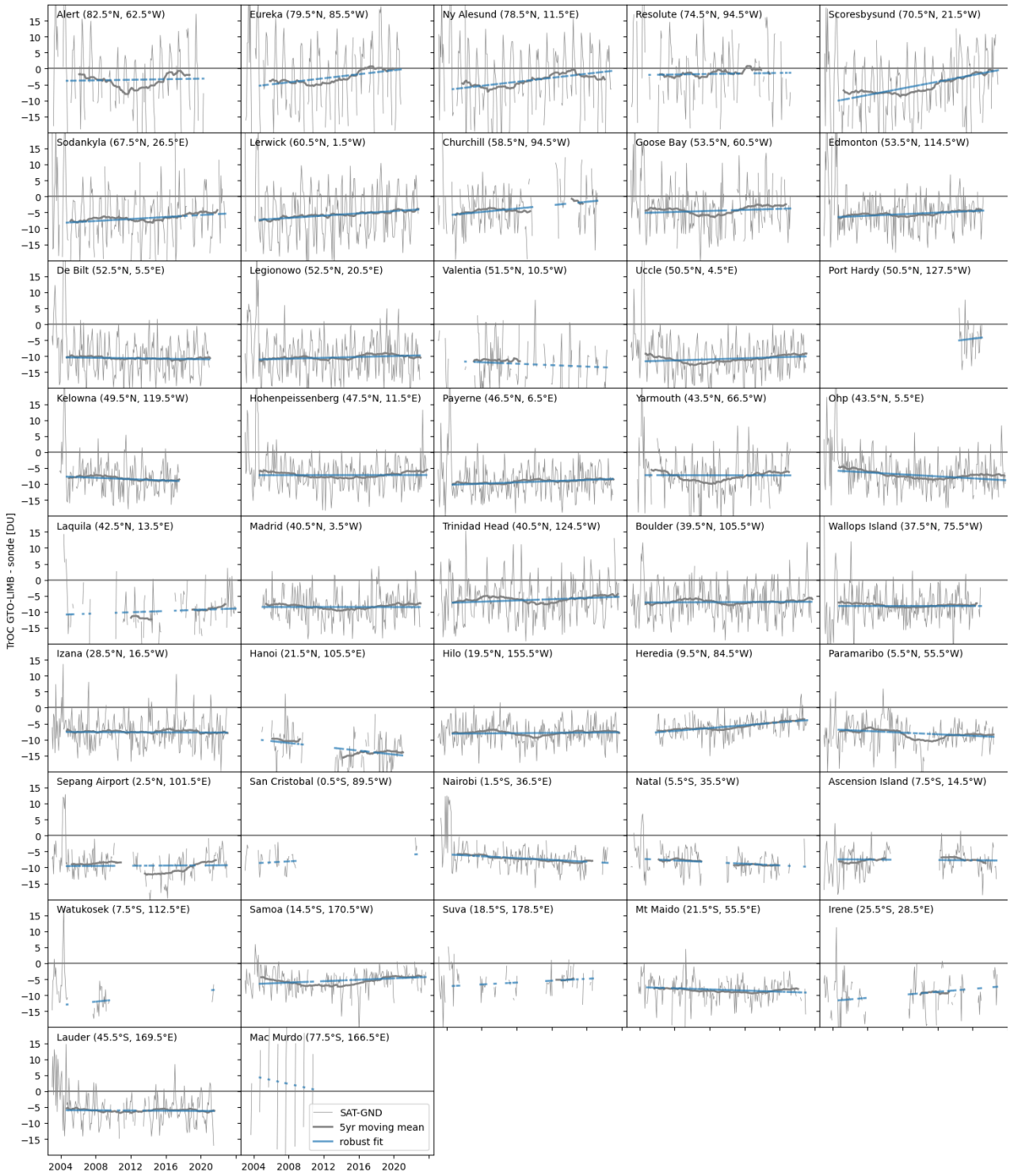

Figure 6.11 – As Figure 6.10, but for GTO-LIMB v1. Comparison data in the period January 2003 to August 2004 are shown but are not considered when computing bias, dispersion or drift.

6.4 *Compliance with user requirements*

From the results reported above, we conclude that the three CCI tropospheric ozone column data records are fully compliant with nearly all user requirements. The main exception is the temporal sampling resolution, which is monthly instead of daily / weekly. Users that require higher temporal resolution are advised to consider the tropospheric layer of the nadir profile products reported in Sect. 4.

Dispersion in pairwise comparisons is known to include a considerable component due to the large differences in sampling by ozonesonde and satellite of the spatio-temporal cells. The dispersion values quoted earlier are therefore too conservative estimates of the random uncertainty of the CCI data records. Further studies are needed to quantify the sampling mismatch term. For now, we assess that all satellite data records comply with the requirement of at most 16 % random uncertainty, with high confidence for OMI-LIMB and GTO-LIMB and medium confidence for GTTO-ECV. There is currently not enough information to verify compliance with the 8 % random uncertainty requirement.

Table 6.1 - Compliance of the considered Ozone_cci+ Level-3 tropospheric ozone data products with user requirements (URD v4.1): full compliance (green), partial compliance (orange) and no compliance (red).

	CCD: GTTO-ECV v6lc	**LNM: OMI-LIMB v1**	**LNM: GTO-LIMB v1**
Time period (1980-)	1995-2023	2004-2023	2004-2023
Observation frequency (daily to weekly)	Monthly	Monthly	Monthly
Horizontal resolution (20-200 km)	1° (~100 km)	1° (~100 km)	1° (~100 km)
Vertical resolution (n/a)	Surface to 270 hPa (~10.5 km)	Surface to thermal tropopause	Surface to thermal tropopause
Uncertainty including only random component (8-16 %)	22 %	18 %	17 %
Dependence on influence quantities	Dispersion increases with latitude.	Seasonal cycle of bias at mid & high latitudes. Dispersion increases with latitude.	Dispersion increases with latitude.
Stability (1-3 %/dec.)	0 ± 1 %/decade	+1 ± 1 %/decade	+1 ± 1 %/decade

7 References

7.1 *Applicable documents*

[RD1] CCI+ SOW: ESA Climate Change Initiative Extension (CCI+) Phase 1: New R&D on CCI ECVs – Statement of Work, Ref. ESA-CCI-EOPS-PRGM-SOW-18-0118, Issue 1 Revision 6, 31/05/2018.

[RD2] CCI+ Ozone Technical Proposal: ESA Ozone_cci+ Technical Proposal – Essential Climate Variable (ECV) - Ozone, Proposal to ESA in response to ITT AO/1-9322/18/I-NB, 14/09/2018.

[RD3] CCI+ Ozone Product Validation Plan: ESA Ozone_cci+ Product Validation Plan (PVP), Ref. Ozone_cci+_D2.4_PVP_v3.1, Issue 3, Revision 1, 17/03/2025.

[RD4] CCI+ Ozone Algorithm Theoretical Basis Document: ESA Ozone_cci+ Algorithm Theoretical Basis Document (ATBD), Ref. Ozone_cci+_D2.1_ATBD_v3.2, Issue 3, Revision 2, 17/03/2025.

[RD5] CCI+ Ozone Product User Guide: ESA Ozone_cci+ Product User Guide (PUG), Ref. Ozone_cci+_D4.2_PUG_v2.1, Issue 2, Revision 1, 17/03/2025.

[RD6] CCI+ Ozone End-to-End ECV Uncertainty Budget: ESA Ozone_cci+ End-to-End ECV Uncertainty Budget (E3UB), Ref. Ozone_cci+_D2.2_E3UB_v6.4, Issue 6, Revision 4, 17/03/2025.

7.2 *Reference documents*

7.2.1 User requirements

[RD7] CMUG: User Requirement Document | Meeting the needs of the Climate Community - Requirements, Deliverable 1.1, Climate Modelling User Group, Issue 2, Revision 1, 11/01/2021.

[RD8] DARD: Ozone CCI Phase II Data Access Requirement Document (DARD), Issue 2, Revision 1, Ref. Ozone_cci_DARD_1.1, 25/05/2016.

[RD9] IGACO: The changing atmosphere. An integrated global atmospheric chemistry observation theme for the IGOS partnership. Report of the Integrated Global Atmospheric Chemistry Observation (IGACO) theme team, Ref. ESA SP-1282, GAW No. 159, WMO-TD No. 1235, 2004.

[RD10] URD: Ozone CCI User Requirement Document, Ref. Ozone_cci+_D1.1_URD_v4.1, Issue 4, Revision 1, 12/05/2025.

[RD11] WMO Observing Systems Capabilities Analysis and Review tool (OSCAR) available on-line from http://www.wmo-sat.info/oscar/observingrequirements

7.2.2 International standards and frameworks

[RD12] CDRH: Center for Devices and Radiological Health (CDRH), General Principles of Software Validation; Final Guidance for Industry and FDA Staff, CBER CDRH/OC Doc. N. 938, January 11, 2002. Publicly available via http://www.fda.gov/MedicalDevices/DeviceRegulationandGuidance

[RD13] CEOS: Committee on Earth Observation Satellites (CEOS): Terms and Definitions and other documents and resources, publicly available on http://calvalportal.ceos.org

[RD14] GUM: Joint Committee for Guides in Metrology (JCGM/WG 1) 100:2008, Evaluation of measurement data – Guide to the expression of uncertainty in a measurement (GUM), http://www.bipm.org/utils/common/documents/jcgm/JCGM_100_2008_E.pdf

[RD15] Larssen, S., R. Sluyter, and C. Helmis, Criteria for EUROAIRNET – The EEA Air Quality Monitoring and Information Network, 1999.

[RD16] Nappo, C.J., Caneill J.Y., Furman R.W., Gifford F.A., Kaimal J.C., Kramer M.L., Lockhart T.J., Pendergast M.M, Pielke R.A., Randerson D., Shreffler J.H., and Wyngaard J.C., The Workshop on the Representativeness of Meteorological Observations, June 1981, Boulder, CO, Bull. Am. Meteorol. Soc. 63, 761-764, 1982.

[RD17] NIST: Prokhorov, A. V., R. U. Datla, V. P. Zakharenkov, V. Privalsky, T. W. Humpherys, and V. I. Sapritsky, Spaceborne Optoelectronic Sensors and their Radiometric Calibration. Terms and Definitions. Part 1. Calibration Techniques, Ed. by A. C. Parr and L. K. Issaev, NIST Technical Note NISTIR 7203, March 2005.

[RD18] VIM: Joint Committee for Guides in Metrology (JCGM/WG 2) 200:2008 & ISO/IEC Guide 99-12:2007, International Vocabulary of Metrology – Basic and General Concepts and Associated Terms (VIM), http://www.bipm.org/en/publications/guides/vim.html

[RD19] WMO Quality Management Framework (QMF), home page at http://www.wmo.int/pages/prog/www/QMF-Web/home.html

[RD20] QA4EO – A Quality Assurance framework for Earth Observation, established by the CEOS. It consists of ten distinct key guidelines linked through an overarching document (the http://qa4eo.org/docs/Guidelines_Framework_v3.0.pdf QA4EO Guidelines Framework) and more community-specific QA4EO procedures, all available on http://qa4eo.org/documentation.html A short QA4EO "user" guide has been produced to provide background into QA4EO and how one would start implementing it (http://qa4eo.org/docs/QA4EO_guide.pdf)

[RD21] ISO Quality Management Principles available at http://www.iso.org/iso/iso9000-14000/understand/qmp.html

[RD22] NetCDF Climate and Forecast Metadata Convention, http://cf-psmdi.llnl.gov

[RD23] Fahre Vik, A., T. Krognes, S-E. Walker, S. Bjørndalsæter, C. Stoll, T. Bårde, R. Paltiel, and B. Gloslie, ESA Campaign Database (CDB) user manual, NILU Technical Note O-103045, 100 pp., April 2006. http://nadir.nilu.no/cdb/doc/CDB_manual_20060405.pdf

[RD24] World Meteorological Organization, WMO Global Atmosphere Watch (GAW) Strategic Plan: 2008-2015, GAW Report No. 172 / WMO TD No. 1384.

7.2.3 Validation measurements, validation methods and assessments

[RD25] Adams, C., A. E. Bourassa, A. F. Bathgate, C. A. McLinden, N. D. Lloyd, C. Z. Roth, E. J. Llewellyn, J. M. Zawodny, D. E. Flittner, G. L. Manney, W. H. Daffer, and D. A. Degenstein. Characterization of Odin-OSIRIS ozone profiles with the SAGE II dataset. Atmos. Meas. Tech., 6 (5): 1447–1459, doi: 10.5194/amt-6-1447-2013, 2013.

[RD26] Adams, C., A. E. Bourassa, V. Sofieva, L. Froidevaux, C. A. McLinden, D. Hubert, J.-C. Lambert, C. E. Sioris, and D. A. Degenstein. Assessment of Odin-OSIRIS ozone measurements from 2001 to the present using MLS, GOMOS, and ozonesondes. Atmos. Meas. Tech., 7 (1): 49–64, doi: 10.5194/amt-7-49-2014, 2014.

[RD27] Backus, G.E., and F. Gilbert, Uniqueness in the Inversion of inaccurate Gross Earth Data, Philosophical Transactions of the Royal Society of London A, 266, 123-192, 1970.

[RD28] Balis, D., J.-C. Lambert, M. Van Roozendael, D. Loyola, R. Spurr, Y. Livschitz, P. Valks, V. Amiridis, P. Gerard, and J. Granville, Ten years of GOME/ERS-2 total ozone data – The new GOME Data Processor (GDP) Version 4: II Ground-based validation and comparisons with TOMS V7/V8, Journal of Geophysical Research – Atmosphere, Vol. 112, D07307, doi:10.1029/2005JD006376, 2007.

[RD29] Bernhard, G., R. D. Evans, G. J. Labow, and S. J. Oltmans, Bias in Dobson total ozone measurements at high latitudes due to approximations in calculations of ozone absorption coefficients and air mass, J. Geophys. Res., 110, D10305, doi:10.1029/2004JD005559, 2005.

[RD30] Bourassa, A. E., Roth, C. Z., Zawada, D. J., Rieger, L. A., McLinden, C. A., and Degenstein, D. A.: Drift-corrected Odin-OSIRIS ozone product: algorithm and updated stratospheric ozone trends, Atmos. Meas. Tech., 11, 489–498, https://doi.org/10.5194/amt-11-489-2018, 2018.

[RD31] Boynard, A., Hurtmans, D., Koukouli, M. E., Goutail, F., Bureau, J., Safieddine, S., Lerot, C., Hadji-Lazaro, J., Wespes, C., Pommereau, J.-P., Pazmino, A., Zyrichidou, I., Balis, D., Barbe, A., Mikhailenko, S. N., Loyola, D., Valks, P., Van Roozendael, M., Coheur, P.-F., and Clerbaux, C.: Seven years of IASI ozone retrievals from FORLI: validation with independent total column and vertical profile measurements, Atmos. Meas. Tech., 9, 4327-4353, doi:10.5194/amt-9-4327-2016, 2016.

[RD32] Boynard, A., D. Hurtmans, K. Garane, F. Goutail, J. Hadji-Lazaro, M. E. Koukouli, C. Wespes, C. Vigouroux, A. Keppens, J.-P. Pommereau, A. Pazmino, D. Balis, D. Loyola, P. Valks, R. Sussmann, D. Smale, P.F. Coheur, and C. Clerbaux: Validation of the IASI FORLI/EUMETSAT O3 products using satellite (GOME-2), ground-based (Brewer-Dobson, SAOZ, FTIR) and ozonesonde measurements, Atmos. Meas. Tech.,https://doi.org/10.5194/amt-11-5125-2018 , 2018.

[RD33] Bramstedt, K., Stone, T. C., Gottwald, M., Noël, S., Bovensmann, H., and Burrows, J. P.: Improved pointing information for SCIAMACHY from in-flight measurements of the viewing directions towards sun and moon, Atmos. Meas. Tech., 10, 2413-2423, doi:10.5194/amt-10-2413-2017, 2017.

[RD34] Burkholder, J.B., and R.K. Talukdar, Temperature dependence of the ozone absorption spectrum over the wavelength range 410 to 760 nm, Geophysical Research Letters, Volume 21, Issue 7, pages 581–584, doi:10.1029/93GL02311, 1994.

[RD35] Calisesi, Y., V. T. Soebijanta, and R. van Oss, Regridding of remote soundings: Formulation and application to ozone profile comparison, J. Geophys. Res., 110, D23306, doi:10.1029/2005JD006122, 2005.

[RD36] Coldewey-Egbers, M., D.G. Loyola, M. Koukouli, D. Balis, J.-C. Lambert, T. Verhoelst, J. Granville, M. van Roozendael, C. Lerot, R. Spurr, S.M. Frith, and C. Zehner, The GOME-type Total Ozone Essential Climate Variable (GTO-ECV) data record from the ESA Climate Change Initiative, Atmos. Meas. Tech., 8, 3923-3940, 2015.

[RD37] Dufour, G., Eremenko, M., Griesfeller, A., Barret, B., LeFlochmoën, E., Clerbaux, C., Hadji-Lazaro, J., Coheur, P.-F., and Hurtmans, D.: Validation of three different scientific ozone products retrieved from IASI spectra using ozonesondes, Atmos. Meas. Tech., 5, 611-630, doi:10.5194/amt-5-611-2012, 2012.

[RD38] Eckert, E., von Clarmann, T., Kiefer, M., Stiller, G. P., Lossow, S., Glatthor, N., Degenstein, D. A., Froidevaux, L., Godin-Beekmann, S., Leblanc, T., McDermid, S., Pastel, M., Steinbrecht, W., Swart, D. P. J., Walker, K. A., and Bernath, P. F.: Drift-corrected trends and periodic variations in MIPAS IMK/IAA ozone measurements, Atmos. Chem. Phys., 14, 2571-2589, doi:10.5194/acp-14-2571-2014, 2014.

[RD39] Frith, S. M., Stolarski, R. S., Kramarova, N. A., and McPeters, R. D.: Estimating uncertainties in the SBUV Version 8.6 merged profile ozone data set, Atmos. Chem. Phys., 17, 14695-14707, doi:10.5194/acp-17-14695-2017, 2017.

[RD40] Garane, K., Lerot, C., Coldewey-Egbers, M., Verhoelst, T., Koukouli, M. E., Zyrichidou, I., Balis, D. S., Danckaert, T., Goutail, F., Granville, J., Hubert, D., Keppens, A., Lambert, J.-C., Loyola, D., Pommereau, J.-P., Van Roozendael, M., and Zehner, C.: Quality assessment of the Ozone_cci Climate Research Data Package (release 2017) – Part 1: Ground-based validation of total ozone column data products, Atmos. Meas. Tech., 11, 1385-1402, https://doi.org/10.5194/amt-11-1385-2018, 2018.

[RD41] Garane, K., Koukouli, M.-E., Verhoelst, T., Lerot, C., Heue, K.-P., Fioletov, V., Balis, D., Bais, A., Bazureau, A., Dehn, A., Goutail, F., Granville, J., Griffin, D., Hubert, D., Keppens, A., Lambert, J.-C., Loyola, D., McLinden, C., Pazmino, A., Pommereau, J.-P., Redondas, A., Romahn, F., Valks, P., Van Roozendael, M., Xu, J., Zehner, C., Zerefos, C., and Zimmer, W.: TROPOMI/S5P total ozone column data: global ground-based validation and consistency with other satellite missions, Atmos. Meas. Tech., 12, 5263–5287, https://doi.org/10.5194/amt-12-5263-2019, 2019.

[RD42] Godin, S., A.I. Carswell, D.P. Donovan, H. Claude, W. Steinbrecht, I.S. McDermid, T.J. McGee, M.R. Gross, H. Nakane, D.P.J. Swart, H.B. Bergwerff, O. Uchino, P. von der Gathen, and R. Neuber, Ozone differential absorption lidar algorithm intercomparison, Appl. Opt. 38, 6225-6236, 1999.

[RD43] Godin, S., Bergeret, V., Bekki, S., David, C., and Mégie, G.: Study of the interannual ozone loss and the permeability of the Antarctic polar vortex from aerosol and ozone lidar measurements in Dumont d'Urville (66.4S, 140E), J. Geophys. Res., 106, 1311-1330, doi:10.1029/2000JD900459, 2001.

[RD44] Hendrick, F., Pommereau, J.-P., Goutail, F., Evans, R. D., Ionov, D., Pazmino, A., Kyrö, E., Held, G., Eriksen, P., Dorokhov, V., Gil, M., and Van Roozendael, M.: NDACC/SAOZ UV-visible total ozone measurements: improved retrieval and comparison with correlative ground-based and satellite observations, Atmos. Chem. Phys., 11, 5975-5995, doi:10.5194/acp-11-5975-2011, 2011.

[RD45] Hubert, D., Lambert, J.-C., Verhoelst, T., Granville, J., Keppens, A., Baray, J.-L., Bourassa, A. E., Cortesi, U., Degenstein, D. A., Froidevaux, L., Godin-Beekmann, S., Hoppel, K. W., Johnson, B. J., Kyrölä, E., Leblanc, T., Lichtenberg, G., Marchand, M., McElroy, C. T., Murtagh, D., Nakane, H., Portafaix, T., Querel, R., Russell III, J. M., Salvador, J., Smit, H. G. J., Stebel, K., Steinbrecht, W., Strawbridge, K. B., Stübi, R., Swart, D. P. J., Taha, G., Tarasick, D. W., Thompson, A. M., Urban, J., van Gijsel, J. A. E., Van Malderen, R., von der Gathen, P., Walker, K. A., Wolfram, E., and Zawodny, J. M.: Ground-based assessment of the bias and long-term stability of 14 limb and occultation ozone profile data records, Atmos. Meas. Tech., 9, 2497-2534, doi:10.5194/amt-9-2497-2016, 2016.

[RD46] Hubert, D., Heue, K.-P., Lambert, J.-C., Verhoelst, T., Allaart, M., Compernolle, S., Cullis, P. D., Dehn, A., Félix, C., Johnson, B. J., Keppens, A., Kollonige, D. E., Lerot, C., Loyola, D., Maata, M., Mitro, S., Mohamad, M., Piters, A., Romahn, F., Selkirk, H. B., da Silva, F. R., Stauffer, R. M., Thompson, A. M., Veefkind, J. P., Vömel, H., Witte, J. C., and Zehner, C.: TROPOMI tropospheric ozone column data: geophysical assessment and comparison to ozonesondes, GOME-2B and OMI, Atmos. Meas. Tech., 14, 7405–7433, https://doi.org/10.5194/amt-14-7405-2021, 2021.

[RD47] Immler, F. J., Dykema, J., Gardiner, T., Whiteman, D. N., Thorne, P. W., and Vömel, H.: Reference Quality Upper-Air Measurements: guidance for developing GRUAN data products, Atmos. Meas. Tech., 3, 1217–1231, https://doi.org/10.5194/amt-3-1217-2010, 2010.

[RD48] Keckhut, P., McDermid, S., Swart, D., McGee, T., Godin-Beekmann, S., Adriani, A., et al., Review of ozone and temperature lidar validations performed within the framework of the Network for the Detection of Stratospheric Change, J. Environ. Monit., 6, 721-733. doi:10.1039/B404256E, 2004.

[RD49] Keppens, A., Lambert, J.-C., Granville, J., Miles, G., Siddans, R., van Peet, J. C. A., van der A, R. J., Hubert, D., Verhoelst, T., Delcloo, A., Godin-Beekmann, S., Kivi, R., Stübi, R., and Zehner, C.: Round-robin evaluation of nadir ozone profile retrievals: methodology and application to MetOp-A GOME-2, Atmos. Meas. Tech., 8, 2093-2120, doi:10.5194/amt-8-2093-2015, 2015.

[RD50] Keppens, A., Lambert, J.-C., Granville, J., Hubert, D., Verhoelst, T., Compernolle, S., Latter, B., Kerridge, B., Siddans, R., Boynard, A., Hadji-Lazaro, J., Clerbaux, C., Wespes, C., Hurtmans, D. R., Coheur, P.-F., van Peet, J. C. A., van der A, R. J., Garane, K., Koukouli, M. E., Balis, D. S., Delcloo, A., Kivi, R., Stübi, R., Godin-Beekmann, S., Van Roozendael, M., and Zehner, C.: Quality assessment of the Ozone_cci Climate Research Data Package (release 2017) – Part 2: Ground-based validation of nadir ozone profile data products, Atmos. Meas. Tech., 11, 3769–3800, doi:10.5194/amt-11-3769-2018, 2018.

[RD51] Keppens, A., Compernolle, S., Verhoelst, T., Hubert, D., and Lambert, J.-C.: Harmonization and comparison of vertically resolved atmospheric state observations: methods, effects, and uncertainty budget, Atmos. Meas. Tech., 12, 4379–4391, doi:10.5194/amt-12-4379-2019, 2019.

[RD52] Kerr, J. B., I. A. Asbridge, and W. F. J. Evans, Intercomparison of total ozone measured by the Brewer and Dobson spectrophotometers at Toronto, J. Geophys. Res., 93 (D9), 11129–11140, 1988.

[RD53] Kiefer, M., T. von Clarmann, U. Grabowski, M. De Laurentis, R. Mantovani, M. Milz, and M. Ridolfi. Characterization of MIPAS elevation pointing. Atmos. Chem. Phys., 7 (6): 1615–1628, doi: 10.5194/acp-7-1615-2007, 2007.

[RD54] Komhyr, W. D., Mateer, C. L., and Hudson, R. D.: Effective Bass-Paur 1985 ozone absorption coefficients for use with Dobson ozone spectrophotometers, J. Geophys. Res., 98, 20451–20465, https://doi.org/10.1029/93JD00602, 1993.

[RD55] Koukouli, M. E., Balis, D. S., Loyola, D., Valks, P., Zimmer, W., Hao, N., Lambert, J.-C., Van Roozendael, M., Lerot, C. and Spurr, R. J. D., Evaluating a new homogeneous total ozone climate data record from GOME/ERS-2, SCIAMACHY/Envisat, and GOME-2/MetOp-A, J. Geophys. Res. Atmos., 120, 12296–12312, doi:10.1002/2015JD023699, 2015.

[RD56] Koukouli, M. E., Zara, M., Lerot, C., Fragkos, K., Balis, D., van Roozendael, M., Allaart, M. A. F., and van der A, R. J.: The impact of the ozone effective temperature on satellite validation using the Dobson spectrophotometer network, Atmos. Meas. Tech., 9, 2055–2065, https://doi.org/10.5194/amt-9-2055-2016, 2016.

[RD57] Kramarova, N. A., Bhartia, P. K., Jaross, G., Moy, L., Xu, P., Chen, Z., DeLand, M., Froidevaux, L., Livesey, N., Degenstein, D., Bourassa, A., Walker, K. A., and Sheese, P.: Validation of ozone profile retrievals derived from the OMPS LP version 2.5 algorithm against correlative satellite measurements, Atmos. Meas. Tech. Discuss., doi:10.5194/amt-2017-431, in review, 2017.

[RD58] Laeng, A., D. Hubert, T. Verhoelst, T. von Clarmann, B.M. Dinelli, A. Dudhia, P. Raspollini, G. Stiller, U. Grabowski, A. Keppens, M. Kiefer, V. Sofieva, L. Froidevaux, K.A. Walker, J.-C. Lambert, C. Zehner, The ozone climate change initiative: Comparison of four Level-2 processors for the Michelson Interferometer for Passive Atmospheric Sounding (MIPAS), Remote Sensing of Environment, 162, 316-343, doi:10.1016/j.rse.2014.12.013, 2015.

[RD59] Laeng, A., Eckert, E., von Clarmann, T., Kiefer, M., Hubert, D., Stiller, G., Grabowski, U., Glatthor, N., Plieninger, J., Kellmann, S., Linden, A., Lossow, S., Babenhauserheide, A., Froidevaux, L., and Walker, K.: On the improved stability of the version 7 MIPAS ozone record, Atmos. Meas. Tech. Discuss., https://doi.org/10.5194/amt-2017-345, in review, 2017.

[RD60] Lambert, J.-C., D. S. Balis, P. Gerard, J. Granville, Y. Livschitz, D. Loyola, R. Spurr, P. Valks, and M. Van Roozendael, UPAS / GDOAS 4.0 Upgrade of the GOME Data Processor for Improved Total Ozone Columns – Delta Validation Report, Ed. by J.-C. Lambert (IASB) and D. Balis (AUTH), Tech. Note ERSE-CLVL-EOPG-TN-04-0001, European Space Agency, Frascati, Italy, 2004.

[RD61] Lambert, J.-C., M. E. Koukouli, D. S. Balis, J. Granville, C. Lerot, D. Pieroux, and M. Van Roozendael, GDP 5.0 - Upgrade of the GOME Data Processor for Improved Total Ozone Column - Validation Report for ERS-2 GOME GDP 5.0 Total Ozone Column, Edited by J.-C. Lambert (IASB) and M. E. Koukouli (AUTH), Tech. Note TN-IASB-GOME-GDP5-VR, Issue/Rev. 1/A, 55 pp., 6 May 2011.

[RD62] Lambert, J.-C., C. De Clercq, and T. von Clarmann, Comparing and merging water vapour observations: A multi-dimensional perspective on smoothing and sampling issues, Chapter 9 (p. 177-199) of book “Monitoring Atmospheric Water Vapour: Ground-Based Remote Sensing and In-situ Methods”, N. Kämpfer (Ed.), ISSI Scientific Report Series, Vol. 10, Edition 1, 326 p., ISBN: 978-1-4614-3908-0, doi:10.1007/978-1-4614-3909-7_2, Springer, New York, 2012.

[RD63] Langerock, B.; De Mazière, M.; Hendrick, F.; Vigouroux, C.; Desmet, F.; Dils, B. and Niemeijer, S., Description of algorithms for co-locating and comparing gridded model data with remote-sensing observations, Geosci. Model Dev., 8, 911-921, 2015.

[RD64] Lerot, C., M. Van Roozendael, R. Spurr, et al., Homogenized total ozone data records from the European sensors GOME/ERS-2, SCIAMACHY/Envisat and GOME-2/Metop-A, Journal of Geophysical Research, 119, 1–20, doi:10.1002/2013JD020831, 2014.

[RD65] Liu, G., D. W. Tarasick, V. E. Fioletov, C. E. Sioris, and Y. J. Rochon, Ozone correlation lengths and measurement uncertainties from analysis of historical ozonesonde data in North America and Europe, J. Geophys. Res., 114, D04112, doi:10.1029/2008JD010576, 2009.

[RD66] Livesey, N. J., Read,W. G.,Wagner, P. A., Froidevaux, L., Lambert, A., Manney, G. L., Millán Valle, L. F., Pumphrey, H. C., Santee, M. L., Schwartz, M. J., Wang, S., Fuller, R. A., Jarnot, R. F., Knosp, B. W., and Martinez, E.: Aura Microwave Limb Sounder (MLS). Version 4.2x Level 2 data quality and description document, Tech. rep. JPL D-33509 Rev. C, Jet Propulsion Laboratory, http://mls.jpl.nasa.gov/data/v4-2_data_quality_document.pdf, 2017.

[RD67] Loyola, D.G., M. Coldewey-Egbers, M. Dameris, H. Garny, A. Stenke, M. van Roozendael, C. Lerot, D. Balis, and M. Koukouli, Global long-term monitoring of the ozone layer – a prerequisite for predictions, Int. J. Remote Sens., 30, 4295-4318, 2009.

[RD68] McCormick, M. P., Lei, L., Hill, M. T., Anderson, J., Querel, R., and Steinbrecht, W.: Early results and validation of SAGE III-ISS ozone profile measurements from onboard the International Space Station, Atmos. Meas. Tech., 13, 1287–1297, https://doi.org/10.5194/amt-13-1287-2020, 2020.

[RD69] McLinden, C., V. Fioletov, C. Haley, N. Lloyd, C. Roth, D. Degenstein, A. Bourassa, C. McElroy, and E. Llewellyn. An evaluation of Odin/OSIRIS limb pointing and stratospheric ozone through comparisons with ozonesondes. Can. J. Phys., 85 (11): 1125–1141, doi:10.1139/P07-112, 2007.

[RD70] Mégie, G., J. Y. Allain, M. L. Chanin, and J. E. Blamont, Vertical profile of stratospheric ozone by lidar sounding from the ground, Nature 270, 329–331, doi:10.1038/270329a0, 1977.

[RD71] Moy, L., Bhartia, P. K., Jaross, G., Loughman, R., Kramarova, N., Chen, Z., Taha, G., Chen, G., and Xu, P.: Altitude registration of limb-scattered radiation, Atmos. Meas. Tech., 10, 167-178, doi:10.5194/amt-10-167-2017, 2017.

[RD72] Nair, P. J., S. Godin-Beekmann, L. Froidevaux, L. E. Flynn, J. M. Zawodny, J. M. Russell III, A. Pazmiño, G. Ancellet, W. Steinbrecht, H. Claude, T. Leblanc, S. McDermid, J. A. E. van Gijsel, B. Johnson, A. Thomas, D. Hubert, J.-C. Lambert, H. Nakane, and D. P. J. Swart, Relative drifts and stability of satellite and ground-based stratospheric ozone profiles at NDACC lidar stations, Atmospheric Measurement Techniques, 5, 1301-1318 doi:10.5194/amt-5-1301-2012, 2012.

[RD73] Ozone_cci+ Climate Assessment Report (CAR), https://climate.esa.int/en/projects/ozone/key-documents, 07/03/2012.

[RD74] Ozone_cci Product Validation and Intercomparison Report (PVIR v2), Ozone_cci_Phase-II_PVIR_2.0, Issue 2.0 / Rev. 0, https://climate.esa.int/en/projects/ozone/key-documents, 30/06/2016.

[RD75] Pommereau, J.P. and Goutail, F., O_3 and NO_2 ground-based measurements by visible spectrometry during arctic winter and spring 1988. Geophysical Research Letters, 15, doi:10.1029/88GL00479, 1988.

[RD76] Rodgers, C. D.: Inverse Methods for Atmospheric Sounding, World Scientific Publishing, Singapore, p. 238, 2000.

[RD77] Rong, P. P., J. M. Russell III, M. G. Mlynczak, E. E. Remsberg, B. T. Marshall, L. L. Gordley, and M. López-Puertas, Validation of Thermosphere Ionosphere Mesosphere Energetics and Dynamics/Sounding of the Atmosphere using Broadband Emission Radiometry (TIMED/SABER) v1.07 ozone at 9.6 µm in altitude range 15–70 km, J. Geophys. Res., 114, D04306, doi:10.1029/2008JD010073, 2009.

[RD78] Sentinel-5 precursor / TROPOMI Level 2 Algorithm Theoretical Basis Document O3 Total Column, DLR/BIRA-IASB, S5P-L2-DLR-ATBD-400A, Issue 2.33, 62pp., https://sentinels.copernicus.eu/documents/247904/2476257/Sentinel-5P-TROPOMI-ATBD-Total-Ozone, 04/06/2021.

[RD79] Sheese, P. E., Walker, K. A., Boone, C. D., Bernath, P. F., Froidevaux, L., Funke, B., Raspollini, P., and von Clarmann, T.: ACE-FTS ozone, water vapour, nitrous oxide, nitric acid, and carbon monoxide profile comparisons with MIPAS and MLS, Journal of Quantitative Spectroscopy and Radiative Transfer, 186, 63-80, doi:10.1016/j.jqsrt.2016.06.026, 2017.

[RD80] Sheese, P. E., Walker, K. A., Boone, C. D., Bourassa, A. E., Degenstein, D. A., Froidevaux, L., McElroy, C. T., Murtagh, D., Russell III, J. M., and Zou, J.: Assessment of the quality of ACE-FTS stratospheric ozone data, Atmos. Meas. Tech., 15, 1233–1249, https://doi.org/10.5194/amt-15-1233-2022, 2022.

[RD81] Simmons, A. J., Poli, P., Dee, D. P., Berrisford, P., Hersbach, H., Kobayashi, S. and Peubey, C., Estimating low-frequency variability and trends in atmospheric temperature using ERA-Interim. Q.J.R. Meteorol. Soc., 140: 329–353. doi: 10.1002/qj.2317, 2014.

[RD82] Smit, H., and the Panel for the Assessment of Standard Operating Procedures for Ozonesondes (ASOPOS), Quality Assurance and Quality Control for Ozonesonde Measurements in GAW, GAW Report No. 201, September 2011.

[RD83] Sofieva, V. F., N. Rahpoe, J. Tamminen, E. Kyrölä, N. Kalakoski, M. Weber, A. Rozanov, C. von Savigny, A. Laeng, T. von Clarmann, G. Stiller, S. Lossow, D. Degenstein, A. Bourassa, C. Adams, C. Roth, N. Lloyd, P. Bernath, R. J. Hargreaves, J. Urban, D. Murtagh, A. Hauchecorne, F. Dalaudier, M. van Roozendael, N. Kalb, and C. Zehner. Harmonized dataset of ozone profiles from satellite limb and occultation measurements. Earth System Science Data, 5 (2): 349–363, doi: 10.5194/essd-5-349-2013, 2013.

[RD84] Sofieva, V. F., Kyrölä, E., Laine, M., Tamminen, J., Degenstein, D., Bourassa, A., Roth, C., Zawada, D., Weber, M., Rozanov, A., Rahpoe, N., Stiller, G., Laeng, A., von Clarmann, T., Walker, K. A., Sheese, P., Hubert, D., van Roozendael, M., Zehner, C., Damadeo, R., Zawodny, J., Kramarova, N., and Bhartia, P. K.: Merged SAGE II, Ozone_cci and OMPS ozone profile dataset and evaluation of ozone trends in the stratosphere, Atmos. Chem. Phys., 17, 12533-12552, doi:10.5194/acp-17-12533-2017, 2017.

[RD85] Staehelin J., J. Kerr, R. Evans and K. Vanicek, Comparison of total ozone measurements of Dobson and Brewer spectrophotometers and recommended transfer functions, WMO TD N. 1147, No 149, 2003.

[RD86] Stauffer, R. M., Thompson, A. M., Kollonige, D. E., Tarasick, D. W., Van Malderen, R., Smit, H. G. J., Vömel, H., Morris, G. A., Johnson, B. J., Cullis, P. D., Rene Stübi, R., Davies, J. and Yan, M. M., An Examination of the Recent Stability of Ozonesonde Global Network Data, Earth and Space Science Open Archive, preprint, https://doi.org/10.1002/essoar.10511590.1, 2022.

[RD87] Thompson, A.M., J.C. Witte, R.D. McPeters, S.J. Oltmans, F.J. Schmidlin, J.A. Logan, M.Fujiwara, V.W.J.H. Kirchhoff, F. Posny, G.J.R. Coetzee, B. Hoegger, S. Kawakami, T. Ogawa, B.J. Johnson, H. Vömel and G. Labow, Southern Hemisphere Additional Ozonesondes (SHADOZ) 1998-2000 Tropical ozone climatology 1. Comparison with Total Ozone Mapping Spectrometer (TOMS) and ground-based measurements, J. Geophys. Res., Vol. 108 No. D2, 8238, doi: 10.1029/2001JD000967, 30 January 2003.

[RD88] Thompson, A.M., J.C. Witte, S.J. Oltmans, F.J. Schmidlin, J.A. Logan, M. Fujiwara, V.W.J.H. Kirchhoff, F. Posny, G.J.R. Coetzee, B. Hoegger, S. Kawakami, T. Ogawa, J.P.F. Fortuin, and H.M. Kelder, Southern Hemisphere Additional Ozonesondes (SHADOZ) 1998-2000 Tropical ozone climatology 2. Tropospheric variability and the zonal wave-one, *J. Geophys. Res.*, Vol. 108 No. D2, 8241, doi: 10.1029/2002JD002241, 31 January 2003.

[RD89] Tukiainen, S., Kyrölä, E., Tamminen, J., Kujanpää, J., and Blanot, L.: GOMOS bright limb ozone data set, Atmos. Meas. Tech., 8, 3107-3115, doi:10.5194/amt-8-3107-2015, 2015.

[RD90] Vandenbussche, S., C. De Clercq, J.-C. Lambert, R. Spurr, and T. von Clarmann. EC FP6 GEOmon Technical note D4.2.1 - Multi-dimensional characterisation of remotely sensed data - Chapter 4: Satellite measurements of limb-scattered ultraviolet-visible light. GEOmon TN-IASB-OBSOP / Chapter 4, BIRA-IASB, July 2010.

[RD91] Vandenbussche, S., J.-C. Lambert, and R. Spurr, EC FP6 GEOmon Technical note D4.2.1 - Multi-dimensional characterisation of remotely sensed data - Chapter 5: Satellite measurements of solar/stellar occultation. GEOmon TN-IASB-OBSOP / Chapter 5, BIRA-IASB, December 2010.

[RD92] Van Malderen, R. et al., Global Ground-based Tropospheric Ozone Measurements : Reference Data and Individual Site Trends (2000-2022) from the TOAR II/HEGFITOM project, submitted, 2024.

[RD93] van Roozendael, M.,P. Peters, H. K. Roscoe, et al., Validation of Ground-Based Visible Measurements of Total Ozone by Comparison with Dobson and Brewer Spectrophotometers, J. Atmos. Chem, 29, 55–83, 1998.

[RD94] von Clarmann, T., C. De Clercq, M. Ridolfi, M. Höpfner, and J.-C. Lambert, The horizontal resolution of MIPAS, Atmos. Meas. Tech., Vol. 2, 47-54, 2009.

[RD95] von Savigny, C., H. Bovensmann, K. Bramstedt, S. Dikty, F. Ebojie, A. Jones, S. Noël, A. Rozanov, and B.-M. Sinnhuber. Indications for long-term trends and seasonal variations in the SCIAMACHY Level 1 version 6.03 tangent height information. Technical Report TN-IUP-scia-pointing-2009-01, IUP Bremen, June 2009.

[RD96] Wang, H. J. R., Damadeo, R., Flittner, D., Kramarova, N., Taha, G., Davis, S., et al. (2020). Validation of SAGE III/ISS solar occultation ozone products with correlative satellite and ground based measurements. Journal of Geophysical Research: Atmospheres, 125, e2020JD032430. https://doi.org/10.1029/2020JD032430, 2020.

[RD97] Waters, J. W. et al., "The Earth observing system microwave limb sounder (EOS MLS) on the aura Satellite," in IEEE Transactions on Geoscience and Remote Sensing, vol. 44, no. 5, pp. 1075-1092, doi:10.1109/TGRS.2006.873771, 2006.

[RD98] World Meteorological Organization, Scientific assessment of ozone depletion: 2006, Global Ozone Res. Monit. Proj., Rep. 50, Geneva, Switzerland, 2006.

8 Terms and definitions

8.1 *Terminology*

In Table 8.1, terms and definitions as recommended by CEOS WGCV and by standards development organisations of international recognition have been transcript from reference documents [RD12] to [RD20]. In some cases, terms and definitions peculiar to forecast systems are also proposed. They are expected to evolve as these organisations regularly update their standards and as further standardisation and harmonisation occur.

Table 8.1 - Recommended terms and definitions.

TERM	DEFINITION	SOURCE
accuracy	closeness of agreement between a quantity value obtained by measurement and the true value of the measurand; note that it is not a quantity and it is not given a numerical quantity value	VIM, GUM
area (volume) of representativeness	the area (volume) in which the concentration does not differ from the concentration at the station by more than a specific range	Larssen
bias	(1) systematic error of indication of a measuring system (2) estimate of a systematic measurement error (3) estimate of a systematic forecast error	VIM VIM GAS
calibration	(1) the process of quantitatively defining the system responses to known, controlled signal inputs (2) operation that, under specified conditions, in a first step, establishes a relation between the quantity values with measurement uncertainties provided by measurement standards and corresponding indications with associated measurement uncertainties and, in a second step, uses this information to establish a relation for obtaining a measurement result from an indication	CEOS VIM
dead band (or neutral zone)	maximum interval through which a value of a quantity being measured can be changed in both directions without producing a detectable change in the corresponding indication	VIM
detection limit	measured quantity value, obtained by a given measurement procedure, for which the probability of falsely claiming the absence of a component, given a probability α of falsely claiming its presence	VIM
error	(1) measured quantity value minus a reference quantity value (2) difference of quantity value obtained by measurement and true value of the measurand (3) difference of forecast value and a, estimate of the true value	VIM CEOS
establish	define, document and implement	CDRH
field-of-regard	an area of the object space scanned by the field-of-view of a scanning sensor	NIST
field-of-view	the solid angle from which the detector receives radiation	NIST
footprint	the area of a target encircled by the field-of-view of a detector of radiation, or irradiated by an active system	NIST

influence quantity	quantity that, in a direct measurement, does not affect the quantity that is actually measured, but affects the relation between the indication and the measurement result	VIM
in situ measurement	(1) a direct measurement of the measurand in its original place (2) any sub-orbital measurement of the measurand	GEOSS
measurand	quantity intended to be measured	VIM
metadata	data about the data; parameters that describe, characterise, and/or index the data	WMO
monitoring	(1) systematic evaluation over time of some quantity (2) by extension, evaluation over time of the performance of a system, of the occurrence of an event etc.	NIST
point-to-area (point-to-volume) representativeness	the probability that a point measurement lies within a specific range of area-average (volume-average) concentration value	Nappo
precision	closeness of agreement between quantity values obtained by replicate measurements of a quantity on the same or similar object under specified conditions	VIM
process validation	establishing documented evidence of a high degree of assurance that a specific process will consistently produce a product meeting its pre-determined specifications and quality characteristics	CDRH
quality assessment (QA)	QA refers to the overall management of the processes involved in obtaining the data	CEOS
quality control (QC)	QC refers to the activities undertaken to check and optimise accuracy and precision of the data after its collection	CEOS
quality indicator (QI)	a means of providing a user of data or derived product with sufficient information to assess its suitability for a particular application. This information should be based on a quantitative assessment of its traceability to an agreed reference or measurement standard (ideally SI) but can be presented as a numeric or a text descriptor, provided the quantitative linkage is defined.	QA4EO
radiometric calibration	a determination of radiometric instrument performance in the spatial, spectral, and temporal domains in a series of measurements, in which its output is related to the true value of the measured radiometric quantity	NIST
random error	(1) component of measurement error that in replicate measurements varies in an unpredictable manner; note that random measurement error equals measurement error minus systematic measurement error (2) component of forecast error that varies in an unpredictable manner	VIM
relative standard uncertainty	standard measurement uncertainty divided by the absolute value of the measured quantity value	VIM
repeatability	measurement precision under set of conditions including the same measurement procedure, same operator, same measuring system, same operating conditions and same location, and replicated measurements over a short period of time	VIM

representativeness	the extent to which a set of measurements taken in a given space-time domain reflect the actual conditions in the same or different space-time domain taken on a scale appropriate for a specific application	Nappo
reproducibility	measurement precision under a set of conditions including different locations, operators, and measuring systems	VIM
resolution	(1) the least angular/linear/temporal/spectral distance between two identical point sources of radiation that can be distinguished according to a given criterion (2) the least vertical/geographical/temporal distance between two identical atmospheric features that can be distinguished in a gridded numerical product or in time series of measurements; resolution is equal to or coarser than vertical/geographical/temporal sampling of the grid or the measurement time series	NIST
stability	ability of a measuring system to maintain its metrological characteristics constant with time	VIM
systematic error	component of measurement error that in replicate measurements remains constant or varies in a predictable manner	VIM
traceability	property of a measurement result relating the result to a stated metrological reference (free definition and not necessarily SI) through an unbroken chain of calibrations of a measuring system or comparisons, each contributing to the stated measurement uncertainty	VIM
tropopause	the region of the atmosphere where the environmental temperature lapse rate changes from positive (in the troposphere) to negative (in the stratosphere) the lowest level at which the lapse rate decreases to 2 °C/km or less, provided that the average lapse rate between this level and all higher levels within 2 km does not exceed 2 °C/km occasionally, a second tropopause may be found if the lapse rate above the first tropopause exceeds 3 °C/km	WMO
uncertainty	non-negative parameter that characterizes the dispersion of the quantity values that are being attributed to a measurand, based on the information used	VIM
validation	(1) the process of assessing, by independent means, the quality of the data products derived from the system outputs (2) verification where the specified requirements are adequate for an intended use (3) the process of assessing, by independent means, the degree of correspondence between the value of the radiometric quantity derived from the output signal of a calibrated radiometric device and the actual value of this quantity. (4) confirmation by examination and provision of objective evidence that specifications conform to user needs and intended uses, and that the requirements implemented through software can be consistently fulfilled	CEOS VIM NIST CDRH

verification	(1) the provision of objective evidence that a given data product fulfils specified requirements; note that, when applicable, measurement uncertainty should be taken into consideration. (2) the provision of objective evidence that the design outputs of a particular phase of the software development life cycle meet all of the specified requirements for that phase	VIM CDRH
vicarious calibration	a post-launch radiometric calibration of sensors performed with the use of natural or artificial sites or objects on the surface of the Earth (as opposed to calibration techniques using onboard standards such as lamps, blackbodies, solar diffuse reflecting panels etc.)	NIST

8.2 *Abbreviations and acronyms*

Note of best practice: Using an acronym is acceptable if it has been defined the first time it appears in a document. The same applies to chemical abbreviations. In documents targeting a wide spectrum of potential readers, like user manuals and validation reports, it is recommended to avoid systematic use of acronyms and abbreviations except for those with frequent occurrence, and those widely understood by the general public. For example, acronyms such as CFCs and ESA are acceptable. Acronyms such as ECSS and ICTT-QMF are not. Before using acronyms and abbreviations, authors should keep in mind that it is annoying and difficult – especially in Web-based documents unless the acronyms are available as hyperlinks – to turn over several pages in a document to verify the meaning.

AK	Averaging Kernel
AMF	Air Mass Factor or optical enhancement factor
ATBD	Algorithm Theoretical Basis Document
AUTH	Aristotle University of Thessaloniki
BIRA-IASB	Belgian Institute for Space Aeronomy
C3S	Copernicus Climate Change Service
CCI	ESA's Climate Change Initiative programme
CEOS	Committee on Earth Observation Satellites
CMUG	Climate Modelling User Group of the CCI programme
CDRP	Climate Research Data Package
CRG	Climate Research Group of the Ozone_cci+ project
DARD	Data Access Requirement Document
DFS	Degree of Freedom of the System
DHF	Data Host Facility
DIAL	Differential Absorption LIDAR
DLR	German Aerospace Centre
DOAS	Differential Absorption Optical Spectroscopy
DU	Dobson Unit – unit of vertical column density (2.69 1016 molec.cm-2)
EC	European Commission
ECMWF	European Centre for Medium-Range Weather Forecasts
ECSS	European Corporation for Space Standardization
Envisat	ESA's Environmental Satellite, launched March 1, 2002
EO	Earth Observation
EOST	Earth Observation Science Teams of the Ozone_cci+ project
EPS	EUMETSAT Polar System
ERA-I	ECMWF ReAnalysis Interim
ERA5	ECMWF ReAnalysis 5
ERS-2	ESA's Earth Remote Sensing satellite 2, launched April 21, 1995
ESA	European Space Agency
ESRIN	European Space Research Institute
EUMETSAT	European Organisation for the Exploitation of Meteorological Satellites
FMI	Finnish Meteorological Institute
FRM	Fiducial Reference Measurements
FTIR	Fourier Transform Infra-Red spectrometer
GAS	GMES Atmospheric Service
GAW	WMO's Global Atmosphere Watch
GCOS	Global Climate Observing System
GDP	GOME Data Processor
GEO	Group on Earth Observation

GEOSS	Global Earth Observation System of Systems
GMES	Global Monitoring for Environment and Security
GOME	Global Ozone Monitoring Experiment
GOMOS	Global Ozone Monitoring by Occultation of Stars
GPS	Global Positioning System
GUM	Guide to the expression of uncertainty in a measurement
HALOE	Halogen Occultation Experiment
ICTT-QMF	Inter-Commission Task Team on Quality Management Framework
IGACO	Integrated Global Atmospheric Chemistry Observation strategy
IGOS	Integrated Global Observation Strategy
INSPIRE	Infrastructure for Spatial Information in the European Community
IPF	Instrument Processing Facility
I/O tools	Input/Output tools
IR	INSPIRE Implementation Rule
ISO	International Organization for Standardization
ISSI	International Space Science Institute
JCGM	Joint Committee for Guides in Metrology
KNMI	Royal Dutch Meteorological Institute
lidar	light detection and ranging
LP	Limb Profile
MetOp	EUMETSAT's Meteorological Operational satellite
MIPAS	Michelson Interferometer for Passive Atmospheric Sounding
MIPAS FR	MIPAS operated at Full (nominal) Resolution
MIPAS RR	MIPAS operated at Reduced (optimised) Resolution
MLS	Microwave Limb Sounder
Multi-TASTE	Technical ASsistance To the multi-mission validation of Envisat and Third Party Missions using spectrometers, radiometers and sondes
MWR	MicroWave Radiometer
NCEP	National Centers for Environmental Prediction
NDACC	Network for the Detection of Atmospheric Composition Change
NH	Northern Hemisphere
NOAA	National Oceanic and Atmospheric Administration
NP	Nadir Profile
O3	Ozone
OE	Optimal Estimation
OMI	Ozone Monitoring Instrument
PSD	Product Specification Document
PVP	Product Validation Plan
QA4EO	Quality Assurance framework for Earth Observation
RAL	Rutherford Appleton Laboratory
S5P	Sentinel-5 Precursor
SAGE	Stratospheric Aerosol and Gas Experiment
SBUV	Solar Backscatter Ultraviolet
SCIAMACHY	SCanning Imaging Absorption spectroMeter for Atmospheric CHartographY
SGP	SCIAMACHY Ground Processor
SH	Southern Hemisphere
SHADOZ	Southern Hemisphere ADditional Ozonesondes
SNPP	Suomi National Polar-orbiting Partnership satellite
SZA	Solar Zenith Angle

TBD	To Be Determined
TEMIS	Tropospheric Emission Monitoring Internet Service
TOC	Total Ozone Column
TOMS	Total Ozone Mapping Spectrometer
TROPOMI	TROPOspheric Monitoring Instrument
UARS	Upper Atmosphere Research Satellite, launched September 15, 1991
ULB	Université Libre de Bruxelles
URD	User Requirement Document
USM	Upper Stratosphere/Mesosphere
UT	Upper Troposphere
UTLS	Upper Troposphere/Lower Stratosphere
UVVIS	DOAS UV-visible spectrometer (generic)
VALT	Validation team of the Ozone_cci+ project
VIM	International Vocabulary of Metrology – Basic and general concepts and associated terms
VMR	Volume Mixing Ratio
WGCV	CEOS Working Group on Calibration and Validation
WMO	World Meteorological Organization
WOUDC	World Ozone and Ultraviolet Radiation Data Center

END OF DOCUMENT